

SSPAs with European GaN Devices Final Report

**ESTEC Contract Number Contrat 4000101119
ESA Technical Officer(s): Amitabh Chowdhary, ESTEC, Noordwijk**

**B.Lefebvre⁽¹⁾, J.Lhortolary⁽¹⁾, A.Benvegnu⁽¹⁾, F.Delahaye⁽¹⁾, M.Delmas⁽¹⁾, V.Leal⁽¹⁾,
A.Guillope⁽¹⁾, JL. Muraro⁽¹⁾, H.Lebfond⁽¹⁾, JF.Villemazet⁽¹⁾
R.Ouhachi⁽²⁾, M.Faure⁽²⁾, C. Charbonniaud⁽²⁾, Raphael Sommet⁽³⁾, Laurent
Favede⁽⁴⁾**

**⁽¹⁾Thales Alenia Space, 26, avenue J.F. Champollion BP 1187, 31037 Toulouse
Cedex 1 France**

⁽²⁾AMCAD Engineering, Bâtiment Galiléo, 20 rue d'Atlantis, 87068 Limoges

**⁽³⁾ XLIM - C2S2 - UMR 7252 Campus universitaire, 16 rue Jules Vallès 19100
Brive la Gaillarde**

**⁽³⁾ UMS, Mosaic Parc de Courtaboeuf - Bat Charmille, 10 Avenue du Québec,
91140 Villebon-sur-Yvette**

Date: 15 February 2019

**EUROPEAN SPACE AGENCY
CONTRACT REPORT**

The work described in this report was done under ESA contract. Responsibility for the contents resides in the author or organisation that prepared it.

ABSTRACT

GaN technology represents a fundamental technological breakthrough for power amplification at microwave frequencies for satellite payload. The introduction of GaN transistors in the new generation of SSPA equipment is significantly improving several performances :

- At electrical level : higher power density, better efficiency, improved robustness, EPC with high voltage value
- At thermal level : higher operational temperature
- At mechanical level : mass reduction, size reduction thanks to higher power density and reduced HPA module number.

Regarding this ARTES 5.1 study, the main conducted activities allowed to evaluate last improvements on European commercial 0.5 μ m (GH50) and 0.25 μ m (GH25) GaN HEMT technologies from United Monolithic Semiconductors Foundry. These two GaN technologies were developed in the frame of the GREAT² ESA contract. These UMS GaN processes, makes them the good candidates for space applications from L-band to Ku-band.

Main activity was to design, manufacture and test:

- **1 hybrid HPA module (two iterations) at L-band and based on the UMS GH50 technology**
- **1 MMIC HPA module at Ku-band and based on the UMS GH25 technology**

As prime contractor of the project, **Thales Alenia Space (TAS)** was in charge of the transistor specification and the design, the manufacture and test of the L-band hybrid HPA module (HPA-1) and the Ku-Band MMIC HPA module (HPA-2). Regarding HPA-2, different architectures were studied (Class AB and Doherty)

United Monolithic Semiconductors (UMS), as sub-contractor and European GaAs and GaN foundry, was in charge of the manufacture and on wafer test of the transistors, power bars and HPA MMIC.

Advanced Modelling Computer Aided Design (AMCAD), as sub-contractor, was in charge of the transistor and power-bar characterization for modelling activity. AMCAD will perform the multi-harmonic load pull measurements for the transistor and power-bar validation after the foundry manufacturing. AMCAD was in charge of the transistor cell non-linear modelling.

The Institut de recherche de l'université de Limoges (XLIM), as sub-contractor, was in charge of the transistor thermal analysis and electro thermal non-linear modelling. XLIM was in charge of the power-bar non-linear modelling and the determination of the operating classes for the L-band hybrid HPA module design.

TABLE OF CONTENTS

1. SSPA FOR FUTURE SPACEBORNE TELECOM APPLICATIONS	18
1.1 Survey on the Market Trends for L/S-band Telecom application	18
1.2 Initial L-Band SSPA equipment analysis based on L-Band GH50 Hybrid HPA module performance	18
1.3 Survey on the Market Trends for Ku-Band Telecom application	21
1.4 Initial Ku-Band SSPA equipment analysis based on Ku-Band GH25 MMIC HPA module performance.....	22
2. DEVELOPMENT OF L-BAND HYBRID GH50 HPA MODULE (HPA-1 MODULE)	25
2.1 Development of L-band hybrid GH50 HPA module (HPA-1 module): Phase 1.....	25
2.1.1 Baseline Design	25
2.1.1.1 Loadpull simulations.....	25
2.1.1.2 Architecture and technologies considerations	29
2.1.1.3 RF performance	30
2.1.1.4 Packaging solution.....	32
2.1.1.5 Thermal simulations.....	33
2.1.2 Manufacture and test the 0.5 μ m transistors and power-bars (GH50). Run-1	36
2.1.3 Characterization and modeling of the 0,5 μ m transistors and power-bars. Run-1	39
2.1.3.1 Unitary cell measurements. Run-1	39
2.1.3.2 Unitary cell modeling activity. Run-1	47
2.1.3.3 Power Bar measurements. Run-1	50
2.1.3.4 Power Bar modeling activity. Run-1	56
2.1.4 Detailed Design. Run-1	60
2.1.5 HPA-1 Module Manufacturing and Tests. Run-1	68
2.1.5.1 [S] Parameter measurements. Run-1	69
2.1.5.2 CW mode power measurements. Run-1	71
2.1.5.3 Multi-carrier mode power measurements. Run-1	75
2.1.5.4 RF step measurements with multi-carrier signal : reliability of GH50-10 technology. Run-1	78
2.2 Development of L-band hybrid GH50 HPA module (HPA-1 module): Phase 2.....	85
2.2.1 Reverse Engineering of HPA-1 module developed in Run-1	85
2.2.1.1 Back-simulations of HPA-1 module Run-1	85
2.2.1.2 CCN on new specification for HPA-1 module	88
2.2.2 Manufacture and test the 0.5 μ m transistors and power-bars (GH50). Run-2	89
2.2.3 Characterization and modeling of the 0,5 μ m transistors and power-bars. Run-2.....	94
2.2.3.1 Unitary cell measurements. Run-2.....	94
2.2.3.2 Unitary cell modeling activity. Run-2	101
2.2.3.3 Power Bar measurements. Run-2.....	107
2.2.3.4 Power Bar modeling activity. Run-2.....	108
2.2.3.5 Synthesis of the performance Gate-Lag and Drain Lag monitored for Sabrina wafer (Run-1) and Stardust wafer (Run-2)	110
2.2.4 Detailed Design. Run-2.....	111
2.2.5 HPA-1 Module Manufacturing and Tests. Run-2.....	119
2.2.5.1 [S] Parameter measurements. Run-2	119
2.2.5.2 CW mode power measurements. Run-2	122
2.2.5.3 Multi-carrier mode power measurements. Run-2	124

2.2.5.4	RF step measurements with multi-carrier signal : reliability of GH50-10 technology. Run-2	126
3.	DEVELOPMENT OF KU-BAND MMIC GH25 HPA MODULES (HPA-2 MODULE)	133
3.1	Market trends survey.....	133
3.2	HPA specifications	134
3.3	Baseline Design	135
3.3.1	Loadpull simulations	135
3.3.2	MMIC architecture	137
3.3.3	RF performance simulation	138
3.3.4	Packaging solution	139
3.3.5	Thermal simulations	139
3.3.5.1	Thermal study of GH25 8x125 μ m transistor.....	140
3.3.5.2	Thermal study of the GH25 8x8x125 μ m power-bar	141
3.3.5.3	Thermal study of the packaging of the power amplifier	142
3.3.5.4	Temperature evaluation	143
3.4	0.25μm Technology Modelling and Performance.....	144
3.4.1	Unitary cell measurements	144
3.4.2	Unitary cell modeling activity.....	149
3.5	Detailed Design	153
3.5.1	Detailed Design of version 1 : HPA-2 module.....	154
3.5.2	Detailed Design of version 2: MMIC Doherty HPA module.....	161
3.5.3	Detailed Design of version 3: MMIC-Hybrid Doherty HPA module	166
3.6	0,25μm MMIC and transistors Manufacturing and on-wafer Test	171
3.6.1	PCM Results	171
3.6.2	HPA-2 MMIC On wafer-measurements	173
3.6.3	Doherty HPA MMIC On wafer-measurements.....	174
3.7	HPA-2 Module and Doherty HPA Module Test	176
3.7.1	HPA-2 Modules test results	177
3.7.1.1	[S] Parameter measurements.	177
3.7.1.2	CW mode power measurements.	180
3.7.1.3	Multi-carrier mode power measurements.	183
3.7.1.4	RF step measurements with multi-carrier signal : reliability of GH25 technology	185
3.7.2	MMIC Doherty HPA Modules test results	191
3.7.2.1	[S] Parameter measurements.....	191
3.7.2.2	CW mode power measurements.	193
3.7.2.3	Multi-carrier mode power measurements.	196
3.7.2.4	Comparison results between HPA-2 module and MMIC Doherty HPA module.....	198
4.	CRITICAL ASSESMENT OF HPA MODULE.....	201
4.1	L-band applications: comparison of SSPA using GaN HPA-1 module with a conventional GaAs flat mounted SSPA and TWTA	201
4.2	Ku-band applications: comparison of SSPA using GaN HPA-2 module with a LC-TWTA equipment.	202

LIST OF FIGURES

FIGURE 1 : LP SIMULATION (8X250MM). THIRD HARMONIC LOAD IMPEDANCE OPTIMIZATION FOR ZL(H1OPT) AND ZL(H2OPT).	27
FIGURE 2 : COMPARISON BETWEEN 6X400 μ M AND 8X250 μ M TRANSISTORS PERFORMANCES WITH OPTIMAL IMPEDANCE	28
FIGURE 3 : POWER BAR CONSIDERED AS MACRO CELL MADE UP OF 2N ELEMENTARY TRANSISTOR	29
FIGURE 4 : OUTPUT NETWORK SCHEMATIC (MOMENTUM) OF THE L-BAND HYBRID HPA	30
FIGURE 5 : HPA-1 MODULE. BASELINE DESIGN. HPA RF PERFORMANCES. POUT(W), PAE(%), GAIN(DB) VERSUS INPUT POWER (DBM) AND FREQUENCY(GHZ).....	31
FIGURE 6 : HPA-1 MODULE. PRELIMINARY GH50 HYBRID HPA SIMULATION RESULTS IN MULTI-CARRIER MODE. PAE(%), NPR(DB), GAIN COMPRESSION(DB) VERSUS OUTPUT POWER(DBM)	32
FIGURE 7 : L40 POWER PACKAGE WITH MDC (METAL DIAMOND COMPOSITE) BASE PLATE.....	33
FIGURE 8 : NON LINEAR THERMAL CONDUCTIVITY OF GAN (LEFT) AND SIC (RIGHT).....	34
FIGURE 9 : CUTPLANE OF ELEMENTARY CELL (LEFT)AND ZOOM ON THE ACTIVE AREA (RIGHT).....	34
FIGURE 10 : TEMPERATURE PROFILE FOR TBASE=75°C AND 32W OF DISSIPATED POWER	35
FIGURE 11 : TEMPERATURE CALCULATION FOR TCASE 75°C 36W DISSIPATED POWER WITH TAB	36
FIGURE 12 : PRELIMINARY THERMAL MODEL WITH 4 CELLS	36
FIGURE 13 : UMS WORKFLOW FOR THE MANUFACTURING AND TEST OF GH50 MASKSET (RUN-1).....	37
FIGURE 14 : RUN-1 0,5 μ M WAFER MANUFACTURING. MAXIMUM STABLE GAIN /MAXIMUM AVAILABLE GAIN FOR 8X250 μ M TRANSISTOR CELL	37
FIGURE 15 : RUN-1 0,5 μ M WAFER TESTS. MEASURED PERFORMANCE OF 8X8X250 μ M POWER-BAR.....	38
FIGURE 16 : AMCAD I(V) AND [S] TEST BENCH FOR TRANSISTORS CHARACTERIZATIONS	39
FIGURE 17 : PRINCIPLE OF THE S-PARAMETERS MEASUREMENTS IN PULSE MODE.....	40
FIGURE 18 : DISPERSIVE [S] MEASUREMENTS ON TRANSISTORS 8X250MM GH50 (BIAS POINTS CORRESPONDING TO SURROUNDED POINTS ON THE I(V) CURVES, VDS=40V).....	41
FIGURE 19 : OUTPUT CURRENT WITH DIFFERENT CHUCK TEMPERATURE (25°C, 60°C, 100°C) TRANSISTOR 8X250 L60 MEASUREMENTS	42
FIGURE 20 : HIGHLIGHTED PHENOMENA TRAPS	42
FIGURE 21 : MAXIMUM GAIN @ VDS0=40V, IDS0=50MA/MM	43
FIGURE 22 : SUMMARY OF THE UNITARY CELL – PULSED I(V) / RF MEASUREMENTS	43
FIGURE 23 : AMCAD VNA-BASED LOAD-PULL SYSTEM	43
FIGURE 24 : POUT / PAE / GAIN VS PIN AFTER LOADPULL OPTIMIZATION. OPTIMIZED LOAD (H1, H2, H3) FOR OPTIMAL PAE PERFORMANCE. VDS=40V, 25MA/MM.	45
FIGURE 25 : LOADPULL MEASUREMENTS. PERFORMANCE VS TECHNOLOGY DISPERSION. 5X TRANSISTOR SAMPLES TESTED. 40V, 25MA/MM.....	45
FIGURE 26 : ELEMENTARY TRANSISTOR CELL 8X250 μ M GH50. MODEL IMPLEMENTED IN ADS.....	47
FIGURE 27 : 8X250 μ M TRANSISTOR MODEL VALIDATION. I(V) CURVES COMPARISON. BIAS CONDITIONS : VDS=40V, IDS0=25MA/MM. TEMP=25°C	47
FIGURE 28 : 8X250 μ M TRANSISTOR MODEL VALIDATION. I(V) CURVES COMPARISON. BIAS CONDITIONS : VDS=0V, VGS=0V. TEMP=60°C.....	48

FIGURE 29 : 8X250 μ M TRANSISTOR MODEL VALIDATION. [S] PARAMETERS COMPARISON. MEASUREMENT. VS MODEL 8X250MM @VDS0=40V AND IDS0=25MA/MM	48
FIGURE 30 : 8X250 μ M TRANSISTOR MODEL VALIDATION. [S] PARAMETERS COMPARISON. MEASUREMENT. VS MODEL 8X250MM @VDS0=40V AND IDS0=25MA/MM	49
FIGURE 31 : 8X250 μ M TRANSISTOR MODEL VALIDATION. SELECTED IMPEDANCES USED FOR LOADPULL SIMULATIONS/MEASUREMENTS COMPARISON.....	49
FIGURE 32 : 8X250 μ M TRANSISTOR MODEL VALIDATION. LOADPULL SIMULATIONS / MEASUREMENTS COMPARISON. VDS0=40V AND IDS0=25MA/MM	50
FIGURE 33 : MEASUREMENT CHRONOGRAM OF THE POWER BAR	51
FIGURE 34 : AMCAD VNA-BASED LOAD-PULL SYSTEM USED FOR LOADPULL MEASUREMENT OF POWER-BAR	51
FIGURE 35 : POWER BAR TEST FIXTURE – TWO TYPES OF MEASUREMENT PLANS	52
FIGURE 36 : MIC_IN / MIC_OUT.....	52
FIGURE 37 : TRL KIT	53
FIGURE 38 : EXAMPLE OF A LOAD IMPEDANCE TRANSFORMATION CAUSED BY THE DE-EMBEDDING (@F0)	54
FIGURE 39 : MEASUREMENTS @ 1.57 GHZ WITH VDS0=45V IDS0=400MA (25MA/MM), POWER BAR REFERENCE PLANE, POWER BAR N°4. OPTIMUM ZLOAD @F0 AND @2F0	55
FIGURE 40 : MEASUREMENTS @ 1.57 GHZ WITH VDS0=45V IDS0=400MA (25MA/MM), POWER BAR REFERENCE PLANE, POWER BAR N°4. GAIN(DB) / POUT(DBM) VS PIN(DBM).....	55
FIGURE 41 : MEASUREMENTS @ 1.57 GHZ WITH VDS0=45V IDS0=400MA (25MA/MM), POWER BAR REFERENCE PLANE, POWER BAR N°4. PAE(%) VS PIN(DBM).....	56
FIGURE 42 : MEASUREMENT TEST SET OFF THE POWER BAR	57
FIGURE 43 : ELECTRO THERMAL MODEL OF THE POWER BAR	58
FIGURE 44 : POUT VS PIN AND DC DRAIN CURRENT VERSUS VS PIN. COMPARISON BETWEEN SIMULATION AND MEASUREMENTS FOR POWER BAR SAMPLE4	58
FIGURE 45 : INPUT REFLECTION COEFFICIENT VERSUS PIN AND PAE VERSUS PIN. COMPARISON BETWEEN SIMULATION AND MEASUREMENTS FOR POWER BAR SAMPLE4	59
FIGURE 46 : POWER GAIN VS PIN AND AMPM VS PIN. COMPARISON BETWEEN SIMULATION AND MEASUREMENTS FOR POWER BAR SAMPLE4.....	59
FIGURE 47 : OPTIMAL LOAD IMPEDANCES FOUND AT FUNDAMENTAL (LEFT) AND 2ND HARMONIC (RIGHT) FREQUENCIES BASED ON 8X250MM TRANSISTOR LOAD-PULL MEASUREMENTS AND SIMULATIONS.	60
FIGURE 48 : OVERVIEW OF THE RF INSERT USED WITH THE CUD PACKAGE	61
FIGURE 49 : S-PARAMETERS WIDE FREQUENCY BAND ANALYSIS	61
FIGURE 50 : S-PARAMETERS IN-BAND FREQUENCY ANALYSIS	62
FIGURE 51 : K STABILITY FACTOR & B STABILITY MEASUREMENTS. WIDE FREQUENCY BAND ANALYSIS.....	62
FIGURE 52 : SYNTHESIZED OUTPUT IMPEDANCES AT FUNDAMENTAL FREQUENCY (H1) FROM 1.52GHZ TO 1.62GHZ.....	63
FIGURE 53 : SYNTHESIZED OUTPUT IMPEDANCES AT 2ND HARMONIC FREQUENCY (H2) FROM 3.04GHZ TO 3.24GHZ.....	63
FIGURE 54 : OUTPUT COMBINER LOSSES (DB) VERSUS RFFREQ AND INPUT POWER(DBM)	64
FIGURE 55 : HPA RF PERFORMANCES. POUT(W), PAE(%), GAIN(DB) VERSUS INPUT POWER (DBM) AND FREQUENCY(GHZ).	64
FIGURE 56 : DRAIN CURRENT AND POWER CONSUMPTION(W) VS. INPUT POWER(DBM) – FROM 1.52 TO 1.65GHZ.....	65

FIGURE 57 : DRAIN CURRENT AND POWER CONSUMPTION(W) VS. INPUT POWER(DBM) – FROM 1.52 TO 1.65GHZ.....	65
FIGURE 58 : HPA PERFORMANCES : POUT(W), PAE(%), GAIN(DB) VERSUS TEMPERATURE [-10°C; 25°C, 85°C] @PIN(MAX PAE).....	66
FIGURE 59 : HPA PERFORMANCES IN MULTI-CARRIER MODE : NPR(DB), COMPRESSION(DB), PAE(%) VERSUS PIN. TEMP=25°C, VDS=40V AND IDS=25MA/MM.....	67
FIGURE 60 : HPA-1 MODULE (#2). [S] PARAMETERS MEASUREMENTS. RF=[DC-10GHZ], VD=45V, FIXED DRAIN CURRENT IDS=400MA @25°C , TEMP=[-20°C , 25°C , 90°C].....	69
FIGURE 61 : HPA-1 MODULE (#2). [S] PARAMETERS MEASUREMENTS. RF=[1.3-1.8GHZ], VD=45V, FIXED DRAIN CURRENT IDS=400MA @25°C , TEMP=[-20°C , 25°C , 90°C].....	70
FIGURE 62 : HPA-1 MODULE (#2). [S] PARAMETERS MEASUREMENTS. RF=[1.3-1.8GHZ],.....	70
FIGURE 63 : HPA-1 MODULES (#2#3#5). [S] PARAMETERS MEASUREMENTS. RF=[1.3-1.8GHZ], VD=45V, DRAIN CURRENT IDS=400MA @25°C . TEMP=[-20°C , 25°C , 90°C].....	71
FIGURE 64 : HPA-1 MODULE (#2). POWER MEASUREMENTS WITH CW SIGNAL. TEMP=[-20°C, 25°C, 90°C], VD=40V, ID=400MA. RF=[1,5425GHZ/1,5675GHZ/1,5925GHZ]. GAIN(DB), PAE(%), POUT(DBM), PHASE(DEG) VS PIN(DBM).....	72
FIGURE 65 : HPA-1 MODULE (#2). POWER MEASUREMENTS WITH CW SIGNAL. TEMP=[-20°C, 25°C, 90°C], VD=40V, ID=400MA. GAIN(DB), PAE(%), POUT(DBM), PHASE(DEG) VS RFFREQ(GHZ) @PAE_MAX.....	72
FIGURE 66 : HPA-1 MODULE (#2). POWER MEASUREMENTS WITH CW SIGNAL. TEMP=[-20°C, 25°C, 90°C], VD=45V, ID=400MA. GAIN(DB), PAE(%), POUT(DBM), PHASE(DEG) VS RFFREQ(GHZ) @PAE_MAX.....	73
FIGURE 67 : HPA#1 MODULE (#5). POWER MEASUREMENTS WITH CW SIGNAL. TEMP=[25°C, 90°C], VD=45V, RF=1,5675GHZ ID=[100MA/200MA/400MA/800MA]. GAIN(DB), PAE(%), POUT(DBM), PHASE(DEG) VS PIN(DBM).....	75
FIGURE 68 : HPA-1 MODULE (#5). SYNTHESIS OF POWER MEASUREMENTS WITH CW SIGNAL. TEMP=[25°C, 90°C], VD=45V, RF=1,5675GHZ ID=[100MA / 200MA / 400MA / 800MA]. GAIN(DB), PAE(%), POUT(DBM), PHASE(DEG) VS PIN(DBM).....	75
FIGURE 69 : HPA-1 MODULE (#5) POWER MEASUREMENTS WITH MULTI-CARRIER SIGNAL. TEMP=-20°C. VDS=45V, RF=1,5675GHZ, SPAN=40MHZ, 3000 CARRIERS, 1% NOTCH. GAIN(DB), PAE(%), NPR(DB) VS POUT(DBM).....	76
FIGURE 70 : HPA-1 MODULE (#5). POWER MEASUREMENTS WITH MULTI-CARRIER SIGNAL. TEMP=+25°C. VDS=45V, RF=1,5675GHZ, SPAN=40MHZ, 3000 CARRIERS, 1% NOTCH. GAIN(DB), PAE(%), NPR(DB) VS POUT(DBM).....	76
FIGURE 71 : HPA-1 MODULE (#5) POWER MEASUREMENTS WITH MULTI-CARRIER SIGNAL. TEMP=+90°C. VDS=45V, RF=1,5675GHZ, SPAN=40MHZ, 3000 CARRIERS, 1% NOTCH. GAIN(DB), PAE(%), NPR(DB) VS POUT(DBM).....	77
FIGURE 72 : HPA-1 MODULE (#5). SYNTHESIS OF POWER MEASUREMENTS WITH MULTI-CARRIER SIGNAL. TEMP=[-20°C, +25°C, +90°C]. VDS=45V, RF=1,5675GHZ, SPAN=40MHZ, 3000 CARRIERS, 1% NOTCH. ID(A) AND IG(A) PIN(DBM).....	77
FIGURE 73 : MULTI-CARRIER TEST BENCH.....	79
FIGURE 74 : PHOTOGRAPHS OF THE MULTI-CARRIER TEST BENCH.....	79
FIGURE 75 : NOISE SIGNAL LEVEL AT DIFFERENT POINT OF THE TEST BENCH.....	80
FIGURE 76 : CCDF VALUE FOR DIFFERENT COMPRESSION VALUES.....	80
FIGURE 77 : PHOTOGRAPHY OF THE CW TEST BENCH FOR CW INITIAL/INTERMEDIATE AND FINAL MEASUREMENTS.....	81
FIGURE 78 : RF STEP STREP MEASUREMENT: INITIAL CHARACTERIZATION OF HPA-1 MODULE (SAMPLE N°5). GAIN(DB) AND POUT(DBM) VERSUS PIN(DBM) FOR 3 DIFFERENT BIAS POINTS: 45V/100MA & 45V/400MA 45V/800MA IN SMALL SIGNAL.....	81

FIGURE 79 : DETECTOR CHARACTERIZATION : DETECTED VOLTAGE VALUE (MV) VERSUS POWER RANGE(DBM).....	82
FIGURE 80 : HPA-1 MODULE (#2). RF STEP STRESS MEASUREMENT. INPUT POWER MONITORING DURING 6DBC COMPRESSION STEP	82
FIGURE 81 : HPA-1 MODULE (#2). RF STEP STRESS MEASUREMENT. TEMPERATURE MONITORING DURING 6DBC COMPRESSION STEP	82
FIGURE 82 : HPA-1 MODULE (#2). RF STEP STRESS MEASUREMENT (6DBC STEP). POUT DRIFT (DETECTED VOLTAGE IN V). DRAIN VOLTAGE DRIFT(V). DRAIN CURRENT DRIFT (MA). GATE VOLTAGE DRIFT (V). VOLTAGE CURRENT DRIFT (MA).....	83
FIGURE 83 : HPA-1 MODULE #3. AMAM AND AMPM CHARACTERIZATION IN CW MODE AFTER EACH COMPRESSION STEP OF THE RF STEP STRESS MEASUREMENTS.....	84
FIGURE 84 : HPA-1 MODULE #3. [S] PARAMETERS MEASUREMENTS AFTER EACH COMPRESSION STEP OF THE RF STEP STRESS MEASUREMENTS	84
FIGURE 85 : HPA-1 MODULE #3. STATIC MEASUREMENTS AFTER EACH COMPRESSION STEP OF THE RF STEP STRESS MEASUREMENTS.....	85
FIGURE 86 : TWO METHODS USED DURING THE REVERSE ENGINEERING OF HPA-1 MODULE RUN-1.....	86
FIGURE 87 : HPA-1 MODULE RUN-1: S-PARAMETER COMPARISON OF MEASUREMENT AND REVERSE ENGINEERING SIMULATIONS	86
FIGURE 88 : HPA-1 MODULE RUN-1: S-PARAMETER COMPARISON ZOOM OF MEASUREMENT AND REVERSE ENGINEERING SIMULATIONS	87
FIGURE 89 : HPA-1 MODULE RUN-1: HPA RF PERFORMANCE VS FREQUENCY COMPARISON OF MEASUREMENT AND REVERSE ENGINEERING SIMULATIONS @ PIN=35DBM.....	87
FIGURE 90 : HPA-1 MODULE RUN-1: HPA RF PERFORMANCE VS PIN COMPARISON OF MEASUREMENT AND REVERSE ENGINEERING SIMULATIONS	88
FIGURE 91 : UMS WORKFLOW FOR THE MANUFACTURING & TEST OF GH50 MASKSET (RUN-2).....	89
FIGURE 92 : STARDUST TILE COMPOSITION	89
FIGURE 93 : 8X250_70 VD=40V ID=50MA/MM. S21 PARAMETER MAPPING AT 40V&ID=50MA/MM	90
FIGURE 94 : ON-WAFER LOADPULL MEASUREMENT OF 8X250 μ M POWER CELL UNIT	91
FIGURE 95 : 8X8X250 μ M POWER-BAR ON-WAFER MEASUREMENTS.....	93
FIGURE 96 : AMCAD I(V) AND [S] TEST BENCH FOR TRANSISTORS CHARACTERIZATIONS. RUN-2	94
FIGURE 97 : DISPERSIVE [S] MEASUREMENTS ON TRANSISTORS 8X250MM GH50. RUN-2 (BIAS POINTS CORRESPONDING TO SURROUNDED POINTS ON THE I(V) CURVES, VDS=40V).....	96
FIGURE 98 : OUTPUT CURRENT WITH DIFFERENT CHUCK TEMPERATURE (25°C, 60°C, 100°C) TRANSISTOR 8X250 μ M SAMPLE W81 MEASUREMENTS. RUN-2	96
FIGURE 99 : OUTPUT CURRENT WITH DIFFERENT CHUCK TEMPERATURE (25°C, 60°C,100°C), TRANSISTOR 8X250 μ M GH50 MEASUREMENTS (BIAS POINTS VDS0=42V, IDS0=100MA)	96
FIGURE 100 : HIGHLIGHTED PHENOMENA TRAPS	97
FIGURE 101: OUTPUT CURRENT, QUIESCENT BIAS: (42V, 100MA), (CHUCK TEMPERATURE = 25°C), TRANSISTOR 8X250 μ M GH50.....	97
FIGURE 102 : MAXIMUM GAIN @ VDS0=40V, IDS0=50MA/MM.....	98
FIGURE 103 : POUT / PAE / GAIN VS PIN AFTER LOADPULL OPTIMIZATION. OPTIMIZED LOAD (H1, H2) FOR OPTIMAL PAE PERFORMANCE. VDS=42V, 50MA/MM.....	100
FIGURE 104 : LOADPULL MEASUREMENTS. PERFORMANCE VS TECHNOLOGY DISPERSION. 3X 8X250 μ M TRANSISTOR SAMPLES TESTED. 42V, 50MA/MM.....	100
FIGURE 105 : ELEMENTARY TRANSISTOR CELL 8X250 μ M GH50. MODEL IMPLEMENTED IN ADS.....	101

FIGURE 106 : ACCESS LINES & TRANSISTOR LAYOUT (ALL VALUES IN μM)	102
FIGURE 107 : MODELED TRANSISTOR.....	102
FIGURE 108 : 8X250 μM TRANSISTOR MODEL VALIDATION. I(V) CURVES COMPARISON. QUIESCENT BIAS CONDITIONS : $V_{DS0}=0\text{V}$, $V_{GS0}=0\text{V}$	103
FIGURE 109 : 8X250 μM TRANSISTOR MODEL VALIDATION. I(V) CURVES COMPARISON. BIAS CONDITIONS : $V_{DS}=0\text{V}$, $V_{GS}=0\text{V}$. $\text{TEMP}=60^{\circ}\text{C}$	103
FIGURE 110 : TRAP EFFECTS	103
FIGURE 111 : 8X250 μM TRANSISTOR MODEL VALIDATION. [S] PARAMETERS COMPARISON. MEASUREMENT. VS MODEL 8X250MM @ $V_{DS0}=42\text{V}$ AND $I_{DS0}=50\text{MA/MM}$	104
FIGURE 112 : 8X250 μM TRANSISTOR MODEL VALIDATION. [S] PARAMETERS COMPARISON. MEASUREMENT. VS MODEL 8X250MM @ $V_{DS0}=42\text{V}$ AND $I_{DS0}=50\text{MA/MM}$	104
FIGURE 113 : CONTOUR OF MAX PAE - MEAS. VS MODEL 8X250 μM	105
FIGURE 114 : CONTOUR OF OPT POUT @ 3DB - MEAS. VS MODEL 8X250 μM	105
FIGURE 115 : 8X250 μM TRANSISTOR MODEL VALIDATION. LOADPULL SIMULATIONS / MEASUREMENTS COMPARISON. $V_{DS0}=42\text{V}$ AND $I_{DS0}=50\text{MA/MM}$	106
FIGURE 116 : SMA REFERENCE PLANE, POWER BAR N°2. POWER GAIN (DB)/ POUT(DBM) / PAE(%) OF THE POWER BAR AFTER FINAL OPTIMIZATION OF ZLOAD @ F0 AND ZLOAD@2F0.....	107
FIGURE 117 : USED POWER BAR CONFIGURATION FOR THE SIMULATION	108
FIGURE 118 : SPARAMETER COMPARISON BETWEEN SIMULATIONS AND MEASUREMENTS FOR POWER BAR JIG_TEST_BARRETTE_N1	109
FIGURE 119 : POUT VS PIN AND DC CURRENT VS PIN. COMPARISON BETWEEN SIMULATION AND MEASUREMENTS FOR POWER BAR N2	109
FIGURE 120 : INPUT REFLEXION COEFFICIENT / PAE / GP / AMPM VERSUS PIN. COMPARISON BETWEEN SIMULATION AND MEASUREMENTS FOR POWERBAR N2.....	110
FIGURE 121 : 8X250 μM TRANSISTOR PERFORMANCE AFTER HARMONICS LOADPULL OPTIMIZATION	112
FIGURE 122 : ADS SCHEMATIC OF THE GH50 8X8X250 μM POWERBAR BASED ON AMCAD TRANSISTOR MODEL.....	113
FIGURE 123 : ADS SCHEMATIC VIEW OF THE HPA-1 MODULE RUN-2	114
FIGURE 124 : HFSS SCHEMATIC VIEW OF THE HPA-1 MODULE RUN-2.....	114
FIGURE 125 : HPA-1 MODULE. RUN-2. SIMULATED S-PARAMETERS WIDE FREQUENCY BAND ANALYSIS	115
FIGURE 126 : HPA-1 MODULE. RUN-2. SIMULATED S-PARAMETERS IN-BAND FREQUENCY ANALYSIS	115
FIGURE 127 : HPA-1 MODULE. RUN-2. SIMULATED PERFORMANCES. POUT(W), PAE(%), GAIN(DB) VERSUS INPUT POWER (DBM) AND FREQUENCY(GHZ).	116
FIGURE 128 : HPA-1 MODULE. RUN-2. SIMULATED PERFORMANCES. POWER DENSITY (W/MM) VS. INPUT POWER(DBM) – FROM 1.50 TO 1.58GHZ	116
FIGURE 129 : HPA-1 MODULE. RUN-2. SIMULATED PERFORMANCES. DRAIN CURRENT AND POWER CONSUMPTION(W) VS. INPUT POWER(DBM) – FROM 1.50 TO 1.58GHZ	117
FIGURE 130 : HPA-1 MODULE. RUN-2. SIMULATED PERFORMANCES : POUT(W), PAE(%), GAIN(DB) VERSUS TEMPERATURE [-10°C; 25°C, 85°C] @PIN(MAX PAE).	117
FIGURE 131 : HPA-1 MODULE. RUN-2. SIMULATED PERFORMANCES IN MULTI-CARRIER MODE : NPR(DB), COMPRESSION(DB), PAE(%) VERSUS PIN. $\text{TEMP}=25^{\circ}\text{C}$, $V_{DS}=40\text{V}$ AND $I_{DS}=50\text{MA/MM}$	118
FIGURE 132 : HPA-1 MODULE. RUN-2. SIMULATED PERFORMANCES IN MULTI-CARRIER MODE : NPR(DB), COMPRESSION(DB), PAE(%) VERSUS PIN. $\text{TEMP}=25^{\circ}\text{C}$, $V_{DS}=45\text{V}$ AND $I_{DS}=50\text{MA/MM}$	118
FIGURE 133 : RUN-2. HPA-1 MODULE(SN#01). [S] PARAMETERS MEASUREMENTS. $\text{RF}=[\text{DC}-10\text{GHZ}]$, $V_{D}=+40\text{V}$, FIXED DRAIN CURRENT $I_{DS}=800\text{MA}$ @ $+25^{\circ}\text{C}$, $\text{TEMP}=[-5^{\circ}\text{C}, +25^{\circ}\text{C}, +85^{\circ}\text{C}]$	120

FIGURE 134 : SN#01 MODULE. [S] PARAMETERS MEASUREMENTS. RF=[1.3-1.8GHZ], VD=+40V, FIXED DRAIN CURRENT IDS=800MA @+25°C, TEMP=[-5°C, +25°C, +85°C]	120
FIGURE 135 : RUN-2. HPA-1 MODULES. SAMPLES SN#01 SN#02 SN#03 MODULES. [S] PARAMETERS MEASUREMENTS. RF=[DC-10GHZ], VD=+40V. FIXED DRAIN CURRENT IDS=800MA @+25°C. TEMP=[-5°C, +25°C, +85°C].....	121
FIGURE 136 : RUN-2. HPA-1 MODULES. SAMPLES SN#01 SN#02 SN#03 MODULES. [S] PARAMETERS MEASUREMENTS. RF=[1.3-1.8GHZ], VD=+40V. FIXED DRAIN CURRENT IDS=800MA @+25°C. TEMP=[-5°C, +25°C, +85°C].....	121
FIGURE 137 : RUN-2. HPA-1 MODULE. SN#01 SAMPLE. POWER MEASUREMENTS WITH CW SIGNAL. TEMP=[-5°C, +25°C, +85°C], VD=+40V, ID=800MA. RF=[1,5135GHZ / 1,5385GHZ / 1,5635GHZ]. GAIN(DB), PAE(%), POUT(DBM), PHASE(DEG) VS PIN(DBM)	122
FIGURE 138 : RUN-2. HPA-1 MODULE. SN#01 MODULE. POWER MEASUREMENTS WITH CW SIGNAL. TEMP=[-5°C, +25°C, +85°C], VD=+40V, ID=800MA. GAIN(DB), PAE(%), POUT(DBM), PHASE(DEG) VS RFFREQ(GHZ) @PAE_MAX.	123
FIGURE 139 : RUN-2. HPA-1 MODULE. SN#01. SYNTHESIS OF POWER MEASUREMENTS WITH CW SIGNAL. TEMP=[-5°C, +25°C, +85°C], VD=+40V, ID=800MA. GAIN(DB), PAE(%), POUT(DBM), PHASE(DEG) VS RFFREQ(GHZ) @PAE_MAX	123
FIGURE 140 : RUN-2. HPA-1 MODULE. SN#02. SYNTHESIS OF POWER MEASUREMENTS WITH CW SIGNAL. TEMP=[-5°C, +25°C, +85°C], VD=+40V, ID=800MA. GAIN(DB), PAE(%), POUT(DBM), PHASE(DEG) VS RFFREQ(GHZ) @PAE_MAX	124
FIGURE 141 : RUN-2. HPA-1 MODULE. SN#03. SYNTHESIS OF POWER MEASUREMENTS WITH CW SIGNAL. TEMP=[-5°C, +25°C, +85°C], VD=+40V, ID=800MA. GAIN(DB), PAE(%), POUT(DBM), PHASE(DEG) VS RFFREQ(GHZ) @PAE_MAX	124
FIGURE 142 : RUN-2. HPA-1 MODULE. SN#02 POWER MEASUREMENTS WITH MULTI-CARRIER SIGNAL. TEMP=[-5°C, +25°C, +85°C]. VDS=40V, RF=1,5385GHZ, GAIN(DB), PAE(%), NPR(DB) VS POUT(DBM).....	125
FIGURE 143 : RUN-2. HPA-1 MODULE. SN#02 MODULE. SYNTHESIS OF POWER MEASUREMENTS WITH MULTI-CARRIER SIGNAL. TEMP=[-20°C, +25°C, +90°C]. VDS=40V,	125
FIGURE 144 : RUN-2. HPA-1 MODULE. SN#04 POWER MEASUREMENTS WITH MULTI-CARRIER SIGNAL. TEMP=[-5°C, +25°C, +85°C]. VDS=40V, RF=1,5385GHZ, GAIN(DB), PAE(%), NPR(DB) VS POUT(DBM).....	126
FIGURE 145 : : RUN-2. HPA-1 MODULE. SN#04 MODULE. SYNTHESIS OF POWER MEASUREMENTS WITH MULTI-CARRIER SIGNAL. TEMP=[-20°C, +25°C, +90°C]. VDS=40V,.....	126
FIGURE 146 : MULTI-CARRIER TEST BENCH.....	128
FIGURE 147 : PHOTOGRAPHY OF THE CW TEST BENCH FOR CW INITIAL/INTERMEDIATE AND FINAL MEASUREMENTS	128
FIGURE 148: DETECTOR CHARACTERIZATION : DETECTED VOLTAGE VALUE (MV) VERSUS POWER RANGE(DBM).....	129
FIGURE 149 : HPA-1 MODULE RUN-2 (#4). RF STEP STRESS MEASUREMENT. INPUT POWER AND OUTPUT POWER MONITORING DURING 5DBC COMPRESSION STEP	130
FIGURE 150 : HPA-1 RUN-2 MODULE (#4). RF STEP STRESS MEASUREMENT (5DBC STEP). DRAIN VOLTAGE DRIFT(V). DRAIN CURRENT DRIFT (MA).	130
FIGURE 151 : HPA-1 RUN-2 MODULE (#4). RF STEP STRESS MEASUREMENT (5DBC STEP). GATE VOLTAGE DRIFT (V) & GATE CURRENT DRIFT (MA).	131
FIGURE 152 : HPA-1 RUN-2 MODULE #4. AMAM AND AMPM CHARACTERIZATION IN CW MODE AFTER EACH COMPRESSION STEP OF THE RF STEP STRESS MEASUREMENTS.....	132
FIGURE 153 : HPA-1 RUN-2 MODULE #4. [S] PARAMETERS MEASUREMENTS AFTER EACH COMPRESSION STEP OF THE RF STEP STRESS MEASUREMENTS.....	133
FIGURE 154 : HPA-1 RUN-2 MODULE #4. STATIC MEASUREMENTS AFTER EACH COMPRESSION STEP OF THE RF STEP STRESS MEASUREMENTS	133

FIGURE 155 : LOADPULL SIMULATION OF GH25 8X125 μ M TRANSISTORS	137
FIGURE 156 : PRELIMINARY TOPOLOGY OF THE GH25 HPA-2	137
FIGURE 157 : PERFORMANCE VERSUS PIN IN CW MODE OF THE GH25 HPA-2. VDS=22,5V, RFFREQ=12.5GHZ	138
FIGURE 158 : LAYOUT OF THE KU-BAND HERMETIC PACKAGE INCLUDING PRELIMINARY MMIC HPA-2	139
FIGURE 159 : DESCRIPTION OF THE THERMAL STACK USED FOR THERMAL SIMULATION: BASEPLATE MATERIAL OF THE PACKAGE: CUW	140
FIGURE 160 : 8X125 μ M TRANSISTOR THERMAL SIMULATIONS	141
FIGURE 161 : 8X8X125 μ M TRANSISTOR THERMAL SIMULATIONS	142
FIGURE 162 : THERMAL STUDY OF THE PACKAGING	143
FIGURE 163 : AMCAD I(V) AND [S] TEST BENCH FOR TRANSISTORS CHARACTERIZATIONS	145
FIGURE 164 : TYPICAL TIMINGS (DC BIAS / RF) USED FOR PULSED MEASUREMENTS	145
FIGURE 165 : OUTPUT CURRENT WITH DIFFERENT CHUCK TEMPERATURE (25°C, 60°C, 100°C), TRANSISTOR 8X125 GH25 MEASUREMENTS (BIAS POINTS VDS0=0V, VGS0=0V)	146
FIGURE 166 : OUTPUT CURRENT WITH DIFFERENT CHUCK TEMPERATURE (25°C, 60°C,100°C), TRANSISTOR 8X125 GH25 MEASUREMENTS (BIAS POINTS VDS0=27V, IDS0=50MA)	146
FIGURE 167 : HIGHLIGHTED PHENOMENA TRAPS	146
FIGURE 168 : OUTPUT CURRENT, QUIESCENT BIAS: (27V, 50MA), (CHUCK TEMPERATURE = 25°C), TRANSISTOR 8X125 GH25	147
FIGURE 169 : MAXIMUM GAIN @ VDS0=27V, IDS0=50MA	147
FIGURE 170 : AMCAD VNA-BASED LOAD-PULL SYSTEM	147
FIGURE 171 : 8X125 μ M PERFORMANCE AT 12.5GHZ AFTER LOADPULL OPTIMIZATION	148
FIGURE 172 : SAMPLE DISPERSION FOR OPTIMAL PAE LOAD IMPEDANCES @ 12.5GHZ (VDS=27V, 50MA)	149
FIGURE 173 : SYNTHESIS OF SAMPLE DISPERSION FOR OPTIMAL PAE LOAD IMPEDANCES @ 12.5GHZ (VDS=27V, 40MA)	149
FIGURE 174 : 3 PORTS TRANSISTOR MODEL	150
FIGURE 175 : MEAS. VS MODEL 8X125MM @ 25°C	150
FIGURE 176 : THERMAL RESISTANCE EXTRACTION FOR 8X125MM	150
FIGURE 177 : MEAS. VS MODEL 8X125MM @ 60°C	151
FIGURE 178 : [S] PARAMETER MEAS. VS MODEL 8X125MM @ 25°C	151
FIGURE 179 : CONTOUR OF MAX PAE - MEAS. VS MODEL 8X125MM	152
FIGURE 180 : GAMMA_IN / IRL / POUT / PAE - MEAS. VS MODEL 8X125MM	152
FIGURE 181 : POWER GAIN / AM-PM / ID - MEAS. VS MODEL 8X125MM	153
FIGURE 182 : HPA-2 MODULE. AMPLIFIER TOPOLOGY	155
FIGURE 183 : HPA-2 MODULE. MMIC CIRCUIT LAYOUT	155
FIGURE 184 : FINAL LOAD-PULL OPTIMIZATION RESULTS	157
FIGURE 185 : S-PARAMETERS SIMULATION (S21, S11, S22) AT ROOM TEMPERATURE	157
FIGURE 186 : HPA-2 MODULE. SIMULATION RESULTS. OUTPUT POWER, POWER GAIN AND PAE PERFORMANCES	158
FIGURE 187 : PAE OF STAGE 1 & 2 VERSUS INPUT POWER	159
FIGURE 188 : TRANSISTOR LOAD-CYCLE AT 11.5GHZ, 12.25GHZ AND 13GHZ (PIN = 28DBM), STAGE 1 & 2	160
FIGURE 189 : DC CURRENT AND POWER CONSUMPTION	160

FIGURE 190 : DOHERTY MMIC HPA MODULE. TOPOLOGY	161
FIGURE 191 : DOHERTY MMIC HPA MODULE. MMIC CIRCUIT LAYOUT	162
FIGURE 192 : LOAD PULL 8X125UM @12.2GHZ @130MA/MM AS CARRIER TRANSISTOR.....	162
FIGURE 193 : LOAD PULL @12.2GHZ @0MA/MM AS PEAKING TRANSISTOR.....	163
FIGURE 194 : S PARAMETERS SIMULATION OF MMIC DOHERTY HPA MODULE	163
FIGURE 195 : COMPARISON BETWEEN DOHERTY AND A CLASSICAL 20W HPA REGARDING PAE PARAMETER	164
FIGURE 196 : MMIC DOHERTY HPA MODULE. PERFORMANCE OVER FREQUENCY FOR TWO DIFFERENT INPUT POWER	164
FIGURE 197 : 2ND STAGE TRANSISTOR LOAD PIN -7 TO 29.5DBM FREQ 11.5 TO 13 GHZ.....	165
FIGURE 198 : MMIC DOHERTY HPA MODULE. NL SIMULATION VERSUS PIN AT 12.25 GHZ	165
FIGURE 199 : MMIC DOHERTY HPA MODULE. PERFORMANCE VERSUS VG PEAKING.....	166
FIGURE 200 : MMIC-HYBRID DOHERTY HPA MODULE. CONFIGURATION USING TWO MMIC TEST CELLS.	166
FIGURE 201 : LOAD PULL SIMULATION AND CARRIER AMPLIFIER	167
FIGURE 202 : LOAD PULL SIMULATION AND PEAKING AMPLIFIER	168
FIGURE 203 : S PARAMETERS SIMULATION OF MMIC-HYBRID DOHERTY HPA	169
FIGURE 204 : COMPARISON BETWEEN DOHERTY AND A CLASSICAL 20W HPA REGARDING PAE PARAMETER	169
FIGURE 205 : MMIC-HYBRID DOHERTY HPA MODULE. PERFORMANCE OVER FREQUENCY FOR DIFFERENT INPUT POWER	170
FIGURE 206 : MMIC-HYBRID DOHERTY HPA MODULE. 2ND STAGE TRANSISTOR OUTPUT LOAD FOR PIN=[-7 TO 30DBM]. FREQ=[11.5 TO 13 GHZ].....	170
FIGURE 207 : MMIC-HYBRID DOHERTY HPA MODULE. AMPLIFIER (CARRIER & PEAKING) LOADS FOR PIN=[-7 TO 30DBM]. FREQ 12.25 GHZ.....	171
FIGURE 208 : PCM RESULTS OF GH25 WAFER.....	172
FIGURE 209 : HPA-2 MMIC ON WAFER-MEASUREMENT. [S] PARAMETER MEASUREMENTS AND SIMULATION.....	173
FIGURE 210 : HPA-2 MMIC ON WAFER-MEASUREMENT. POWER MEASUREMENTS. POUT AND PAE VS PIN AT 12,25 GHZ	174
FIGURE 211: HPA-2 MMIC ON WAFER-MEASUREMENT. POWER MEASUREMENTS. POUT AND PAE VS FREQ AT PIN=27 DBM	174
FIGURE 212 : DOHERTY HPA MMIC ON WAFER-MEASUREMENT. [S] PARAMETER MEASUREMENTS AND SIMULATION	175
FIGURE 213 : DOHERTY HPA MMIC ON WAFER-MEASUREMENT. POWER MEASUREMENTS. POUT AND PAE VS PIN AT 12,25 GHZ	175
FIGURE 214 : DOHERTY HPA MMIC ON WAFER-MEASUREMENT. POUT & PAE VS FREQ MEASUREMENTS AND SIMULATION AT PIN=20&30 DBM	176
FIGURE 215 : PHOTOGRAPHY OF HPA-2 MODULES AND DOHERTY HPA MODULES	177
FIGURE 216 : HPA-2 #1 MODULE. [S] PARAMETERS MEASUREMENTS. RF=[DC-20GHZ], VD=30V, FIXED DRAIN CURRENT IDS=450MA @25°C, TEMP=[-10°C, 25°C, 85°C].....	178
FIGURE 217 : HPA-2 #1 MODULE. [S] PARAMETERS MEASUREMENTS. RF=[10-14GHZ], VD=30V, FIXED DRAIN CURRENT IDS=450MA @25°C, TEMP=[-10°C, 25°C, 85°C].....	179
FIGURE 218 : HPA-2 #1 HPA-2 #2 HPA-2 #3 HPA-2 #4 MODULES. [S] PARAMETERS MEASUREMENTS. RF=[DC-20 GHZ], VD=30 V. FIXED DRAIN CURRENT IDS=450MA @25°C. TEMP=[-10°C, 25°C, 85°C].....	179
FIGURE 219 : HPA-2 #1 HPA-2 #2 HPA-2 #3 HPA-2 #4 MODULES. [S] PARAMETERS MEASUREMENTS. RF=[10- 14GHZ], VD=30 V, FIXED DRAIN CURRENT IDS=450MA @25°C. TEMP=[-10°C, 25°C, 85°C].	180

FIGURE 220: HPA-2 #1 MODULE. POWER MEASUREMENTS WITH CW SIGNAL. TEMP=[-10°C, 25°C, 85°C], VD=30 V, ID=450MA. RF=[11,5 GHZ TO 13 GHZ]. GAIN(DB), PAE(%), POUT(DBM), PHASE(DEG) VS PIN(DBM).....	181
FIGURE 221 : HPA-2 #1 MODULE. POWER MEASUREMENTS WITH CW SIGNAL. TEMP=[-10°C, 25°C, 85°C], VD=30 V, ID=450MA. GAIN(DB), PAE(%), POUT(DBM), PHASE(DEG) VS RFFREQ(GHZ) @PAE_MAX.....	181
FIGURE 222 : HPA-2 #1 MODULE. POWER MEASUREMENTS WITH MULTI-CARRIER SIGNAL. TEMP=[-10°C, 25°C, 85°C]. VDS=30V, RF=12GHZ, SPAN=1GHZ, 3000 CARRIERS, 1% NOTCH. GAIN(DB), PAE(%), NPR(DB), POUT(DBM) VS PIN(DBM).....	183
FIGURE 223 : KU-BAND MULTI-CARRIER TEST BENCH	186
FIGURE 224 : PHOTOGRAPHS OF THE KU-BAND MULTI-CARRIER TEST BENCH	186
FIGURE 225 : NOISE SIGNAL LEVEL AT DIFFERENT POINT OF THE TEST BENCH	187
FIGURE 226 : PHOTOGRAPHY OF THE CW TEST BENCH FOR CW INITIAL/INTERMEDIATE AND FINAL MEASUREMENTS	187
FIGURE 227 : DETECTOR CHARACTERIZATION : DETECTED VOLTAGE VALUE (MV) VERSUS POWER RANGE(DBM).....	188
FIGURE 228 : HPA-2 MODULE (#2). RF STEP STRESS MEASUREMENT. MONITORING OF POUT DRIFT (DETECTED VOLTAGE IN V) DURING 8DBC COMPRESSION STEP.....	188
FIGURE 229 : HPA-2 MODULE (#2). RF STEP STRESS MEASUREMENT. MONITORING OF GATE CURRENT DRIFT DURING 8DBC COMPRESSION STEP	189
FIGURE 230 : HPA-2 MODULE (#2). RF STEP STRESS MEASUREMENT. MONITORING OF DRAIN CURRENT DRIFT DURING 8DBC COMPRESSION STEP	189
FIGURE 231 : HPA-2 MODULE #2. AMAM CHARACTERIZATION IN CW MODE AFTER EACH COMPRESSION STEP OF THE RF STEP STRESS MEASUREMENTS.....	190
FIGURE 232 : HPA-2 MODULE #2. [S] PARAMETERS MEASUREMENTS AFTER EACH COMPRESSION STEP OF THE RF STEP STRESS MEASUREMENTS	191
FIGURE 233 : HPA-2 MODULE #2 STATIC MEASUREMENTS AFTER EACH COMPRESSION STEP OF THE RF STEP STRESS MEASUREMENTS.....	191
FIGURE 234 : MMIC DOHERTY HPA MODULE #1 (FULL MMIC). [S] PARAMETERS MEASUREMENTS. RF=[DC-20GHZ], VD=30V. FIXED IDS_CARRIER=400MA (80MA/MM) AND FIXED IDS_PEAKING=100MA (20MA/MM) @25°C, TEMP=[-10°C, 25°C, 85°C]	192
FIGURE 235 : MMIC DOHERTY HPA MODULE #1 (FULL MMIC). [S] PARAMETERS MEASUREMENTS. RF=[10-14GHZ], VDS=30V. FIXED IDS_CARRIER=400MA (80MA/MM) AND FIXED IDS_PEAKING=100MA (20MA/MM) @25°C, TEMP=[-10°C, 25°C, 85°C]	192
FIGURE 236 : 3X MMIC DOHERTY HPA MODULE (FULL MMIC). [S] PARAMETERS MEASUREMENTS. RF=[DC-20 GHZ]. VDS=30V. FIXED IDS_CARRIER=400MA (80MA/MM) AND FIXED IDS_PEAKING=100MA (20MA/MM) @25°C, TEMP=[-10°C, 25°C, 85°C]	193
FIGURE 237 : 3X MMIC DOHERTY HPA MODULE (FULL MMIC). [S] PARAMETERS MEASUREMENTS. RF=[10-14 GHZ]. VDS=30V. FIXED IDS_CARRIER=400MA (80MA/MM) AND FIXED IDS_PEAKING=100MA (20MA/MM) @25°C, TEMP=[-10°C, 25°C, 85°C]	193
FIGURE 238 : MMIC DOHERTY HPA MODULE#1 (FULL MMIC). POWER MEASUREMENTS WITH CW SIGNAL. VDS=30V. FIXED IDS_CARRIER=400MA (80MA/MM) AND FIXED IDS_PEAKING=100MA (20MA/MM) @25°C. TEMP=[-10°C, 25°C, 85°C]. RF=[11,5 GHZ TO 13 GHZ]. GAIN(DB), PAE(%), POUT(DBM), PHASE(DEG) VS PIN(DBM).....	194
FIGURE 239 : MMIC DOHERTY HPA MODULE#1 (FULL MMIC). POWER MEASUREMENTS WITH CW SIGNAL. TEMP=[-10°C, 25°C, 85°C]. VDS=30V. FIXED IDS_CARRIER=400MA (80MA/MM) AND FIXED IDS_PEAKING=100MA (20MA/MM) @25°C. GAIN(DB), PAE(%), POUT(DBM), PHASE(DEG) VS RFFREQ(GHZ) @PAE_MAX.	195
FIGURE 240 : MMIC DOHERTY HPA MODULE#1 (FULL MMIC). SYNTHESIS OF POWER MEASUREMENTS WITH CW SIGNAL. TEMP=[-10°C, 25°C, 85°C], VDS=30V. FIXED IDS_CARRIER=400MA (80MA/MM) AND FIXED	

IDS_PEAKING=100MA (20MA/MM) @25°C. GAIN(DB), PAE(%), POUT(DBM), PHASE(DEG) VS RFFREQ(GHZ) @PAE_MAX	195
FIGURE 241 : MMIC DOHERTY HPA MODULE#2 (FULL MMIC). SYNTHESIS OF POWER MEASUREMENTS WITH CW SIGNAL. TEMP=[-10°C, 25°C, 85°C], VDS=30V. FIXED IDS_CARRIER=400MA (80MA/MM) AND FIXED IDS_PEAKING=100MA (20MA/MM) @25°C. GAIN(DB), PAE(%), POUT(DBM), PHASE(DEG) VS RFFREQ(GHZ) @PAE_MAX	196
FIGURE 242 : MMIC DOHERTY HPA MODULE#3 (FULL MMIC). SYNTHESIS OF POWER MEASUREMENTS WITH CW SIGNAL. VDS=30V. FIXED IDS_CARRIER=400MA (80MA/MM) AND FIXED IDS_PEAKING=100MA (20MA/MM) @25°C. GAIN(DB), PAE(%), POUT(DBM), PHASE(DEG) VS RFFREQ(GHZ) @PAE_MAX.....	196
FIGURE 243 : MMIC DOHERTY HPA MODULE#1 (FULL MMIC). OPTIMIZATION OF THE BIASING POINT. MULTI-CARRIER MEASUREMENTS. TEMP=25°C.....	197
FIGURE 244 : DOHERTY HPA MODULE#1 (FULL MMIC). POWER MEASUREMENTS WITH MULTI-CARRIER SIGNAL. TEMP=[-10°C, 25°C, 85°C]. VDS=30V, RF=12GHZ, SPAN=1GHZ, 3000 CARRIERS, 1% NOTCH. GAIN(DB), PAE(%), NPR(DB), POUT(DBM) VS PIN(DBM).....	197
FIGURE 245 : DOHERTY HPA MODULE#1 (FULL MMIC). SYNTHESIS OF POWER MEASUREMENTS WITH MULTI-CARRIER SIGNAL. TEMP=[-10°C, +25°C, +85°C]. VDS=30V, RF=12GHZ, SPAN=1GHZ, 3000 CARRIERS, 1% NOTCH.	198
FIGURE 246 : DOHERTY HPA MODULE#2 (FULL MMIC). SYNTHESIS OF POWER MEASUREMENTS WITH MULTI-CARRIER SIGNAL. TEMP=[-10°C, +25°C, +85°C]. VDS=30V, RF=12GHZ, SPAN=1GHZ, 3000 CARRIERS, 1% NOTCH.	198
FIGURE 247 : DOHERTY HPA MODULE#3 (FULL MMIC). SYNTHESIS OF POWER MEASUREMENTS WITH MULTI-CARRIER SIGNAL. TEMP=[-10°C, +25°C, +85°C]. VDS=30V, RF=12GHZ, SPAN=1GHZ, 3000 CARRIERS, 1% NOTCH.	198

LIST OF TABLES

TABLE 1 : INITIAL L-BAND SSPA EQUIPMENT, RF ANALYSIS SYNTHESIS.....	20
TABLE 2 : INITIAL KU-BAND SSPA EQUIPMENT, RF ANALYSIS SYNTHESIS.....	23
TABLE 3 : HPA-1 REQUIRED PERFORMANCES.....	26
TABLE 4 : MATERIALS TABLE CONSIDERED FOR THE HPA (INPUT AND OUTPUT NETWORK).....	29
TABLE 5 : POWER BARS COMBINATIONS CONSIDERED AS BACKUP SOLUTIONS.....	32
TABLE 6 : LINEAR THERMAL PROPERTIES OF THE MATERIALS.....	34
TABLE 7 : MAXIMUM TEMPERATURE (°C) FOR VARIOUS BASEPLATE TEMPERATURES AND DISSIPATED POWER.....	35
TABLE 8 : SUMMARY OF PERFORMANCE MONITORED DURING LOADPULL MEASUREMENTS. VDS=40V AND IDS=25MA/MM.....	46
TABLE 9 : SUMMARY OF PERFORMANCE MONITORED DURING LOADPULL MEASUREMENTS. VDS=40V AND IDS=50MA/MM.....	46
TABLE 10 : SUMMARY OF PERFORMANCE MONITORED DURING LOADPULL MEASUREMENTS. VDS=40V AND IDS=75MA/MM.....	46
TABLE 11 : HPA PERFORMANCES IN MULTICARRIER MODE @NPR=15DB. TEMP=25°C. VDS=40V, IDS=25MA/MM.....	67
TABLE 12 : HPA PERFORMANCES IN MULTICARRIER MODE @NPR=15DB. TEMP=25°C. VDS=45V, IDS=30MA/MM.....	67
TABLE 13 : SUMMARY OF SIMULATED CW PERFORMANCES AT HPA LEVEL.....	68
TABLE 14 : SUMMARY OF SIMULATED MULTI-CARRIERS PERFORMANCES AT HPA LEVEL.....	68
TABLE 15 : HPA-1 MODULE (#2). SYNTHESIS OF POWER MEASUREMENTS WITH CW SIGNAL. TEMP=[-20°C, 25°C, 90°C], VD=40V & VD=45V, ID=400MA. GAIN(DB), PAE(%), POUT(DBM), PHASE(DEG) VS RFFREQ(GHZ) @PAE_MAX.....	73
TABLE 16 : HPA-1 MODULE (#3). SYNTHESIS OF POWER MEASUREMENTS WITH CW SIGNAL. TEMP=[-20°C, 25°C, 90°C], VD=40V & VD=45V, ID=400MA. GAIN(DB), PAE(%), POUT(DBM), PHASE(DEG) VS RFFREQ(GHZ) @PAE_MAX.....	74
TABLE 17 : HPA-1 MODULE (#5). SYNTHESIS OF POWER MEASUREMENTS WITH CW SIGNAL. TEMP=[-20°C, 25°C, 90°C], VD=40V & VD=45V, ID=400MA. GAIN(DB), PAE(%), POUT(DBM), PHASE(DEG) VS RFFREQ(GHZ) @PAE_MAX.....	74
TABLE 18 : TEST PLAN FOR RF STEP STRESS MEASUREMENTS OF L-BAND GH50 HPA-1 MODULE.....	78
TABLE 19 : SUMMARY OF PERFORMANCE MONITORED DURING LOADPULL MEASUREMENTS. VDS=42V AND IDS=50MA/MM.....	101
TABLE 20 : MONITORING OF THE UMS 0.5 MM GAN PROCESS EVOLUTION. DRAIN-LAG AND GATE-LAG.....	111
TABLE 21 : HPA-1 MODULE. NEW REQUIRED PERFORMANCES FOR RUN-2.....	112
TABLE 22 : 8X250µM TRANSISTOR PERFORMANCE AFTER HARMONICS LOADPULL OPTIMIZATION.....	113
TABLE 23 : SUMMARY OF SIMULATED MULTI-CARRIERS PERFORMANCES AT HPA-1 MODULE. RUN-2. VD=450V AND VD=45V.....	119
TABLE 24 : TEST PLAN FOR RF STEP STRESS MEASUREMENTS OF L-BAND GH50 HPA-1 MODULE.....	127
TABLE 24 : HPA-2 SPECIFICATIONS (INITIAL VERSION FROM ESA PROPOSAL).....	135
TABLE 25 : NEW HPA-2 SPECIFICATIONS AFTER CCN.....	135
TABLE 26 : PERFORMANCE IN MULTI-CARRIER MODE OF THE GH25 HPA-2. VDS=22,5V, RFFREQ=12,5GHZ.....	138

TABLE 27 : GH25 8X125 μ M TRANSISTOR. THERMAL RESISTANCE($^{\circ}$ C/W) FOR VARIOUS BASE PLATE TEMPERATURES AND DISSIPATED POWER.	140
TABLE 28 : GH25 8X8X125 μ M POWER-BAR. THERMAL RESISTANCE($^{\circ}$ C/W) FOR VARIOUS BASE PLATE TEMPERATURES AND DISSIPATED POWER.	141
TABLE 29 : 8X125 μ M PERFORMANCE AT 12.5GHZ AFTER LOADPULL OPTIMIZATION	148
TABLE 30 : SPECIFICATIONS OF THE HPA-2 MODULE AND DOHERTY HPA MODULES.....	154
TABLE 31 : HPA-2 MMIC ON WAFER-MEASUREMENTS. TEST CONDITIONS	173
TABLE 32 : DOHERTY HPA MMIC ON WAFER-MEASUREMENTS. TEST CONDITIONS	174
TABLE 33 : HPA-2 #1 MODULE. SYNTHESIS OF POWER MEASUREMENTS WITH CW SIGNAL. TEMP=[-10 $^{\circ}$ C, 25 $^{\circ}$ C, 85 $^{\circ}$ C], VD=30V, ID=450MA. GAIN(DB), PAE(%), POUT(DBM), PHASE(DEG) VS RFFREQ(GHZ) @PAE_MAX	182
TABLE 34 : HPA-2 #2 MODULE. SYNTHESIS OF POWER MEASUREMENTS WITH CW SIGNAL. TEMP=[-10 $^{\circ}$ C, 25 $^{\circ}$ C, 85 $^{\circ}$ C], VD=30V, ID=450MA. GAIN(DB), PAE(%), POUT(DBM), PHASE(DEG) VS RFFREQ(GHZ) @PAE_MAX	182
TABLE 35 : HPA-2 #3 MODULE. SYNTHESIS OF POWER MEASUREMENTS WITH CW SIGNAL. TEMP=[-10 $^{\circ}$ C, 25 $^{\circ}$ C, 85 $^{\circ}$ C], VD=30V, ID=450MA. GAIN(DB), PAE(%), POUT(DBM), PHASE(DEG) VS RFFREQ(GHZ) @PAE_MAX	183
TABLE 36 : HPA-2 #4 MODULE. SYNTHESIS OF POWER MEASUREMENTS WITH CW SIGNAL. TEMP=[-10 $^{\circ}$ C, 25 $^{\circ}$ C, 85 $^{\circ}$ C], VD=30V, ID=450MA. GAIN(DB), PAE(%), POUT(DBM), PHASE(DEG) VS RFFREQ(GHZ) @PAE_MAX	183
TABLE 37 : HPA-2 #1 MODULE. SYNTHESIS OF POWER MEASUREMENTS WITH MULTI-CARRIER SIGNAL. TEMP=[-10 $^{\circ}$ C, +25 $^{\circ}$ C, +85 $^{\circ}$ C]. VDS=30V, RF=12GHZ, SPAN=1GHZ, 3000 CARRIERS, 1% NOTCH	184
TABLE 38 : HPA-2 #2 MODULE. SYNTHESIS OF POWER MEASUREMENTS WITH MULTI-CARRIER SIGNAL. TEMP=[-10 $^{\circ}$ C, +25 $^{\circ}$ C, +85 $^{\circ}$ C]. VDS=30V, RF=12GHZ, SPAN=1GHZ, 3000 CARRIERS, 1% NOTCH.	184
TABLE 39 : HPA-2 #3 MODULE. SYNTHESIS OF POWER MEASUREMENTS WITH MULTI-CARRIER SIGNAL. TEMP=[-10 $^{\circ}$ C, +25 $^{\circ}$ C, +85 $^{\circ}$ C]. VDS=30V, RF=12GHZ, SPAN=1GHZ, 3000 CARRIERS, 1% NOTCH.	184
TABLE 40 : HPA-2 #4 MODULE. SYNTHESIS OF POWER MEASUREMENTS WITH MULTI-CARRIER SIGNAL. TEMP=[-10 $^{\circ}$ C, +25 $^{\circ}$ C, +85 $^{\circ}$ C]. VDS=30V, RF=12GHZ, SPAN=1GHZ, 3000 CARRIERS, 1% NOTCH	185
TABLE 41 : TEST PLAN FOR RF STEP STRESS MEASUREMENTS OF KU-BAND GH25 HPA-2 MODULE.....	185
TABLE 42 : COMPARISON RESULTS BETWEEN HPA-2 MODULE AND MMIC DOHERTY HPA MODULE.....	199
TABLE 43 : TRADE-OFF GAAS SSPA VS GAN SSPA (USING HPA-1 MODULE) VS TWTA	201
TABLE 44 : CURRENT COMPARISON BETWEEN KU-BAND A LC-TWTA AND A LC-SSPA BASED ON THE GH25 GAN TECHNOLOGY ASSOCIATED TO THE SPACE COMBINER TECHNIQUE.....	203

1. SSPA FOR FUTURE SPACEBORNE TELECOM APPLICATIONS

1.1 Survey on the Market Trends for L/S-band Telecom application

In order to identify the optimal target with regard to the market needs, TAS has realized a market trends survey for telecom applications in L/S-band.

This survey has been conducted in collaboration with the Telecom Business Line and the SSPA product line.

Two power amplifier families for L/S-band Telecom market have been identified:

- **Mobile Satellite Service (MSS) Market:**
 - Considered as market of opportunities with high quantities of SSPAs (GB2, Inmarsat) and Medium power requirements [25W-40W] in CW mode.
 - In 2014, a prediction on the power requirements would be: [50W-60W] in CW mode.
 - Only one hybrid HPA GaN module will be required for the last output stage of the SSPA to fulfil the specifications.
- **Fixed Service Satellite (FSS) & Data Relay Market:**
 - Considered as stabilized market with limited quantities and high power requirements [25W-85W] in CW mode.
 - In 2014, a prediction on the power requirements would be: [110W-130W] in CW mode.
 - Two to three GaN HPA hybrid modules for the last output stage of the SSPA will be required to fulfil the specifications.

Based on the design of the GH50 hybrid HPA module from WP3100 (baseline design), TAS would be able to address both demands:

- 1x HPA module would be used in the SSPA for the future MSS market.
- 2x HPA modules would be used in the SSPA for the future FSS market.

The introduction of the UMS GaN technology in the future L/S-band SSPA equipments will allow to solve the problem of ITAR restrictions. Thanks to this new GaN SSPA equipment, TAS should increase its market share concerning the L/S-band SSPA for Telecom applications.

To conclude: a 30W multi-carrier L-band SSPA equipment based on a single GaN HPA module is the optimal target with regard to the market need, the RF performance (PAE) and the competitiveness.

1.2 Initial L-Band SSPA equipment analysis based on L-Band GH50 Hybrid HPA module performance

This task has been dedicated to:

- Provide electrical analysis at equipment level of a L-band SSPA using GaAs and GaN Technologies
 - Three L-band SSPA equipment have been studied:
 - “Globalstar2” (GB2) L/S-band SSPA
 - 30W L/S-band SSPA using 2 GaAs hybrid HPA modules
 - 30W L-band SSPA using a single GaN hybrid HPA module designed in WP3100
 - Based on the previous analysis on 30W L-band SSPA equipments (GaAs and GaN), the following aspects have been quantified:
 - Targets for efficiency improvement
 - Targets for DC power consumption reduction and dissipated power reduction
- Provide a preliminary design at equipment level of these SSPA
 - Preliminary mechanical design has been performed on:
 - A 30W L/S-band SSPA using 2 GaAs hybrid HPA modules
 - A 30W L-band SSPA using a single GaN hybrid HPA module designed in WP3100
 - Based on these mechanical designs, following aspects have been quantified:
 - Targets for mass reduction and impact expected
 - Targets for cost reduction including ease of tuning, reduction of number of modules etc...
- Provide thermal analysis on the L-band SSPA preliminary design using GaN technology. The following aspect has been quantified:
 - Operation at a higher base-plate temperature (e.g. 85 to 100deg for a qualification temperature instead of 65deg as proposed today)
- Identify the critical areas related to the usage of the selected GaN technology.

The synthesis of the RF analysis done on L/S-band SSPAs is presented below.

	30W L/S-band SSPA using 2 GaAs HPA modules	30W L/S-band SSPA using GaN
Topology of the SSPA output section		
Performances in CW mode of the MLA module	@Maximum PAE: Pout=38,6dBm PAE=42% Gain compression=2dBc	@Maximum PAE: Pout=33,6dBm PAE=38,7% Gain compression=7dBc
Hybrid HPA module topology	1 stage with 4x14mm GaAs power bar (hypothesis)	1 stage with 1x16mm GaN power bar
Performances in CW mode of the HPA module	@ Maximum Pout: Pout=45,4dBm, PAE=57,7%, Gain compression=2dBc, Power density=0,61W/mm	Pout=44,4dBm, PAE=43,2%, Gain compression=2dBc, Power density=1,73W/mm Pout=46,6dBm, PAE=54,7%, Gain compression=3dBc, Power density=2,88W/mm @Max output power & PAE: Pout=47,9dBm, PAE=63%, Gain compression=5,1dBc, Power density=3,91W/mm
Performances in multi-carrier mode of the HPA module	Pout=42,78dBm (19W) NPR=15dB PAE=48,7% Gain compression=1,26dBc Power density= 0,33W/mm	Pout=45,2dBm (33,5W) NPR=15dB PAE=49,7% Gain compression=2,5dBc Power density= 2,09W/mm
RF performances in CW mode of the SSPA RF chain. Simulation done @Pout max	Pout=47,74dBm(59,4W) PAE=48,8% Gain compression=3,3dBc	Pout=47,77dBm (58,23W) PAE=57,7% Gain compression=5,5dBc
RF performances in multi-carrier mode of the SSPA RF chain	Pout=44,85dBm (30,57W) NPR=15,1dB PAE=38,3% Gain compression=1,37dBc Pdc=79,77W Pdissp=49,2W	Pout=44,9dBm (30,9W) NPR=15,04dB PAE=43,4% (+5points versus 30W GaAs SSPA) Gain compression=3,9dBc Pdc=71,24W (-10% versus 30W GaAs SSPA) Pdissp=40,33W (-18% versus 30W GaAs SSPA)

Table 1 : Initial L-band SSPA equipment, RF analysis synthesis

Regarding a future 30W L/S-band SSPA equipment, the preliminary comparison between the two previous GaAs and GaN versions shows important improvements and points to be addressed further:

- Improvement of PAE performance: +5 points
 - Reduction of the number of HPA modules for the last power stage: 2 modules \Rightarrow 1 module
 - Suppression of combiner losses : 2 ways power combiner (0.3dB losses) \Rightarrow single HPA module (no loss)
 - PAE_RF_chain_SSPA_GaAs=38% \Rightarrow PAE_RF_chain_SSPA_GaN=43%
- Reduction of the total power consumption and the total dissipated power
 - Pdc: 80W \Rightarrow 71W (-10%)
 - Pdiss: 49W \Rightarrow 40W (-18%)
- Increase of the dissipated power at transistor level in the HPA module
 - 0,31W/mm with GaAs technology \Rightarrow 2,09W/mm with GaN technology
 - Need for an advanced packaging technology
- With a higher baseplate temperature set to +85°C a t equipment level, the GH50 Hybrid HPA module maximum temperature is 160°C
- Increase of the Gain compression level compared to the GaAs SSPA
 - 30W SSPA with 2 GaAs HPA modules: Gain compression=1,4dBc
 - 30W SSPA using GaN: Gain compression=3.9dBc

- Despite this compression level, the compromise Pout/PAE/linearity remains in favour of the GaN technology in simulation.
- Gain compression has to be confirmed by measurement at power bar level. The gain compression could be reduced by further improvements of the GaN power device technology in the near future.
- Further reliability analysis should demonstrate that this selected operating power (corresponding to the maximum of PAE) remains in the Safe Operating Area of the chosen GaN technology.
- Reduction of HPA module number (2 ⇒ 1) will allow significant improvements at SSPA equipment level in term of size, mass and cost reductions (indeed manufacturing, tuning and assembly phases will be reduced).
 - Footprint reduction : -16%
 - Mass reduction: -20%
 - Cost reduction estimation: -15% in comparison with the 30W L/S-band GaAs SSPA using 2 HPA modules.

This synthesis and the preliminary conclusion are considered as initial and are updated at the end of the study using the measured performance of the developed L-band GaN HPA module. Updated analysis and conclusions (including also comparison with LTWTA equipment) are presented in chapter 4.1

1.3 Survey on the Market Trends for Ku-Band Telecom application

In order to identify the optimal target with regard to the market needs, TAS has realized a market trends survey for applications in Ku-band.

This survey has been conducted in collaboration with the Telecom Business Line and the SSPA product line.

Two markets are identified: TX for TTC and SSPA for Telecom.

- Regarding TX for TTC applications in Ku-band, the main characteristics of the market which is targeted:
 - Required quantity: 8x equipment to be delivered per year
 - Pout>20W in CW mode
- Regarding GaN LC-SSPA for Telecom in Ku-band:
 - Objective would be to replace current LCTWTA solutions
 - Expected quantity: 200x SSPA to be delivered per year
- Regarding satellites constellation for Ku-band internet data application:
 - Pout>20W in CW mode
 - Pout=10W in multi-carrier mode at 15dB
 - Expected quantity: 900x satellites

1.4 Initial Ku-Band SSPA equipment analysis based on Ku-Band GH25 MMIC HPA module performance

This task has been be dedicated to:

- Identify the topology of a SSPA equipment for the market of active antennas at Ku band
- Provide electrical analysis at equipment level on L-band SSPA using GaAs and GaN Technology
 - Two Ku-band SSPA equipment have been studied:
 - 7W Ku-band SSPA using 2 GaAs hybrid HPA modules (MT-SAT2 equipment)
 - 7W Ku-band SSPA using single GaN hybrid HPA module (GH25 technology)
 - Based on the previous analysis on 7W Ku-band SSPA equipments (GaAs and GaN),following aspects have been quantified:
 - Targets for efficiency improvement
 - Targets for DC power consumption reduction and dissipated power reduction
- Provide a preliminary design at equipment level of Preliminary mechanical design has been realized on:
 - 7W Ku-band SSPA using single GaN hybrid HPA module
 - Based on this preliminary mechanical design and the existing design with GaAs technology ,following aspects have been quantified:
 - Targets for mass reduction and impact expected
 - Targets for cost improvement including ease of tuning, reduction of modules etc...
- Provide thermal analysis on the Ku-band SSPA preliminary design using GaN technology. Following aspects have been quantified:
 - Operations at higher base-plate temperature (e.g. 85 to 100deg for a qualification temperature as opposed to 65deg today)
- Identify the critical areas related to the usage of the selected GaN technologies.

The synthesis of the RF analysis done on Ku-band SSPAs is presented below.

	6/7W MT-SAT2 Ku-band GaAs SSPA	6/7W MTSAT2 Ku-band GaN SSPA
Topology of the SSPA output section		
Performances in CW mode of the Driver module	@Maximum PAE: Pout=34dBm PAE=37,5% Gain compression=4dBc	@Maximum PAE: Pout=28,7dBm PAE=22,3% Gain compression=4dBc
HPA module topology	2 stages hybrid HPA Stage 1: 2x4,8mm GaAs power bar Stage 2: 4x4,8mm GaAs power bar	2 stages MMIC HPA Stage 1: 4x8x75µm GaN transistors Stage 2: 8x8x100µm GaN transistor
Performances in CW mode of the HPA module	@ Maximum PAE: Pout=38,6dBm, PAE=30%, Gain compression=2dBc, Power density=0,37W/mm @ Maximum Pout: Pout=39dBm, PAE=29%, Gain compression=3dBc, Power density=0,41W/mm	Pout=31dBm, PAE=9,3%, Gain compression=2dBc Pout=33,9dBm, PAE=14,6%, Gain compression=3dBc Pout=38,5dBm, PAE=26,5%, Gain compression=5dBc @ Maximum PAE: Pout=42dBm, PAE=37%, Gain compression=8dBc, Power density=2,47W/mm @ Maximum Pout: Pout=42,5dBm, PAE=34%, Gain compression=10dBc Power density=2,77W/mm
Performances in multi-carrier mode of the HPA module	Pout=36,5dBm (4,4W) NPR=15dB, PAE=23,5% Gain compression=2dBc Power density= 0,23W/mm	Pout=39dBm (8W) NPR=15dB, PAE=28,7% Gain compression=6,5dBc Power density= 1,24W/mm
RF performances in CW mode of the SSPA RF chain.	@Maximum PAE: Pout=40,6dBm (11,48W), PAE=23,6% Gain compression=1,54dBc @Maximum Pout: Pout=41,53dBm (14,2W), PAE=21,7% Gain compression=6,5dBc	@Maximum PAE: Pout=41,9dBm (15,5W), PAE=33,2% Gain compression=7dBc @Maximum Pout: Pout=42,3dBm (17,09W), PAE=30,8% Gain compression=11,5dBc
RF performances in multi-carrier mode of the SSPA RF chain	Pout=38,67dBm (7,36W) NPR=15,1dB PAE=17,88% Gain compression=2,03dBc Pdc=41,15W Pdissp=33,8W	Pout=39,1dBm (8,13W) NPR=15,0dB PAE=25,3% (+7points versus Ku-band GaAs SSPA) Gain compression=6,1dBc Pdc=32,1W (-22% versus Ku-band GaAs SSPA) Pdissp=23,99W (-29% versus Ku-band GaAs SSPA)

Table 2 : Initial Ku-band SSPA equipment, RF analysis synthesis

Regarding a future 7W Ku-band SSPA equipment, the preliminary comparison between the two previous GaAs and GaN versions shows important improvements and points to be addressed further:

- Improvement of PAE performance: +7 points
 - Reduction of the number of HPA modules for the last power stage: 2 modules ⇒ 1 module
 - Suppression of combiner losses : 2 ways power combiner (0.6dB losses) ⇒ single HPA module (no loss)
 - PAE_RF_chain_SSPA_GaAs=18%⇒ PAE_RF_chain_SSPA_GaN=25%
- Reduction of the total power consumption and the total dissipated power:
 - Pdc: 41W ⇒ 32W (-22%)
 - Pdiss: 33,8W ⇒ 24W (-29%)
- Increase of the dissipated power at HPA module level:
 - 13,4W with GaAs HPA module⇒20,2W with GaN HPA module
 - Need for an advanced packaging technology
- Increase of the Gain compression level compared to the GaAs SSPA
 - 7W Ku-band SSPA with 2 GaAs HPA modules: Gain compression=2dBc
 - 7W Ku-band SSPA using GaN: Gain compression=6,1dBc

- Despite this compression level, the compromise Pout/PAE/linearity remains in favour of the GaN technology in simulation.
- Gain compression has to be confirmed by measurement at transistor level. The gain compression could be reduced by further improvements of the GaN power device technology in the near future.
- Further reliability analysis should demonstrate that this selected operating power (corresponding to the maximum of PAE) remains in the Safe Operating Area of the chosen GaN technology.
- Reduction of HPA module number (2 \Rightarrow 1) will allow significant improvements at SSPA equipment level in term of size, mass and cost reductions (indeed manufacturing, tuning and assembly phases will be reduced):
 - Footprint reduction : -28%
 - Mass reduction: -20%
 - Cost reduction estimation: -17% in comparison with the 7W Ku-band GaAs SSPA using 2 HPA modules.

This synthesis and the preliminary conclusions are considered as initial and are updated at the end of the study using the measured performance of the developed Ku-band GaN HPA module. Updated analysis and conclusions (including also comparison with LTWTA equipment) are presented in chapter 4.2

2. DEVELOPMENT OF L-BAND HYBRID GH50 HPA MODULE (HPA-1 MODULE)

This activity is composed of two contractual phases:

- Phase 1 for the first iteration of HPA-1 module (based on 0.5 μ m process)
- Phase 2 for a second iteration of HPA-1 module (based on 0.5 μ m process)

Each phases is composed of 5x main activities:

1. A baseline design according to the specified target performances and based on the UMS GH50 characteristics. Using UMS GH50 design kit, load-pull simulations are launched on transistor cell level in order to optimize power bar characteristics (number of transistor cells, total periphery and size of each finger). Thermal analysis on the transistor and the whole structure including the transistor physical description and packaging environment are performed in order to evaluate junction temperature. In order to improve the way to match GaN components, the use of hybrid substrate with high dielectric constant have been considered.
2. The manufacture of the 0.5 μ m transistors and power-bars (GH50) and the associated on wafer tests.
3. The characterization and modeling of the 0,5 μ m transistors and power-bars in order to develop an electro-thermal nonlinear model.
4. The detailed design of the hybrid HPA module using electrical transistor and power-bar models from previous activity
5. The manufacture and test of the HPA-1 modules. These tests are carried out in in order to verify if the performance fulfills the requirements defined in the ESA SOW. Multi-carriers RF step stress on 3 hybrid HPA modules manufactured and mounted in test jig are also performed in order to identify the safe operating area related to UMS GH50 process.

2.1 Development of L-band hybrid GH50 HPA module (HPA-1 module): Phase 1

2.1.1 Baseline Design

2.1.1.1 Loadpull simulations

This activity is dedicated to the definition of the HPA-1 baseline design and the transistor level requirements to achieve the following technical performances :

Performance within Environmental Requirements	L-Band HPA				
	Value	Test condition	C/NC	Proposed value	Comments
Nominal Output power with Multicarrier Signal	>30W	@15dB NPR Worst case over temperature	C		
Power Added Efficiency with Multicarrier Signal	>55%	@15dB NPR Worst case over temperature	-	>45%	
Centre frequency	1.5675 GHz	L-Band	C		
Bandwidth	>50MHz	@ Nominal output power	C		
Gain flatness	+/- 0.25dB	Over the whole BW for fixed input power	C		
Gain with Multicarrier Signal	>16dB	@15dB NPR Worst case over temperature	C		
Gain compression level with Multicarrier Signal	Max. 2dB	@15dB NPR Worst case over temperature		Max. 4dB	@15dB NPR worst case over temperature
Maximum phase shift	<15 deg	From 30dB back-off to 4dB compression	C		
Deviation from linear phase	2 deg pk-pk	versus frequency within BW	C		
Input reflexion coefficient	<-10dB	@ Nominal output power over BW	C		
2nd Harmonic rejection	>30dBc		C		
Main DC voltage supply	>50V		-	40V	Confirmed with UMS
Temperature	-10 deg / +85 deg		C		
Pressure	Ambient and 10e-6 mbar		C		Multipactor free operation will be demonstrated by calculation with a sufficient margin

Table 3 : HPA-1 required performances

The HPA-1 being a low frequency version and the UMS 0.5 μ m GaN process (GH50) being primarily a discrete transistor process; the HPA-1 is based on hybrid technology.

This study has been achieved by applying the following work philosophy :

- Load pull simulation of elementary transistors. Different sizes and different biasing points have been simulated to find the best possible power added efficiency (PAE), output power trade-off for each transistor size.
- Starting from remarkable load-pull simulations, "VOLTI" analysis have been performed to evaluate NPR performances. Thus, optimum transistor size, biasing point and load impedances at fundamental frequency and up to the 3rd harmonic have been highlighted.
- Power bar size has been chosen to reach the output power performances by direct scaling of an elementary transistor.
- Preliminary design of the HPA has been undertaken. Different materials have been studied to enable optimum input and output matching networks design.
- "VOLTI" analysis have validated the PAE, Pout and NPR trade-off feasibility at HPA level and pointed out the RF performances margin regarding the design risks.

Loadpull simulations have been conducted on two different transistor sizes: 8x250 μ m and 6x400 μ m.

Main conclusions about the smith chart analysis for peak PAE performances are:

- H2 is very critical for the PAE performance. PAE gradient is high over the whole smith chart and PAE performances can varies from 72% to 43% in the worst case (Zworstcase = 0.97 / 110°). H2 sweet spot impedances is located between Zload 0.97/0° to 0.97/70°. H2 optimization also enables the best output power for PAE peak performance.
- Fine tuning of H1 have to be undertaken in order to maximize PAE performances (+8points PAE) or to find the best trade-off between output power level and PAE.
- H3 allows only a slight improvement of the maximum PAE compared to the re-tuning of H1 with H2 optimized (+2points of PAE). Nevertheless, and even if a wide part of the smith chart is not critical for PAE performances, upper-left side impedances of the smith chart must to be avoided during the design phase because it will lead to a drop of 20 points of PAE in the worst case.
- We notice that PAE peak performance is always correlated to a high level of gain compression around 10dBcomp.

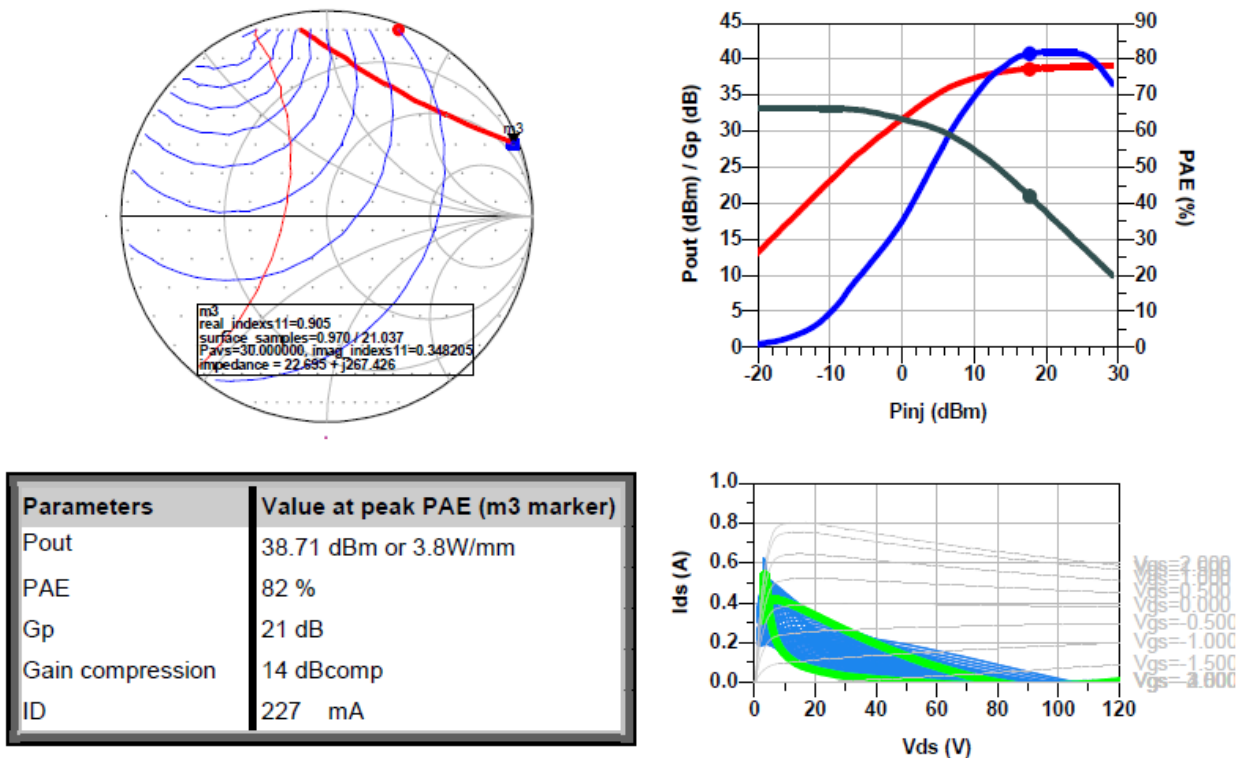


Figure 1 : LP simulation (8x250µm). Third harmonic load impedance optimization for ZL(H1opt) and ZL(H2opt).

A comparison between the 8x250µm and 6x400µm transistor when they are both optimized for maximum PAE up to the 3rd harmonic. A focus is done on output power, power gain and PAE.

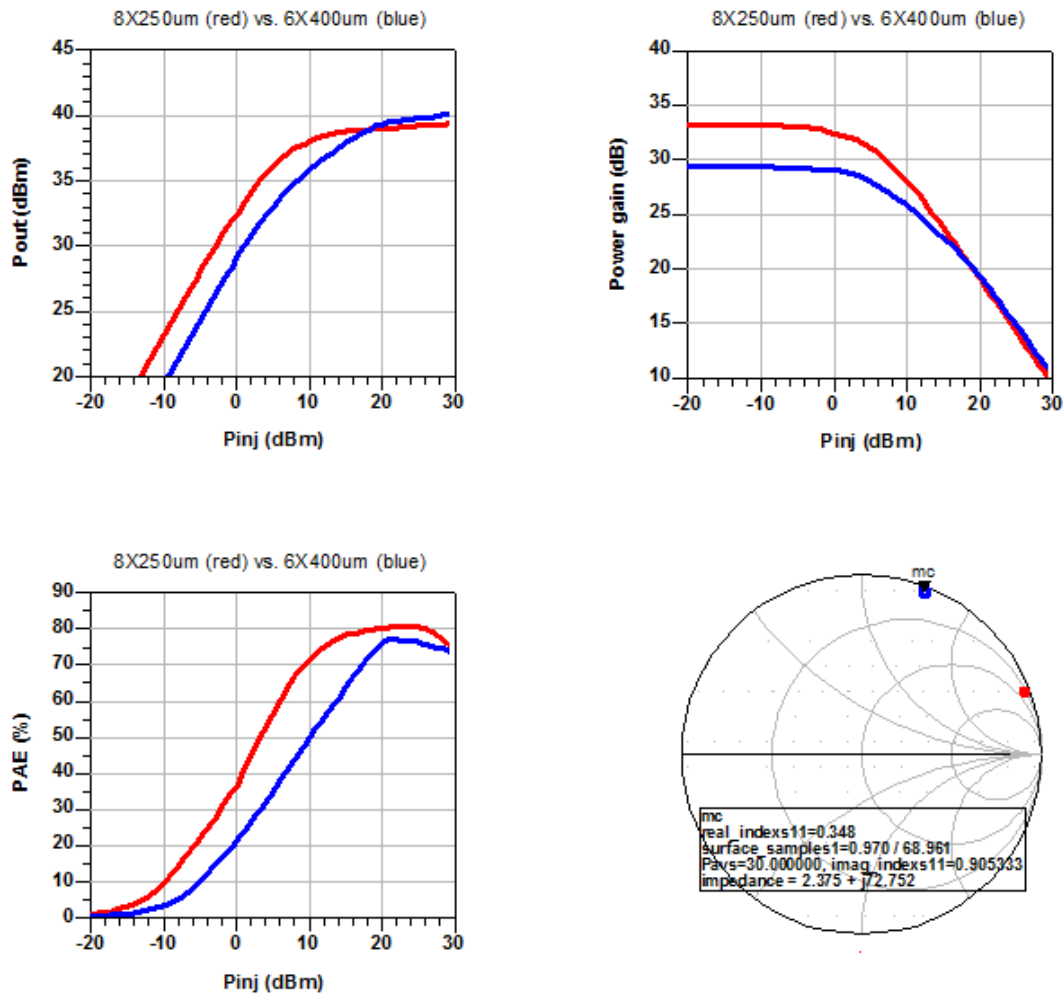


Figure 2 : Comparison between 6x400µm and 8x250µm transistors performances with optimal impedance

As expected, 6x400µm transistor delivers higher output power ($P_{out} > 40\text{dBm}$) than 8x250µm transistor ($P_{out} = 39\text{dBm}$) in saturation mode. Moreover, power gain behavior is also coherent with the respective size of the two transistors. In addition, the key point of the comparison is the power added efficiency performances because 8x250µm transistor, in our simulation condition, is far superior to the 6x400µm transistor. It reaches better PAE performances over a wider input power range near the peak PAE than 6x400µm. Finally, when used in back-off mode, PAE is up to 20points better than its competitor. As a consequence, 8x250µm transistor offers the best trade-off for our HPA RF performances requirements where PAE is of primary concern.

Due to its better PAE performances, the L-Band HPA is based on $8 \times 250 \mu\text{m}$ transistors. Only one stage is necessary regarding the power gain requirements at compression level and the output power performances will be reached using 8 transistors in parallel. Thus, the circuit definition have to be done with UMS $8 \times 8 \times 250 \mu\text{m}$ power bar to matched as close as possible the overall required HPA performances.

2.1.1.2 Architecture and technologies considerations

Regarding the elementary transistor cell combination, the 8 transistor power bar (2^n) have been selected. It gives less output power margin regarding the size of the power bar but PAE will be maximized. Moreover, transistor balance is directly linked to the overall HPA stability. This second approach is enhancing PAE by 3 to 5 points.

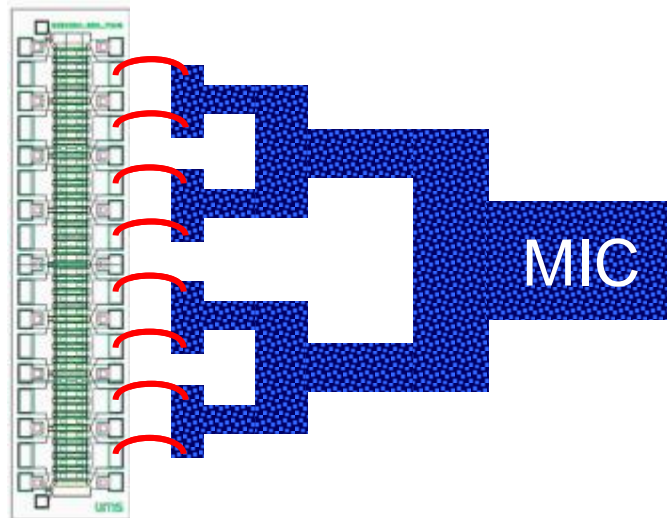


Figure 3 : Power bar considered as macro cell made up of 2^n elementary transistor

To design the matching networks, different materials have been evaluated from low to high dielectric constant (ϵ_r). See Table Below

Material	Permittivity (ϵ_r)	Thickness (μm)	TanD
Al_2O_3	9.9 ± 0.2	254	$2e-4$
OxTi	40	381	
NTK material L	93 ± 2	635 / 1016	$6.25e-4$

Table 4 : Materials table considered for the HPA (input and output network)

Titanium oxide (OxTi) has been found very suitable for compact design, especially for the input matching network where it gives a balanced trade-off between losses, matching accuracy, and physical dimensions. In a first approach, an input matching network made up of standard microstrip lines model has been implemented in ADS and simulated.

Regarding the output matching network, transistor recombination have been performed as close as possible to the power bar in order to obtain the best possible harmonic symmetry.

Due to the biasing current, a minimum micro-strip line width have to be respected and it implies a careful choice of the material used behind the transistor power bar. In our case, high Er materials are not suitable because it doesn't allow an accurate load impedance synthesis with respect of line width current density constraints.

Thus accurate load impedance synthesis up to the 3rd harmonic as been obtained with Al₂O₃ material. In a second time, output combiner downsizing was realized by the use of OxTi material to enable its integration in L40 package. As a consequence, the second part of the output combiner has been replaced with OxTi material as shown on figure below.

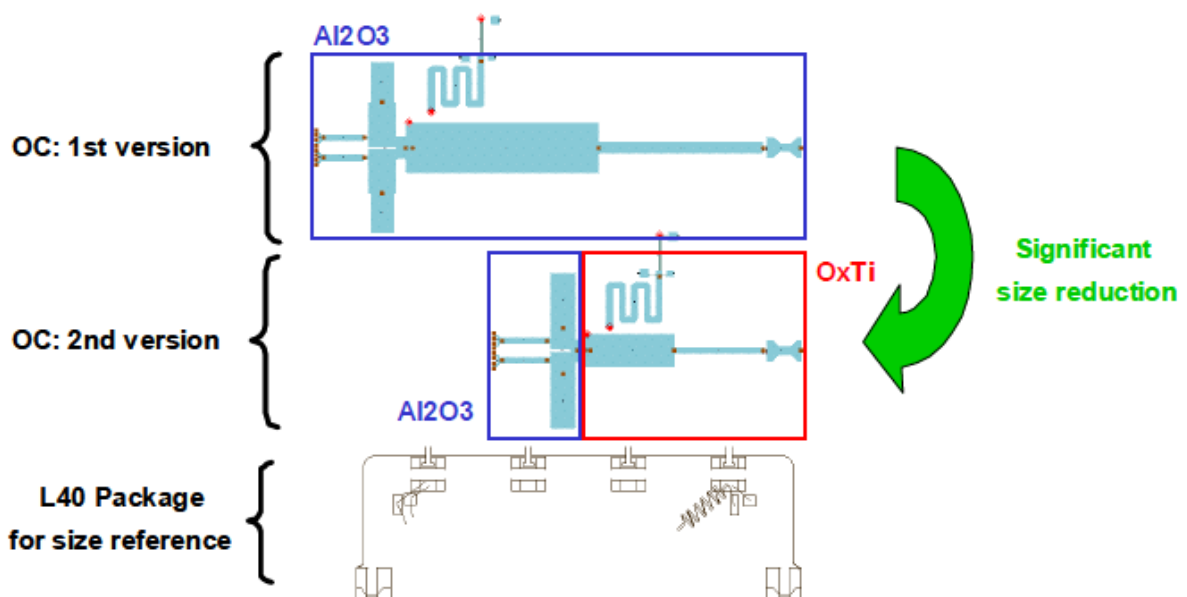


Figure 4 : Output network schematic (Momentum) of the L-band hybrid HPA

2.1.1.3 RF performance

The main RF performances obtained, output power, PAE and power gain are presented below versus input power and versus frequency :

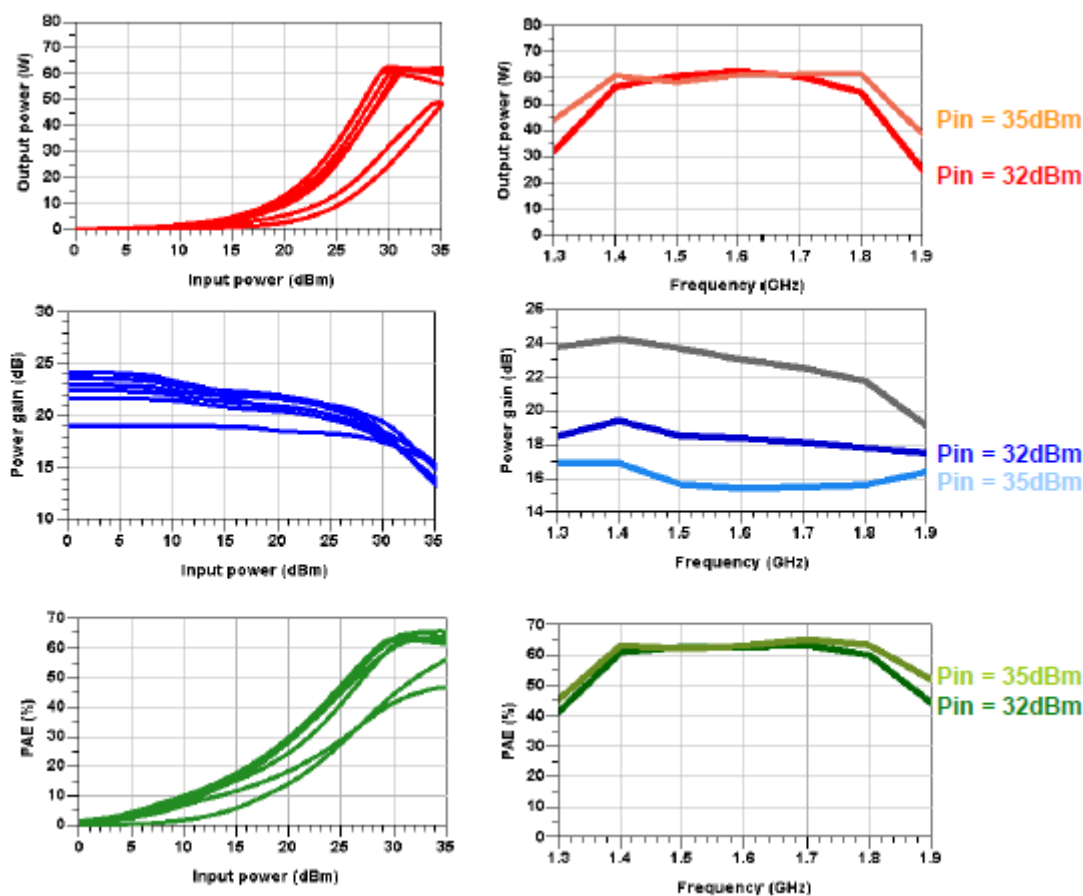


Figure 5 : HPA-1 Module. Baseline Design. HPA RF performances. Pout(W), PAE(%), Gain(dB) versus input power (dBm) and Frequency(GHz).

The frequency bandwidth reaches 400MHz for a centre frequency of 1.6GHz (25% of relative bandwidth). The maximum overall power added efficiency varies from 60 to 65% and is associated to an output power of 60W. It corresponds to a $P_{out} = 4W/mm$ in saturation mode.

Finally, a Volti analysis has been done at HPA level to check the feasibility of the PAE, output power, NPR trade-off with a multi-carrier signal. On figure below, PAE, NPR and gain compression are drawn versus output power.

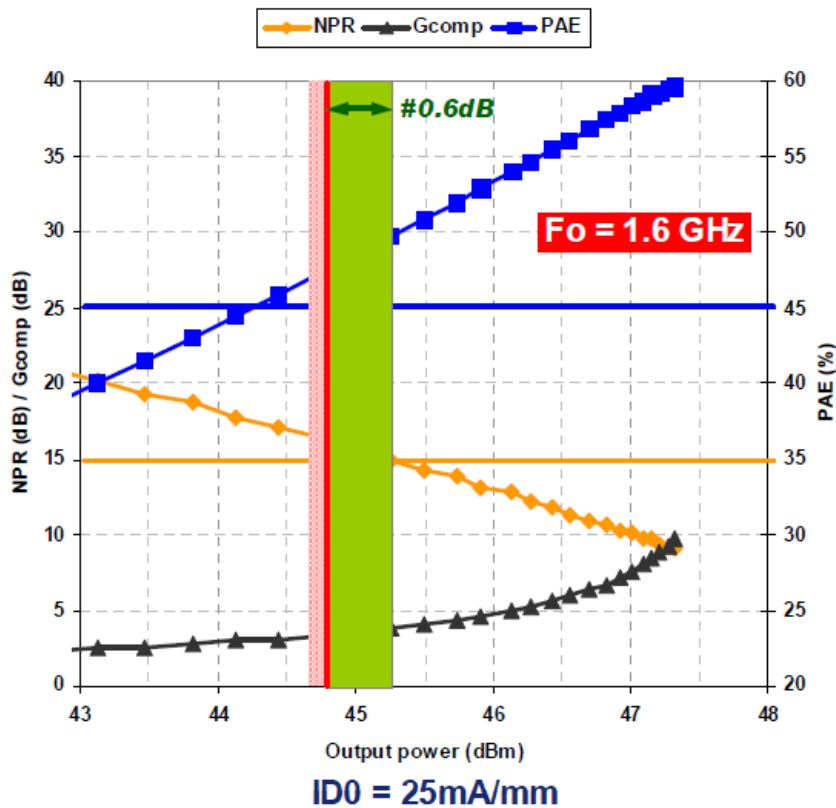


Figure 6 : HPA-1 module. Preliminary GH50 hybrid HPA simulation results in multi-carrier mode. PAE(%), NPR(dB), Gain compression(dB) versus output power(dBm)

As shown below, with an hybrid HPA based on a 8x8x250µm power bar there is very few margin to match both output power, power added efficiency and NPR specifications. So ,different backup solutions, with different power bar setup have been also considered. Table below summarizes these different solutions.

POWER BAR SIZE	GATE LENGTH DEV.	ΔPOUT	PRIORITY	COMMENTARY
8x8x250µm	16 mm	0 dB	+++	
8x8x300µm	19.6 mm	+0.8dB	++	
2x8x8x250µm	32 mm	+3dB	+	2 nominal power bars in // (complex)
10x8x250µm	20 mm	+1dB	-	Not suitable for MMIC design approach
2x8x8x150µm	19,2mm	+0,6dB	-	Complex / high gain

Table 5 : Power bars combinations considered as backup solutions.

2.1.1.4 Packaging solution

The HPA will be integrated in a L40 power package with MDC (Metal Diamond Composite) base plate.

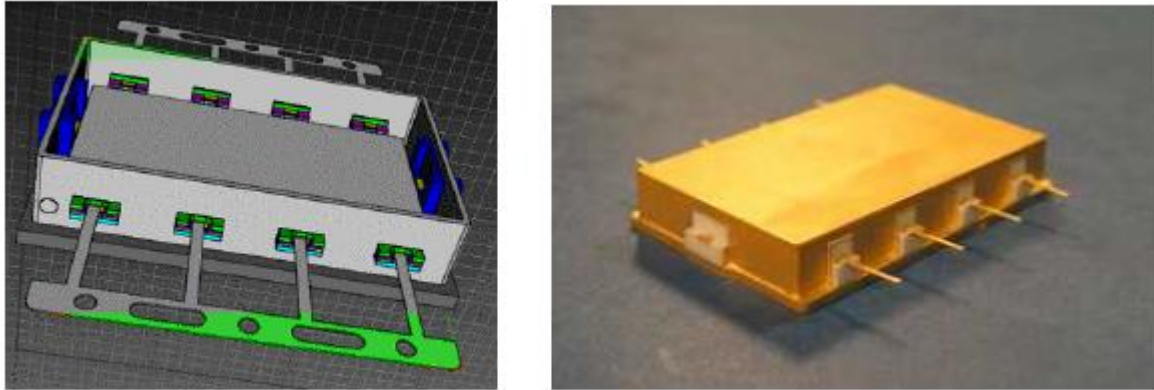


Figure 7 : L40 power package with MDC (Metal Diamond Composite) base plate

This package is space compliant and have been developed by TAS in the frame of the AGAPAC project. Its main characteristics are:

- Able to dissipate up to 100W thermal power (100W dissipated power has been measured in the frame of AGAPAC study where a 36mm power bar has been integrated in this L-band package.
- Overall footprint of the micro-package is set to 20x40 mm.
- Minimized micro-package thermal resistance.
- The L40 package have also been designed taking into account both electrical and mechanical design constraints, multi-pactor and DC current constraints on RF feedthrough.

2.1.1.5 Thermal simulations

Thermal analysis on the transistor and the whole structure including the transistor physical description and packaging environment have been conducted in order to evaluate junction temperature. The thermal behavior of the device represented by a multi-port inputs and outputs SPICE thermal circuit has been generated and used for non-linear modeling activities. These activities are conducted by XLIM.

Thermal simulations are performed with ANSYS software. The job has consisted first to model the transistor structure in 2D and then to extrude it in 3D. The inputs are the geometry of the device: layout and elevations. A very important part of the job is also the mesh of the structure. The knowledge of the thermal properties of materials is also very important. Some materials are considered nonlinear. It is essentially the case for GaN and the SiC substrate which has a significant thickness. Linear thermal properties of the materials are provided below:

Material	K (W/(m.K))	Cp (J/(Kg.K))	ρ (Kg/m ³)
Au	315	130	19320
SiN	35	680	3200
Ni	90	444	8900
AlGaN	40	604	5184
GaN	130	490	6150
AlN	285	600	3230
Diamond Copper	400		
AuSn	58.5		
Al	165		
Glue	2		

Table 6 : Linear thermal properties of the materials

Nonlinear thermal conductivity has been used for thermal simulations. Figure below shows the thermal conductivity of GaN and SiC:

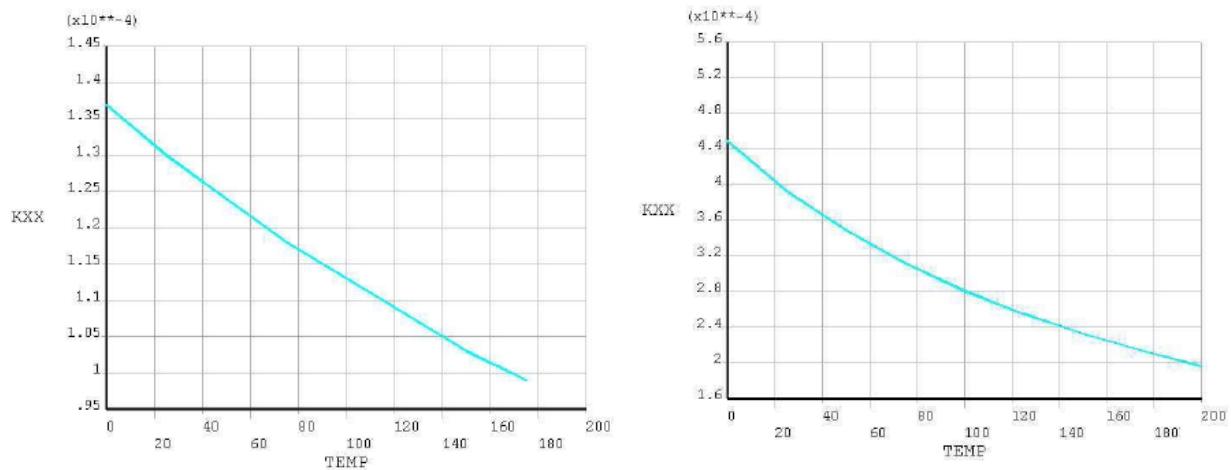


Figure 8 : Non linear thermal conductivity of GaN (left) and SiC (right)

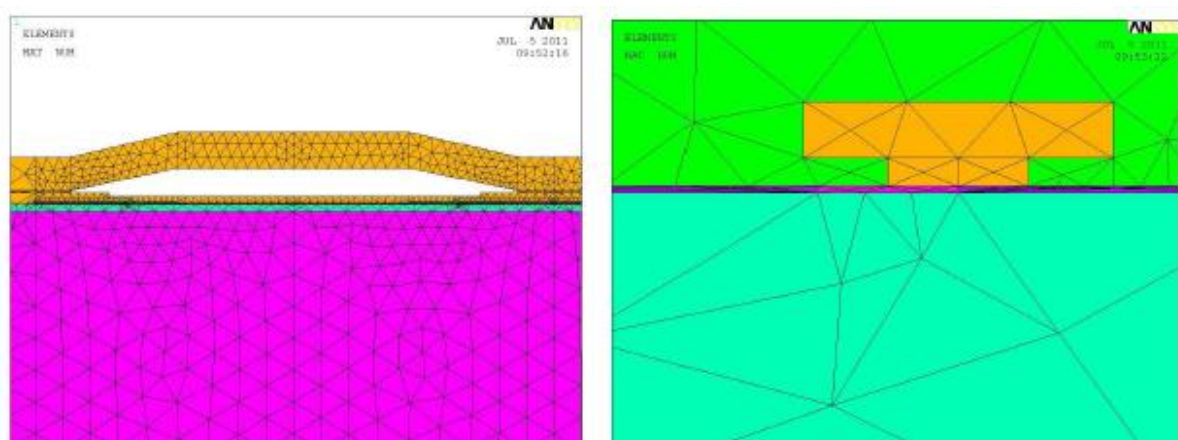


Figure 9 : Cutplane of elementary cell (left)and zoom on the active area (right)

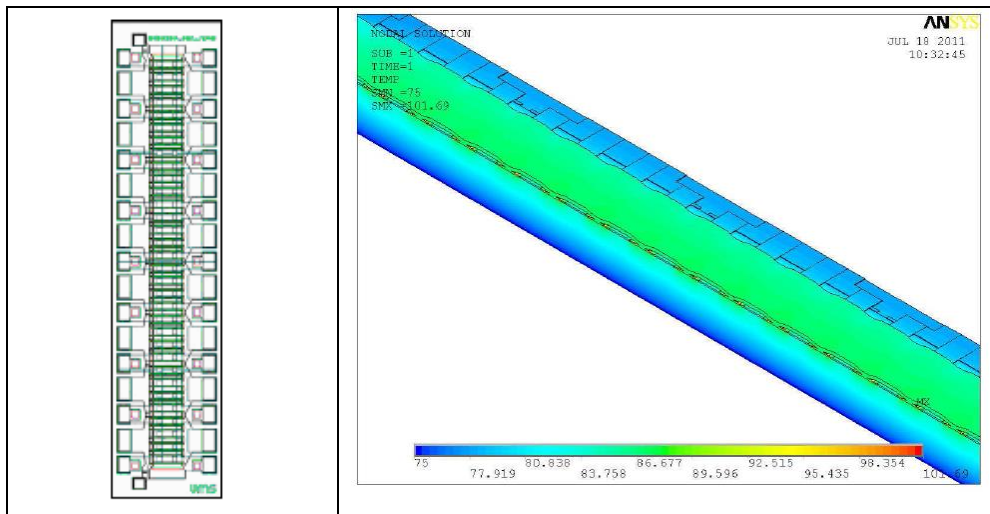


Figure 10 : Temperature profile for Tbase=75°C and 32W of dissipated power

Baseplate\Dissipated Power	28W	32W	36W	40W	44W
50°C	71.87	75.1	78.29	81.55	84.76
75°C	98.28	101.69	105.1	108.58	112
100°C	124.73	128.35	131.98	135.64	139.25
125°C	151	154.78	158.56	162.4	166.16

Table 7 : Maximum Temperature (°C) for various baseplate temperatures and dissipated power

For a power bar build with 8x8x250µm transistor cells, the thermal resistance varies from 6.25°C/W and 7.48°C/W. which is very close to the value obtained for a single elementary cell. This reveals a poor thermal coupling from cell to cell and a quasi-constant temperature along fingers. The third study has been performed to quantify the influence of the packaging. Two different cases have been considered: with or without tab. The first conclusion is that at least 5°C can be gained without tab.

The second one is that the poor thermal conductivity of the glue is clearly a problem. Almost 15°C are lost in this layer. This thermal interface material is not efficient.

To compute the junction temperature of the power bar, the several contributions have been taken into account:

Tcase: 75°C and 36W dissipated power bar. Tab considered

- $T_{junction} = T_{case} + DT_{case_to_baseplate} + DT_{baseplate_to_junction}$
- $DT_{case_to_baseplate} = 1.286 \cdot 36 = 46.3^\circ\text{C}$
- $DT_{baseplate_to_junction} = (0.888 + (0.932 - 0.888) \cdot (121.3 - 100) / 25) \cdot 36 = 33.31^\circ\text{C}$
- $T_{junction} = 154.6^\circ\text{C}$

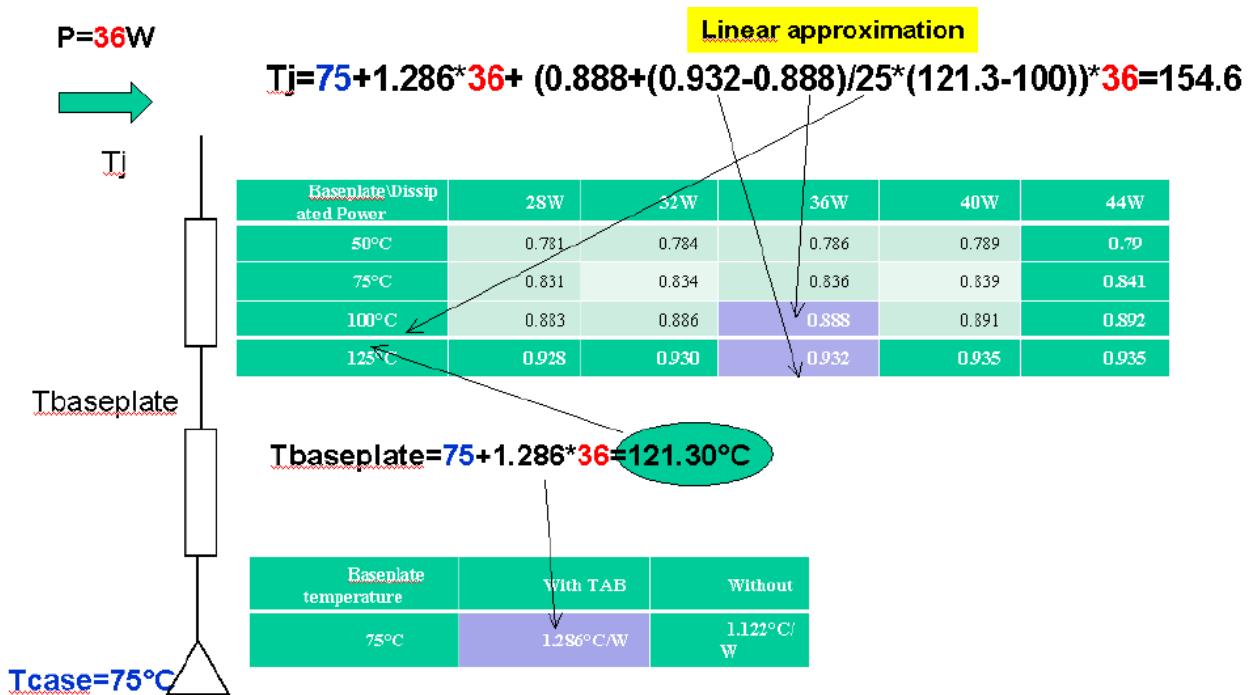


Figure 11 : Temperature calculation for Tcase 75°C 36W dissipated power with tab

Thermal capacitance behavior and equivalent schematic will be implement in the thermal model and include in the modeling report.

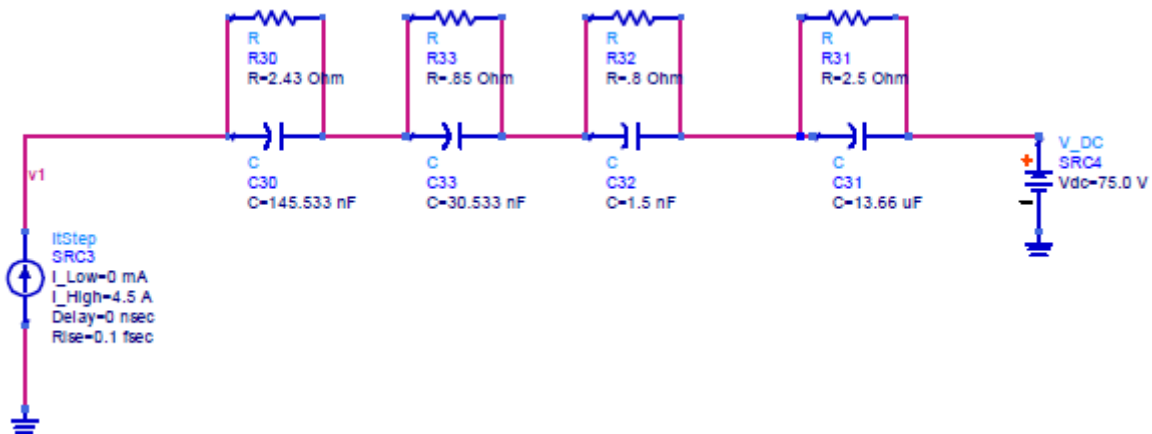


Figure 12 : Preliminary thermal model with 4 cells

2.1.2 Manufacture and test the 0.5µm transistors and power-bars (GH50). Run-1

One specific mask-set called “SABRINA” has been designed, manufactured and tested by UMS. The workflow were as follows :

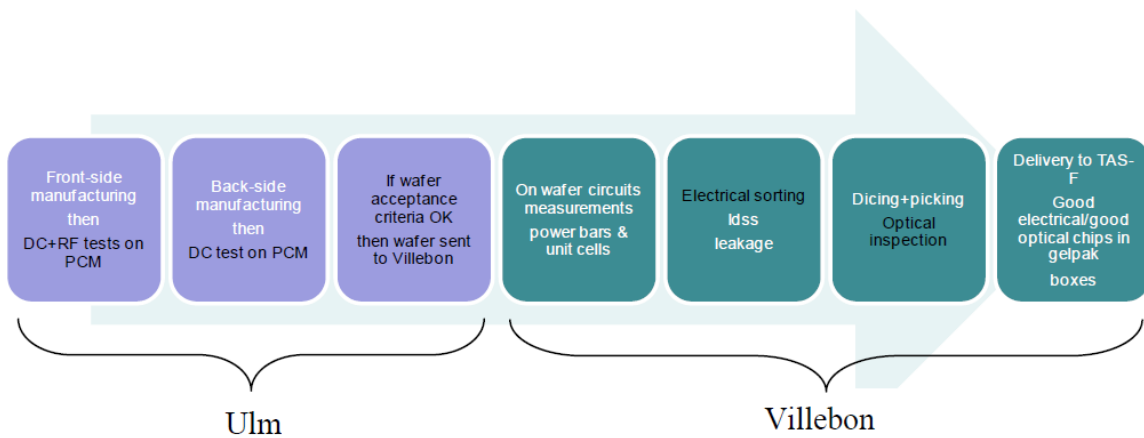


Figure 13 : UMS workflow for the manufacturing and test of GH50 maskset (Run-1)

The PCM tests have shown that the Sabrina wafer 3R034 was in good agreement with the GH50-10 acceptance criteria.

Three power unit cells were included on the Sabrina mask-set :

- 8x150 μ m
- 8x250 μ m
- 8x300 μ m

S parameter measurements were carried out on ten samples located at the center of the wafer. The measurements conditions were as follows:

- Frequency range : 0.5-21GHz
- Frequency step : 250MHz
- Biasing points : Id=50mA/mm Vd=10&40V

For 8x250 μ m transistor cell, the maximum stable gain /maximum available gain are plotted on the following graph, showing clearly the impact of the biasing conditions as well as the transistor size. A good homogeneity chip to chip is noticed.

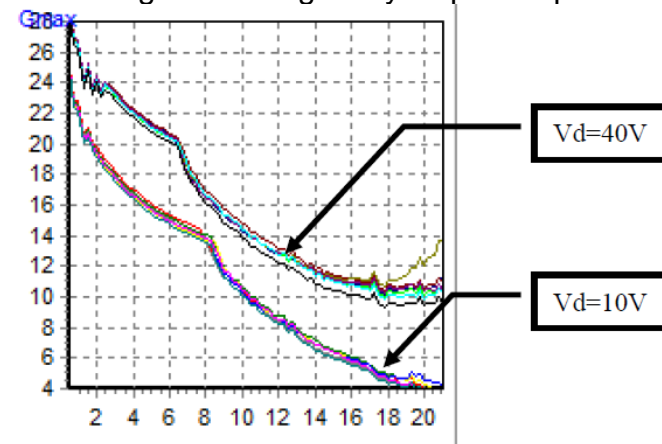


Figure 10- 8x250 Vd=10-40V Id=50mA/mm

Figure 14 : Run-1 0,5 μ m wafer manufacturing. Maximum stable gain /maximum available gain for 8x250 μ m transistor cell

Four power bars were included on the Sabrina mask-set :

- 8x8x150µm
- 8x8x250µm
- 8x8x300µm
- 10x8x250µm

These Power bars were measured in DC mode thanks to specific probe card. Schottky diode, saturated drain current , pinch-off voltage and gate/drain current leakage were measured on every power bar of the whole wafer. Measured performance of 8x8x250µm power-bar are presented below:

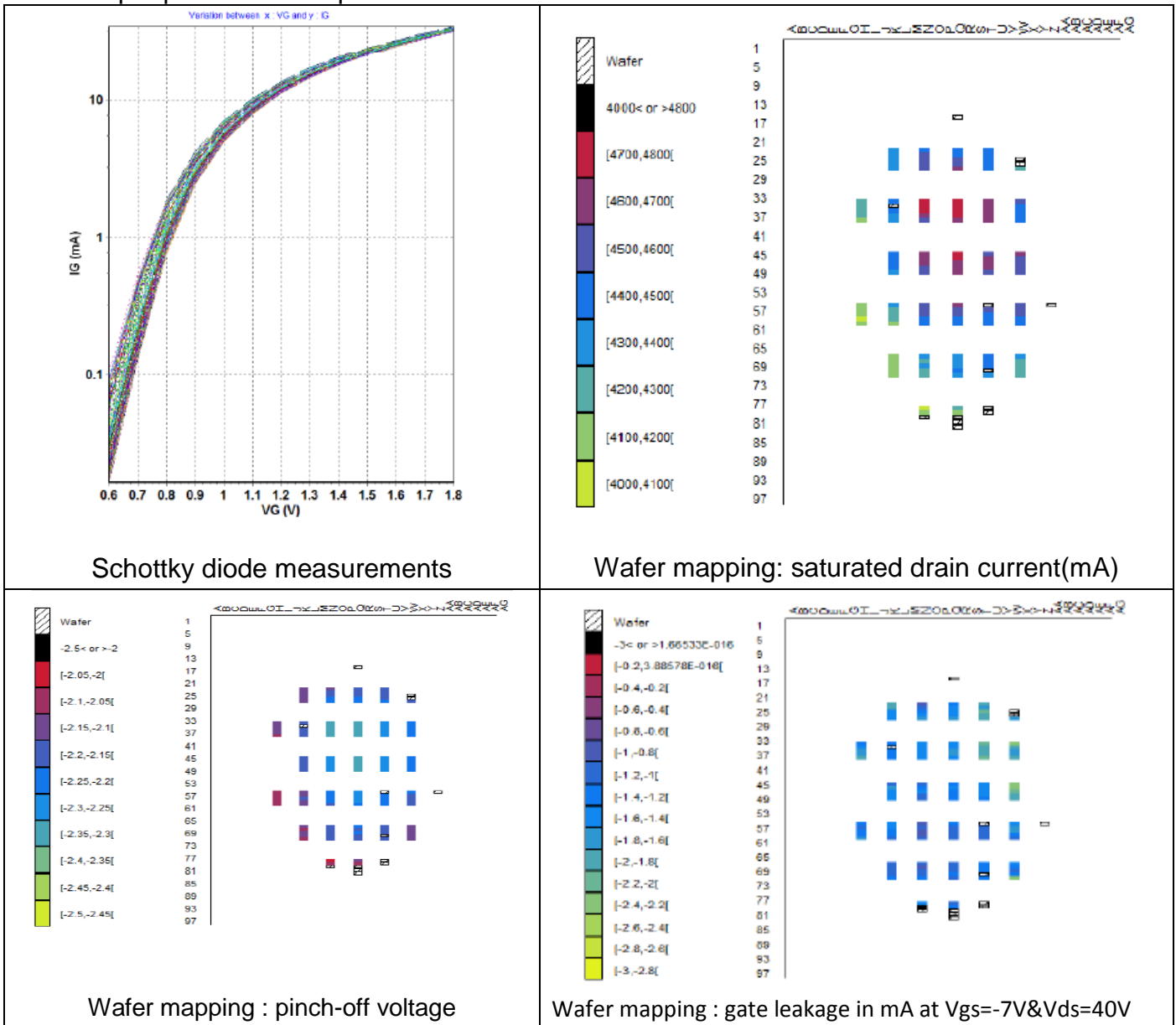


Figure 15 : Run-1 0,5µm wafer tests. Measured performance of 8x8x250µm power-bar

In this paragraph, the whole on-wafer tests carried out on the Sabrina wafer(Ref.K514111 3R034) have been depicted. The PCM tests have shown that the Sabrina wafer 3R034 was in good agreement with the GH50-10 acceptance criteria. The power bars tests have enabled to screen the die and to provide good electrical chips to TAS-F. That is also useful to know accurately each power bar for building HPA with chips as close as possible in term of electrical performance.

2.1.3 Characterization and modeling of the 0,5 μ m transistors and power-bars. Run-1

This paragraph gathers AMCAD Engineering and XLIM tasks achieved within the framework of the ARTES 5.1 SSPAs with European GaN Devices, Phase1 (Run-1). For unitary cell, AMCAD Engineering tasks consisted in pulsed I(V) with pulsed [S] measurements, load pull measurements and devices modeling. For power bar, AMCAD Engineering tasks consisted in load pull measurements. For power bar model, XLIM tasks consisted in the de development and validation of the 8x8x250 μ m nonlinear electro-thermal model.

2.1.3.1 Unitary cell measurements. Run-1

A pulsed I(V) / RF test bench is used for the measurements. Test bench is described in the figure below.

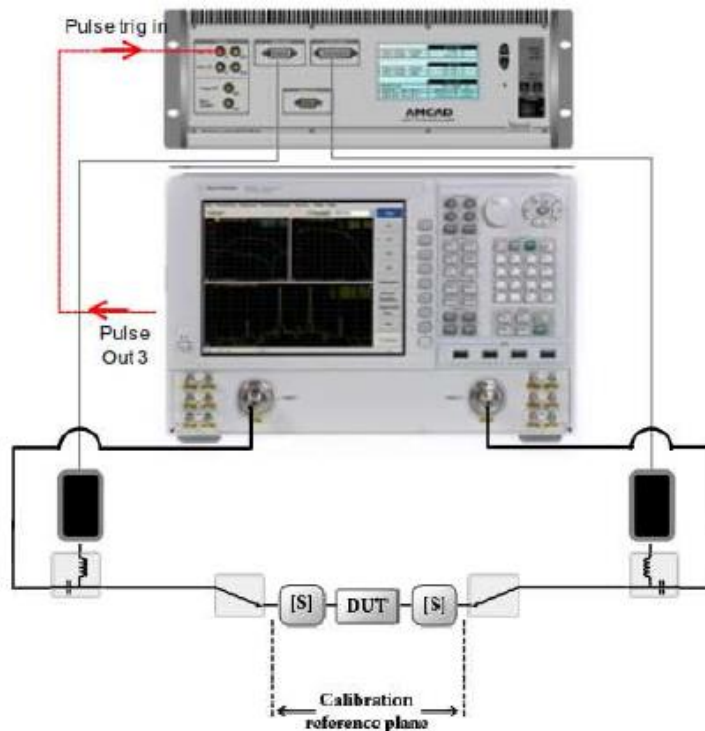


Figure 16 : AMCAD I(V) and [S] test bench for transistors characterizations

The principle of pulsed measurement is to describe the I(V) network by quasi-isothermal measurements using short pulses around a quiescent bias point selected. The quiescent bias point of rest is provided by the voltage levels and V_{gs0} v_{ds0} . This results in a current I_{ds0} polarization. Pulses, whose levels are represented by V_{gs1} , I_{gs1} , V_{ds1} I_{ds1} and describe all the characteristics of input and output of the transistors.

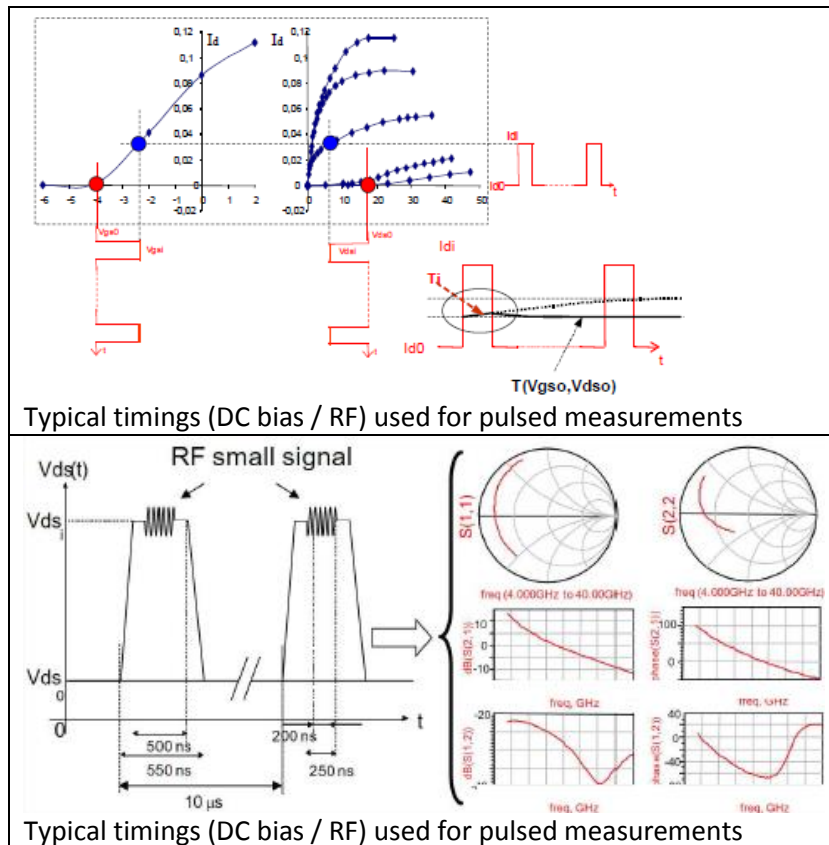


Figure 17 : Principle of the S-parameters measurements in pulse mode

Preliminary pulsed I(V)/RF measurements have been performed on three samples of each topology in order to estimate the process dispersion and to select the most representative samples for the complete characterizations. These dispersive measurements have been performed at ambient temperature (25°C). The results for the different transistor are shown hereafter.

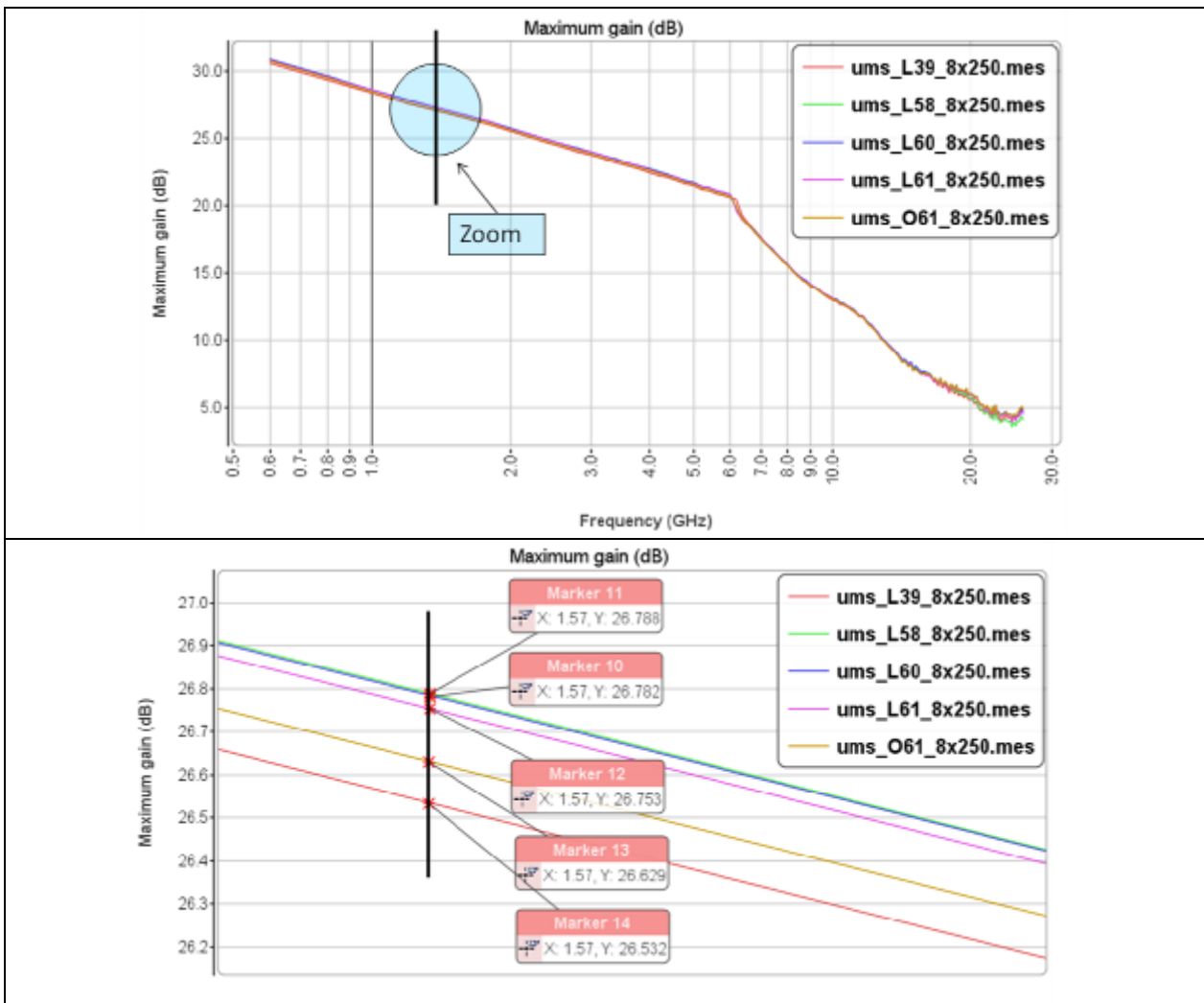


Figure 18 : Dispersive [S] measurements on transistors 8x250µm GH50 (bias points corresponding to surrounded points on the I(V) curves, Vds=40V)

The representative samples chosen are referred L60. Measurements with temperature have been performed at 25°C, 60°C and 90°C. The results obtained are shown hereafter.

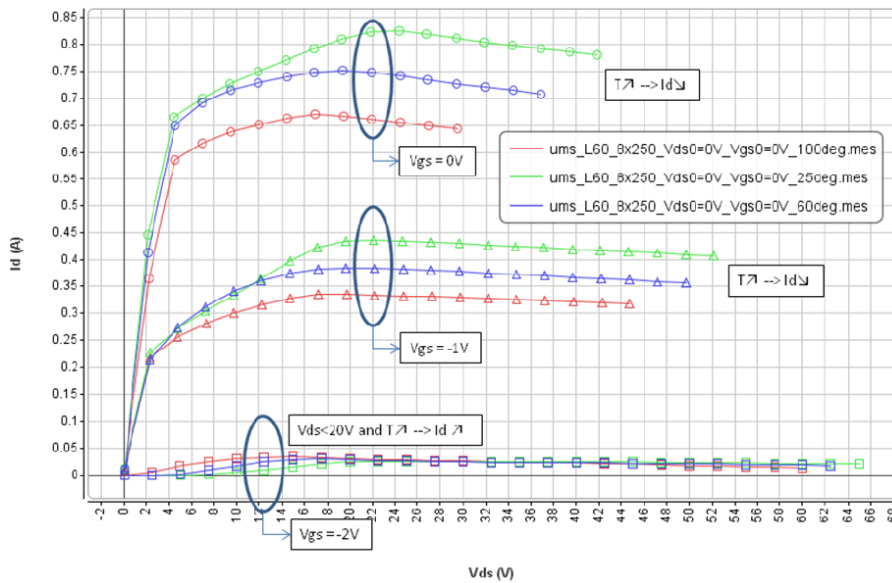


Figure 19 : Output current with different chuck temperature (25°C, 60°C, 100°C) transistor 8x250 L60 measurements

Idss is reduced by 20% to a rise of 75 ° C the chuck temperature.

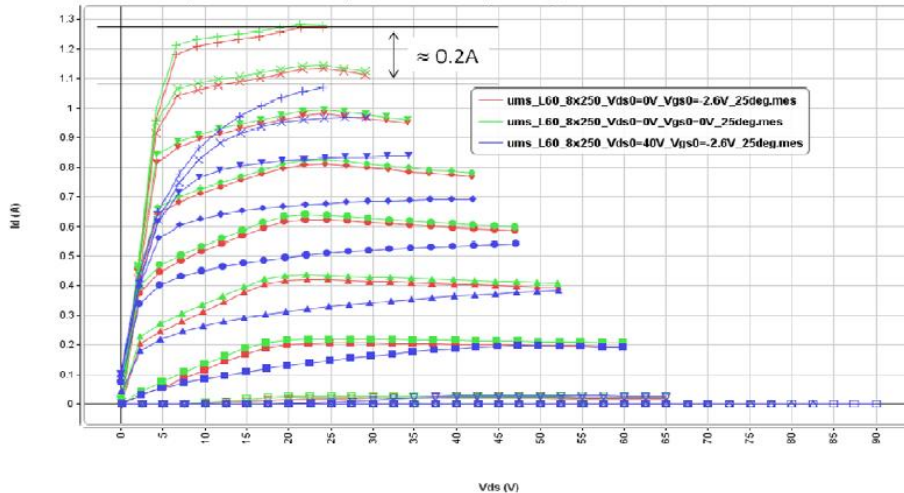


Figure 20 : Highlighted phenomena traps

Only the drain-lag effects are present. The effect on the output characteristic is a reduction of the drain current of 15%. Maximum gain has been plotted for different quiescent bias (40V and Ids from 25mA/mm to 75mA/mm). Example for quiescent bias of 50mA/mm is given below.

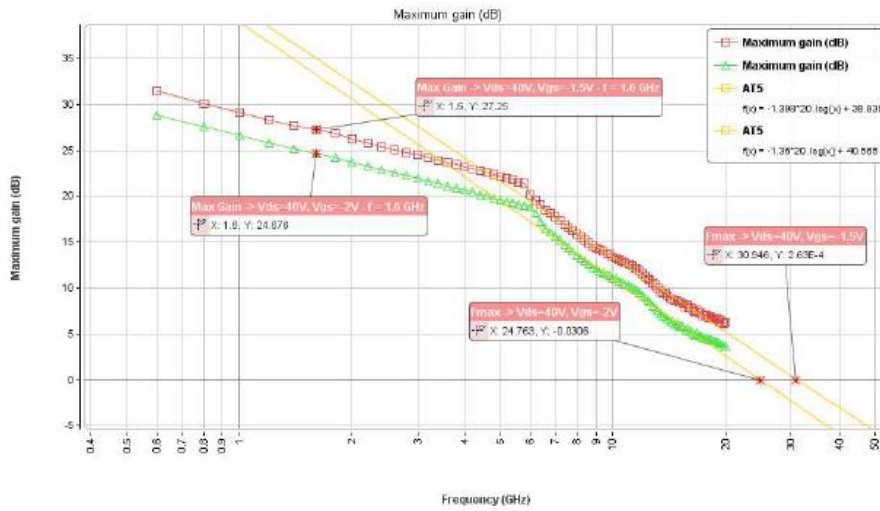


Figure 21 : Maximum Gain @ Vds0=40V, Ids0=50mA/mm

Summary of the unitary cell pulsed i(V) / RF measurements is given in the following table:

Transistor	Dispersion	Idss (A) @ Vds=10V	Max Gain (40V, 50mA)	Fmax (40V, 50mA)
8x250µm L39	✓	0.635		
8x250µm L58	✓	0.632		
8x250µm L60	✓	0.629	24.85dB @ 1.6GHz	24.75 GHz
8x250µm L61	✓	0.621		
8x250µm 061	✓	0.651		

Figure 22 : Summary of the unitary cell – pulsed I(V) / RF Measurements

Load Pull measurements were performed in CW mode at a 1.57GHz. The impedances were optimized at the fundamental frequency and the harmonics 2 and 3. The system set up for the devices characterization is described below.

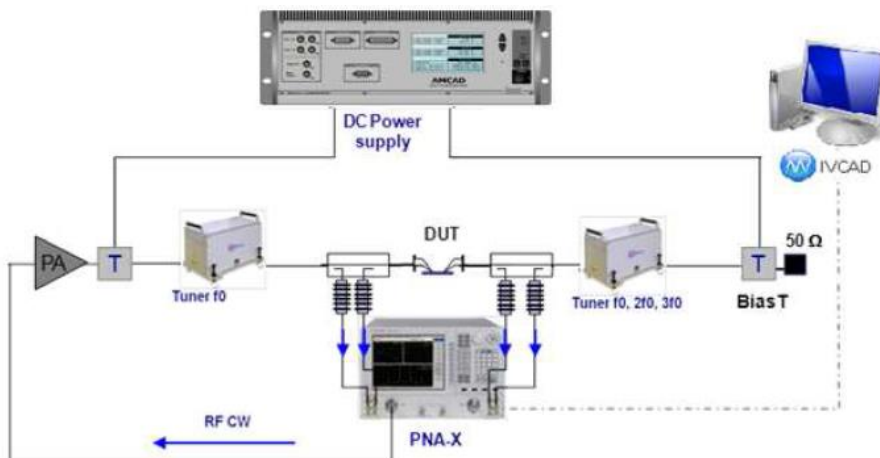


Figure 23 : AMCAD VNA-based load-pull system

The objective is to find the optimal load impedance added power efficiency (PAE) for $f_0 = 1.57\text{GHz}$ CW mode. Impedances harmonics $2f_0$ and $3f_0$ are also optimized to achieve maximum performance. The $8 \times 250\mu\text{m}$ component is polarized:

- $V_{ds0}=40\text{V}$, $I_{ds0}=50\text{mA}$ (25mA/mm).
- $V_{ds0}=40\text{V}$, $I_{ds0}=100\text{mA}$ (50mA/mm).
- $V_{ds0}=40\text{V}$, $I_{ds0}=150\text{mA}$ (75mA/mm).

The source tuner is set at 50Ohms. The reference sample is selected transistor L60 ($8 \times 250\mu\text{m}$), several samples will be used to validate end optimization measures and study the dispersion technology.

The loadpull Optimization methodology used during this campaign is:

- Optimization of f_0 load impedance: A first optimization of the load impedance is made at low level to determine the optimal impedance zone when the transistor operates in the linear regime. For this impedance, a power sweep is then performed in order to observe the performance obtained. The power that provides the maximum added power efficiency is raised to perform a second optimization of the load impedance (nonlinear regime). During these optimizations, the load impedances at $2f_0$ and $3f_0$ are equal to 50 ohms. During these first measures it appeared that the transistors are conditionally stable, this was confirmed by S-parameter measurements (measurements made on 50Ohms support and source). These Sparameter measurements give a good indication of the places of the Smith chart for which the transistor may be unstable. For biasing point $V_d=40\text{V}$ & 25mA/mm, $Z_{load} @ f_0 = (0.56, 43^\circ)$, transistor reaches a 64.3% PAE.
- Optimization of $2f_0$ load impedance: the load impedance at f_0 is now set to the optimum impedance PAE. An impedance sweep at $2f_0$ is now performed to a input power level within the transistor to obtain the maximum PAE. The impedance at $3f_0$ remains at 50Ohms. For biasing point $V_d=40\text{V}$ & 25mA/mm , $Z_{load} @ 2f_0 = (0.85, 18^\circ)$, transistor reaches a 71.6% PAE.
- New optimization of the f_0 load impedance: with this new optimization of f_0 load impedance, the PAE reaches 77.4% ($2f_0$ load impedance is fixed on its optimal and $3f_0$ is set to 50 Ohms).
- Measurement and Optimization of $3F_0$: The load impedances at f_0 and $2f_0$ are now set to the optimum impedance PAE. An impedance sweep at $3f_0$ is now performed to a input power level within the transistor to obtain the maximum PAE. For biasing point $V_d=40\text{V}$ & 25mA/mm, $Z_{load} @ 3f_0 = (0.63, -125^\circ)$, transistor reaches a 77.2% PAE. With the help of this impedance sweep it's possible to conclude than $3f_0$ load impedance do not have a dramatic influence on the PAE performances.

Measured performances are synthesized below:

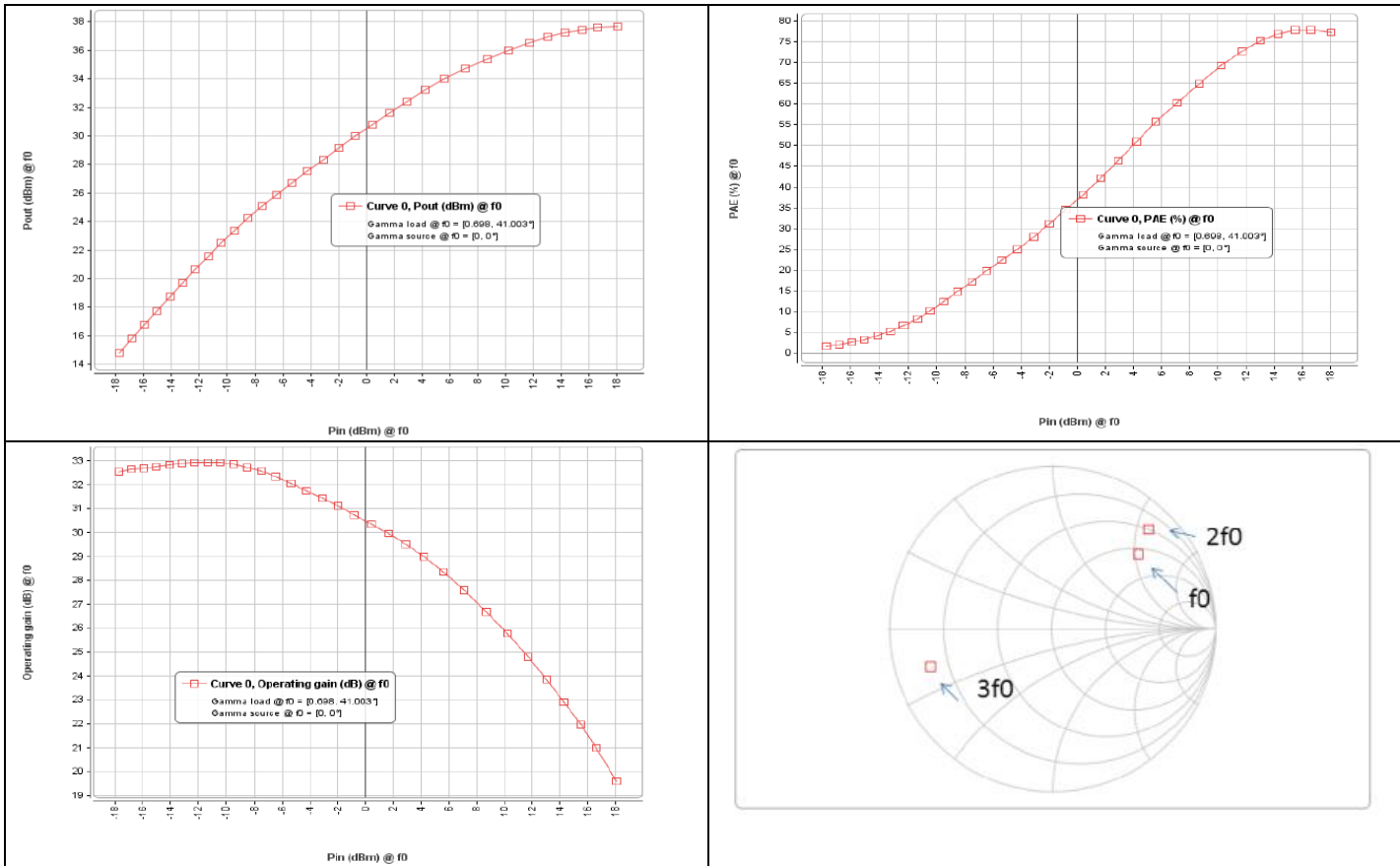


Figure 24 : Pout / PAE / Gain vs Pin after loadpull optimization. Optimized load (H1, H2, H3) for optimal PAE performance. Vds=40V, 25mA/mm.

Regarding the RF performance vs Technology Dispersion, the load impedances are substantially similar to the fundamental frequency and harmonic frequency.

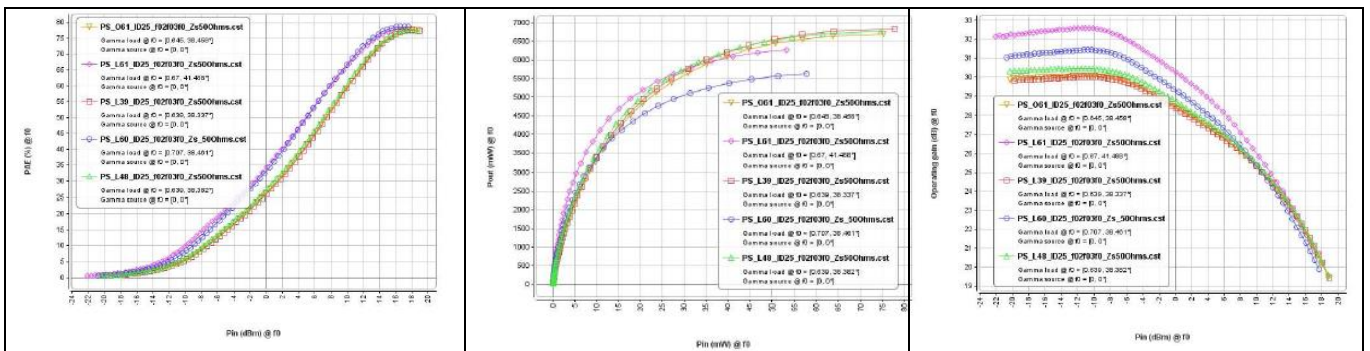


Figure 25 : Loadpull measurements. Performance vs Technology Dispersion. 5x transistor samples tested. 40V, 25mA/mm.

Tables which summarized the load-pull performance monitored during loadpull measurements on different samples are provided below.

Sample	Linear Gain (dB)	Output Power (W)	PAE max (%)	Zload f0 opt PAE (Ω)	Zload 2f0 opt PAE (Ω)	Zload 3f0 opt PAE (Ω)	Zsource (Ω)
L39	29.7	5.8	77.7	72.9+j97.2	23.3+j115.5	5.9-j5.3	50
L48	30.3	6.7	77.5	72.8+j97.5	23.3+j115.5	5.9-j5.2	50
L60	31.0	5.6	78.8	63.6+j112	24.6+j116.8	5.9-j4.5	50
L61	32.1	6.2	77.8	61.9+j99.6	23.2+j116.5	6.2-j6.3	50
O61	29.8	6.7	77.8	71.9+j98.8	23.7+j116.1	6.0-j5.3	50

Table 8 : Summary of performance monitored during loadpull measurements. Vds=40V and Ids=25mA/mm

Sample	Linear Gain (dB)	Output Power (W)	PAE max (%)	Zload f0 opt PAE (Ω)	Zload 2f0 opt PAE (Ω)	Zload 3f0 opt PAE (Ω)	Zsource (Ω)
L39	29.7	6.9	77.3	77+j97.6	23.2+j115.2	5.9-j5.1	50
L48	30.5	6.7	77	72.9+j97.6	23.2+j115.5	5.9-j5.0	50
L60	31.4	6.0	78.2	63.8+j107.5	25.4+j119.1	6.6-j7.4	50
L61	32.0	6.3	77.3	61.9+j99.7	23.8+j118.2	6.2-j6.1	50
O61	30.2	6.7	77.4	71.8+j98.7	23.3+j114.9	6.0-j5.1	50

Table 9 : Summary of performance monitored during loadpull measurements. Vds=40V and Ids=50mA/mm

Sample	Linear Gain (dB)	Output Power (W)	PAE max (%)	Zload f0 opt PAE (Ω)	Zload 2f0 opt PAE (Ω)	Zload 3f0 opt PAE (Ω)	Zsource (Ω)
L39	29.5	7.0	76.7	72.9+j97.5	23.0+j114.6	5.9-j5.1	50
L48	30.1	6.8	76.3	72.8+j97.6	23.4+j115.7	5.9-j5.0	50
L60	31.6	6.2	77.7	61.4+j103.6	28.5+j133.6	8.3-j9.9	50
L61	31.5	6.2	77.4	61.5+j103.7	28.8+j134.4	8.2-j9.7	50
O61	29.9	6.8	76.8	72+j98.9	23.6+j115.7	6.0-j5.4	50

Table 10 : Summary of performance monitored during loadpull measurements. Vds=40V and Ids=75mA/mm

2.1.3.2 Unitary cell modeling activity. Run-1

The model provided is a 3 ports transistor model. It is an electro-thermal model. All parameters of the models are available as well as the temperature variable. The model topology is illustrated below.

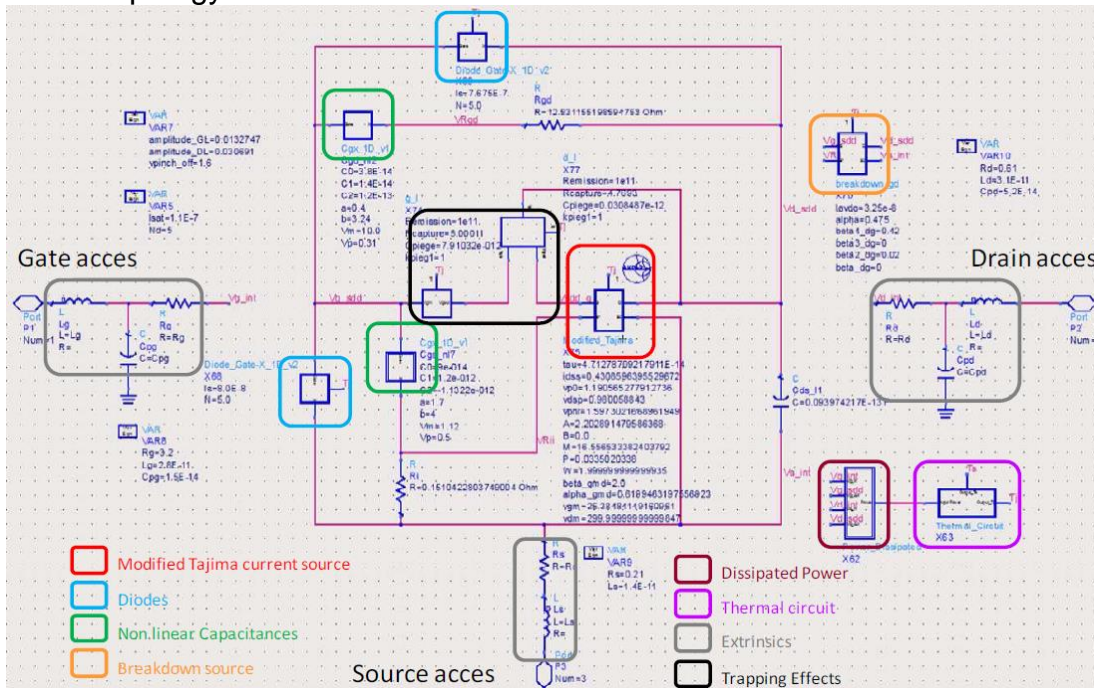


Figure 26 : Elementary transistor cell 8x250µm GH50. Model implemented in ADS

The model adjustment still be a trade-off between all the type of measurements (I(V), [S], load-pull...) and the different operating conditions (bias, temperature, frequency...) in order to have a coherent model. Some comparison (measurements/simulations) are provided below the very good accuracy of the transistor model.

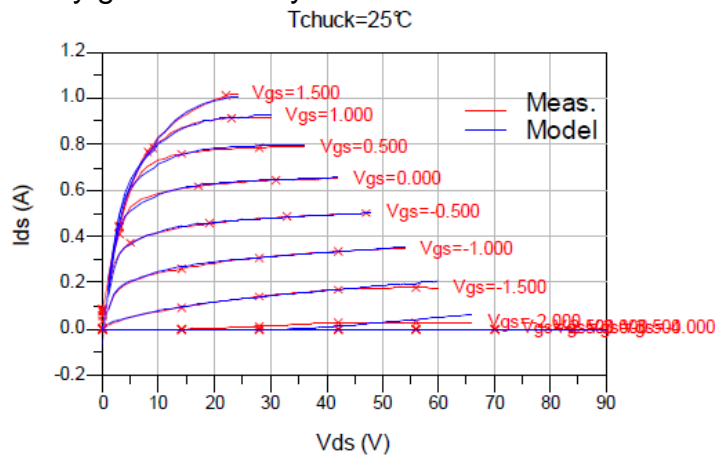


Figure 27 : 8x250µm transistor model validation. I(V) curves comparison. Bias conditions : Vds=40V, Ids0=25mA/mm. Temp=25°C

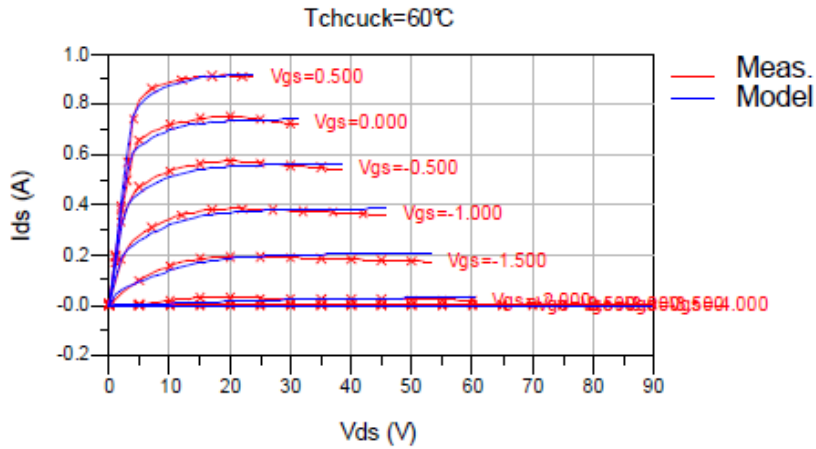


Figure 28 : 8x250µm transistor model validation. I(V) curves comparison. Bias conditions : $V_{ds}=0V$, $V_{gs}=0V$. Temp=60°C

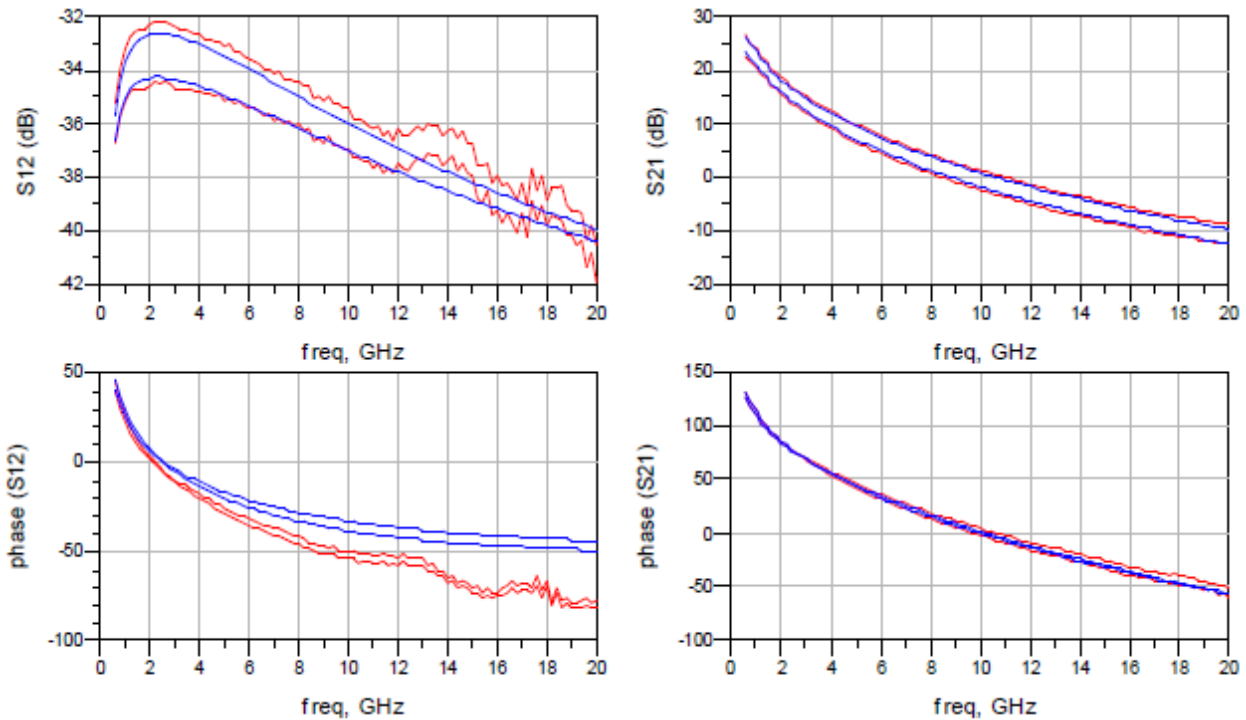


Figure 29 : 8x250µm transistor model validation. [S] parameters comparison. Measurement. vs Model 8x250µm @ $V_{ds0}=40V$ and $I_{ds0}=25mA/mm$

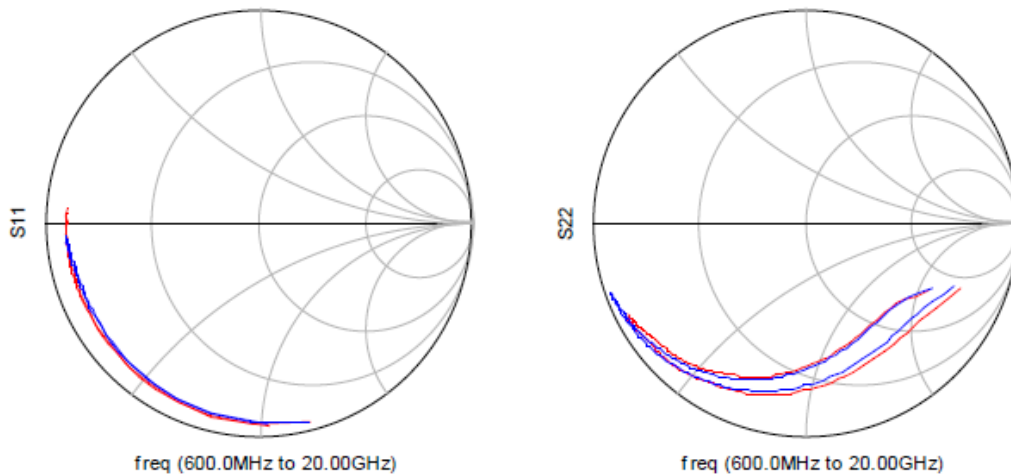


Figure 30 : 8x250µm transistor model validation. [S] parameters comparison. Measurement. vs Model 8x250µm @Vds0=40V and Ids0=25mA/mm

In the load-pull configuration, the comparison is performed at RF_freq=1,57GHz and for several load impedances including the optimum ones.

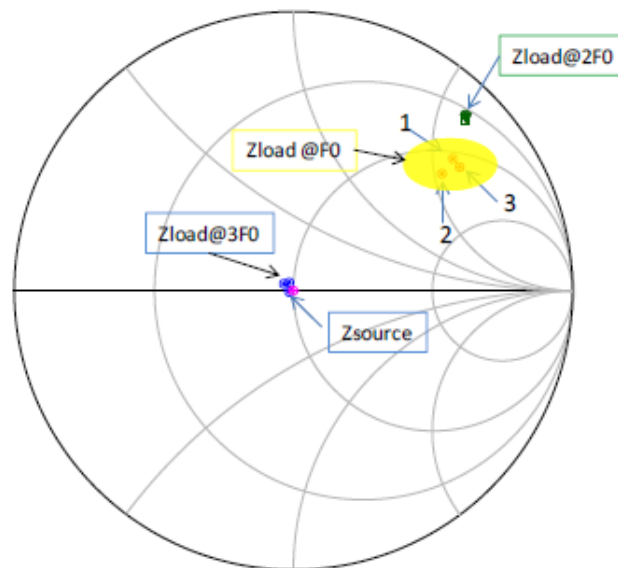


Figure 31 : 8x250µm transistor model validation. Selected impedances used for loadpull simulations/measurements comparison

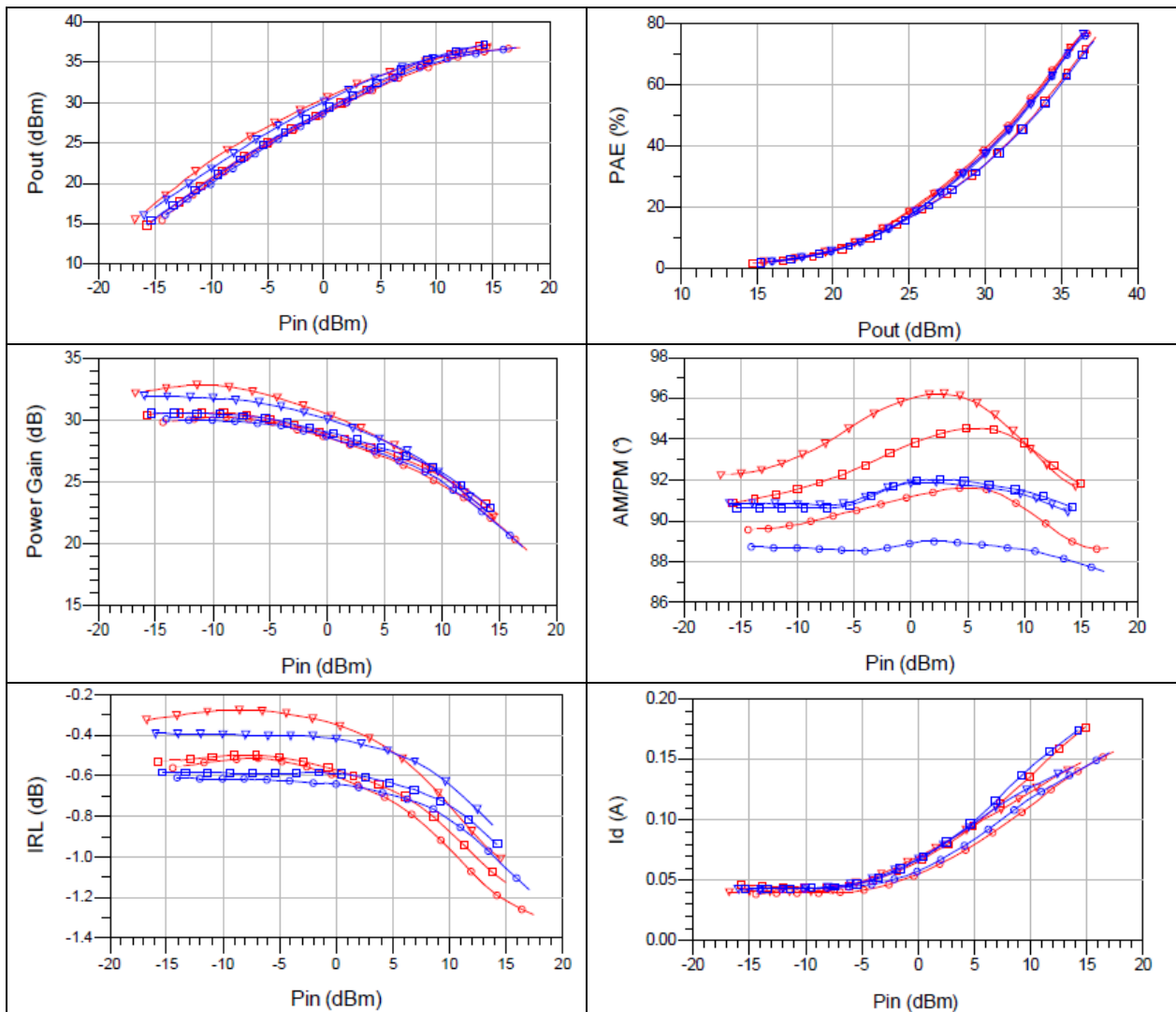


Figure 32 : 8x250µm transistor model validation. Loadpull simulations / measurements comparison. Vds0=40V and Ids0=25mA/mm

2.1.3.3 Power Bar measurements. Run-1

This paragraph sums AMCAD Engineering works achieved on the GaN Power Bar (8x8x250um) provided by Thales Alenia Space: Load-pull measurements PAE optimization (f0, 2f0). The tasks consisted in :

- load-pull measurements to determine the optimum load impedances for the best PAE,
- source impedance is set in order to obtain max Pin.

During the power bar measurements, the operating conditions used are the following:

- RF signal is in pulse mode: F0=1.57 GHz,
- Pulse width=100µs, Duty cycle=5%.

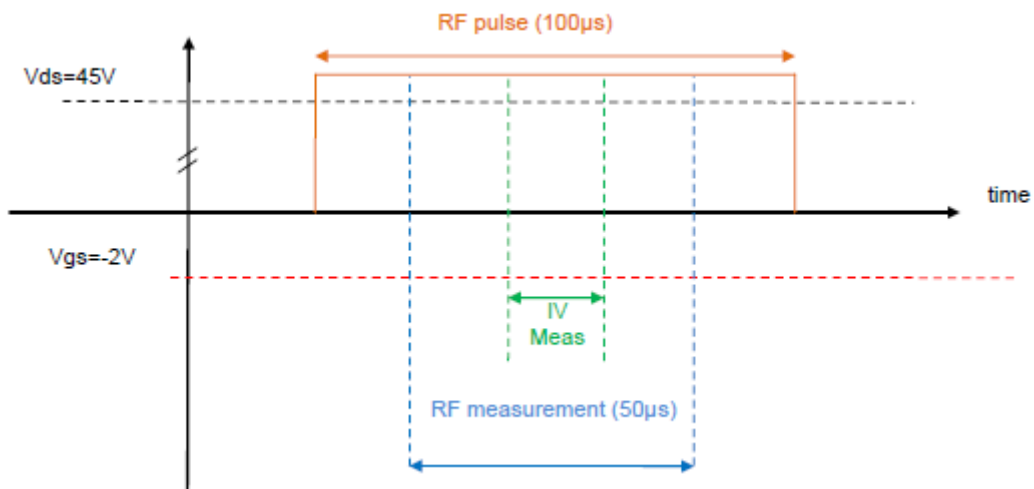


Figure 33 : Measurement chronogram of the Power bar

The Load-pull test bench used during power bar measurement is described below:

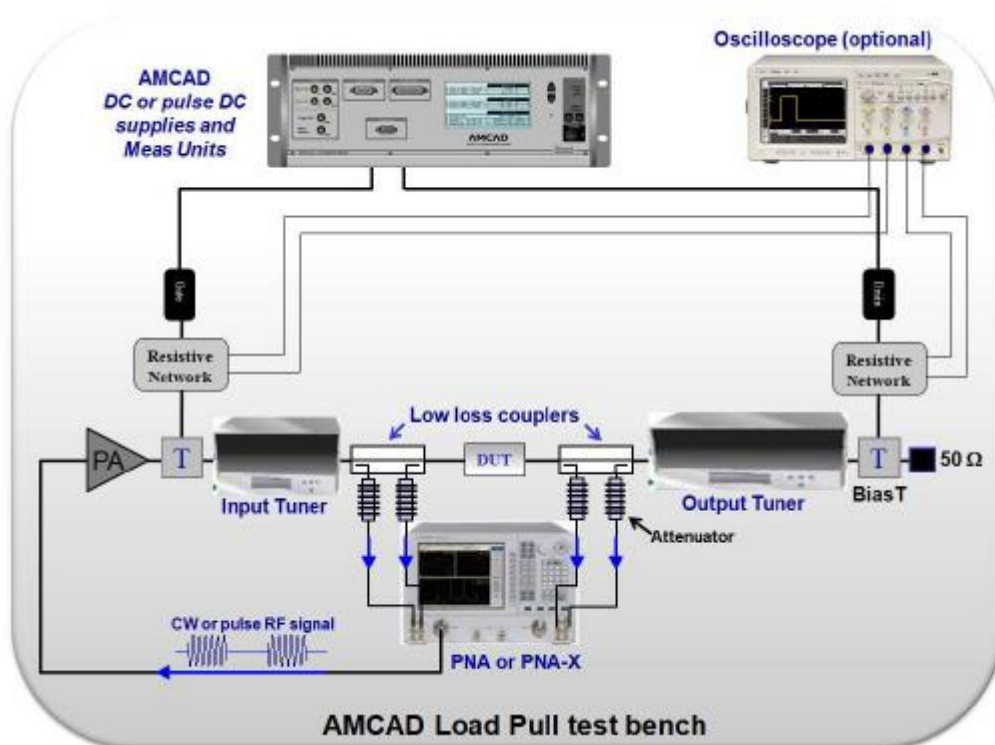


Figure 34 : AMCAD VNA-based load-pull system used for loadpull measurement of power-bar

Two types of measurements are made:

- Direct measurements in the SMA connectors plans
- Measurements in the power bar plans with a de-embedding step

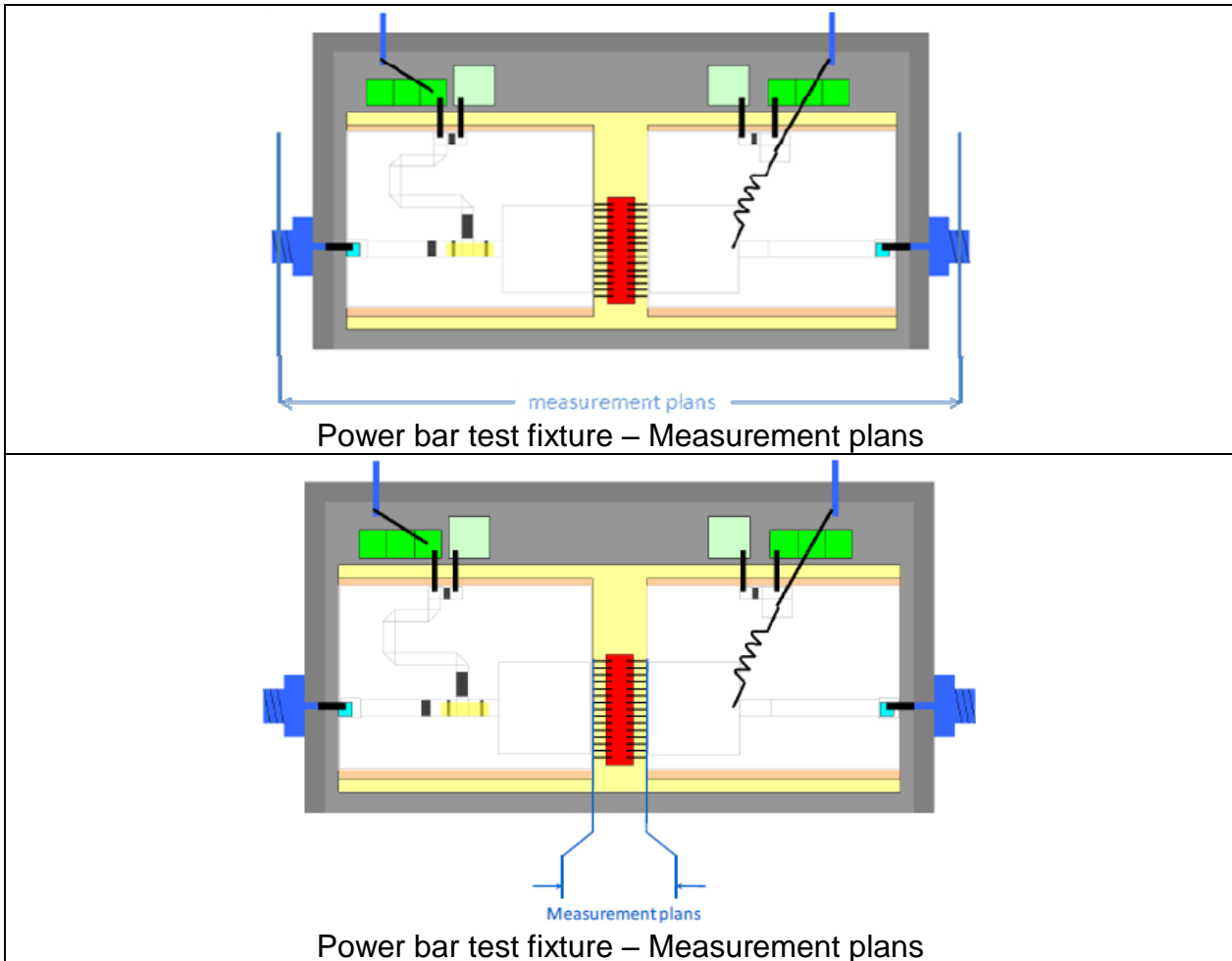


Figure 35 : Power bar test fixture – two types of measurement plans

In order to provide measurements to the power bar plan a TRL kit has been provided by Thales Alenia Space. From the calibration kit provided, S-parameters files representative of the input circuit (Mic_IN) and output circuit (MIC_Out) of the power bar have been built.

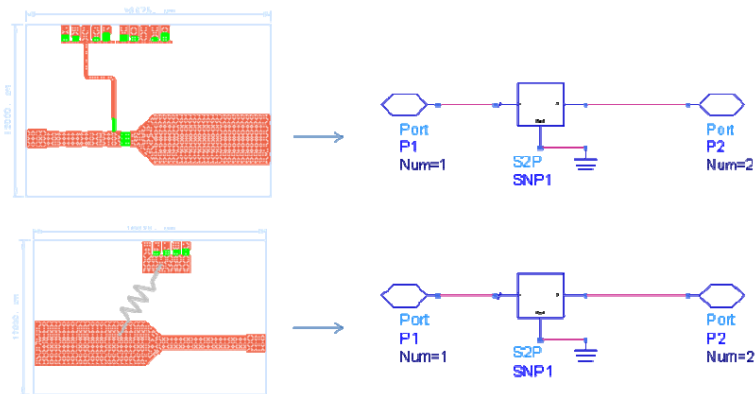


Figure 36 : MIC_In / MIC_Out

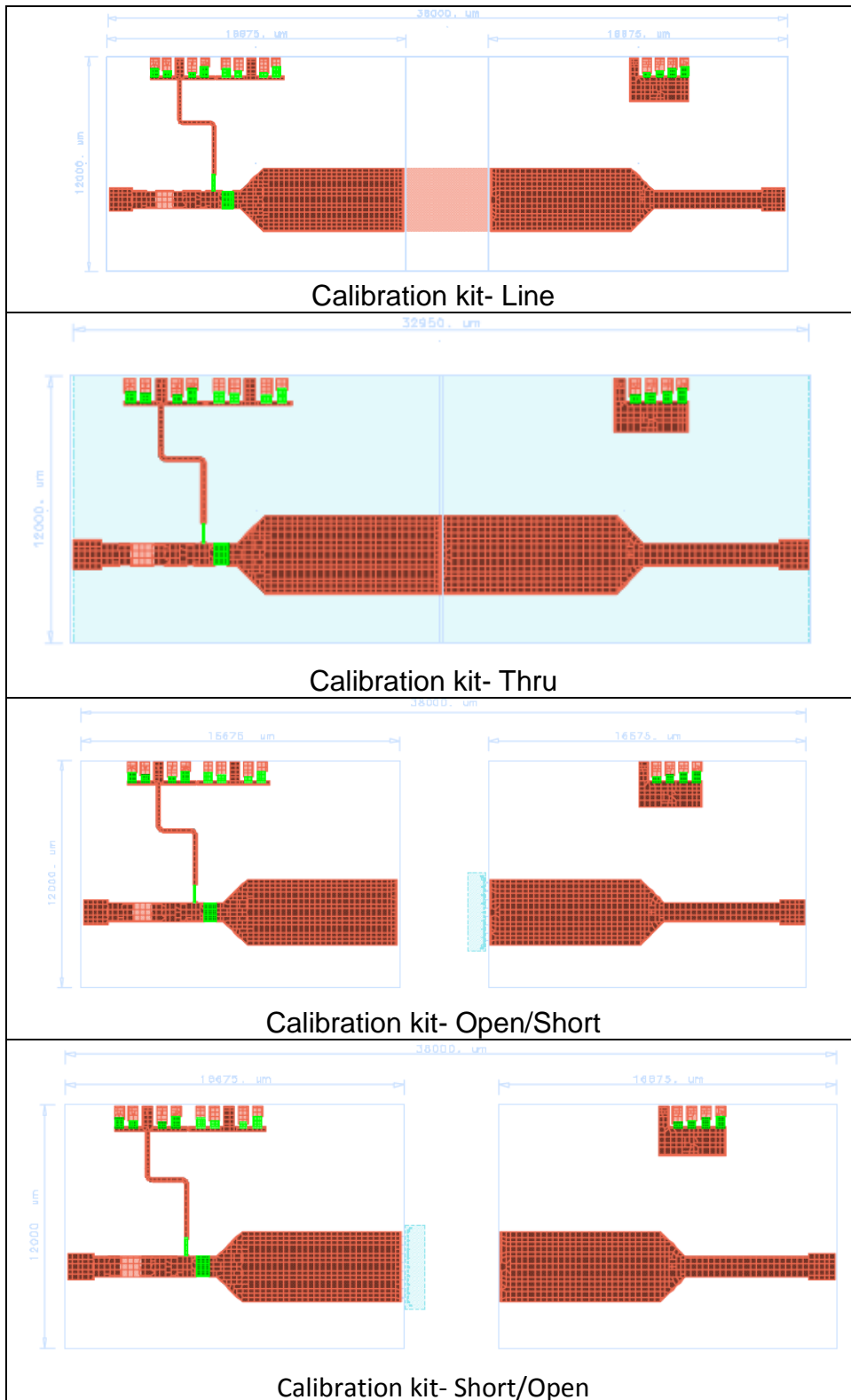


Figure 37 : TRL kit

The power bar characteristics could be defined using measured S-parameters files of the input and output fixture. With the de-embedding files all the performances are transformed.

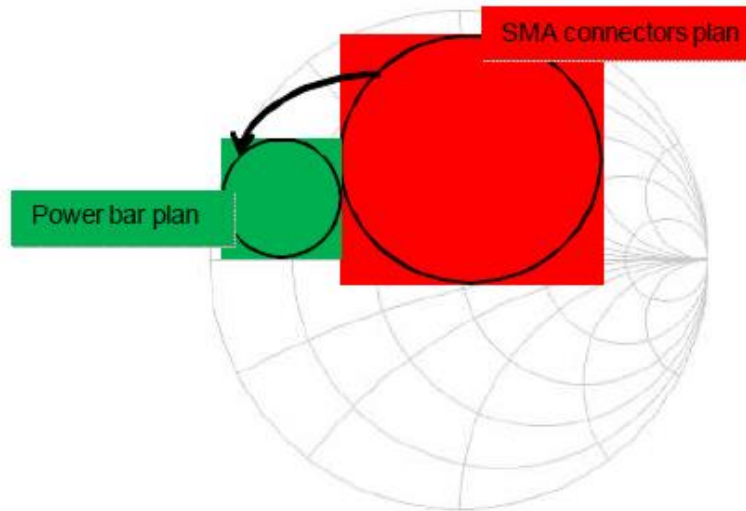


Figure 38 : Example of a load impedance transformation caused by the de-embedding (@F0)

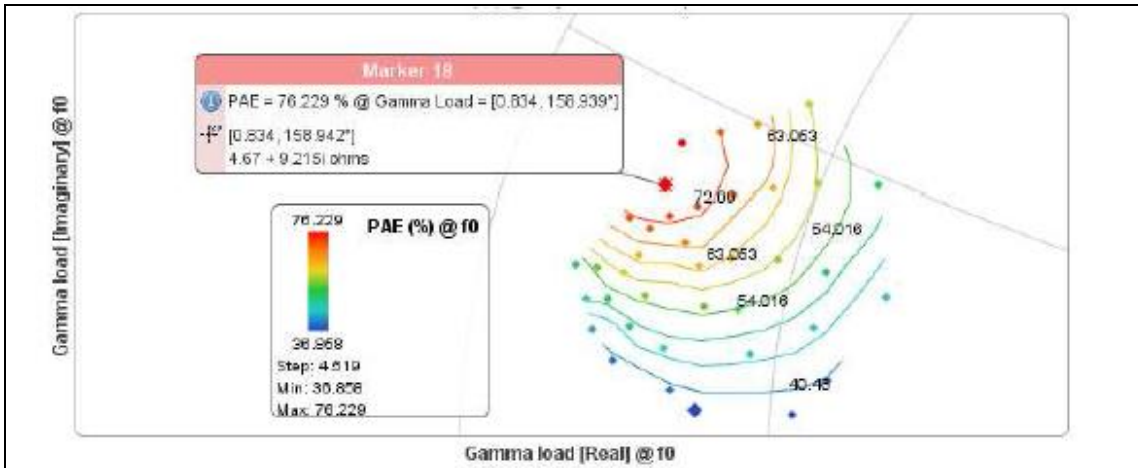
2x power bars have been measured with load-pull test bench under the following conditions

- Measurements @ 1.57 GHz with $V_{ds0}=45V$ $I_{ds0}=400mA$ (25mA/mm), SMA reference plane, power bar n°4
- Measurements @ 1.57 GHz with $V_{ds0}=45V$ $I_{ds0}=400mA$ (25mA/mm), SMA reference plane, power bar n°2
- Measurements @ 1.57 GHz with $V_{ds0}=45V$ $I_{ds0}=400mA$ (25mA/mm), Power Bar reference plane, power bar n°4
- Measurements @ 1.57 GHz with $V_{ds0}=45V$ $I_{ds0}=400mA$ (25mA/mm), Power Bar reference plane, power bar n°2

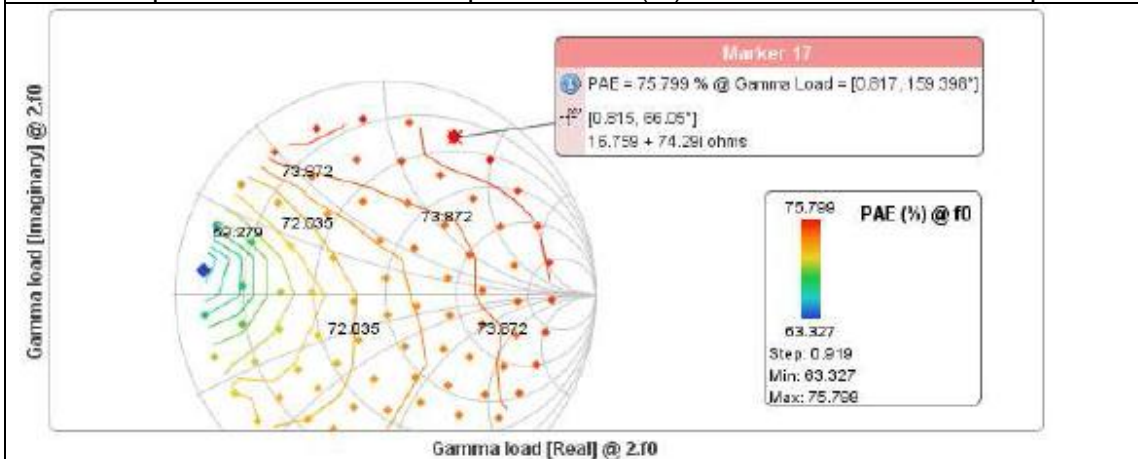
For each power bar, the loadpull optimization methodology used during the campaign is:

- First optimization of Z_{load} @ F_0 (fundamental frequency)
- Optimization of Z_{load} @ $2F_0$
- New optimization of Z_{load} @ F_0 with $Z_{load}@2F_0$ optimized
- Final monitoring of the performance of the power bar for the load impedance ($Z_{load}@F_0$ and $Z_{load}@2F_0$) around the optimum PAE

Performance of the Power bar n°4 monitored in the Power-Bar reference plan are presented below:



Final optimum Zload @F0 on optimum PAE (%). Power Bar n°4 reference plan



Final optimum Zload @2F0 on optimum PAE (%). Power Bar n°4 reference plan

Figure 39 : Measurements @ 1.57 GHz with Vds0=45V Ids0=400mA (25mA/mm), Power Bar reference plane, power bar n°4. Optimum Zload @f0 and @2f0

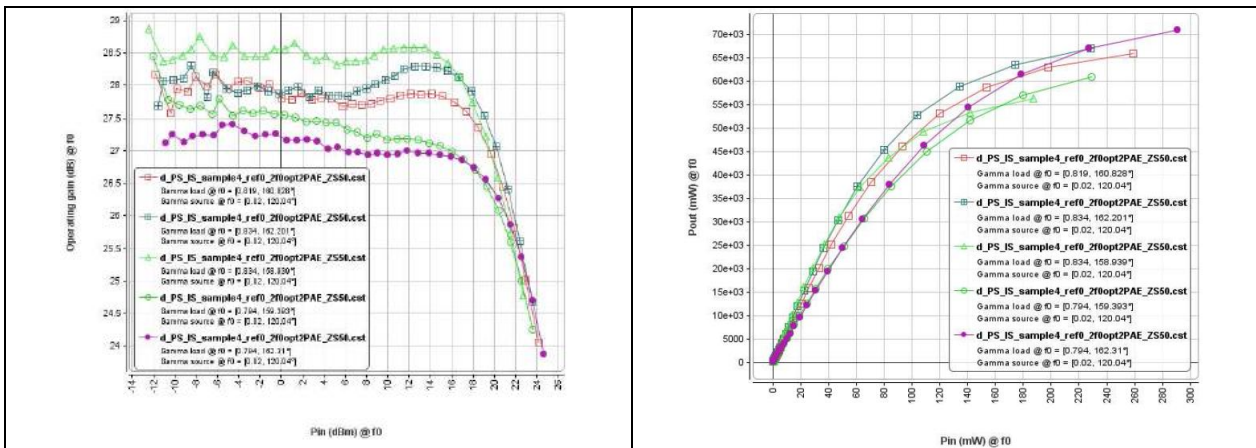


Figure 40 : Measurements @ 1.57 GHz with Vds0=45V Ids0=400mA (25mA/mm), Power Bar reference plane, power bar n°4. Gain(dB) / Pout(dBm) vs Pin(dBm)

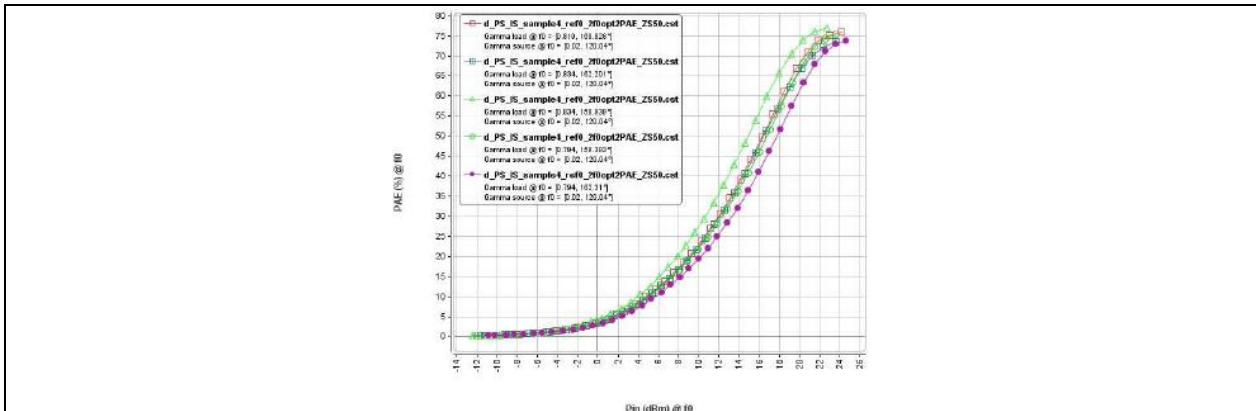


Figure 41 : Measurements @ 1.57 GHz with $V_{ds0}=45V$ $I_{ds0}=400mA$ (25mA/mm), Power Bar reference plane, power bar n°4. PAE(%) vs Pin(dBm)

Load pull measurements demonstrate that power bar $8x8x250\mu m$ could reach more than 67% PAE (sample 2) in the SMA connectors and more than 77% (sample 2) in the power bar plan. The maximum PAE was obtained with a superior 60W output power. The two samples presented in this manuscript (sample 4 and sample 2) have equivalent performance (Pout, PAE, Power Gain, ...). The optimum impedances area is the same.

2.1.3.4 Power Bar modeling activity. Run-1

The objectives have consisted to validate the nonlinear electro-thermal model of the power bar $8x8x250\mu m$ based on UMS GH50_10 technology. The power bar is based on the assembly of 8 transistors of GH50_10 Technology. Each transistor is made of 8 fingers of $250\mu m$ width. The electrical part of the transistor model has been performed by AMCAD Engineering, the thermal part by XLIM. This report takes into account of the results obtained and mentioned in the AMCAD and XLIM reports. Loadpull measurements performed by AMCAD for the power bar have been used for extraction as well as TAS simulations. The test set is presented in figure below. Two types of measurements have been considered: deem bedded or in the SMA connector planes. The deem bedding circuits have been either measured by AMCAD or simulated by TAS.

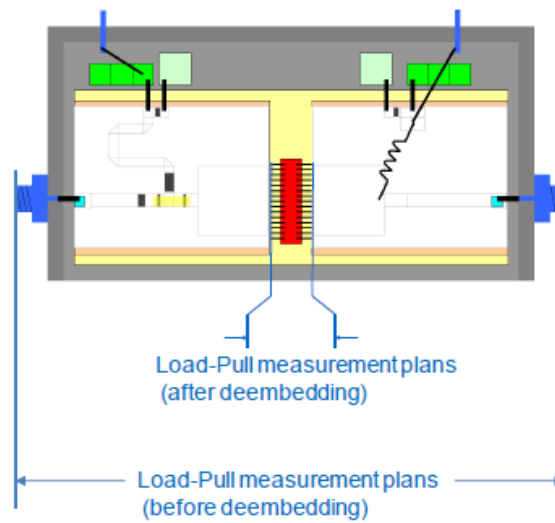
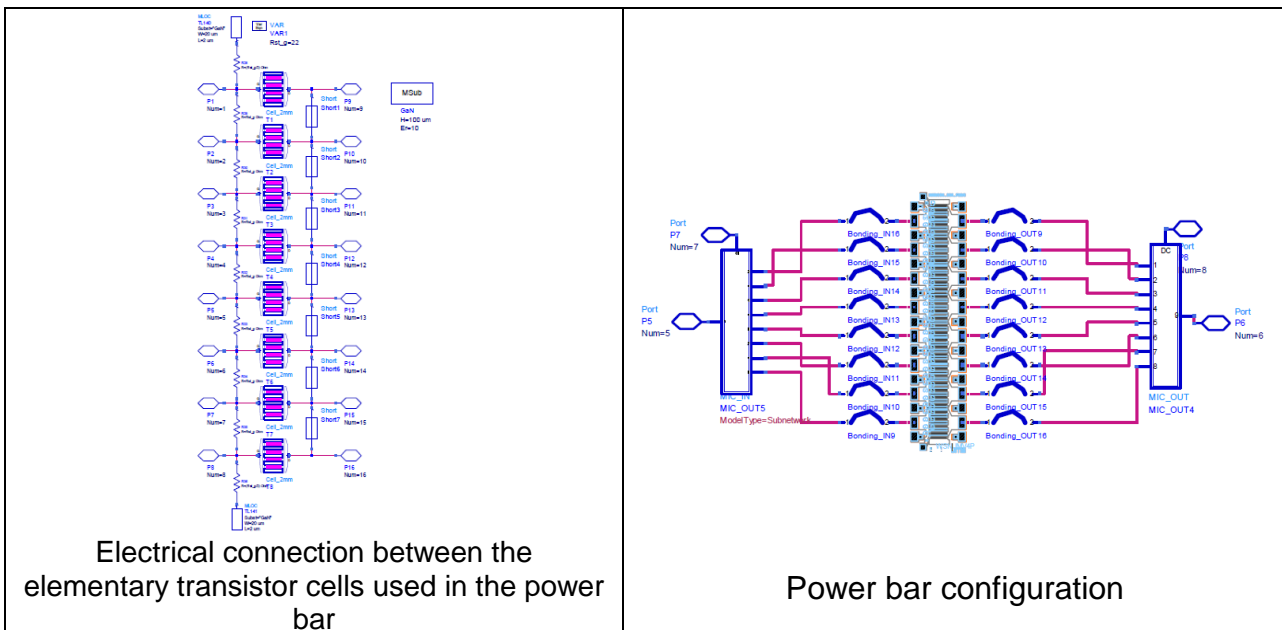


Figure 42 : Measurement test set off the power bar

The 2mm elementary transistor cells are connected at the drain with a short circuit and connected through a resistor at the gate as shown in figure below. According to the thermal study performed by XLIM, coupling circuit are necessary between the elementary transistor cells. For measuring this power bar, an input circuit and an output circuit have been added. The power bar is connected through wire bondings to input and output circuit as shown in figure below. Wire bondings are represented by their S parameters. Input circuit and output circuit are represented either by what a simulated circuit or S parameters of these circuits.



Electrical connection between the elementary transistor cells used in the power bar

Power bar configuration

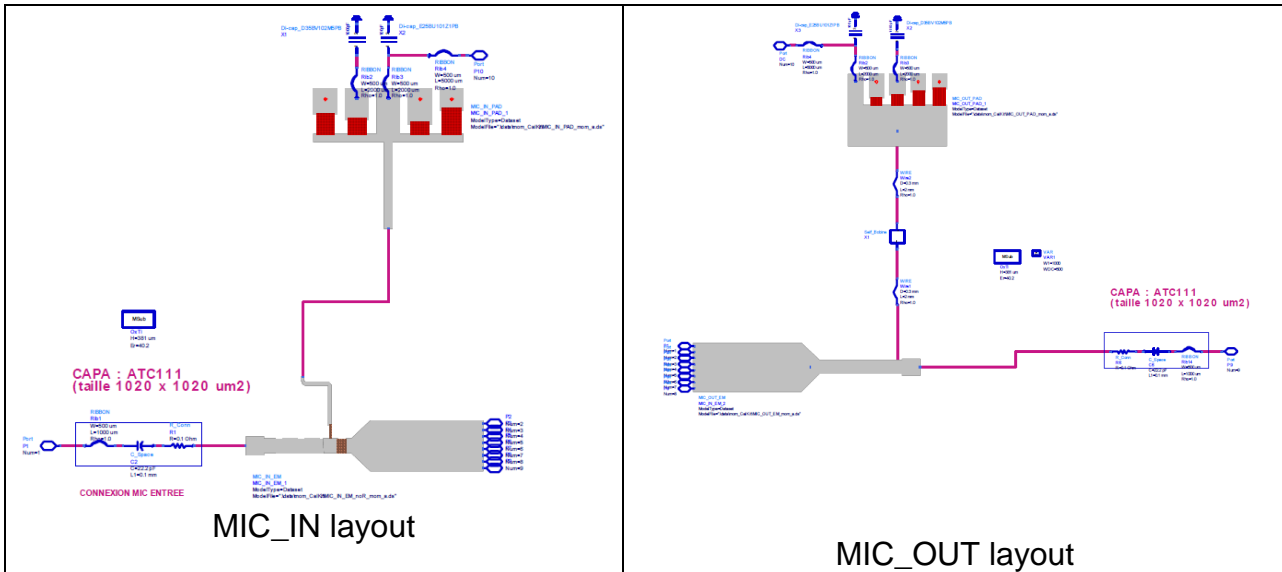


Figure 43 : Electro thermal Model of the Power bar

For measurements and simulations comparison, 3 samples have been considered. They are called sample 2, 4 and 5 to keep the same names as those given by AMCAD during measurements.

A first simulation has been performed in the SMA connector planes. This simulation reveals results which are not sensitive to variation of power bar parameters.

Then, simulation have been performed in the power bar reference plan: deem bedded results before wire bondings for the input and after wire bondings in output have been considered.

Several cases have been considered to sweep loads in term of power optimization or PAE optimization. The results are presented below for sample n°4. The results presented are the output power versus the input power, the PAE versus the input power the DC drain current, the power gain, and the Gamma in (input reflection coefficient). The time domain waveform of current and drain voltage is also presented.

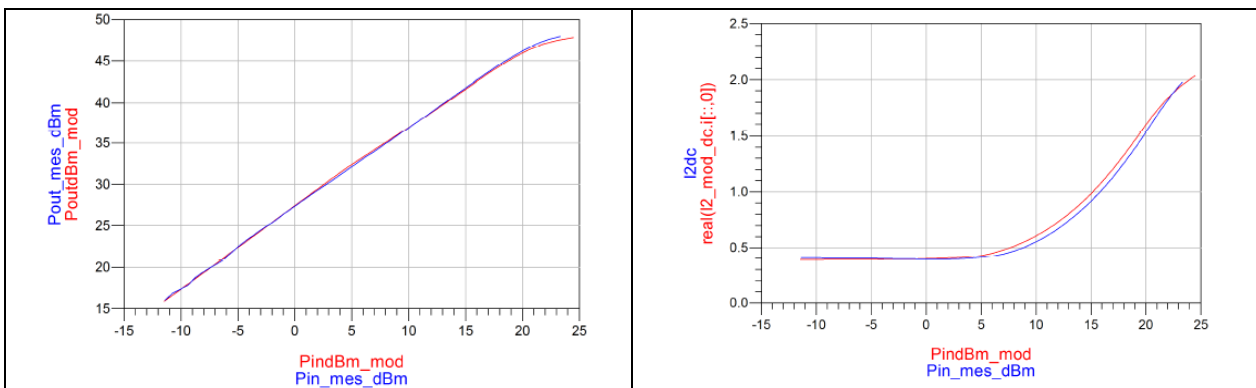


Figure 44 : Pout vs Pin and DC drain current versus vs Pin. Comparison between simulation and measurements for power bar sample4

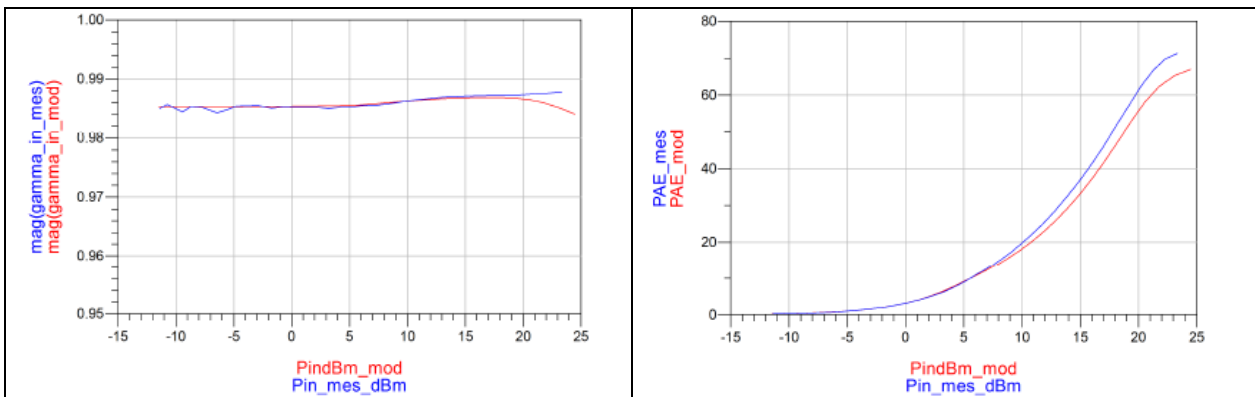


Figure 45 : Input reflection coefficient versus Pin and PAE versus Pin. Comparison between simulation and measurements for power bar sample4

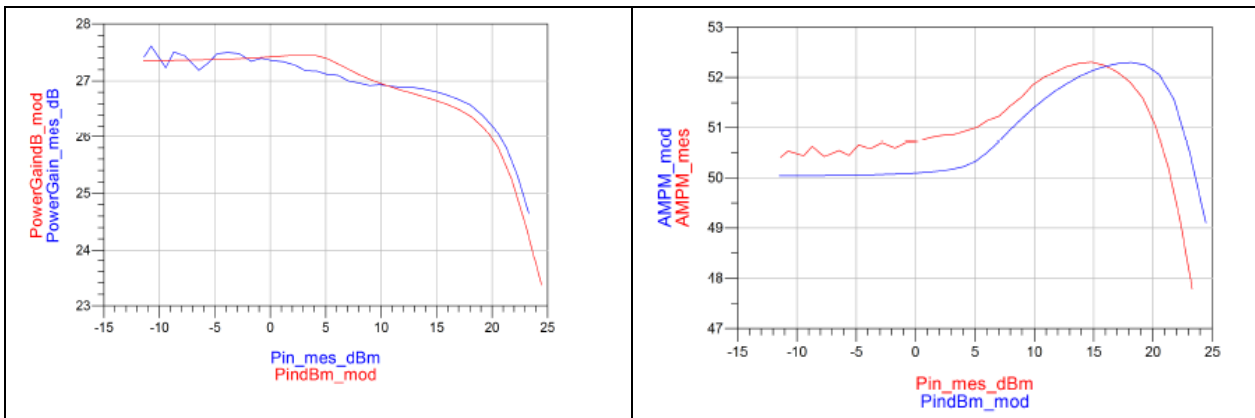


Figure 46 : Power Gain vs Pin and AMPM vs Pin. Comparison between simulation and measurements for power bar sample4

Comparing measurement to simulation obtained from the nonlinear electro-thermal model lead to the following remarks:

- It is crucial to perform the comparison in the plane where changes in the model parameters provide reasonable changes in the observed performances. Clearly, connector planes are not adequate for this.
- Wire bondings must be accurately modeled mainly from the point of view of the losses as they largely impact the input reflection coefficient of the power bar which is close to 1. When the losses of the input are poorly modeled, they must be compensated in the simulation to reach consistent results.
- On key point which still remains unclear is the behavior of the drain current as the input power increases the modeled one is always larger than the measured one. This could be due to traps that are activated when the device reaches pinch-off and reduce the current, but this phenomenon does not clearly appears in the unit cell. Works still have to be performed on this particular point.

2.1.4 Detailed Design. Run-1

Starting from baseline design performed in WP3100 and presented in chapter 2.1.1, design has been finalized with NL electro-thermal model of the power bar provided by AMCAD and XLIM.

Simulations results are presented in this report:

- S-Parameters simulations
- Non-linear simulations with CW signal
- Stability analysis (STAN)
- HPA analysis with multicarrier signal

Design of the HPA has been undertaken to reach the best possible performances with priority on PAE. First of all, optimal output load impedances at fundamental, second and third harmonic frequency have been searched and identified

GH50 technology enables designs up to 53.3V (AMR) of drain voltage. In the following study, spatial derating ratio of 75% has been applied regarding AMR drain voltage, leading to a maximum biasing drain voltage $VD0 = 40V$. This value has been confirmed by UMS. According to the baseline design, load-pull measurements and simulations have been compared at the following transistor quiescent point:

Frequency	Vdso	Idso	Simulation type
1.57 GHz	40 V	25 mA/mm	CW

Optimum $8 \times 250 \mu m$ transistor output loads have been determined at both fundamental (H1) and second harmonic (H2) frequency using AMCAD $8 \times 250 \mu m$ transistor load-pull measurements data of baseline design. In addition, load-pull simulations with both UMS and AMCAD transistor models have been performed to confirm these data.

Crossing load-pull measurements and simulation results at transistor level have allowed us to define an optimum load impedance area at both H1 and H2.

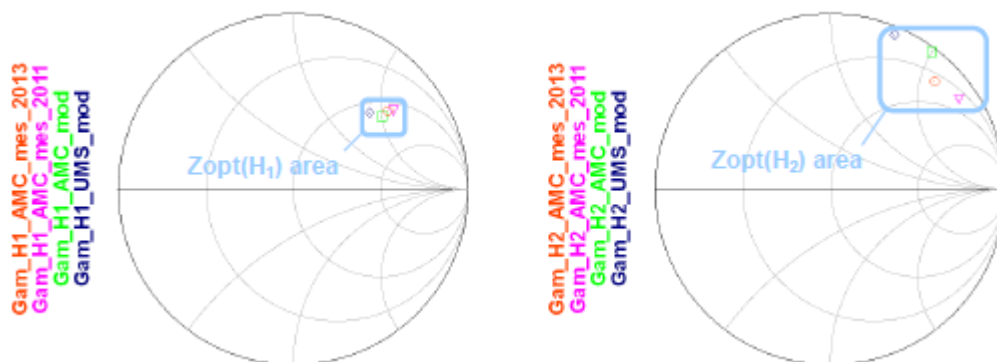


Figure 47 : Optimal load impedances found at fundamental (left) and 2nd harmonic (right) frequencies based on $8 \times 250 \mu m$ transistor load-pull measurements and simulations.

As a result, $Z_{opt}(H1)$ & $Z_{opt}(H2)$ area have been taken as load impedance goals to design the HPA. Load-pull measurements have pointed out that PAE performances are not sensitive to the third harmonic frequency over a wide load impedance area

($\pm 2\%$). This is the reason why the Zopt(H3) area have been optimized to be kept in this sweet spot area during the HPA design.

In order to optimize and predict accurately the HPA performances, package RF insert, capacitors and inductors have been carefully simulated and/or measured to secure the design result.

To simulate input and output package RF ports, simulations have been performed using insert model based on HFSS 3D electromagnetic simulations.

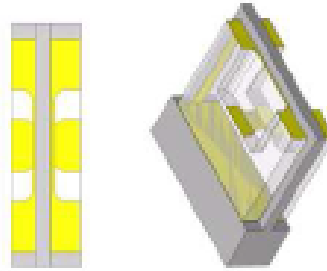


Figure 48 : Overview of the RF insert used with the CuD package

In order to optimize the simulation results, homemade discrete capacitors model have been used whereas S-parameter files (coming from measurements data) have been used to simulate discrete self inductors used for DC biasing. Due to both input and output matching networks size constraints and the need of high distributed capacitance effect to synthesize appropriate input and output load impedances, high dielectric constant material has been used : $\epsilon_r = 40$; $T = 381\mu\text{m}$; $\text{TanD} = 0.0003$

Input and output combiners have been fully optimized by means of EM simulation up to 10GHz. Engrave resistance sheet has been chosen as low as possible ($6\text{W}/\square$) to enable the design of resistors in series with the gate of each transistor. In this way, both even and odd mode stability issues have been managed at the same time.

The following figures shows the small signal behavior of the HPA in a wide frequency range

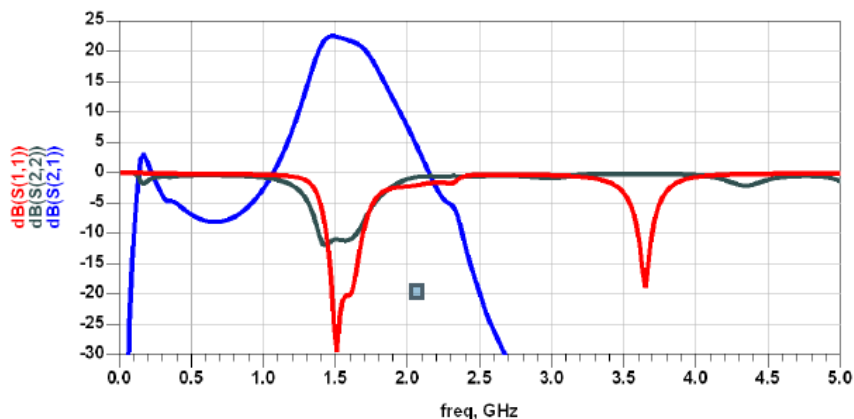


Figure 49 : S-parameters wide frequency band analysis

S21 parameter drops below 0dB for frequency higher than 2.2GHz. HPA design

have been managed to break the very high gain of the power bar at frequency below 1GHz. In that way, low frequency and Fo/2 oscillation issues will be prevented.

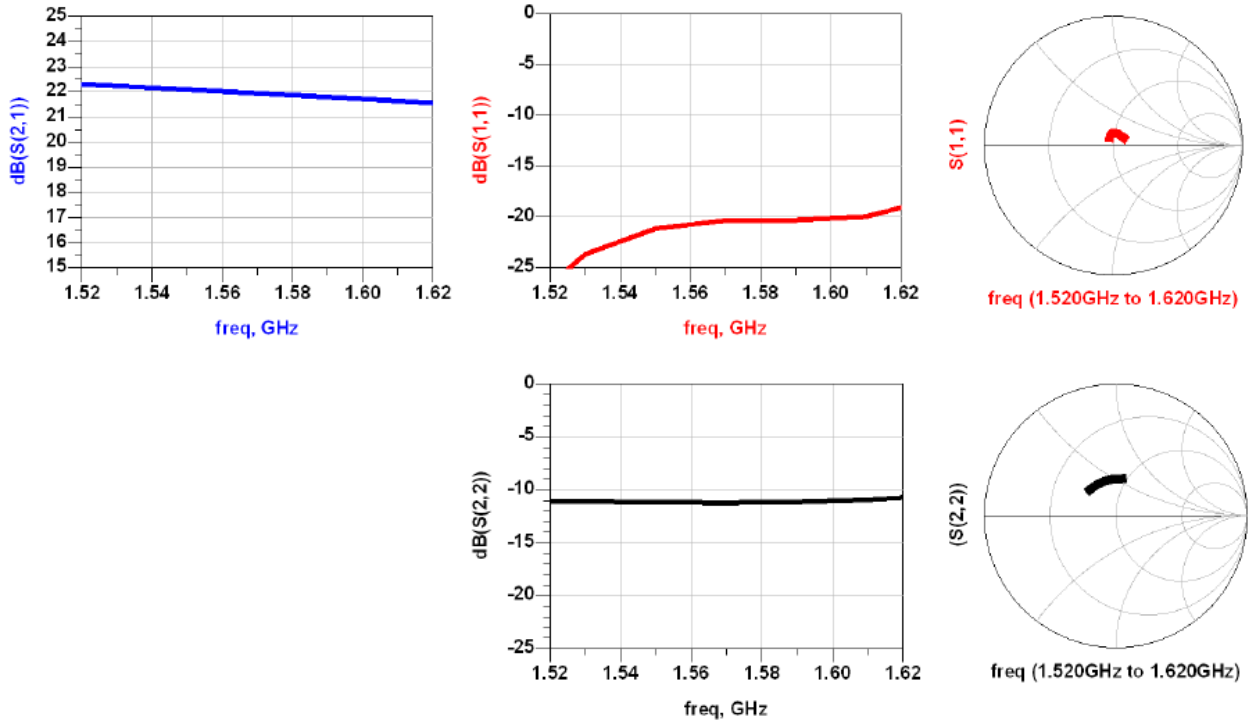


Figure 50 : S-parameters in-band frequency analysis

We can see that the HPA exhibits a S21 of 22dB at center frequency with a slight negative slop over the frequency bandwidth of interest. In addition, we can focus on the S11 that have been optimized to enable an in-band input return loss better than -20dB.

The necessary and sufficient conditions for unconditional stability are that the K stability factor is greater than unity and the B stability measure is positive. K factor and B stability measure are given below. According to the unconditional stability definition, no stability issues have been highlighted at small signal level.

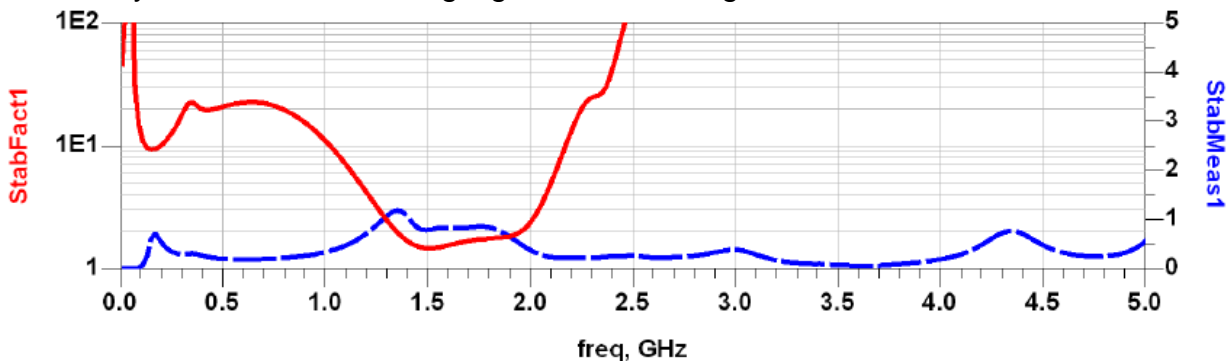


Figure 51 : K stability factor & B stability measurements. Wide frequency band analysis.

To point out the consistency of the HPA optimization, synthesized output load impedances at H1 and H2 are shown below.

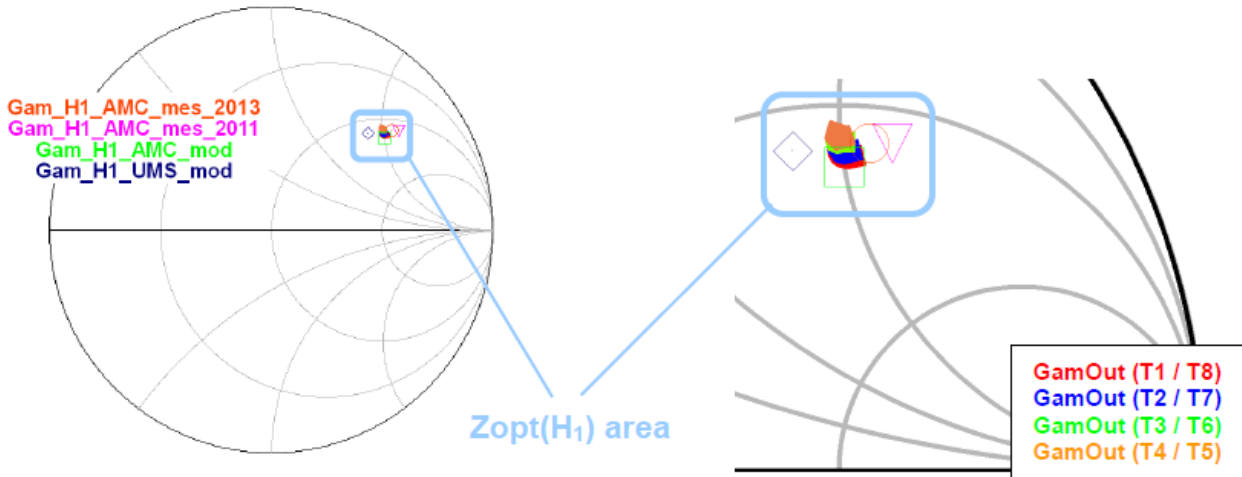


Figure 52 : Synthesized output impedances at fundamental frequency (H1) from 1.52GHz to 1.62GHz

Previous figure shows the load impedances synthesized at the output of each transistor of the $8 \times 8 \times 250 \mu\text{m}$ power-bar. Due to the symmetry of the output combiner design, impedances of the transistor are superimposed 2 by 2. Zload(H1) between elementary transistor are very well balanced and perfectly match the targeted load impedance area.

Regarding 2nd harmonic load impedance behavior we can see that, again, even at H2 frequency all the transistors exhibits a very good load impedances balance. The targeted impedance area is also matched.

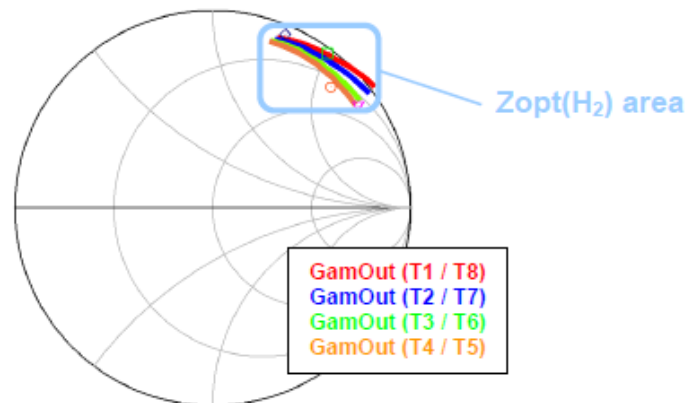


Figure 53 : Synthesized output impedances at 2nd harmonic frequency (H2) from 3.04GHz to 3.24GHz

Note that the design enable H2 load impedance tuning quasi-independently of the load impedance at the fundamental frequency by connecting metallization pads.

On top of that, output losses are given versus frequency on Figure 54, with input power in parameter. This confirm that low losses are simulated which should ensure PAE performances.

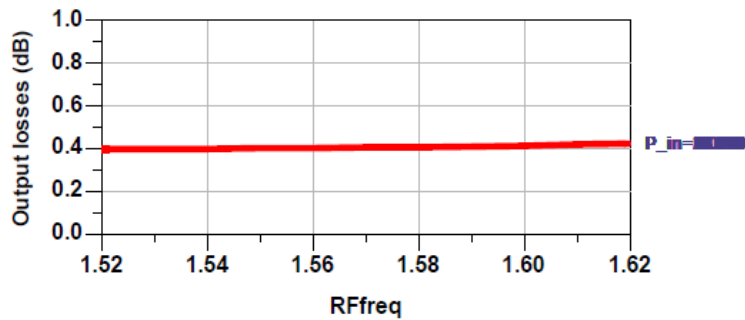


Figure 54 : Output combiner losses (dB) versus RFreq and input power(dBm)

The main RF performances obtained, output power, PAE and power gain are presented below versus input power and versus frequency.

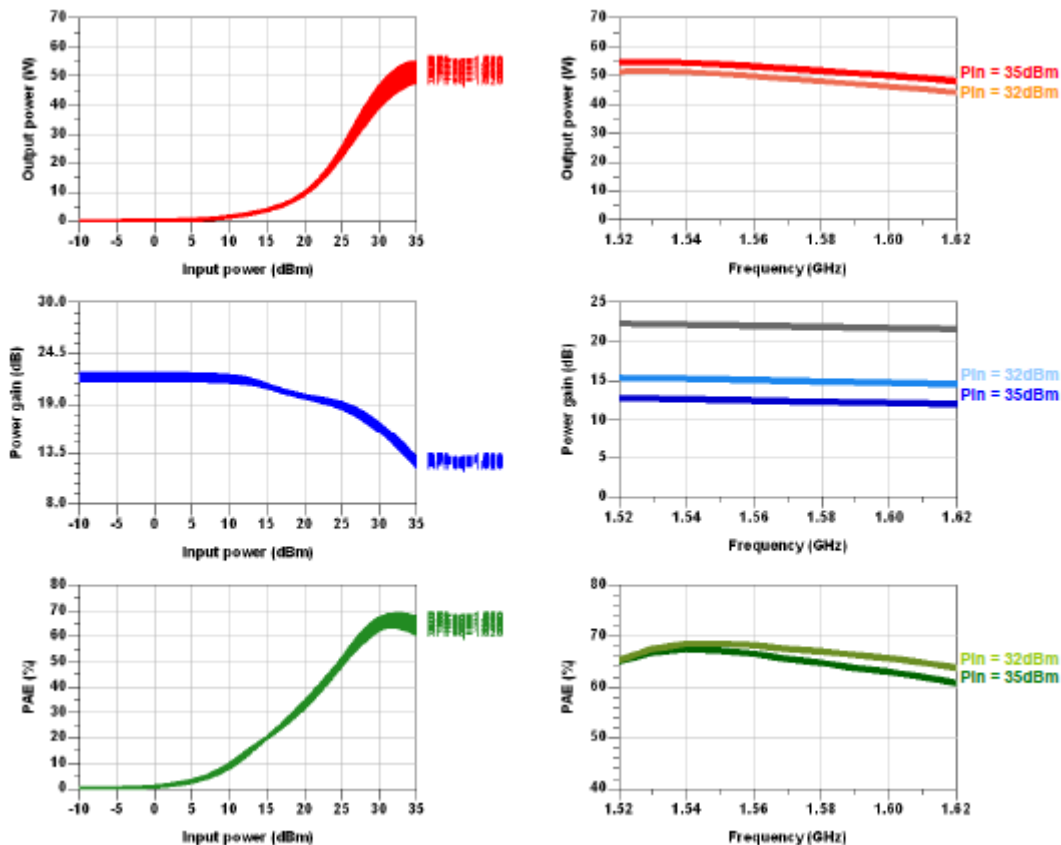


Figure 55 : HPA RF performances. Pout(W), PAE(%), Gain(dB) versus input power (dBm) and Frequency(GHz).

The frequency bandwidth reaches 100MHz for a center frequency of 1.57GHz. The maximum overall power added efficiency varies from 65 to 68% at $P_{in} = 32\text{dBm}$ and is associated to an output power of 45W to 52W. Figure 56 below, shows that between 32dBm and 35dBm of input power, the mean output power density is around 3.5W/mm.

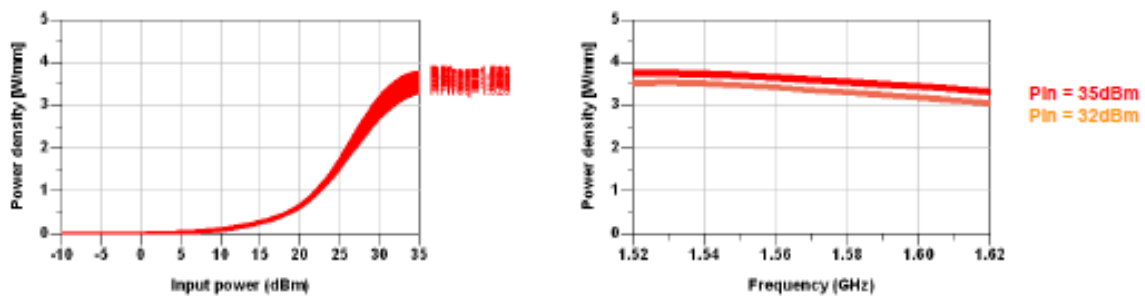


Figure 56 : Drain current and power consumption(W) vs. input power(dBm) – from 1.52 to 1.65GHz

DC drain and gate currents as well as DC power consumption have been drawn on figure below.

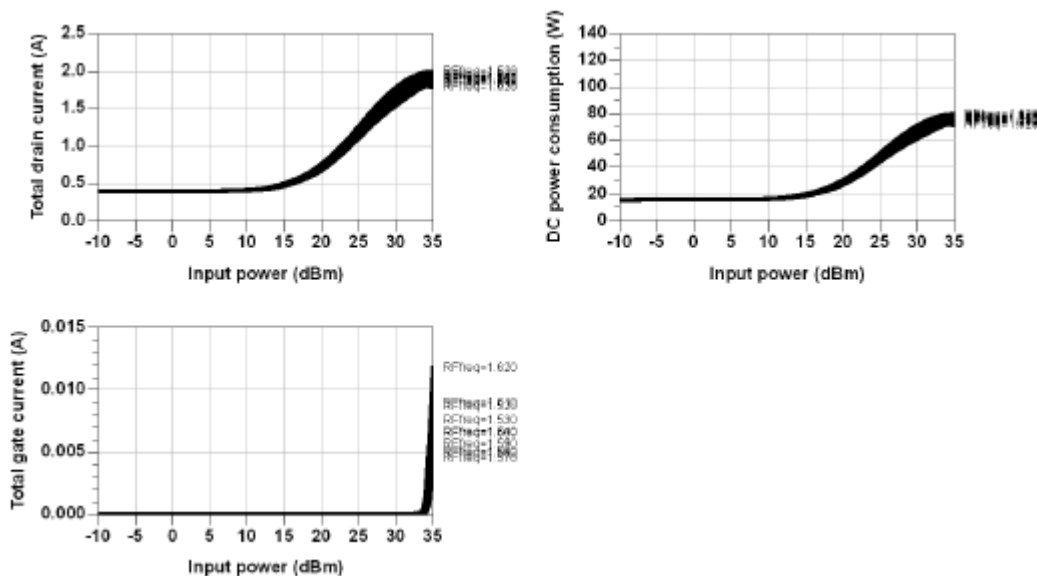


Figure 57 : Drain current and power consumption(W) vs. input power(dBm) – from 1.52 to 1.65GHz

Thanks to the electro-thermal capability of the transistor model, the main RF performances; output power, PAE and power gain; of HPA has been checked versus a temperature range from -10°C to 85°C . Main HPA performances are shown for an input power (@32dBm) corresponding to the maximum of PAE ($P_{in} = 32\text{dBm}$)

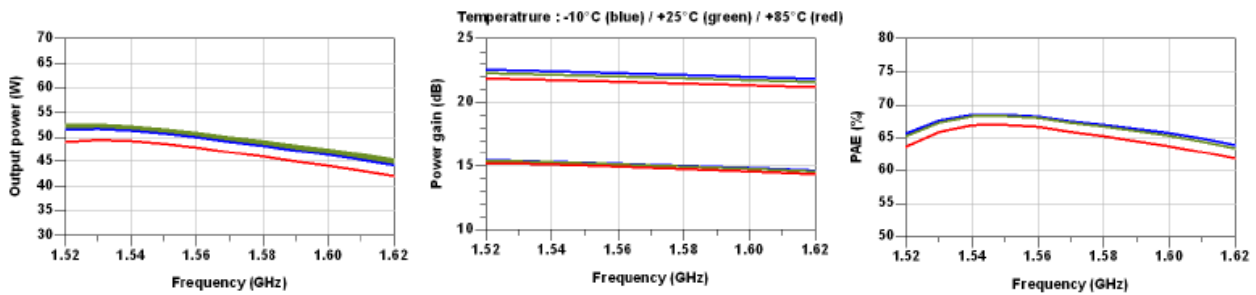


Figure 58 : HPA performances : Pout(W), PAE(%), Gain(dB) versus temperature [-10°C; 25°C, 85°C] @Pin(max PAE).

Performances are not very sensitive to the temperature, and RF performances slightly decrease by - 0.2dB on Pout and -2pts on PAE at high temperature. This phenomenon is mainly due to the power gain level drop as a function of the temperature.

HPA non-linear stability analysis has been performed using STAN software. Current probe was placed on transistor gate. The STAN analysis setup is given below:

- Temperature applied on transistor model: -10°C (wo rst case)
- Frequency pump (Fp): 1.57 GHz, 1.54 GHz, 1.6 GHz
- Frequency Band Analysis (FBA) : [0.05-2GHz]
- Nb of points within FBA: 300 up (arbitrary 15 to 20MHz step)
- Input power sweep (for each Fp) : [10 to 32]dBm / step 1dB
- Max. phase error tolerance : 10-1

According to results monitored during stability analysis, NO stability issues have been highlighted. Nevertheless, we have to point out that these results have to be taken with care because the transistor model is only validated for a drain voltage of 40V. Thus, all others drain voltage simulation results are extrapolated.

Finally, a Volti analysis has been done at HPA level to check the feasibility of the PAE, output power, NPR trade-off. Quiescent point used for multi-carrier simulation are: Vds=40V and Ids=25mA/mm. On the following figure, PAE, NPR and gain compression are drawn versus output power.

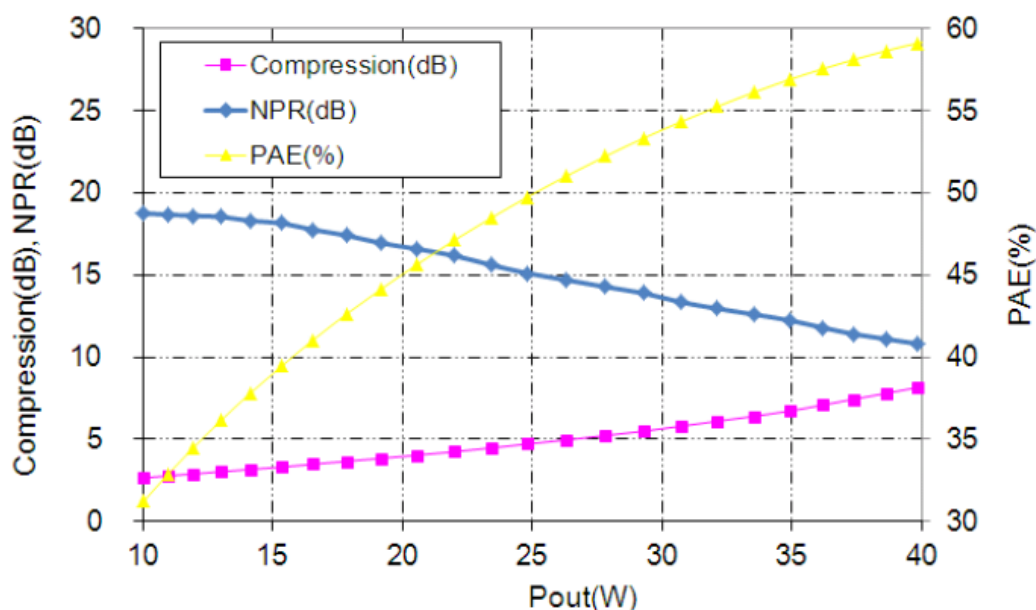


Figure 59 : HPA performances in multi-carrier mode : NPR(dB), compression(dB), PAE(%) versus Pin. Temp=25°C, Vds=40V and Ids=25mA/mm

RF SECTION		Gain	Cumul Gain	NF	Cumul NF	Signal Level	Signal level	NPR	Pdc	Pdiss	PAE	EPC	Gain Comp
N°	Elements	dB	dB	dB	dB	dBm	W	dB	W	W	%	N°	dB
INPUT													
1	Fixed ATT	0,00	0,00	0,00	0,00	27,00	0,5012	387,60	0,00	0,00	0,00		0,00
2	HPA_40V_VG_1_85V	16,96	16,96	10,00	10,00	43,96	24,8684	15,18	46,44	22,07	52,47	3	4,71
Total RF Section			16,96		10,00	43,96	24,87	15,18	46,44	22,07	52,47		4,71

Table 11 : HPA performances in multicarrier mode @NPR=15dB. Temp=25°C. Vds=40V, Ids=25mA/mm

RF SECTION		Gain	Cumul Gain	NF	Cumul NF	Signal Level	Signal level	NPR	Pdc	Pdiss	PAE	EPC	Gain Comp
N°	Elements	dB	dB	dB	dB	dBm	W	dB	W	W	%	N°	dB
INPUT													
1	Fixed ATT	0,00	0,00	0,00	0,00	27,30	0,5623	398,93	0,00	0,00	0,00		0,00
2	HPA_45V_VG_1_85V	17,45	17,45	10,00	10,00	44,95	31,2862	15,05	58,43	27,71	52,58	3	4,57
Total RF Section			17,45		10,00	44,95	31,29	15,05	58,43	27,71	52,58		4,57

Table 12 : HPA performances in multicarrier mode @NPR=15dB. Temp=25°C. Vds=45V, Ids=30mA/mm

Main performances (Pout/PAE/NPR) in multicarrier mode are compliant with specifications by using the quiescent point Vds=45V and Ids=30mA/mm

Following tables summarize the HPA performances reached for the center frequency 1.57GHz in both CW and multi-carriers mode.

CW mode : PAE peak performance for an input power of 32dBm. Vds=40V and Ids=25mA/mm.	
Parameters	Typ.
Output Power	50W
PAE	67%
Gain compression	7dBcomp (15dB)
Dissipated power	25W

Table 13 : Summary of simulated CW performances at HPA level

In CW mode, the simulated HPA performances match the RF specifications 50W output power and more than 65% of peak PAE in the 1.52GHz-1.62GHz bandwidth at 32dBm of input power. These performances are associated to a power gain of 15dB.

Multi-carrier mode : VOLT analysis Vds=45V and Ids=30mA/mm.	
Parameters	Typ.
Output Power	31.3W
PAE	52,5%
Gain compression	4,5dB
NPR	15dB

Table 14 : Summary of simulated multi-carriers performances at HPA level

In multi-carrier mode with NPR=15dB, the simulated HPA performances match the RF specification of 30W output power and more than 52% of PAE in the 1.52GHz-1.62GHz bandwidth. These performances are associated to a power gain of 17,5dB.

2.1.5 HPA-1 Module Manufacturing and Tests. Run-1

This paragraph establishes the report of tests performed on 3 L-band GaN HPA Modules.

3x L-band GaN HPA modules have been manufactured and tested: HPA#2 HPA#3 HPA#5. In the frame of this study, tuning of the HPA modules has been performed at Temp=25°C with CW signal in order to achieve maximum of PAE. Then [S] parameter measurements and power measurements with multi-carrier signal has been conducted.

The results are presented with the following outline

- [S] parameters measurements versus Temp=[-20°C , 25°C , 90°C] for HPA#2 module
- [S] parameter measurements versus Vd=[20V/25V/30V/40V/45V]. Temp=25°C for HPA#2 module.

- [S] parameters measurements versus Temp=[-20°C , 25°C , 90°C] for three HPA modules
- Power measurements (CW signal) versus Pin. Temp=[-20°C , 25°C , 90°C]. Vds=40V and Vds=45V, RF=[1,5425GHz / 1,5675GHz / 1,5925GHz] for three HPA modules
- Power measurements versus Pin. Temp=[25°C , 90°C]. Vds=45V, RF=1,5675GHz, Ids=[100mA / 200mA / 400mA / 800mA] for HPA#5 module
- Power measurements (multi-carrier signal) versus Pin. Temp=[-20°C , 25°C , 90°C]. Vds=45V. Ids=[100mA / 200mA / 400mA / 800mA] for HPA#5 module
- RF step stress measurements for three HPA module

2.1.5.1 [S] Parameter measurements. Run-1

Hereafter, on figure below the HPA-1 module (#2) S-parameters are given over a DC to 10GHz bandwidth with drain voltage of 45V and Ids=400mA (25mA/mm) fixed at Temp=25°C . Measurements are performed versus Temp=[-20°C , 25°C , 90°C]

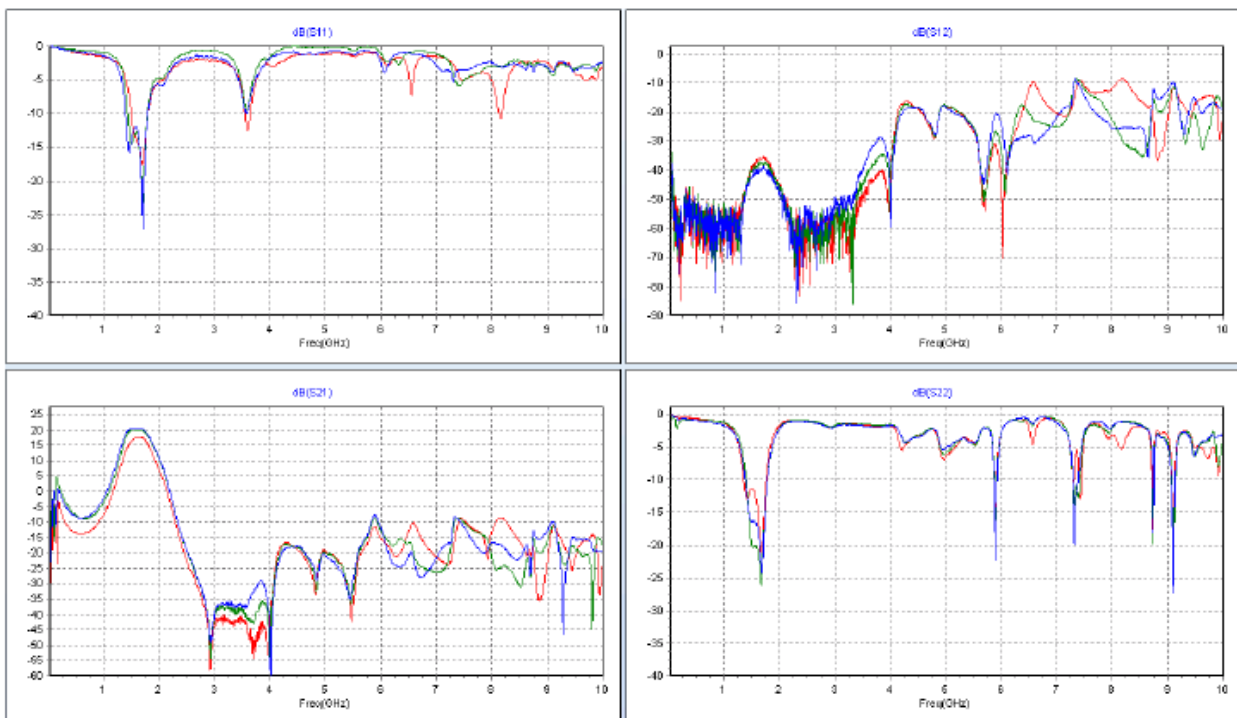


Figure 60 : HPA-1 module (#2). [S] parameters measurements. RF=[DC-10GHz], Vd=45V, Fixed drain current Ids=400mA @25°C , Temp=[-20°C , 25°C , 90°C]

On following figures, we focus on the HPA-1 module (#2) in-band frequency behavior. Figure shows that S11 and S22 parameters varies not in the same way:

- Input return loss is optimum at hot temperature
- Output return loss is optimum at room temperature.

S21 variation is about 3dB between -20°C to 90°C at 1.55GHz. At constant gate voltage current, the gain variation versus temperature is $0,25\text{dB}/^{\circ}\text{C}$.

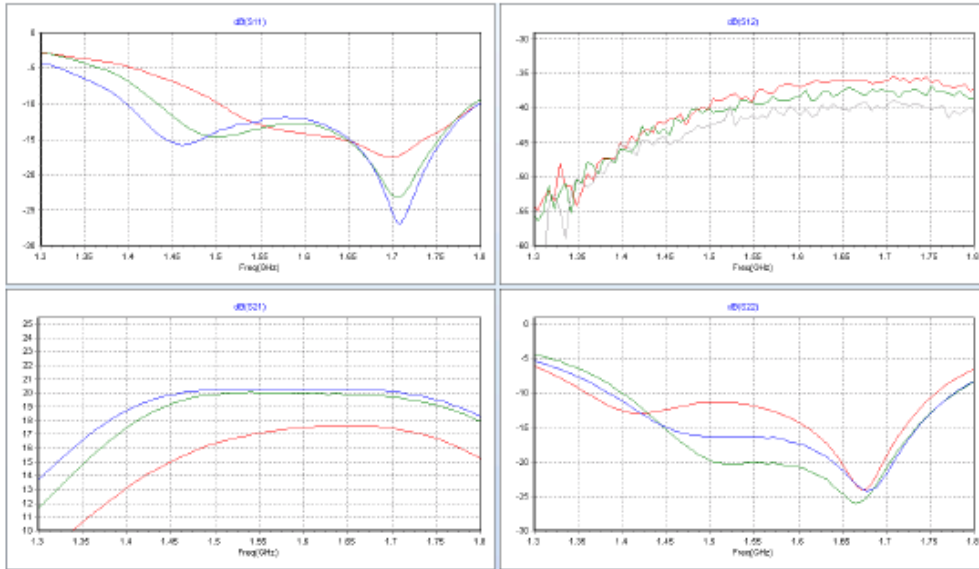


Figure 61 : HPA-1 module (#2). [S] parameters measurements. RF=[1.3-1.8GHz], Vd=45V, Fixed drain current Ids=400mA @25°C , Temp=[-20°C , 25°C , 90°C]

On following figures, we focus on the HPA#2 module in-band frequency behavior versus drain voltage variation. Figures show that S22 parameters varies versus drain voltage value and is optimum at $V_{ds}=40\text{V}$. S21 variation is about 4dB between 20V to 45V at 1.55GHz. At constant gate voltage current, the gain variation versus drain voltage value is $0,16\text{dB}/\text{V}$.

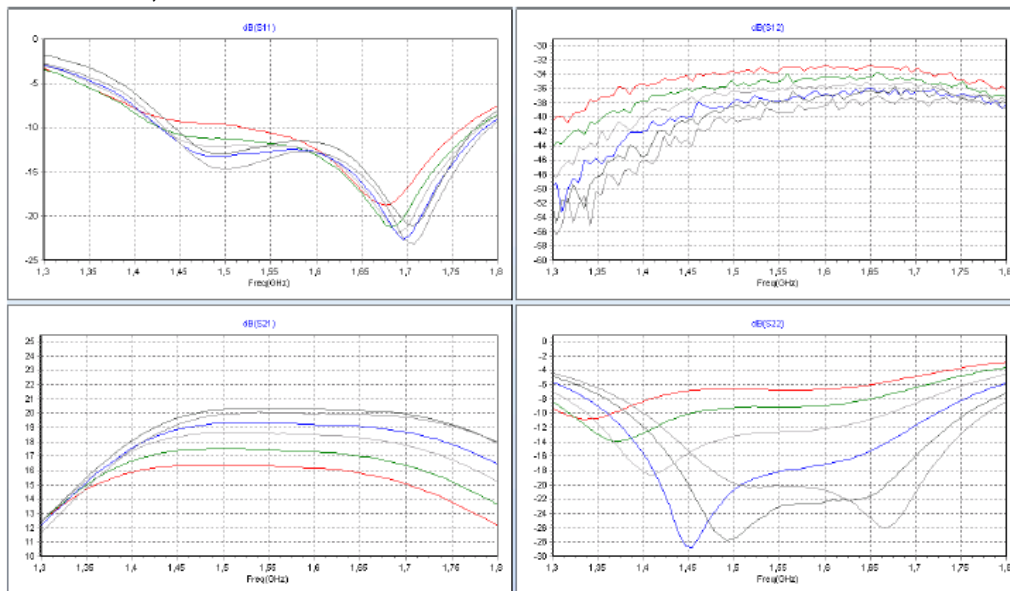


Figure 62 : HPA-1 module (#2). [S] parameters measurements. RF=[1.3-1.8GHz], Vd=[20V/25V/30V/40V/45V]. Fixed drain current Ids=400mA @25°C . Temp= 25°C

Hereafter, for three HPA modules, the S-parameters are given over a DC to 10GHz bandwidth with drain voltage of 45V and $I_{ds}=400\text{mA}$ (25mA/mm) fixed at $\text{Temp}=25^{\circ}\text{C}$. Measurements are performed versus $\text{Temp}=[-20^{\circ}\text{C}, 25^{\circ}\text{C}, 90^{\circ}\text{C}]$

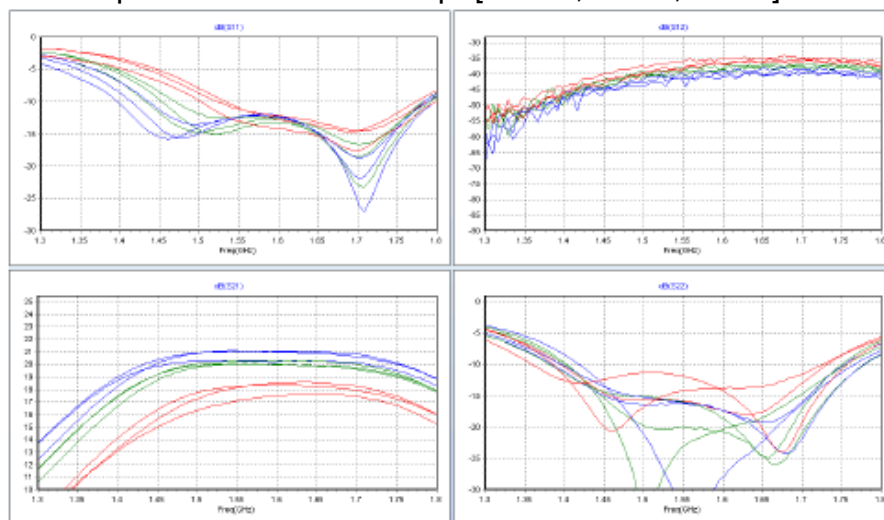


Figure 63 : HPA-1 modules (#2#3#5). [S] parameters measurements. RF=[1.3-1.8GHz], $V_d=45\text{V}$, Drain current $I_{ds}=400\text{mA}$ @ 25°C . $\text{Temp}=[-20^{\circ}\text{C}, 25^{\circ}\text{C}, 90^{\circ}\text{C}]$.

Regarding S21 parameter, at 1,55GHz, a maximum dispersion of 1dB is observed between the three HPA modules. Regarding S11 parameter, at 1,55GHz, a maximum dispersion of 2dB is observed between the three HPA modules. Regarding S22 parameter, dispersion is higher compared to the previous parameters. Indeed, depending of the HPA modules, the settings applied on the output combiner to obtain maximum of PAE have an impact of the output return loss behavior.

2.1.5.2 CW mode power measurements. Run-1

The main RF performances obtained, output power, PAE, power gain and phase are presented below versus input power and three frequency points [1,5425GHz, 1,5675GHz, 1,5925GHz]. Measurements have been performed versus $\text{Temp}=[-20^{\circ}\text{C}, 25^{\circ}\text{C}, 90^{\circ}\text{C}]$. For each frequency and each temperature, drain current has been tuned in small signal: $I_{ds}=400\text{mA}$ with $V_{ds}=40\text{V}$.

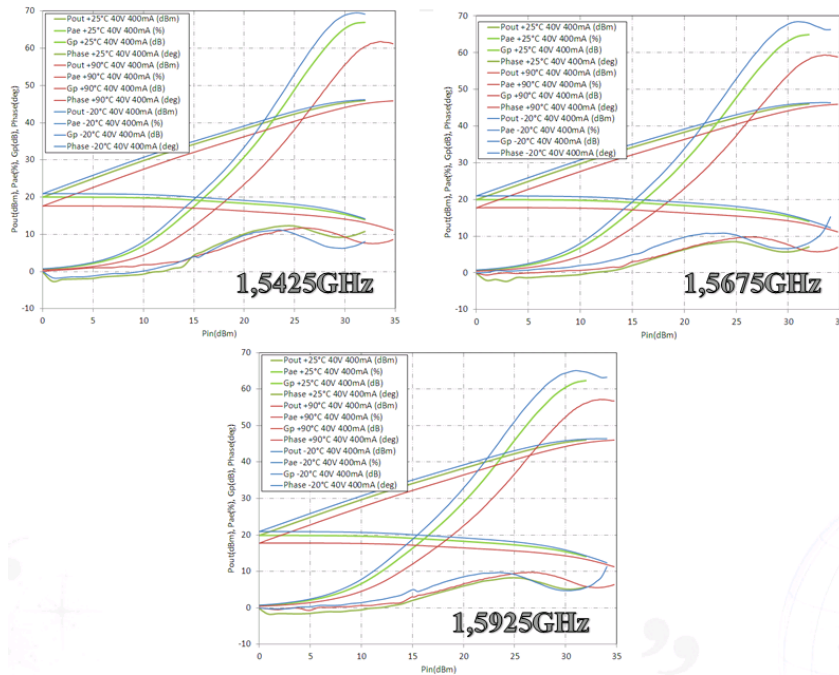


Figure 64 : HPA-1 module (#2). Power measurements with CW signal. Temp=[-20°C, 25°C, 90°C], Vd=40V, Id=400mA. RF=[1,5425GHz/1,5675GHz/1,5925GHz]. Gain(dB), PAE(%), Pout(dBm), Phase(deg) vs Pin(dBm)

In figure below, the results (Pout, Gain, PAE) are presented versus frequency and temperature. Pin is fixed to obtain maximum of PAE.

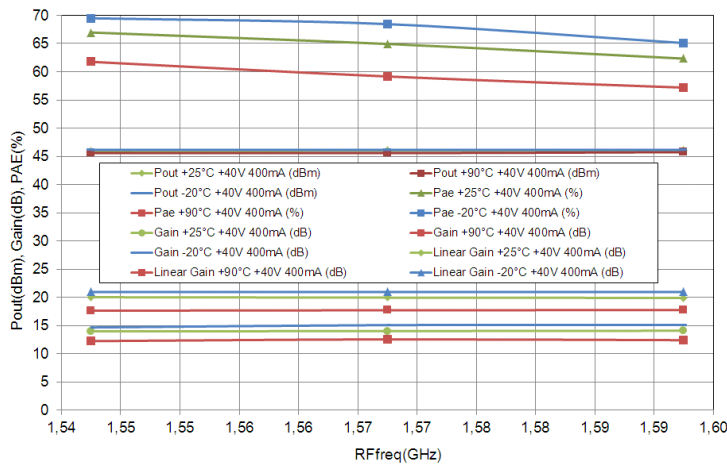


Figure 65 : HPA-1 module (#2). Power measurements with CW signal. Temp=[-20°C, 25°C, 90°C], Vd=40V, Id=400mA. Gain(dB), PAE(%), Pout(dBm), Phase(deg) vs RFfreq(GHz) @PAE_max

At Vds=40V and room temperature, the maximum overall power added efficiency varies from 62 to 67% and is associated to an output power of 39,4W to 40,4W.

The main RF performances obtained, output power, PAE, power gain and phase are presented below versus input power and three frequency points [1,5425GHz, 1,5675GHz, 1,5925GHz]. Measurements have been performed versus Temp=[-20°C, 25°C, 90°C]. For each frequency and each temperature, drain current has been tuned in small signal: Ids=400mA with Vds=45V.

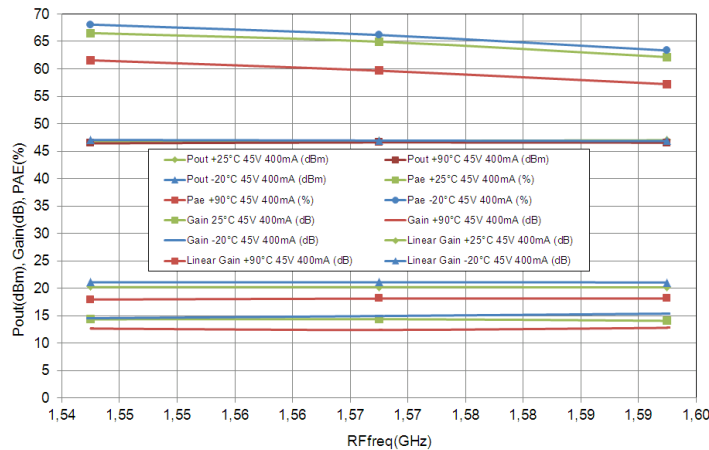


Figure 66 : HPA-1 module (#2). Power measurements with CW signal. Temp=[-20°C, 25°C, 90°C], Vd=45V, Id=400mA. Gain(dB), PAE(%), Pout(dBm), Phase(deg) vs RFreq(GHz) @PAE_max

At Vds=45V and room temperature, the maximum overall power added efficiency varies from 62 to 66,5% and is associated to an output power of 48,2W to 50W. Synthesis of the RF performances measured with CW signal are provided in the following table

Temp (°C)	Biasing Point	RFreq (GHz)	Linear Gain (dB)	Pout (dBm)	Pout (W)	Power Density (W/mm)	Max_PAE (%)	Gain (dB)	Compression (dB)
90	Vd=40V, Id=400mA	1.54	17.63	45.61	36.39	2.27	61.76	12.24	5.39
		1.57	17.71	45.57	36.06	2.25	59.17	12.55	5.16
		1.59	17.75	45.75	37.58	2.35	57.19	12.41	5.34
25	Vd=40V, Id=400mA	1.54	20.03	45.95	39.36	2.46	66.97	13.97	6.06
		1.57	19.95	46.01	39.90	2.49	64.93	14.02	5.93
		1.59	19.90	46.06	40.36	2.52	62.33	14.08	5.82
-20	Vd=40V, Id=400mA	1.54	20.96	46.14	41.11	2.57	69.49	14.66	6.30
		1.57	20.97	46.15	41.21	2.58	68.45	15.08	5.89
		1.59	20.94	46.14	41.11	2.57	65.10	15.12	5.82
90	Vd=45V, Id=400mA	1.54	17.94	46.43	43.95	2.75	61.57	12.65	5.29
		1.57	18.12	46.60	45.71	2.86	59.67	12.40	5.72
		1.59	18.12	46.55	45.19	2.82	57.21	12.79	5.33
25	Vd=45V, Id=400mA	1.54	20.23	46.83	48.19	3.01	66.53	14.34	5.89
		1.57	20.22	46.87	48.64	3.04	64.96	14.38	5.84
		1.59	20.17	46.99	50.00	3.13	62.15	14.06	6.11
-20	Vd=45V, Id=400mA	1.54	21.08	47.04	50.58	3.16	68.09	14.54	6.54
		1.57	21.10	46.94	49.43	3.09	66.18	14.94	6.16
		1.59	21.07	46.85	48.42	3.03	63.36	15.38	5.69

Table 15 : HPA-1 module (#2). Synthesis of power measurements with CW signal. Temp=[-20°C, 25°C, 90°C], Vd=40V & Vd=45V, Id=400mA. Gain(dB), PAE(%), Pout(dBm), Phase(deg) vs RFreq(GHz) @PAE_max

HPA-1 modules (#3 and #5) have been tested with the same approach. Synthesis of the measurements results are presented in the table below.

Temp (°C)	Biasing Point	RFfreq (GHz)	Linear Gain (dB)	Pout (dBm)	Pout (W)	Power Density (W/mm)	Max_PAE (%)	Gain (dB)	Compression (dB)
90	Vd=40V, Id=400mA	1.54	17.54	45.59	36.22	2.26	58.62	11.68	5.86
		1.57	17.76	45.94	39.26	2.45	63.70	11.99	5.77
		1.59	17.86	46.00	39.81	2.49	62.22	12.09	5.77
25	Vd=40V, Id=400mA	1.54	20.04	46.51	44.77	2.80	58.41	12.50	7.54
		1.57	20.07	46.71	46.88	2.93	66.02	13.65	6.42
		1.59	20.05	46.81	47.97	3.00	67.64	12.81	7.24
25	Vd=40V, Id=400mA	1.54	20.94	46.36	43.25	2.70	55.87	13.32	7.62
		1.57	20.83	46.66	46.34	2.90	63.32	13.62	7.21
		1.59	20.93	46.71	46.88	2.93	67.16	14.70	6.23

Temp (°C)	Biasing Point	RFfreq (GHz)	Linear Gain (dB)	Pout (dBm)	Pout (W)	Power Density (W/mm)	Max_PAE (%)	Gain (dB)	Compression (dB)
90	Vd=45V, Id=400mA	1.54	18.00	46.20	41.69	2.61	54.23	11.75	6.25
		1.57	18.23	46.75	47.32	2.96	62.35	12.31	5.92
		1.59	18.34	46.88	48.75	3.05	62.45	12.46	5.88
25	Vd=45V, Id=400mA	1.54	20.28	46.97	49.77	3.11	53.33	12.44	7.84
		1.57	20.31	47.39	54.83	3.43	61.94	13.38	6.93
		1.59	20.30	47.53	56.62	3.54	65.66	14.06	6.24
25	Vd=45V, Id=400mA	1.54	21.07	46.78	47.64	2.98	51.30	13.24	7.83
		1.57	21.12	47.21	52.60	3.29	59.64	14.16	6.96
		1.59	21.09	47.43	47.43	2.96	64.13	14.49	6.60

Table 16 : HPA-1 module (#3). Synthesis of power measurements with CW signal. Temp=[-20°C, 25°C, 90°C], Vd=40V & Vd=45V, Id=400mA. Gain(dB), PAE(%), Pout(dBm), Phase(deg) vs RFfreq(GHz) @PAE_max

Temp (°C)	Biasing Point	RFfreq (GHz)	Linear Gain (dB)	Pout (dBm)	Pout (W)	Power Density (W/mm)	Max_PAE (%)	Gain (dB)	Compression (dB)
90	Vd=40V, Id=400mA	1.54	17.75	45.60	36.31	2.27	64.69	12.58	5.17
		1.57	17.75	45.69	37.07	2.32	62.56	12.61	5.14
		1.59	17.78	45.73	37.41	2.34	59.34	12.76	5.02
25	Vd=40V, Id=400mA	1.54	19.86	45.92	39.08	2.44	67.74	12.94	6.92
		1.57	19.84	45.97	39.54	2.47	67.61	13.49	6.35
		1.59	19.78	46.07	40.46	2.53	64.64	13.58	6.20
-20	Vd=40V, Id=400mA	1.54	20.94	46.06	40.36	2.52	68.88	13.53	7.41
		1.57	21.00	46.02	39.99	2.50	69.92	14.52	6.48
		1.59	20.94	45.99	39.72	2.48	68.93	13.98	6.96

Temp (°C)	Biasing Point	RFfreq (GHz)	Linear Gain (dB)	Pout (dBm)	Pout (W)	Power Density (W/mm)	Max_PAE (%)	Gain (dB)	Compression (dB)
90	Vd=45V, Id=400mA	1.54	18.31	46.51	44.77	2.80	64.15	12.98	5.33
		1.57	18.33	46.60	45.71	2.86	63.41	13.08	5.25
		1.59	18.27	46.64	46.13	2.88	60.30	13.16	5.11
25	Vd=45V, Id=400mA	1.54	20.18	46.78	47.64	2.98	65.91	13.29	6.89
		1.57	20.18	46.86	48.53	3.03	67.47	13.84	6.34
		1.59	20.16	46.84	48.31	3.02	64.98	14.38	5.78
25	Vd=45V, Id=400mA	1.54	21.23	46.82	48.08	3.01	65.80	13.81	7.42
		1.57	21.22	46.95	49.55	3.10	68.97	14.45	6.77
		1.59	21.19	46.99	50.00	3.13	67.26	14.99	6.20

Table 17 : HPA-1 module (#5). Synthesis of power measurements with CW signal. Temp=[-20°C, 25°C, 90°C], Vd=40V & Vd=45V, Id=400mA. Gain(dB), PAE(%), Pout(dBm), Phase(deg) vs RFfreq(GHz) @PAE_max

HPA module-1 (#5) has been tested with different biasing point [100mA / 400mA / 800mA] and Temp=[25°C/90°C].

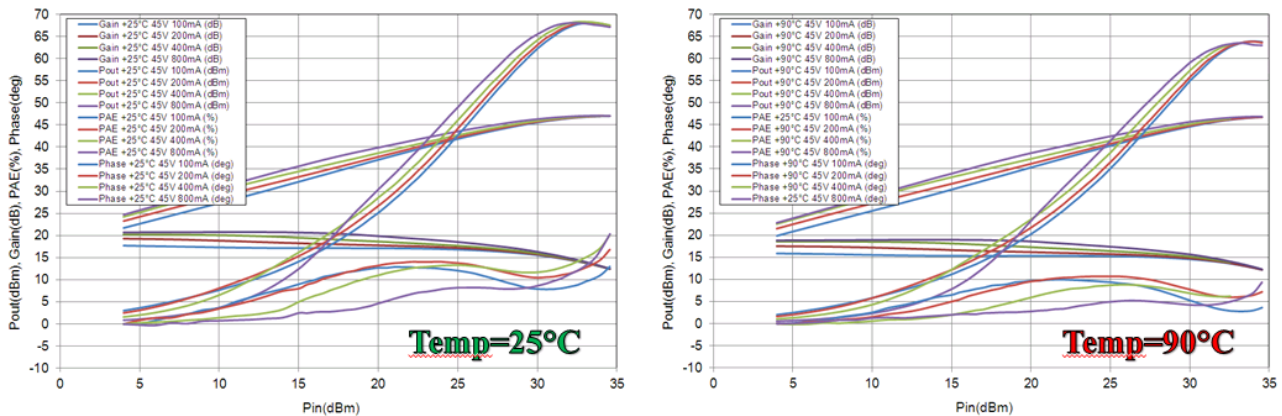


Figure 67 : HPA#1 module (#5). Power measurements with CW signal. Temp=[25°C, 90°C], Vd=45V, RF=1,5675GHz Id=[100mA/200mA/400mA/800mA]. Gain(dB), PAE(%), Pout(dBm), Phase(deg) vs Pin(dBm)

Synthesis of the results are presented in figure below. Biasing point has no impact on PAE performances. On the other hand, the selected biasing point will have an impact on gain compression and power density.

Temp (°C)	Frequency (GHz)	Drain Voltage (V)	Drain Current (mA)	Linear Gain (dB)	Pout (dBm)	Pout (W)	Power Density (W/mm)	Max_PAE (%)	Gain (dB)	Compression (dB)
85	1,57	45	100	15.88	46.62	45.92	2.87	63.91	12.57	3.31
			200	17.52	46.67	46.45	2.90	63.83	12.63	4.89
			400	18.57	46.66	46.34	2.90	63.85	13.13	5.44
			800	18.82	46.72	46.99	2.94	63.53	13.69	5.13
25	1,57	45	100	17.72	46.89	48.87	3.05	68.04	13.34	4.38
			200	19.29	46.86	48.53	3.03	68.28	13.82	5.47
			400	20.24	46.94	49.43	3.09	68.31	13.90	6.34
			800	20.71	46.91	49.09	3.07	68.05	14.85	5.86

Figure 68 : HPA-1 module (#5). Synthesis of power measurements with CW signal. Temp=[25°C, 90°C], Vd=45V, RF=1,5675GHz Id=[100mA / 200mA / 400mA / 800mA]. Gain(dB), PAE(%), Pout(dBm), Phase(deg) vs Pin(dBm)

2.1.5.3 Multi-carrier mode power measurements. Run-1

In the following part, multicarrier measurements are presented. HPA-1 module (#5) has been tested with Vds=45V and different biasing point fixed in small signal (Ids=100mA / 200mA / 400mA / 800mA). Multi-carrier measurements have been performed at Temp=[-20°C, 25°C, 90°C].

The multicarrier signal characteristics are:

- 3000 carriers
- Span=40MHz
- Fc=1.5675GHz
- Notch: 1%

At Temp=-25°C, HPA-1 module (#5) power measurements are given versus Pout.

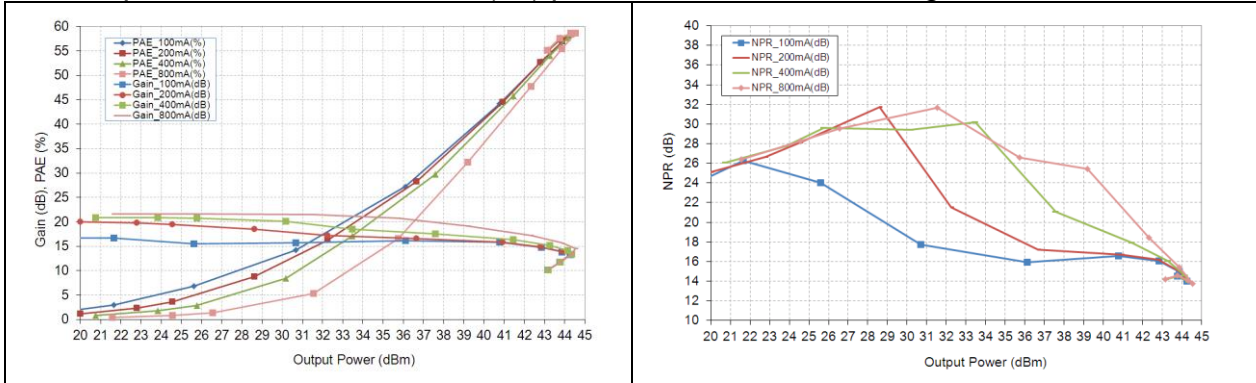


Figure 69 : HPA-1 module (#5) Power measurements with multi-carrier signal. Temp=-20°C. Vds=45V, RF=1,5675GHz, Span=40MHz, 3000 carriers, 1% notch. Gain(dB), PAE(%), NPR(dB) vs Pout(dBm)

At Temp=-25°C, HPA-1 module (#5) power measurements are given versus Pout.

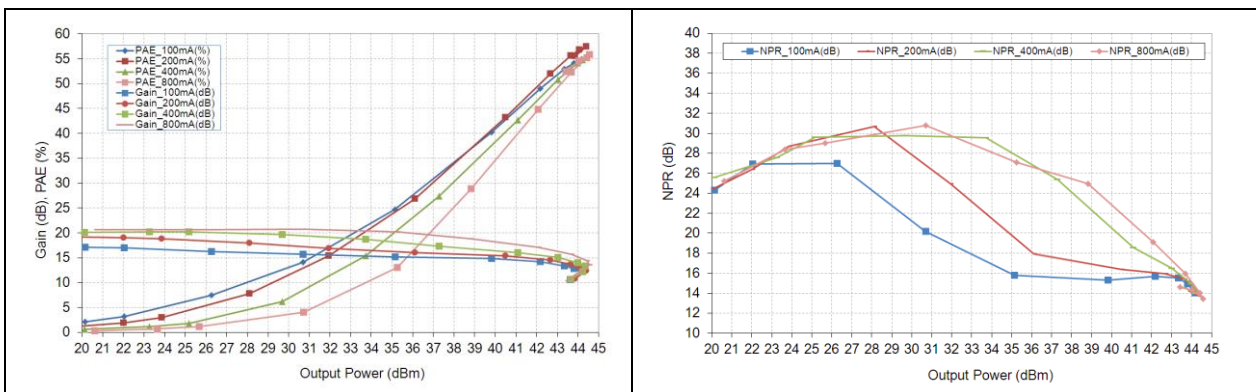


Figure 70 : HPA-1 module (#5). Power measurements with multi-carrier signal. Temp=+25°C. Vds=45V, RF=1,5675GHz, Span=40MHz, 3000 carriers, 1% notch. Gain(dB), PAE(%), NPR(dB) vs Pout(dBm)

At Temp=90°C, HPA-1 module (#5) power measurements are given versus Pout.

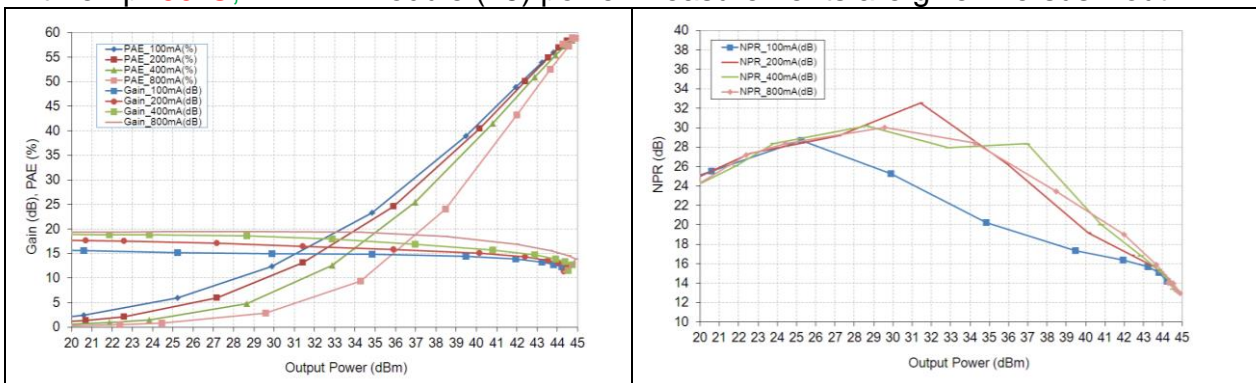


Figure 71 : HPA-1 module (#5) Power measurements with multi-carrier signal. Temp=+90°C. Vds=45V, RF=1,5675GHz, Span=40MHz, 3000 carriers, 1% notch. Gain(dB), PAE(%), NPR(dB) vs Pout(dBm)

In the following table are summarized the main parameters measured during multi-carrier measurements : Pout and power density / NPR / PAE / Compression. This table will be used to select the best biasing point for the HPA module in order to achieve the RF performances in multi-carrier mode required at HPA level. In term of power density, the results are optimum with Ids=800mA. However, the gain compression is increased this representing a risk with respect to the reliability

	Linear Gain(dB)	Pin(dBm)	Pout (dBm)	Pout(W)	PAE (%)	NPR (dB)	Gain (dB)	Compression (dB)
Vd=45V, Id=100mA, Temp=-20°C	17,0	30,0	43,9	24,3	56,8	15,0	13,9	3,1
		31,0	44,3	26,7	58,1	14,0	13,3	3,7
Vd=45V, Id=200mA, Temp=-20°C	20,0	30,0	43,9	24,5	57,0	15,0	13,9	6,1
		31,0	44,3	26,9	58,3	14,0	13,3	6,7
Vd=45V, Id=400mA, Temp=-20°C	20,8	29,1	43,7	23,5	55,9	15,3	14,6	6,2
		31,0	44,3	27,2	58,6	14,0	13,3	7,5
Vd=45V, Id=800mA, Temp=-20°C	21,6	29,1	44,2	26,3	57,0	14,6	15,1	6,5
		31,0	44,3	27,0	58,7	14,1	13,3	8,3
Vd=45V, Id=100mA, Temp=25°C	17,6	31,0	43,8	24,0	54,2	15,0	12,8	4,8
		32,0	44,2	26,1	54,9	14,0	12,2	5,4
Vd=45V, Id=200mA, Temp=25°C	19,2	30,5	43,9	24,3	56,2	15,0	13,4	5,8
		31,5	44,2	26,5	57,2	14,2	12,7	6,5
Vd=45V, Id=400mA, Temp=25°C	20,1	30,0	44,0	25,0	54,1	15,0	14,0	6,1
		31,0	44,3	27,2	55,3	14,0	13,3	6,8
Vd=45V, Id=800mA, Temp=25°C	20,6	29,0	44,1	25,4	53,8	15,0	15,1	5,6
		30,0	44,4	27,7	55,2	14,0	14,4	6,2
Vd=45V, Id=100mA, Temp=90°C	15,9	31,0	43,8	24,0	56,0	15,1	12,8	3,1
		32,0	44,2	26,5	57,2	14,2	12,3	3,6
Vd=45V, Id=200mA, Temp=90°C	18,0	31,0	44,1	25,5	56,9	14,8	13,1	5,0
		32,0	44,5	28,1	58,3	13,9	12,5	5,5
Vd=45V, Id=400mA, Temp=90°C	18,9	30,0	43,9	24,7	55,5	15,2	13,9	5,0
		31,0	44,4	27,4	57,2	14,2	13,4	5,5
Vd=45V, Id=800mA, Temp=90°C	19,1	29,0	44,1	25,7	54,9	14,9	15,1	4,0
		30,0	44,6	28,5	57,2	14,0	14,6	4,6

Figure 72 : HPA-1 module (#5). Synthesis of power measurements with multi-carrier signal. Temp=[-20°C, +25°C, +90°C]. Vds=45V, RF=1,5675GHz, Span=40MHz, 3000 carriers, 1% notch. Id(A) and Ig(A) Pin(dBm)

2.1.5.4 RF step measurements with multi-carrier signal : reliability of GH50-10 technology. Run-1

This paragraph summarizes the reliability test performed on GaN HPA L Band in the frame of the ARTES 5.1 "SSPAs with European GaN Devices" study. The goal of this reliability study is to define a Safe Operating Area through RF Multicarrier step stress (2 dB compression, 4 dB compression, 6 dB compression, 8 dB compression, 10 dB compression). For that, a dedicated multicarrier test bench have been developed. Intermediate RF measurements and in situ monitoring are performed during this qualification.

Test plan is provided in the following table:

DC Life test	Function	HPA 50 WATTS 16 mm
	Process	UMS GH50-10
	Frequency	1.56 GHz
	DC Bias	$V_d=45V$, $I_d = 100\text{ mA}$ (6,25 mA / mm) ² samples + 1 sample $I_d=400\text{ mA}$ (25 mA / mm)
	Number of Sample	NA
	T° JUNCTION (Objective)	NA
RF Life test	Electrical constraint	NA
	Duration	NA
	Number of Sample	3 + 1
	T°	25°C
	DC Biases	Nominal DC biases
	Electrical Constraint	Multicarrier
		1 - Step stress :
		2 weeks / step from 4 dBc to 8 dBc
		2 - RF Life test :
		2000 hours @ X_{dBc} - 2 dB or max PAE
Monitoring	Gate, drain current, Input, output power	
Initial, Final & Intermediate Measurement	RF Characteristic : Pout, Gain, Id, Ig vs Pin, Phase vs input power	

Table 18 : Test plan for RF step stress measurements of L-band GH50 HPA-1 module

3 samples have been tested during RF step stress with multicarrier signal:

- HPA-1 module (#2) = Sample n°2 = SN2
- HPA-1 module (#3) = Sample n°3 = SN3
- HPA-1 module (#5) = Sample n°5 = SN5

Multi carrier signal is generated using white noise source. The « white noise » bandwidth is = 28 MHz. All the spike > 40 dBc outside the signal band width are eliminated. Synoptic and photographs of the multi-carrier test bench are provided in the following figures.

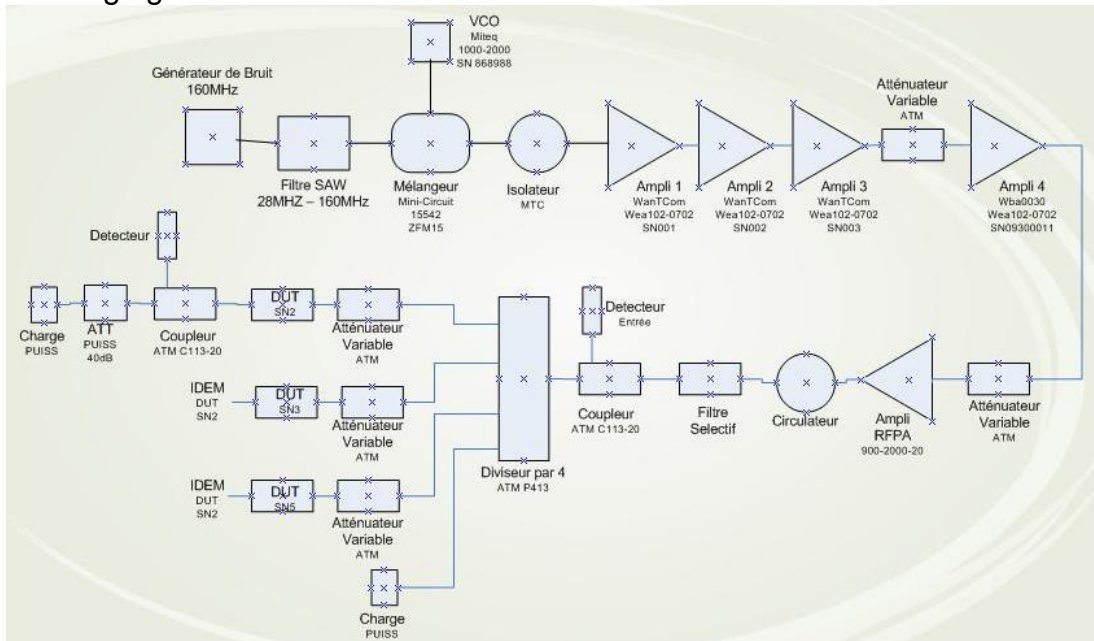


Figure 73 : Multi-carrier test bench

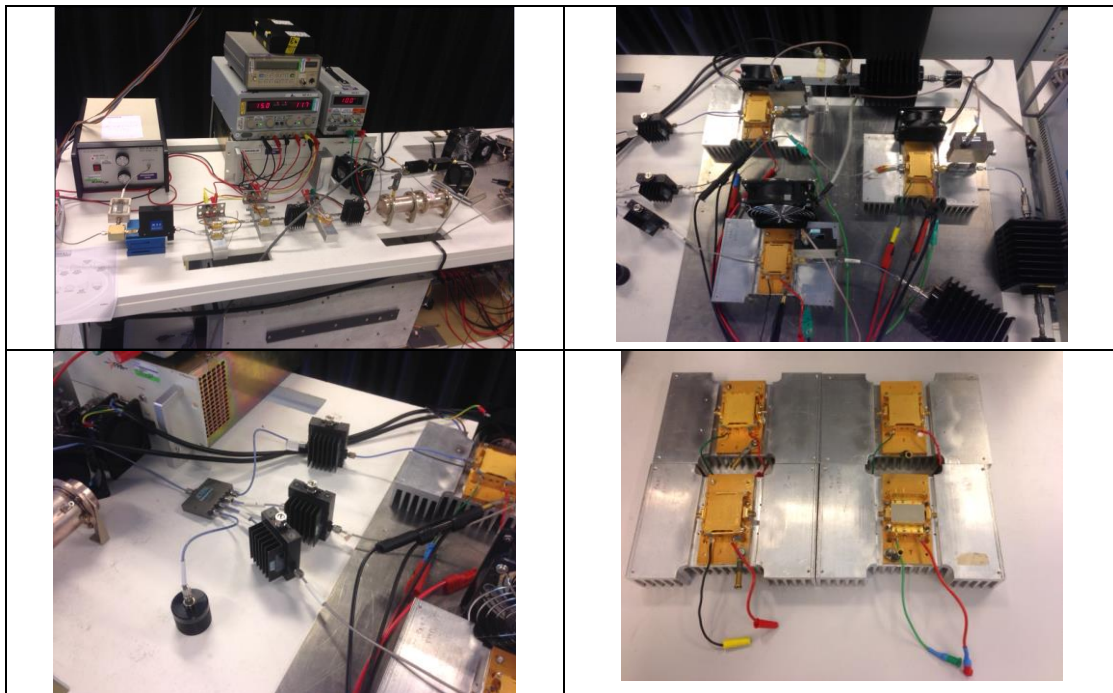


Figure 74 : Photographs of the multi-carrier test bench

The figure here above describes the signal level respectively after the mixer, the amplifier 1, 2,3 and amplifier RFPA + filter

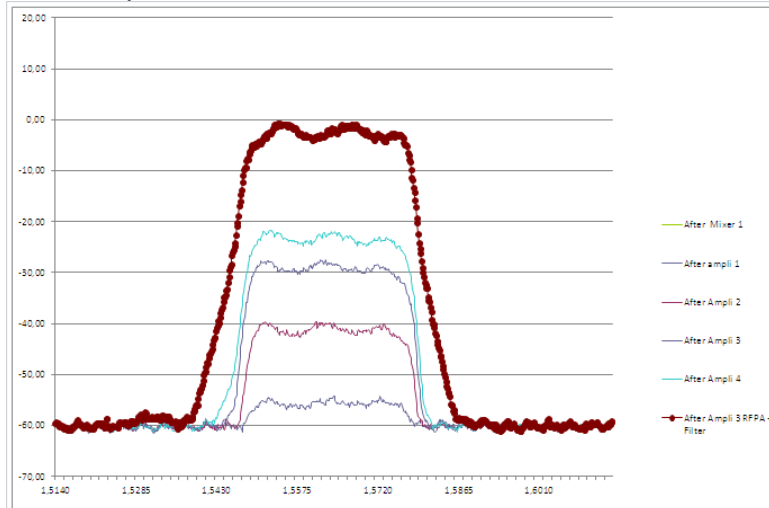


Figure 75 : Noise signal level at different point of the test bench

CCDF measurement (Complementary Cumulative Distribution Function) consist to analyze multi carrier signal in order to determine a probability that a phase recombination generate a signal higher than the average level signal.

Examples :

- For a CCDF = 1, we will have 1 spike / 10 000 = average level signal + 1 dB. (probability= 0.01%)
- For a CCDF = 9, we will have 1 spike / 10 000 = average level signal + 9 dB. (probability= 0.01%)

In the frame of this study, we need to obtain the highest value of CCDF. This value depends on the compression of the different amplifier. The more the compression is high, the more the value of the CCDF is low. The CCDF obtained is = 6.5 dB.

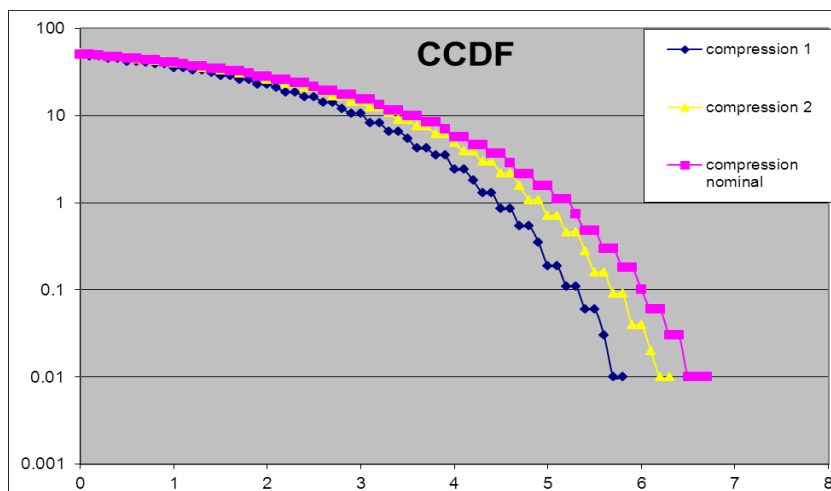


Figure 76 : CCDF Value for different compression values

A dedicated test bench for initial, intermediate and final measurement bench is used for [S], AM/AM and AM/PM measurements after each step of compression (2 weeks / step from 4dBc to 8dBc). Synoptic and photographs of this test bench are provided in the following figures.

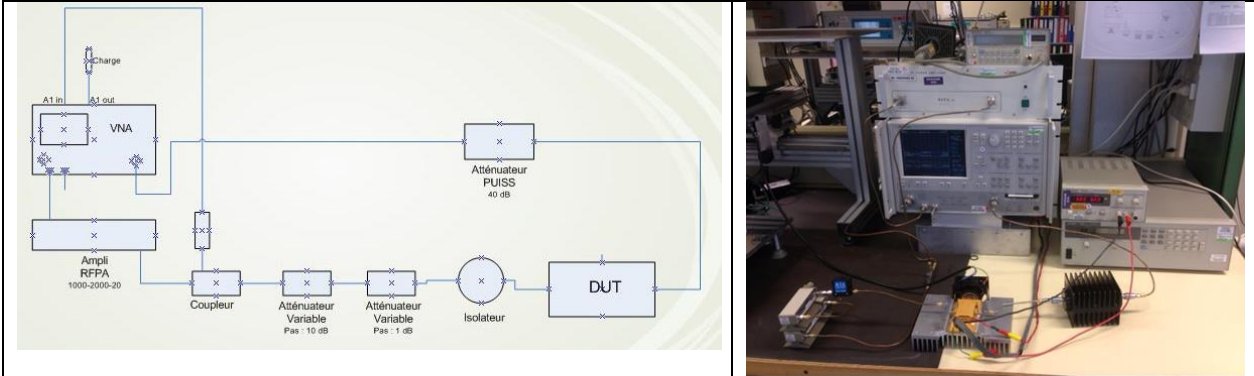


Figure 77 : Photography of the CW test bench for CW initial/intermediate and final measurements

Before starting the RF step stress campaign, initial characterization with the multicarrier signal have been performed in order to determine the non-linear characteristic of each samples. Example for HPA-1 module (#5) is given below:

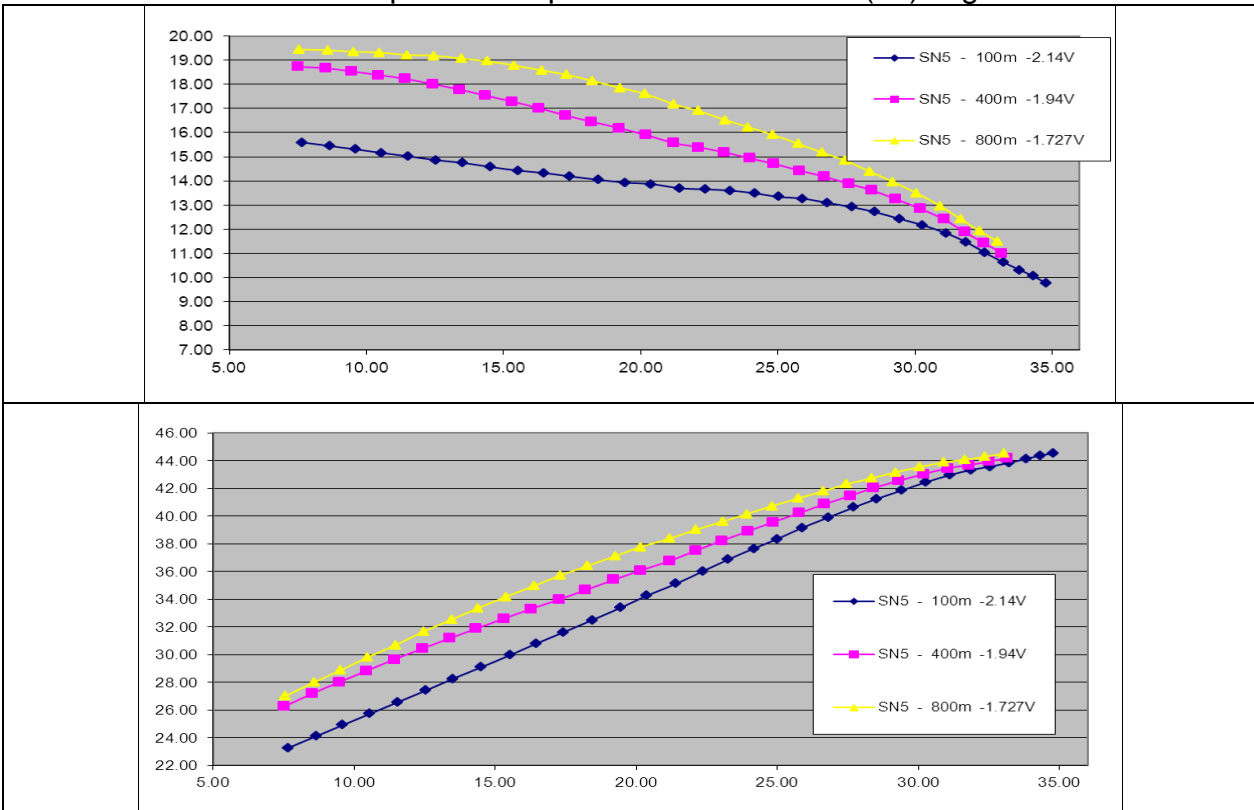


Figure 78 : RF step stress measurement: initial characterization of HPA-1 module (Sample n°5). Gain(dB) and Pout(dBm) versus Pin(dBm) for 3 different bias points: 45V/100mA & 45V/400mA 45V/800mA in small signal.

In order to determine the power value during the in situ monitoring we use a detector. The power value versus the detected voltage is represented in the following graph.

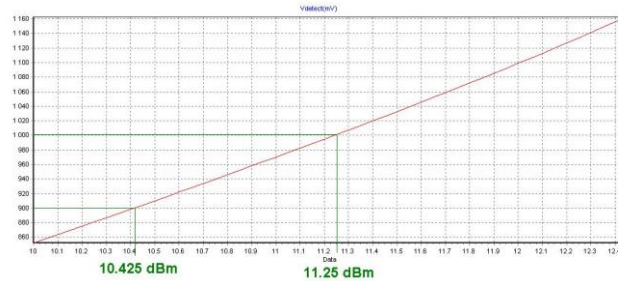


Figure 79 : Detector characterization : Detected voltage value (mV) versus power range(dBm)

The detector sensibility is : 0.825dB / 100mV that means 0.1dB / 12mV. This value must be applied for all the power in situ measurements. The detectors are used during power monitoring (input power and output power)

On three HPA-1 modules (#2, #3, [5], in Situ measurements have been continuously performed during steps @2dB, @4dB, 6dB, 8dB compression. The different parameters monitored are:

- Input power (dBm) and output power (dBm)
- Temperature (°C)
- Drain voltage (V) and Drain current (mA)
- Gate voltage (V) and gate current (mA)

An example of the in situ monitoring performed on HPA-1 module (#2) at Step 6dB compression is presented below:

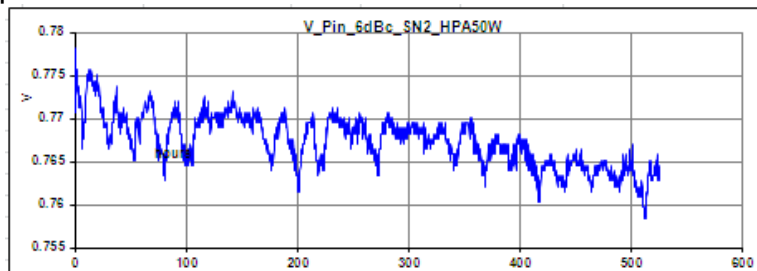


Figure 80 : HPA-1 module (#2). RF step stress measurement. Input power monitoring during 6dBc compression step

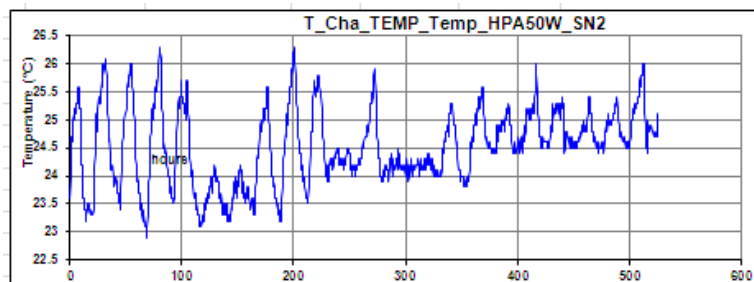


Figure 81 : HPA-1 module (#2). RF step stress measurement. Temperature monitoring during 6dBc compression step

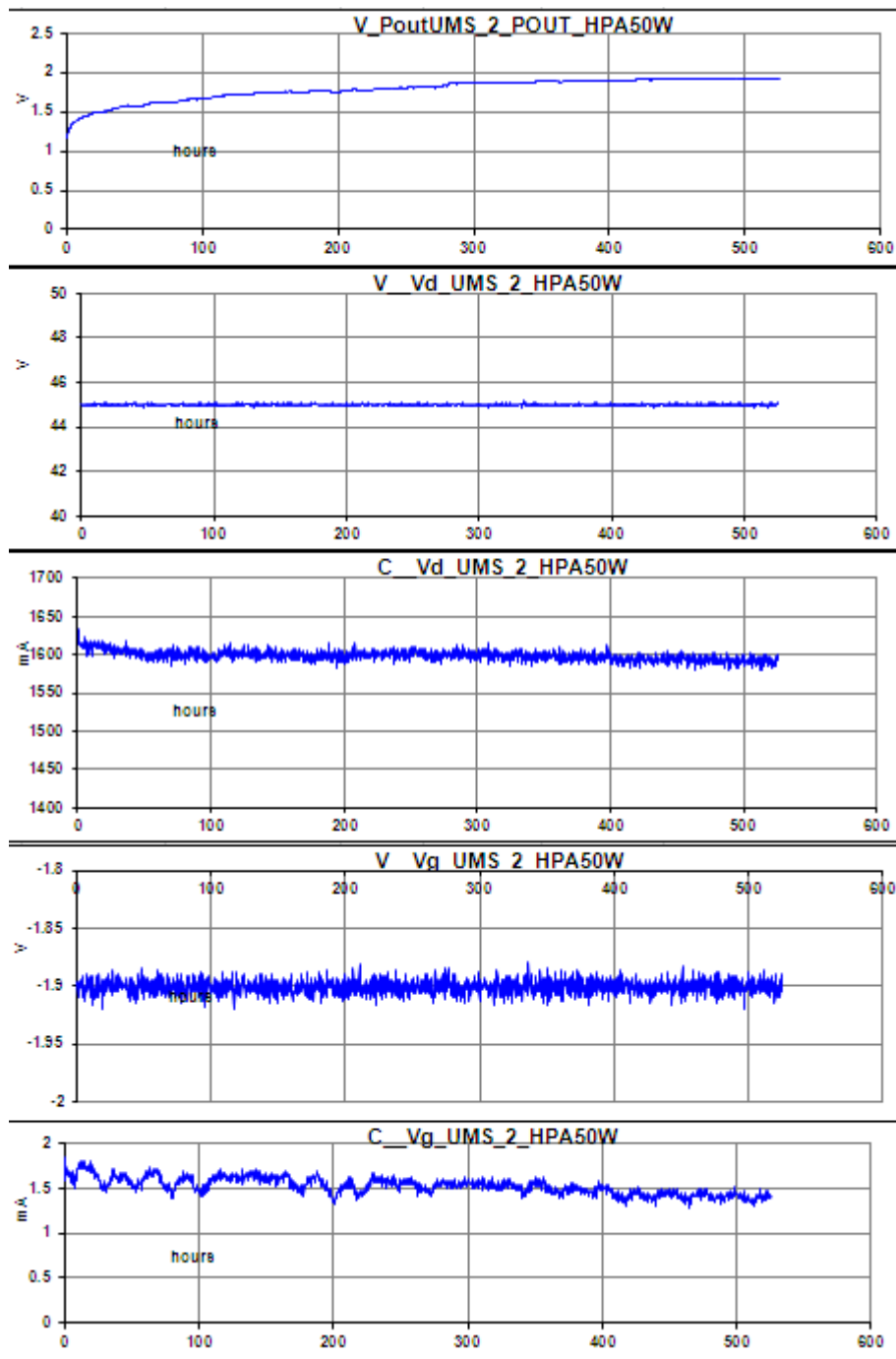


Figure 82 : HPA-1 module (#2). RF step stress measurement (6dBc step). Pout drift (detected voltage in V). Drain voltage drift(V). Drain current drift (mA). Gate voltage drift (V). Voltage current drift (mA)

For each HPA-1 module (#2, #3, #5), initial, intermediate and final have been performed. These measurements have consisted of:

- [S] parameters measurements

- CW characterizations (AMAM and AMPM)
- Static measurements

Measurement data are presented for HPA-1 module #3 in the following graphs. For the following graphs, the legend is:

- Et0 -> Initial measurements
- Et1 -> Measurements after step @ 2 dBc
- Et2 -> Measurements after step @ 4 dBc
- Et3 -> Measurements after step @ 6 dBc
- Et4 -> Measurements after step @ 8 dBc
- Et5 -> Measurements after step @ 10 dBc (for sample n° 3)

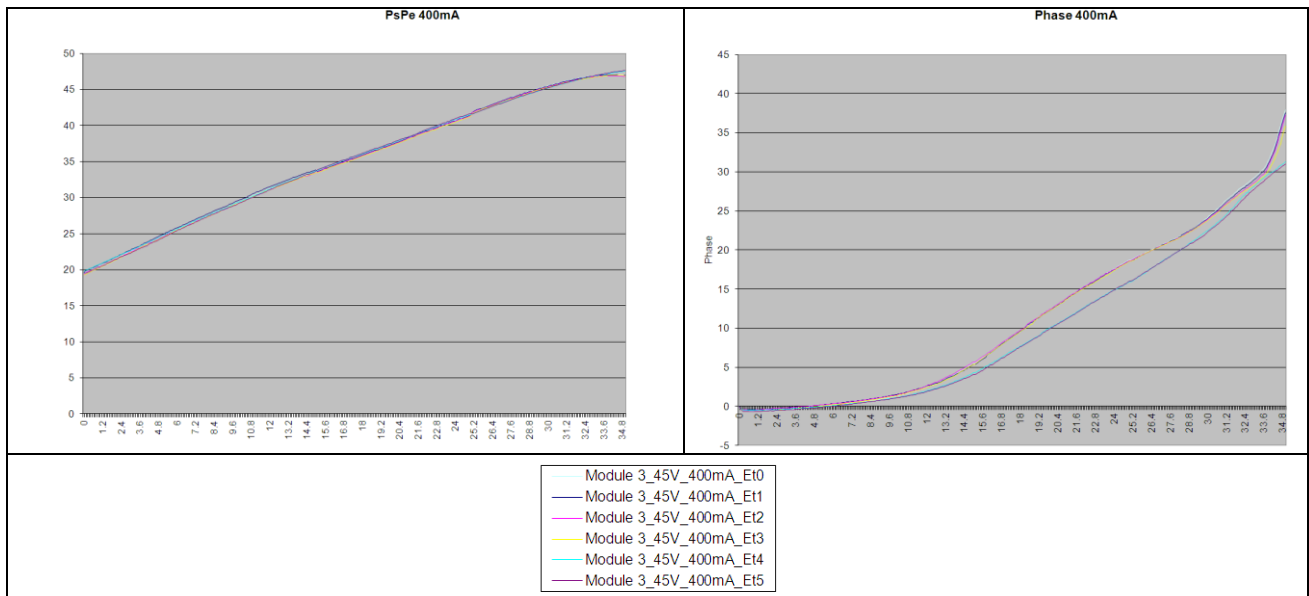


Figure 83 : HPA-1 module #3. AMAM and AMPM characterization in CW mode after each compression step of the RF step stress measurements

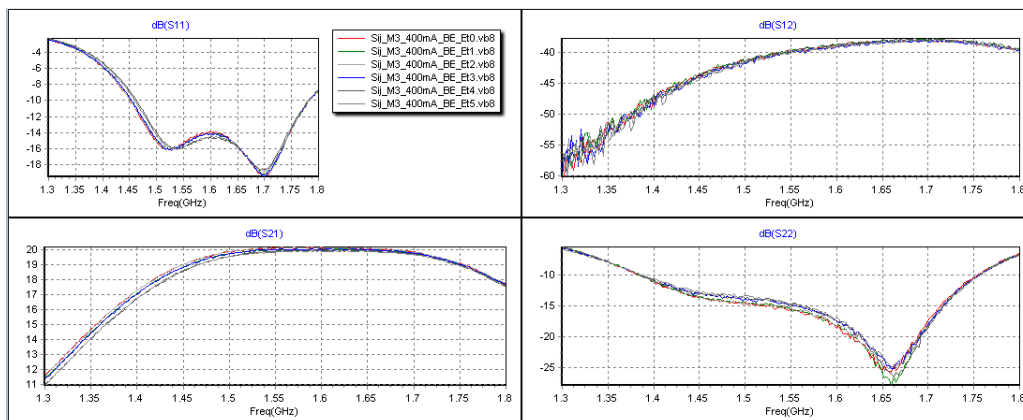


Figure 84 : HPA-1 module #3. [S] parameters measurements after each compression step of the RF step stress measurements

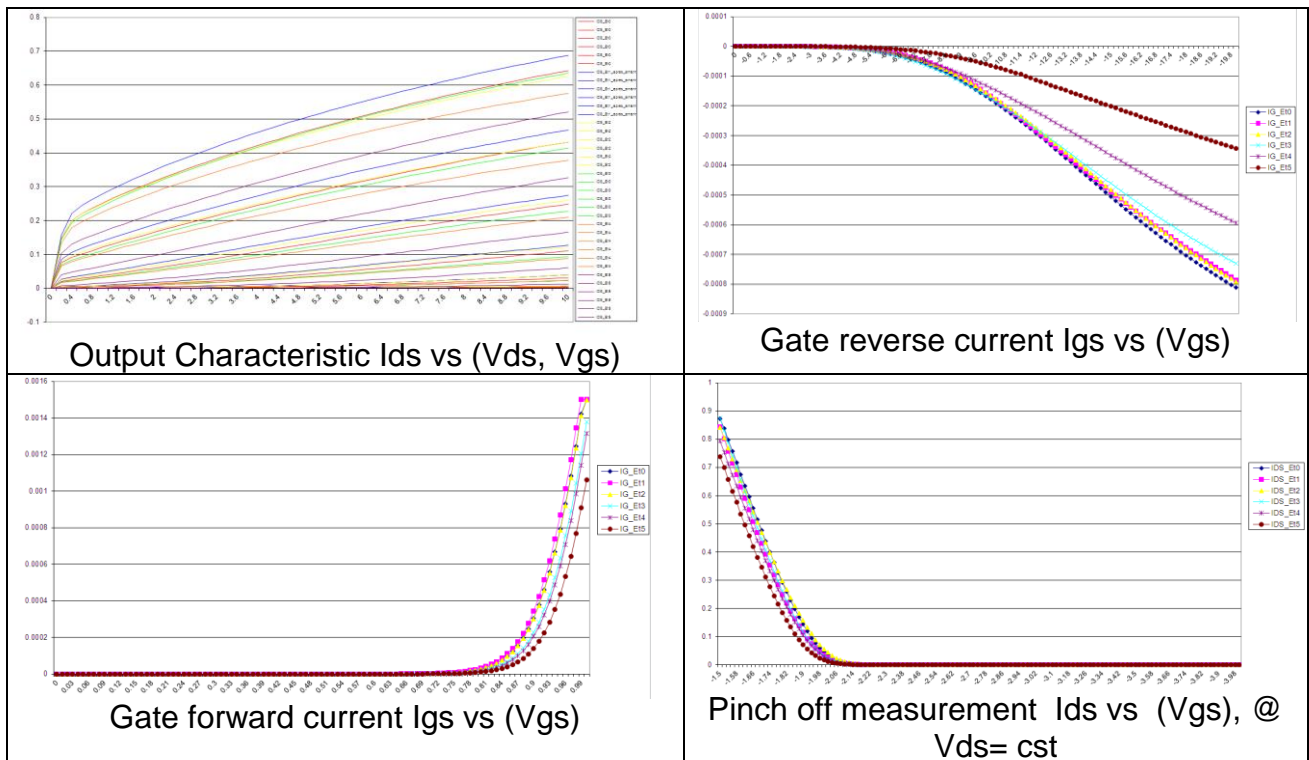


Figure 85 : HPA-1 module #3. Static measurements after each compression step of the RF step stress measurements

Regarding the compression parameter of 6,5dBc obtained at NPR=15dB: the RF step stress measurements have been performed up to 8dBc gain compression for two HPA modules and 10dBc gain compression for HPA#3 module. No degradation has been observed on dynamic performances, showing that high level of compression (6,5dBc) could be used.

2.2 Development of L-band hybrid GH50 HPA module (HPA-1 module): Phase 2

2.2.1 Reverse Engineering of HPA-1 module developed in Run-1

2.2.1.1 Back-simulations of HPA-1 module Run-1

Before presenting the detailed design of HPA-1 module (Run-2) , the following section summarizes the reverse engineering study of HPA-1 module (Run-1) designed during the phase 1 . Two methods have been used during the reverse engineering:

- Simulations based on a classical technique (Momentum simulation for passive networks and HFSS simulation for RF feed-through)
- Simulations based on advanced technique (full HFSS simulation)

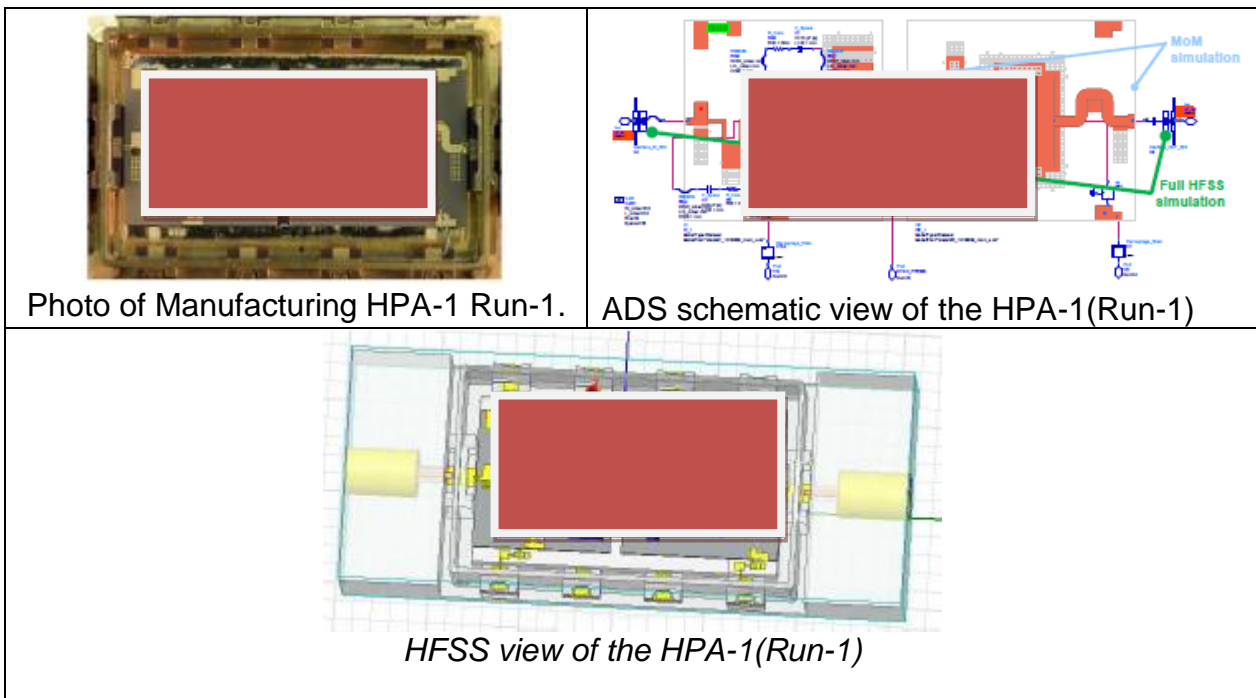


Figure 86 : Two methods used during the reverse engineering of HPA-1 module Run-1

The comparison of reverse engineering simulations are shown below

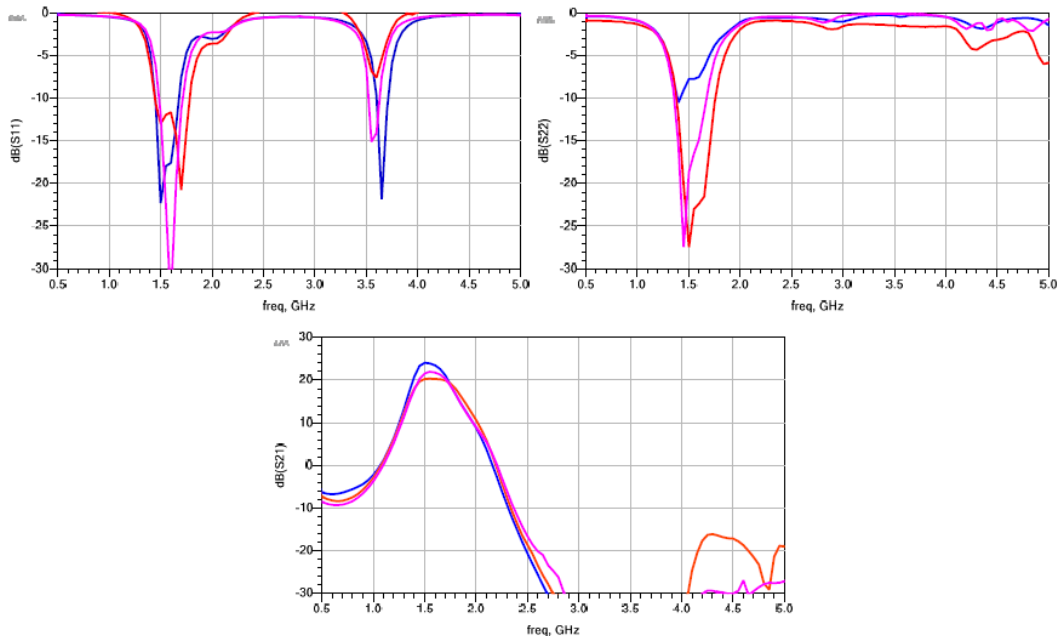


Figure 87 : HPA-1 module Run-1: S-parameter comparison of measurement and reverse engineering simulations

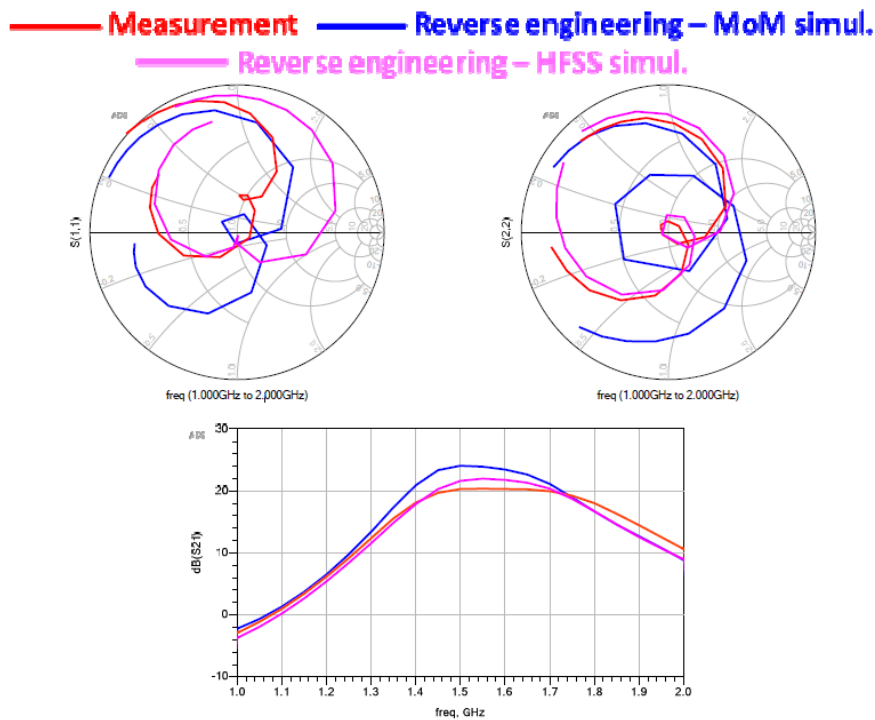


Figure 88 : HPA-1 module Run-1: S-parameter comparison zoom of measurement and reverse engineering simulations

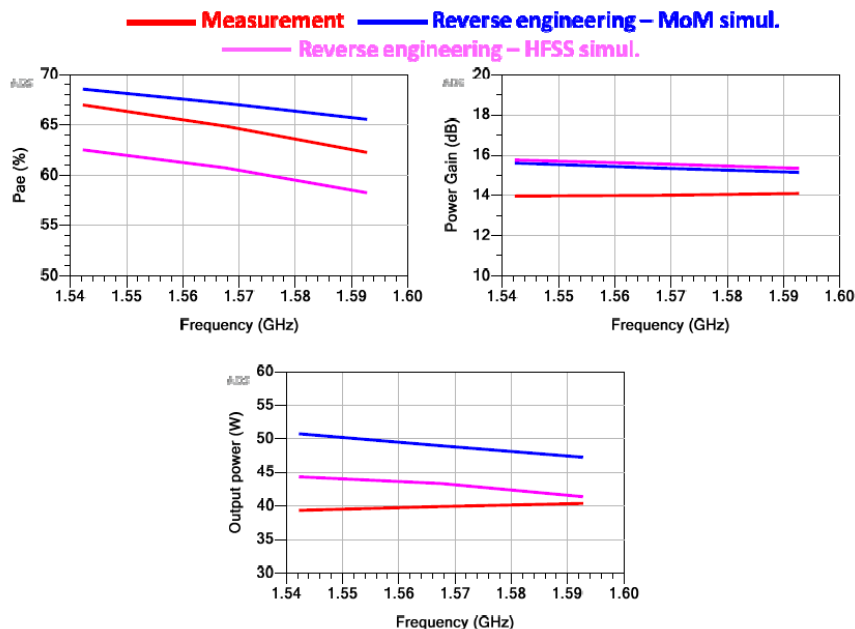


Figure 89 : HPA-1 module Run-1: HPA RF performance vs frequency comparison of measurement and reverse engineering simulations @ Pin=35dBm

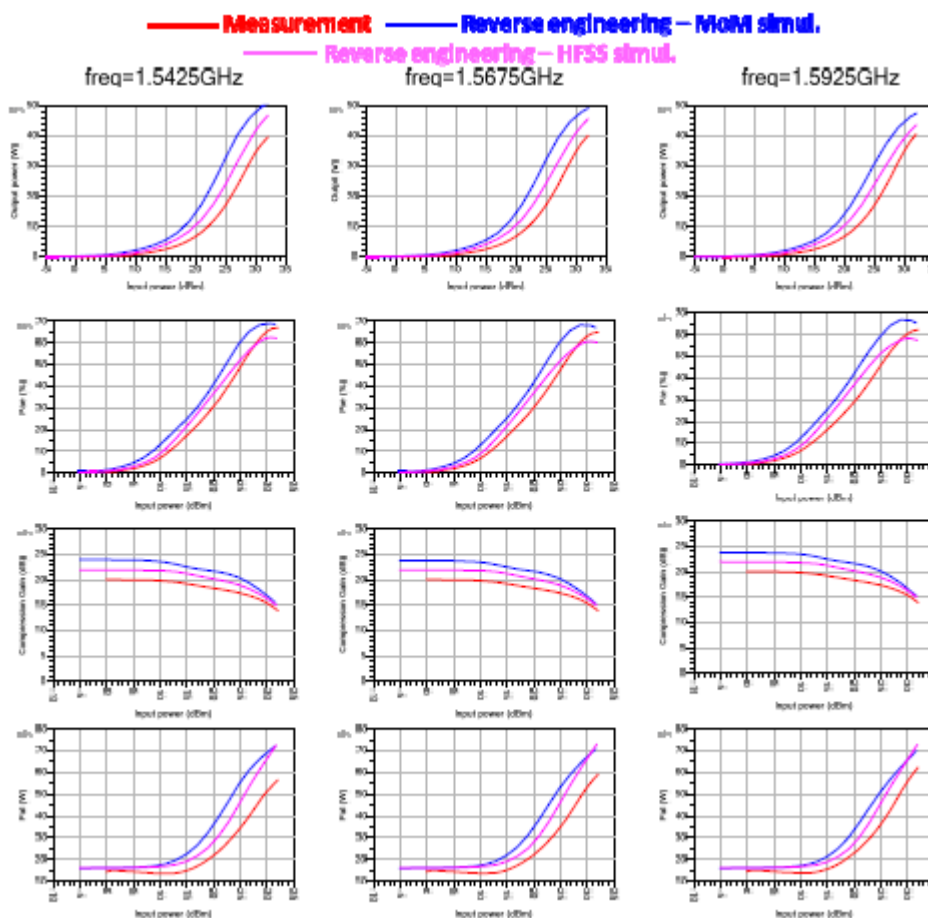


Figure 90 : HPA-1 module Run-1: HPA RF performance vs Pin comparison of measurement and reverse engineering simulations

In conclusion, in L-Band both MoM and HFSS simulation have similar behavior, but the HFSS simulation seems more realistic. Therefore, the design philosophy for the HPA design during phase is to obtain the RF performances with MoM simulation and the validation of such RF performance with HFSS simulations.

2.2.1.2 CCN on new specification for HPA-1 module

Through a CCN, TAS proposed to modify the center frequency from 1,5675GHz to 1,5385GHz. Indeed, this L-band HPA module is used as power stage of a new L-band GaN SSPA for MSS applications. The useful frequency range shall be [1,518-1,559 GHz] instead of [1,5425- 1,5925GHz]. This new equipment will be dedicated to the entire renewal market of constellations of mobile communications satellites. Thus, in phase 2, HPA-1 module are centered at 1.5385GHz.

2.2.2 Manufacture and test the 0.5µm transistors and power-bars (GH50). Run-2

In the frame of the Phase 2 of “SSPA with European Gan Devices” contract, one 3GH50-10 wafer has been manufactured by UMS. For this run, one specific mask-set, named “STARDUST”, was developed in collaboration with TAS-F. UMS was in charge of wafer manufacturing, on wafer tests and delivery. This paragraph report summarizes on-wafer measurements carried out on the Stardust wafer, referenced S355015/1R036. The workflow is as follows:

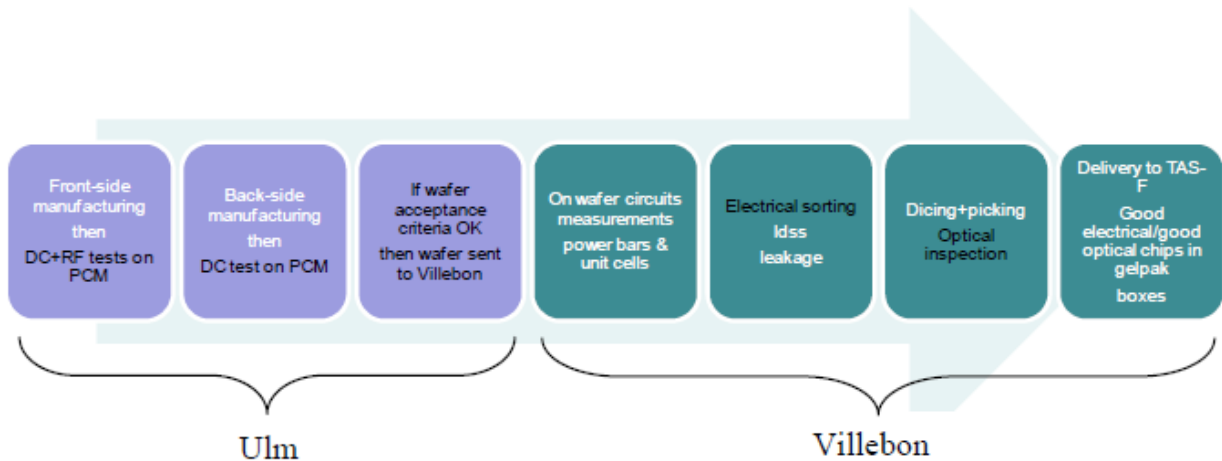


Figure 91 : UMS workflow for the manufacturing & test of GH50 maskset (Run-2)

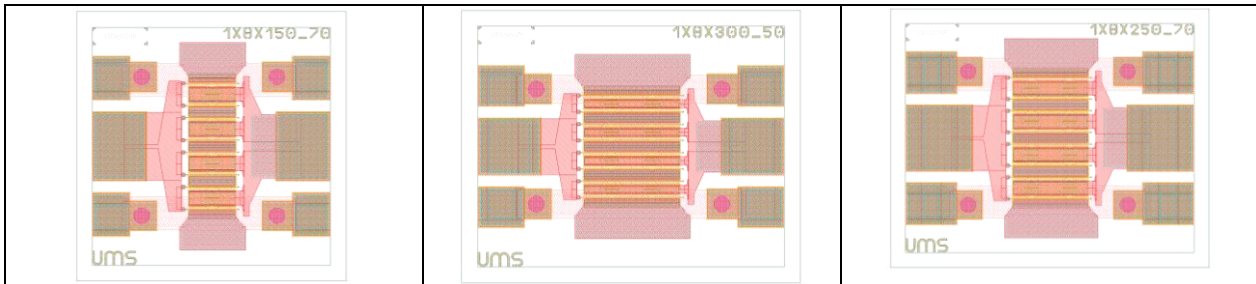
Tile composition and dimension are presented in the following figure

	Y	3,38	4,09	0,85	1,41
X	1,05	PCM1	PCM3	2,4mm 8x300µm Pitch 50µm	PCM5
	0,85	2cells 2,4mm (2x8x150µm) Pitch 70µm	9,6mm 8x8x150µm Pitch 70µm	1,2mm 8x150µm Pitch 70µm	2,4mm 2x8x150µm Pitch 70µm
	0,85	9,6mm 8x8x150µm Pitch 50µm	9,6mm 8x8x150µm Pitch 70µm	1,2mm 8x150µm Pitch 50µm	2,4mm 2x8x150µm Pitch 50µm
	0,85	9,6mm 8x8x150µm Pitch 50µm	12mm 8x10x150µm Pitch 50µm	1,5mm 10x150µm Pitch 50µm	3mm 2x10x150µm Pitch 50µm
	0,85	9,6mm 8x8x150µm Pitch 50µm	12mm 8x10x150µm Pitch 50µm	1,5mm 10x150µm Pitch 50µm	3mm 2x10x150µm Pitch 50µm
	1,05	11,8mm 8x8x185µm Pitch 50µm	11,8mm 8x8x185µm Pitch 70µm	1,48mm 8x185µm Pitch 70µm	1,48mm 8x185µm Pitch 50µm
	1,1	25,6mm 8x8x400µm Pitch 50µm	32mm 8x10x400µm Pitch 50µm	4mm 10x400µm Pitch 50µm	8mm 2x10x400µm Pitch 50µm
	1,05	11,8mm 8x8x185µm Pitch 50µm	20mm 8x10x250µm Pitch 50µm	2,5mm 10x250µm Pitch 50µm	5mm 2x10x250µm Pitch 50µm
	1,05	19,2mm 8x8x300µm Pitch 50µm	16mm 8x8x250µm Pitch 70µm	2mm 8x250µm Pitch 70µm	4mm 2x8x250µm Pitch 70µm
	1,05	11,8mm 8x8x185µm Pitch 50µm	11,8mm 8x8x185µm Pitch 70µm	3mm 10x300µm Pitch 50µm	2,95mm 2x8x185µm Pitch 50µm
	1,05	19,2mm 8x8x300µm Pitch 50µm	24mm 8x10x300µm Pitch 50µm	2,4mm 8x300µm Pitch 50µm	6mm 2x10x300µm Pitch 50µm
	1,05	19,2mm 8x8x300µm Pitch 50µm	12mm input H2 matching 8x10x150µm Pitch 50µm	1,5mm 10x150µm Pitch 50µm H2 input matching	PCM6

Figure 92 : Stardust Tile composition

In the case of the Stardust wafer 1R036 (Run-2), as well as Sabrina wafer in 2011 (Run-1), we can notice that all the parameters concerning the PCM are well centered. As regards to the PCM parameters both Run-1 and Run-2 exhibit very close features.

Some layouts of the power unit cell integrated into the Stardust wafer are presented below:



Regarding the power unit cells, S parameter measurements were carried out on the full wafer map for all the test cells. The measurements conditions were as follows:

- Frequency range : 0.5-21GHz
- Frequency step : 250MHz
- Biasing points : $I_d=50\text{mA/mm}$ $V_d=10\text{-}20\text{-}40\text{V}$

As example for the $8\text{x}250\mu\text{m}$ unit cell, the maximum stable gain /maximum available gain is plotted on the following graphs for the highest drain voltage bias point $V_{ds}=40\text{V}$. We can notice the good homogeneity chip to chip.

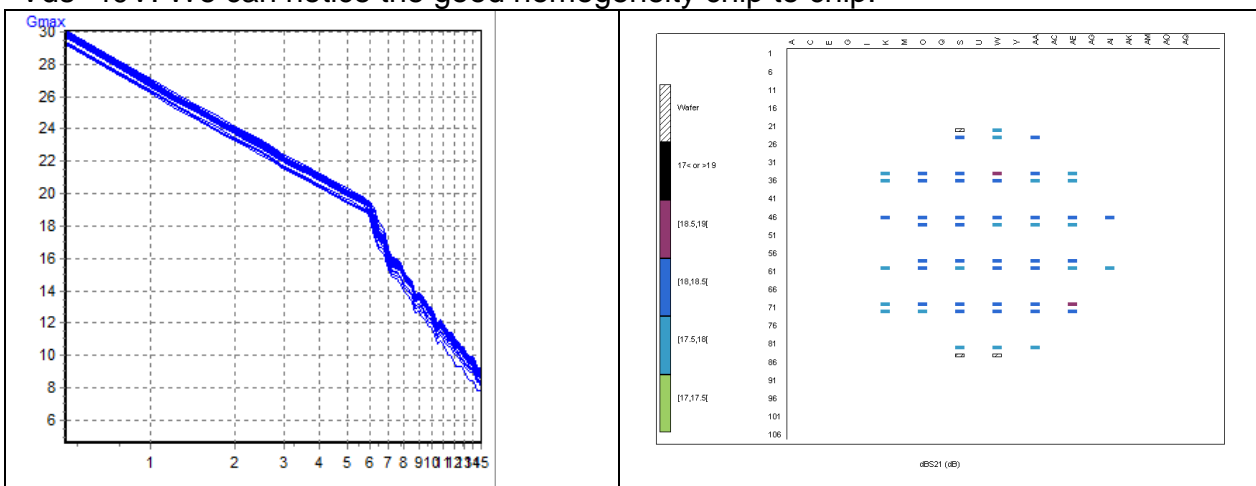


Figure 93 : $8\text{x}250_70$ $V_d=40\text{V}$ $I_d=50\text{mA/mm}$. S21 parameter mapping at 40V & $I_d=50\text{mA/mm}$

Specific load-pull measurements have been carried out in order to get more information about the large signal performance homogeneity on a whole wafer. Measurements have been carried out at 4Ghz on three topologies: $1\text{x}8\text{x}150_50$, $1\text{x}8\text{x}150_70$ and $1\text{x}8\text{x}250_70$

For each topology, about 30 samples have been tested on the Stardust wafer S355015/1R036. The next graphs show for $8\text{x}250\mu\text{m}$ unit cell the performance homogeneity we could expect at transistor level matched with fixed loads at the input and the output. The output impedances at fundamental frequency and second harmonics have been chosen for maximizing PAE.

The impedances are set up to:

- Gsource@fo=0.7/165.1°
- Gload@fo=0.59/97.9°
- Gload@2fo=0.8/90°
- Gload@3fo=0.0

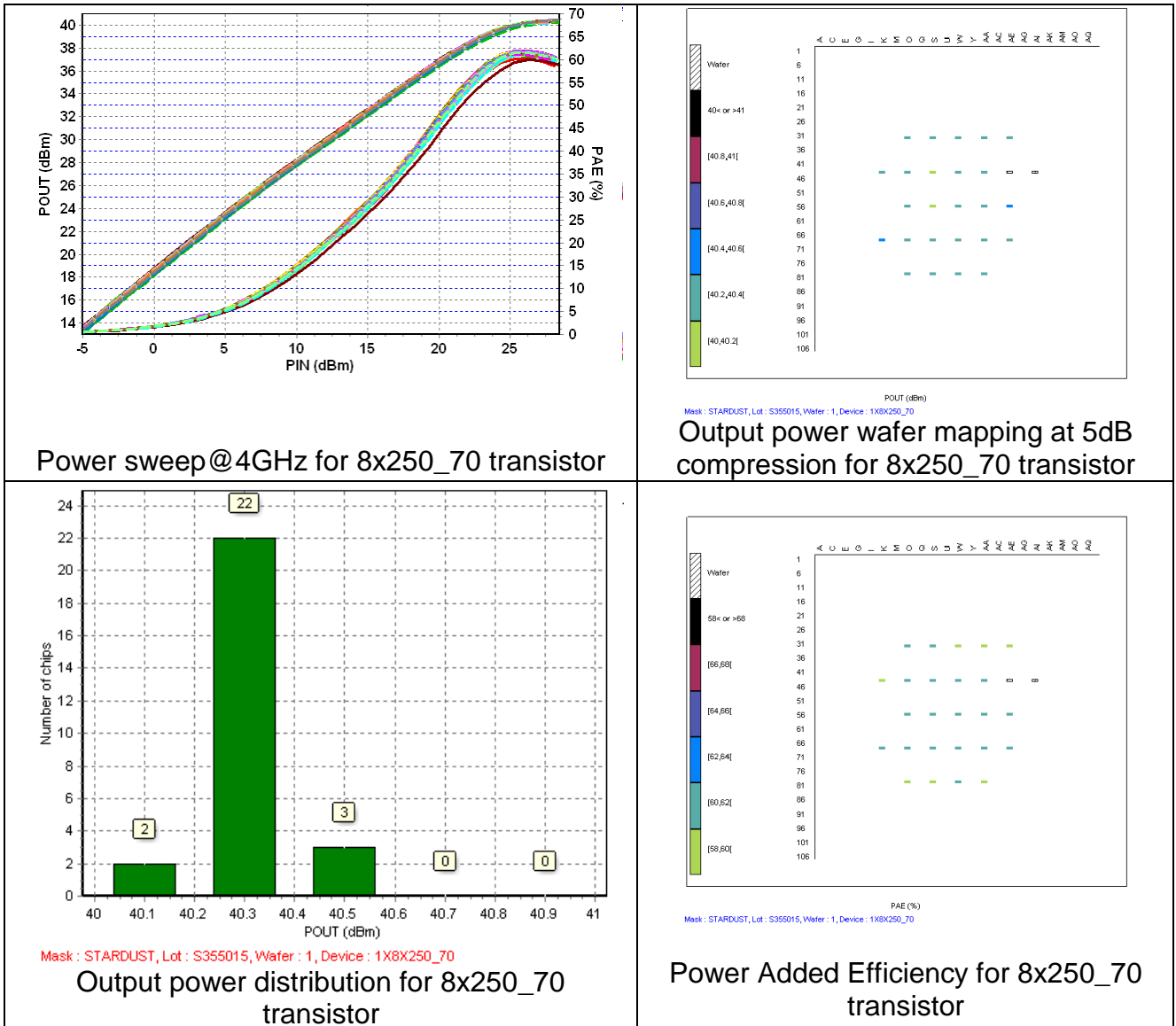
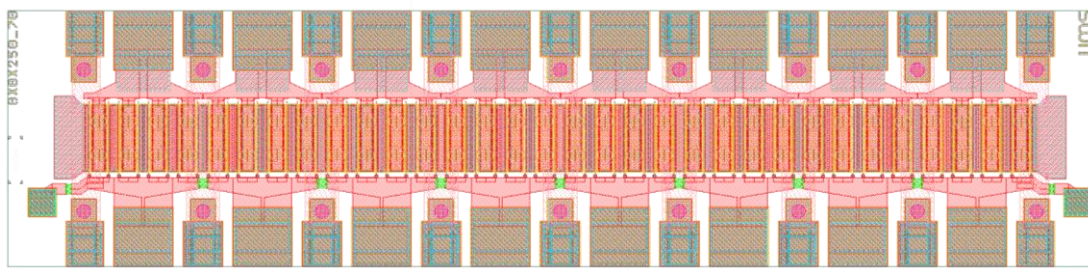


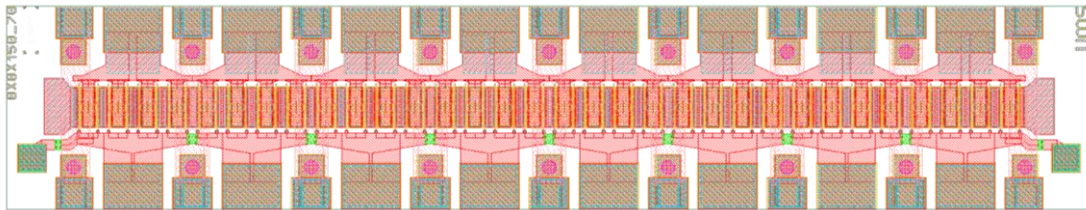
Figure 94 : On-wafer loadpull measurement of 8x250µm power cell unit

Some layouts of the power unit cell integrated into the Stardust wafer are presented below

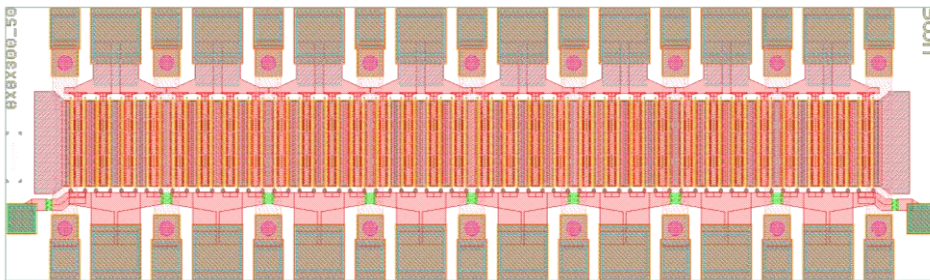
- 8x8x250_70: Xwith dicing street=4.19mm Ywith dicing street=1.15mm



- 8x8x150_70: Xwith dicing street=4.19mm Ywith dicing street=0.95mm



- 8x8x300_50: Xwith dicing street=3.48mm Ywith dicing street=1.15mm



These Power bars are measured in DC mode thanks to specific probe card, more. All signal pads are connected together as well as ground pads through the probes card.

The screening procedure applied on every power bar of the whole wafer is:

- Schottky diode: A gate voltage swing is applied on the power bar with an open circuit on the drain. The gate current is measured. This enables to check the behaviour of the gate- source schottky diode. The results are gathered per power bar topology.
- Saturated drain current: Saturated drain current is measured in pulse mode for thermal issue. The biasing conditions are $V_{gs}=0V$ and $V_{ds}=10V$. On the next graphs we can look at the saturated drain current mapping for each power bar topology.
- Pinch-off voltage: During this measurement, a current loop looks for $I_{dss}/100$, and then the associated gate voltage is defined as the "pinch-off voltage". All the results are summarized in two charts. One is depicted the V_p spread per topology.
- Gate/drain current leakage: a leakage test is performed; the power bars are pinched-off under $-7v$ with an associated drain voltage of $40V$. The gate and drain currents are measured.
- were measured on every power bar of the whole wafer.

Measured performance of 8x8x250µm power-bar are presented below.

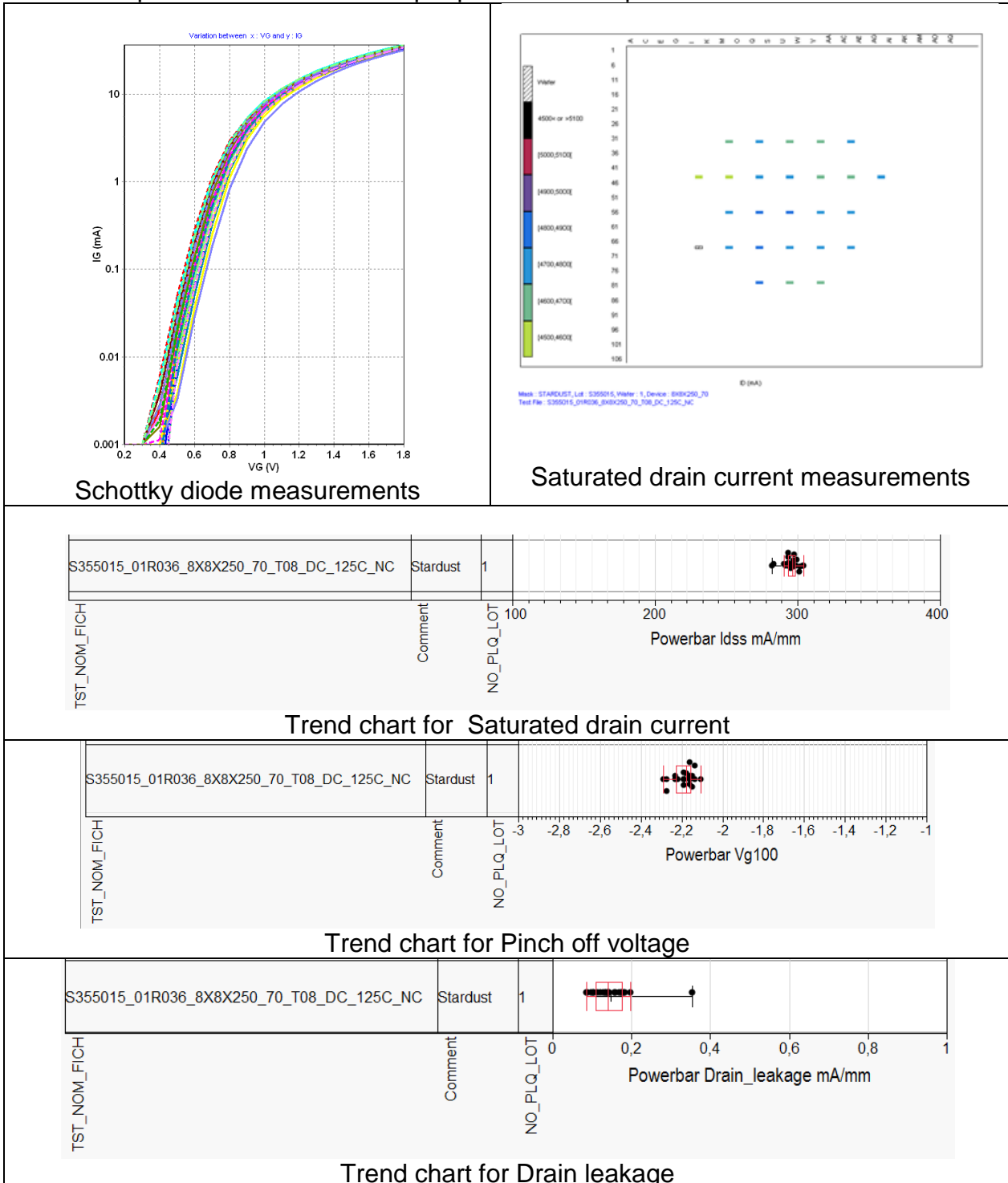


Figure 95 : 8x8x250µm power-bar on-wafer measurements

The PCM data have shown that this Stardust wafer is in agreement with the 3-GH50-10 technology acceptance criteria. On-wafer electrical characterizations have been

carried out on all the devices. All transistors and power bars have been tested. Power bars have been tested following the UMS standard “screening procedure” for GaN devices. All the tests performed, S parameter, load-pull and DC screening have shown a very good homogeneity of the performance whatever the devices location on the wafer. As a results, the electrical yield should be very good.

2.2.3 Characterization and modeling of the 0,5 μ m transistors and power-bars. Run-2

2.2.3.1 Unitary cell measurements. Run-2

This paragraph gathers AMCAD Engineering and XLIM tasks achieved within the framework of the ARTES 5.1 SSPAs with European GaN Devices, Phase2 (Run-2). For unitary cell, AMCAD Engineering tasks consisted in pulsed I(V) with pulsed [S] measurements, load pull measurements and devices modeling. For power bar, AMCAD Engineering tasks consisted in load pull measurements. For power bar model, update of the model has been performed by AMCAD based on load-pull measurements.

The system set up for the transistor (8x250 μ m UMS) characterization is described below. The bias voltages and S-parameters are performed in CW mode.

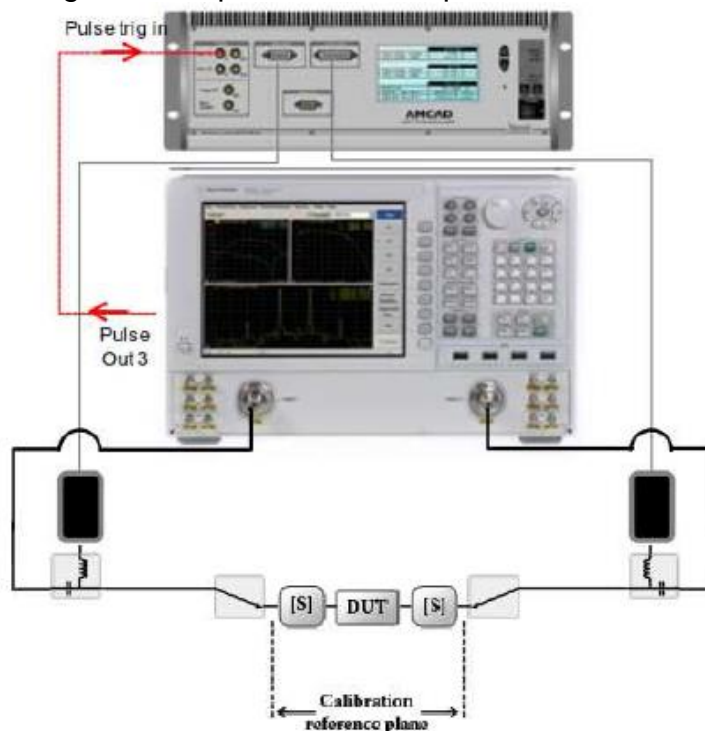


Figure 96 : AMCAD I(V) and [S] test bench for transistors characterizations. Run-2

The principle of pulsed measurement is to describe the I(V) network by quasi-isothermal measurements using short pulses around a quiescent bias point selected. The quiescent bias point of rest is provided by the voltage levels and V_{gs0} v_{ds0} . This results in a current I_{ds0} polarization. Pulses, whose levels are represented by V_{GSI} , I_{GSI} , V_{DSI} I_{DSI} and describe all the characteristics of input and output of the transistors. Principle of the S-parameters measurements in pulse mode is the same than the one used in Phase 1 (Figure 17)

5 samples are supplied by UMS:
-> Ref: W81, W69, AA33, AA57, AA45

Preliminary pulsed I(V)/RF measurements have been performed on each sample of order to estimate the process dispersion and to select the most representative samples for the complete characterizations. These dispersive measurements have been performed at ambient temperature (25°C). The results for the different transistor are shown hereafter.

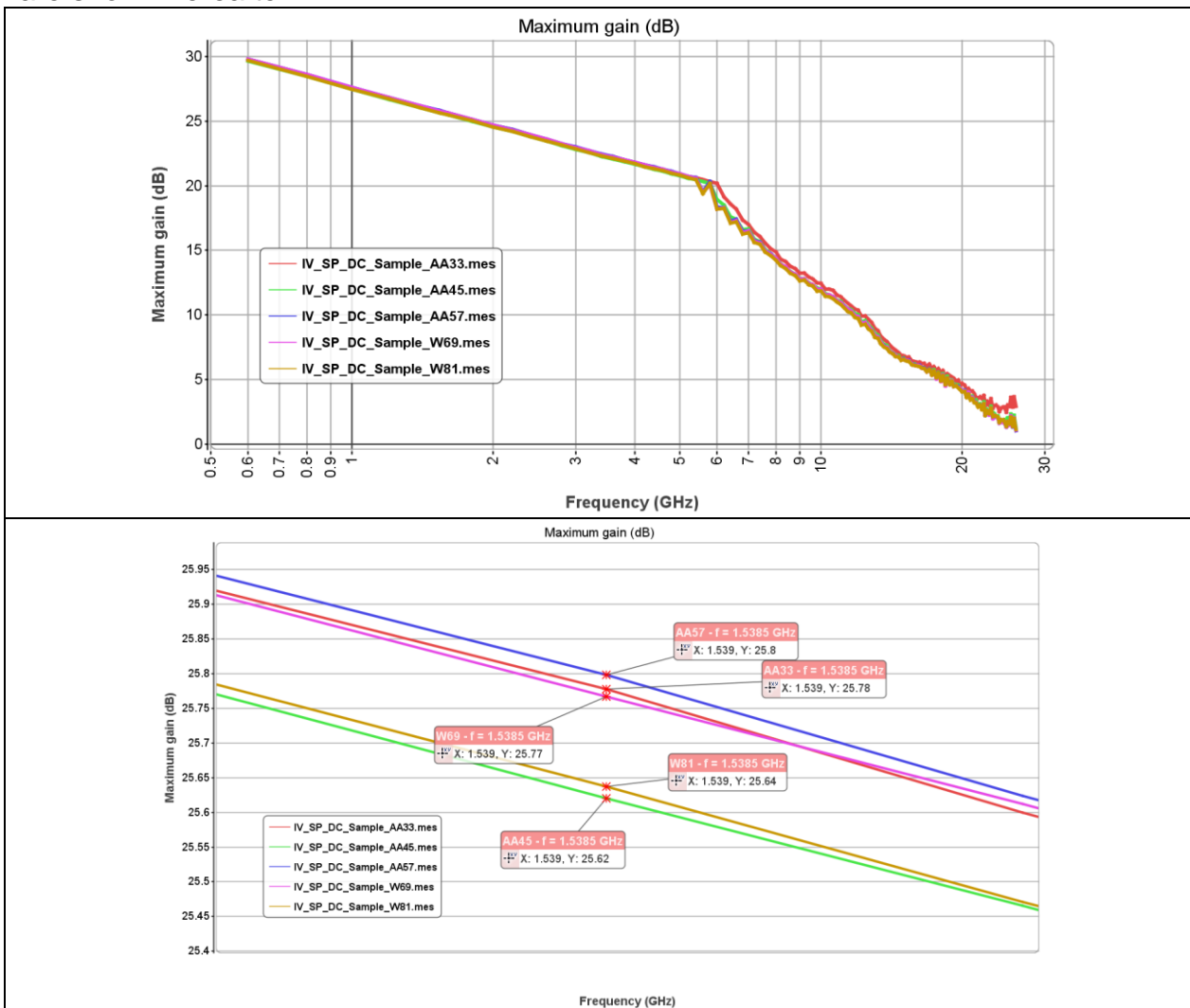


Figure 97 : Dispersive [S] measurements on transistors 8x250µm GH50. Run-2 (bias points corresponding to surrounded points on the I(V) curves, Vds=40V)

The representative samples chosen are referred W81. Measurements with temperature have been performed at 25°C, 60°C and 90°C. The results obtained are shown hereafter.

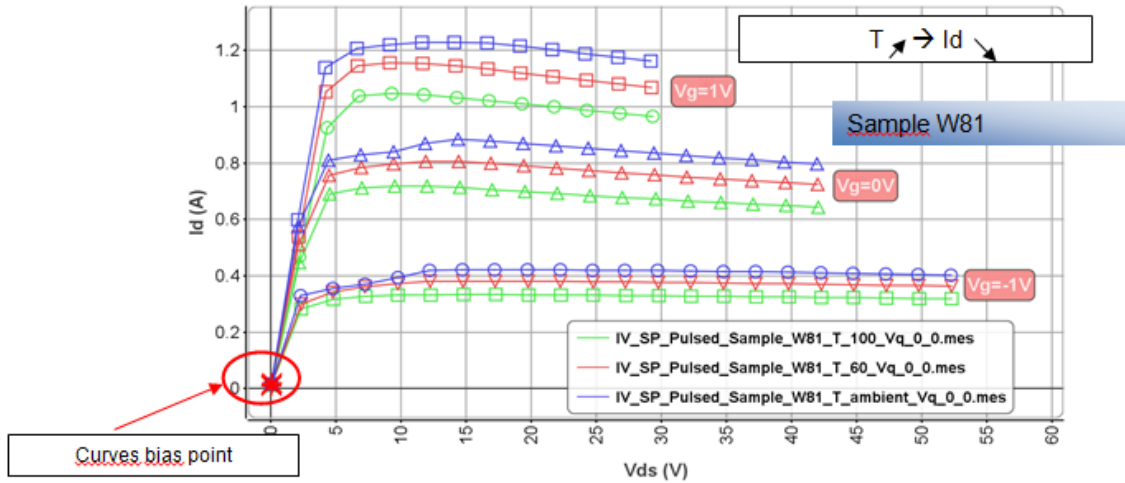


Figure 98 : Output current with different chuck temperature (25°C, 60°C, 100°C) Transistor 8x250µm Sample W81 measurements. Run-2

Idss is reduced by 8% to a rise of 75 ° C the chuck temperature.

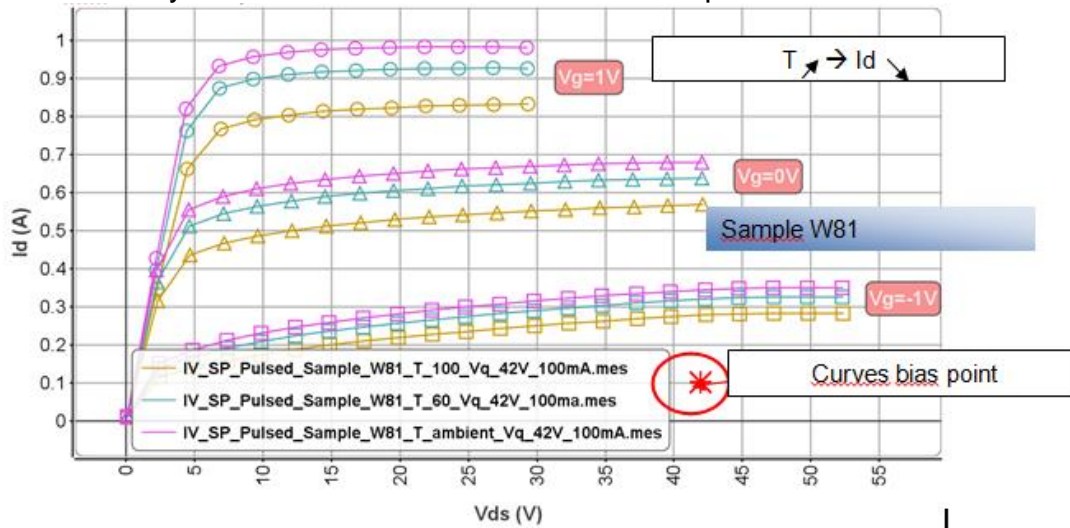


Figure 99 : Output current with different chuck temperature (25°C, 60°C,100°C), transistor 8x250µm GH50 measurements (bias points Vds0=42V, Ids0=100mA)

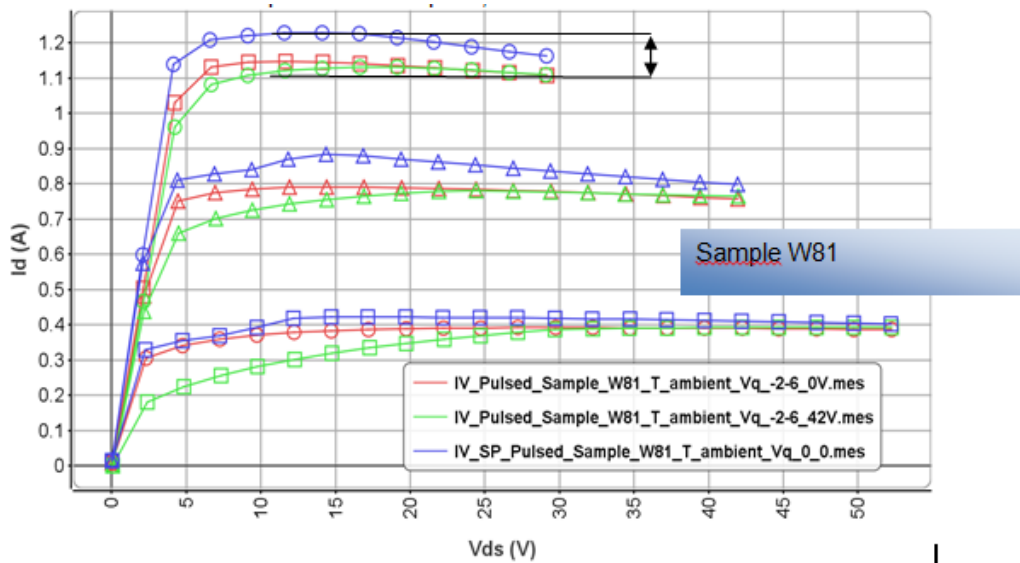


Figure 100 : Highlighted phenomena traps

The effect on the output characteristic is a reduction of the drain current of 8%

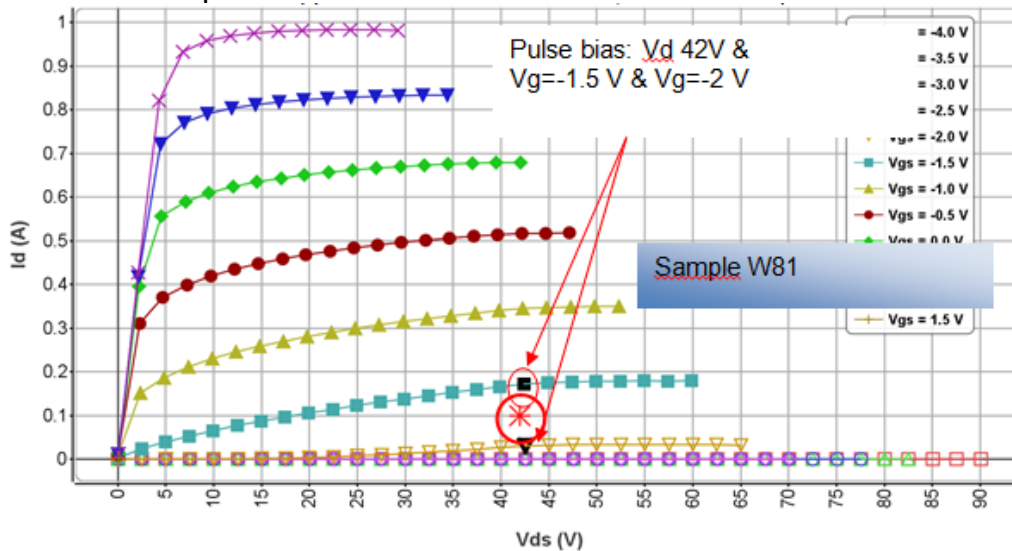


Figure 101: Output current, quiescent bias: (42V, 100mA), (chuck temperature = 25°C), transistor 8x250 μ m GH50

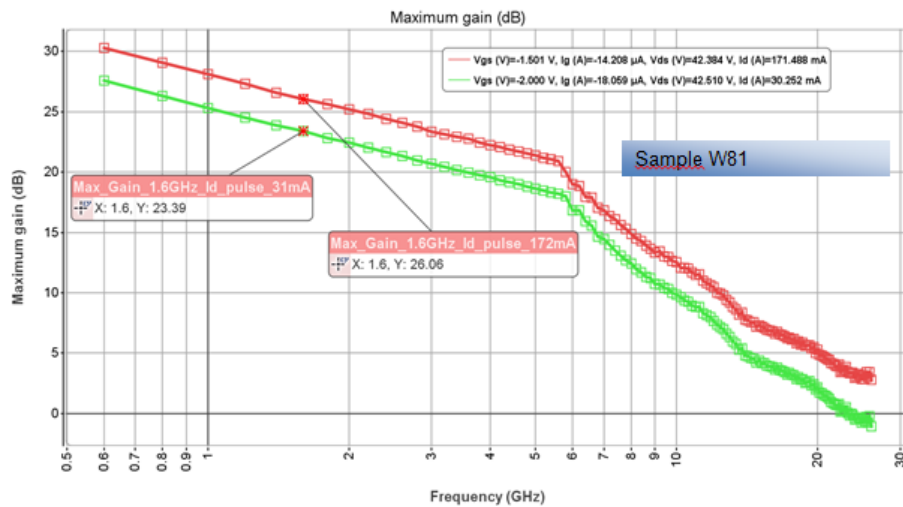


Figure 102 : Maximum Gain @ Vds0=40V, Ids0=50mA/mm

Load Pull measurements were performed in CW mode at a 1.5385GHz. The impedances were optimized at the fundamental frequency and the harmonics 2 and 3. The system set up for the devices characterization is the same used in phase 1 (Figure 23).

The objective is to find the optimal impedances in order to have the best power added efficiency (PAE) for $f_0 = 1.5385\text{GHz}$ CW mode. Load Impedance harmonic $2f_0$ is also optimized to achieve maximum PAE. It is optimized in active mode. Source impedance f_0 is optimized to find the best Pin for a similar Psource. Source impedance harmonic $2 f_0$ is also optimized to achieve maximum PAE. It is optimized in active mode.

The $8 \times 250\mu\text{m}$ components are polarized in DC mode:

- $V_{ds0}=42\text{V}$, $I_{ds0}= 50\text{mA/mm}$

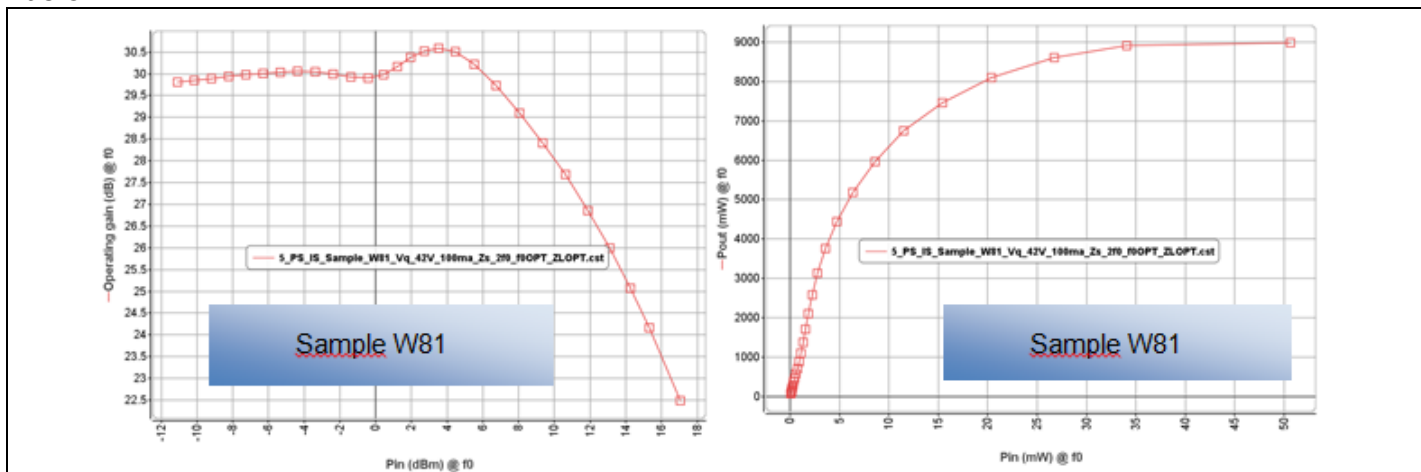
The reference sample W81 is the selected transistor to realize the study. Several samples will be used to validate end optimization measures and study the dispersion.

The load-pull Optimization methodology used during this campaign is:

- Optimization of f_0 load impedance: A first optimization of the load impedance is made at low level to determine the optimal impedance zone when the transistor operates in the linear regime. For this impedance, a power sweep is then performed in order to observe the performance obtained. The power that provides the maximum added power efficiency is raised to perform a second optimization of the load impedance (nonlinear regime). During these optimizations, the load impedances at $2f_0$ and $3f_0$ are equal to 50 ohms. During these first measures it appeared that the transistors are conditionally stable, this was confirmed by S-parameter measurements (measurements made on 50Ohms support and source). These Sparameter measurements give a good indication of the places of the Smith chart for which the transistor may be unstable. For $\Gamma_{load}@f_0=0.483, 50.5^\circ$, transistor reaches a 66.08% PAE.

- Optimization of 2f0 load impedance: the load impedance at f0 is now set to the optimum impedance PAE. An impedance sweep at 2f0 is now performed to a input power level within the transistor to obtain the maximum PAE. The impedance at 3f0 remains at 50Ohms. For $\Gamma_{load@2f0}=0.986/44.99^\circ$, transistor reaches a 76.36% PAE. (10 points increasing).
- New optimization of the f0 load impedance: With this new optimization of f0 load impedance, the PAE reaches 79.66% (4 pts increasing, 2f0 load impedance is fixed on its optimal).
- Measurement and optimization of f0 Source. Source impedance f0 is optimized to find the best Pin for a similar Psource. $Z_{source@2f0}$ is set to 50Ω , $Z_{load@f0\&2f0}$ are set to PAE optimum ($\Gamma_{load@f0}=0.599/44.61^\circ$, $\Gamma_{load@2f0}=0.986/44.99^\circ$). We obtain a maximum Pin for $\Gamma_{source@f0}=0.801/141.7^\circ$, Pin reaches a 17.33 dBm for 18.27dBm of Psource, the PAE reaches 82% (2,5 points increasing)
- Optimization of 2f0 source impedance. For this optimization, source impedance 2f0 is optimized. $\Gamma_{load@f0\&2f0}$ are set to PAE optimum ($\Gamma_{load@f0}=0.599/44.61^\circ$, $\Gamma_{load@2f0}=0.986/44.99^\circ$) and $\Gamma_{source@f0}$ is set to Pin optimum $\Gamma_{source@f0}=0.801/141.7^\circ$. For $\Gamma_{source@2f0}=0.845/14.9^\circ$, the PAE reaches 82.4%. The 2f0 source impedance doesn't permit to increase the PAE.

The performances obtained for these optimal PAE load impedances are depicted below.



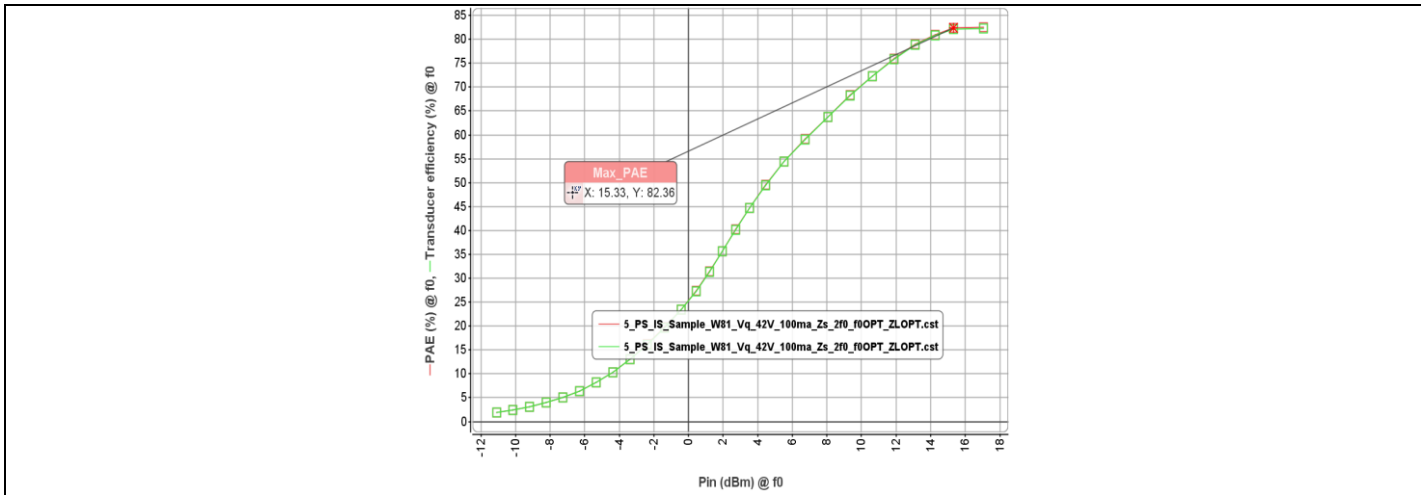


Figure 103 : Pout / PAE / Gain vs Pin after loadpull optimization. Optimized load (H1, H2) for optimal PAE performance. Vds=42V, 50mA/mm.

Regarding the RF performance vs Technology Dispersion, the load impedances are substantially similar to the fundamental frequency and harmonic frequency.

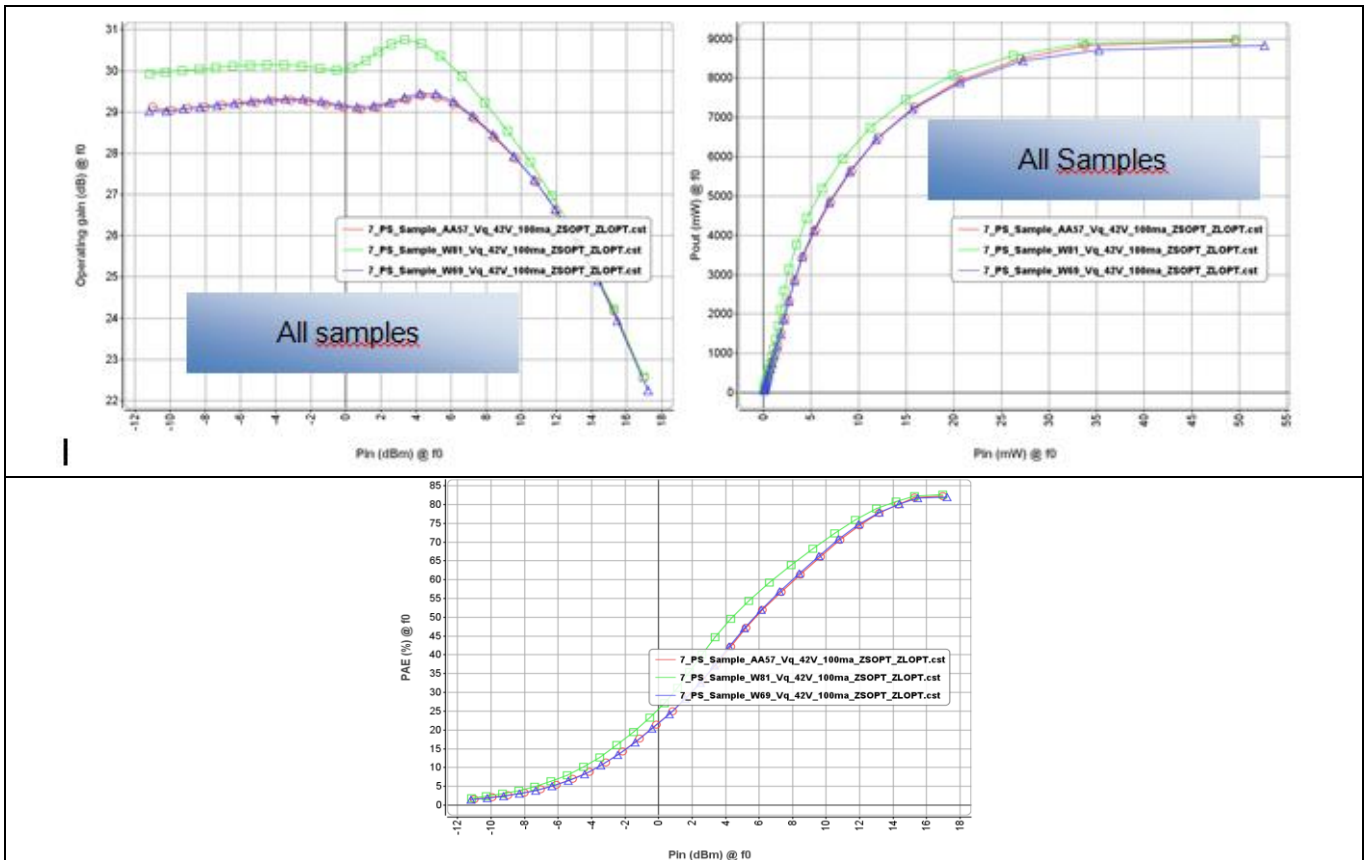


Figure 104 : Loadpull measurements. Performance vs Technology Dispersion. 3x 8x250µm transistor samples tested. 42V, 50mA/mm.

Table which summarized the load-pull performance monitored during loadpull measurements on different samples is provided below.

Sample	Linear Gain (dB)	Output Power (W)	PAE f0 OPT(%)	PAE all OPT(%)	Zload f0 opt PAE (Ω)	Zload 2f0 opt PAE (Ω)	Zsource f0 (Ω)	Zsource 2f0 (Ω)
W81	29.92	8.97	71.4	82.61	63.27+j83.22	2.08+115.5j	6.17+17.13j	172+266.5j
W69	29.02	8.84	No data	82.02	63.27+j83.22	2.08+115.5j	6.17+17.13j	172+266.5j
AA57	29.12	8.95	No data	82.29	63.27+j83.22	2.08+115.5j	6.17+17.13j	172+266.5j

Table 19 : Summary of performance monitored during loadpull measurements. Vds=42V and Ids=50mA/mm

2.2.3.2 Unitary cell modeling activity. Run-2

The provided model is a 3 ports transistor. All the parameters are available as well as the chuck temperature and selfheating effects. The model topology is illustrated below..

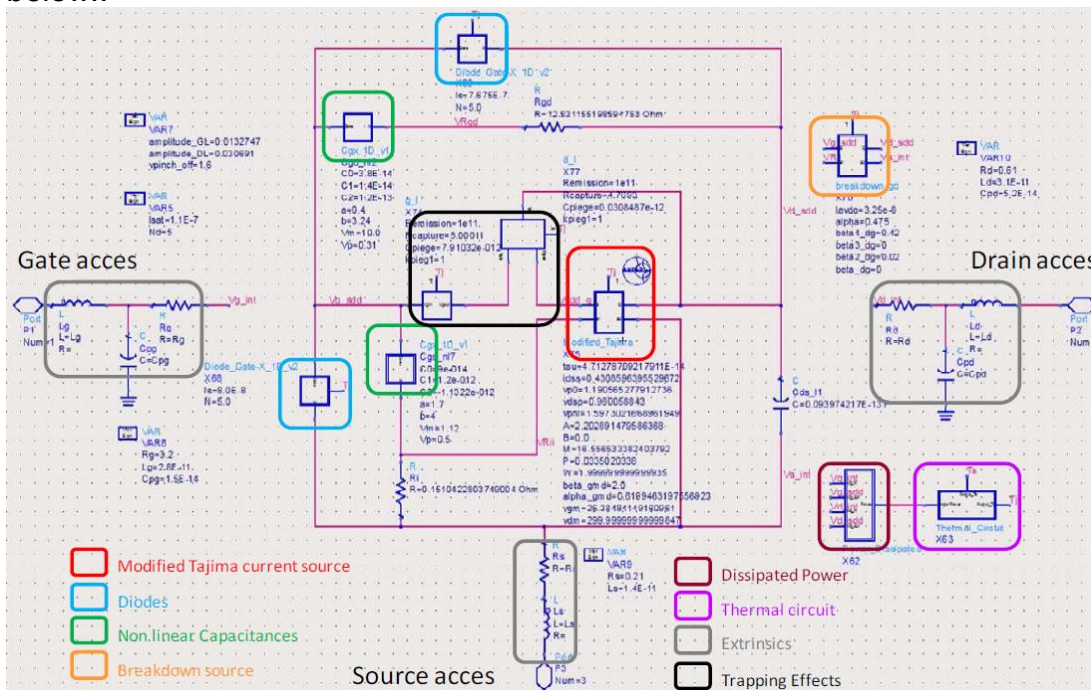


Figure 105 : Elementary transistor cell 8x250µm GH50. Model implemented in ADS

Input/output access lines: Line_port1 & Line_port2 (Figure II.1) are used for deembedding to consider the transistor plan. All measurements are de-embedded on IVCAD knowing S-Parameters of these input/output access lines inside the transistor plan.

These later were calculated from the provided layout (STARDUST), by THALES ALENIA SPACE. In this chapter, all the comparisons (measurements / model) will be presented in the transistor plan

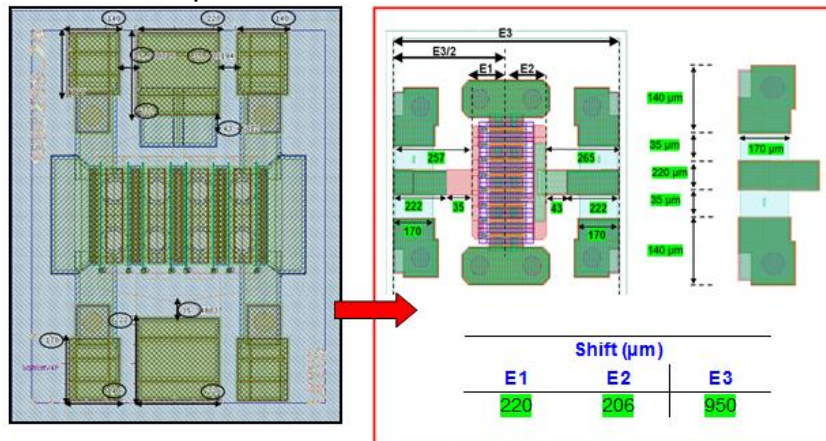


Figure 106 : Access lines & Transistor Layout (All values in μm)

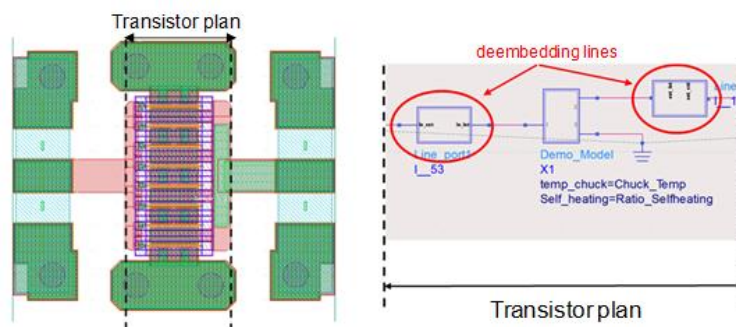


Figure 107 : Modeled Transistor

The model is adjusted through several measurements (I(V), [S], load-pull...) in different operating conditions (bias, temperature, frequency...) in order to have a coherent model. Some comparison (measurements/simulations) are provided below the very good accuracy of the transistor model.

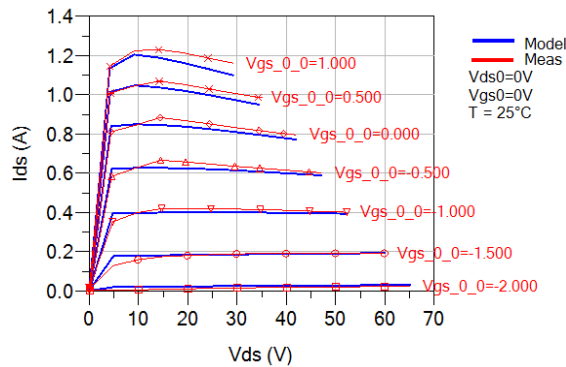


Figure 108 : 8x250µm transistor model validation. I(V) curves comparison. Quiescent bias conditions : Vds0=0V, Vgs0=0V

Thermal network was provided by XLIM through ANSYS. Rth and Cth were then directly implemented on ADS

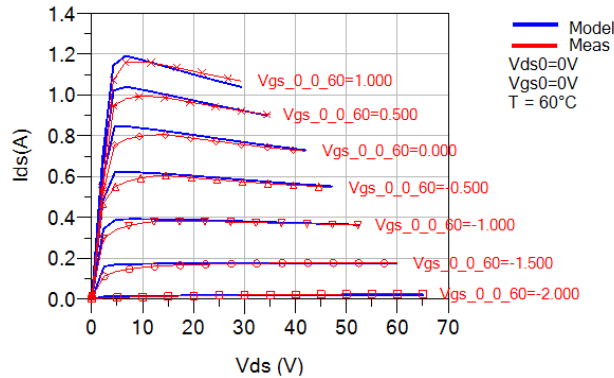


Figure 109 : 8x250µm transistor model validation. I(V) curves comparison. Bias conditions : Vds=0V, Vgs=0V. Temp=60°C

Comparisons between the pulsed I(V) measurements and the model @ _chuck=25°C are illustrated below, for the quiescent bias conditions : Vds0=0V, Vgs0=-2.6V, Vds0=42V, Vgs0=-2.6V.

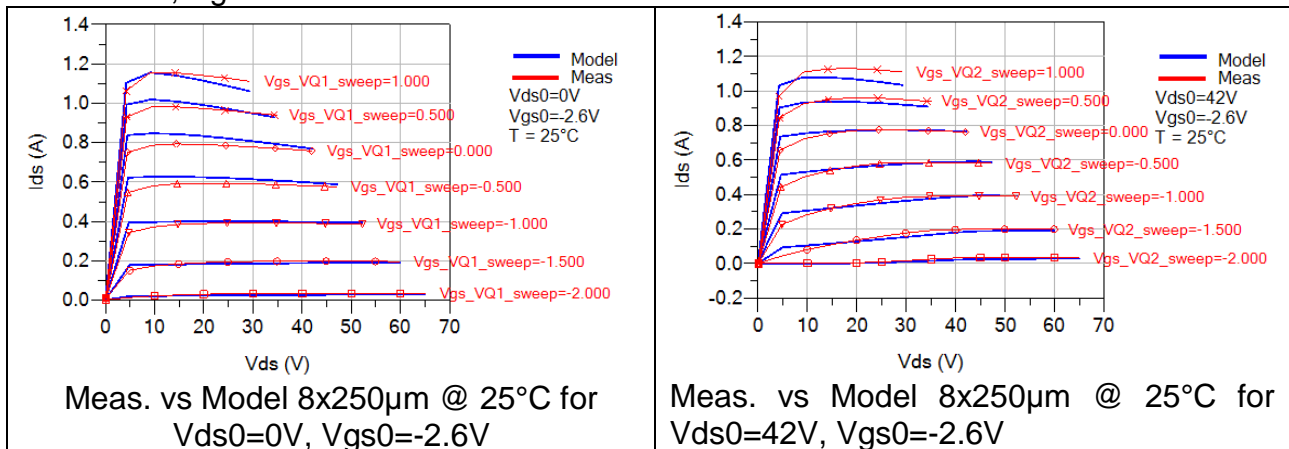


Figure 110 : Trap effects

For S parameters [0.6 to 26 GHz] validation, the model is compared to the measurement on several bias points.

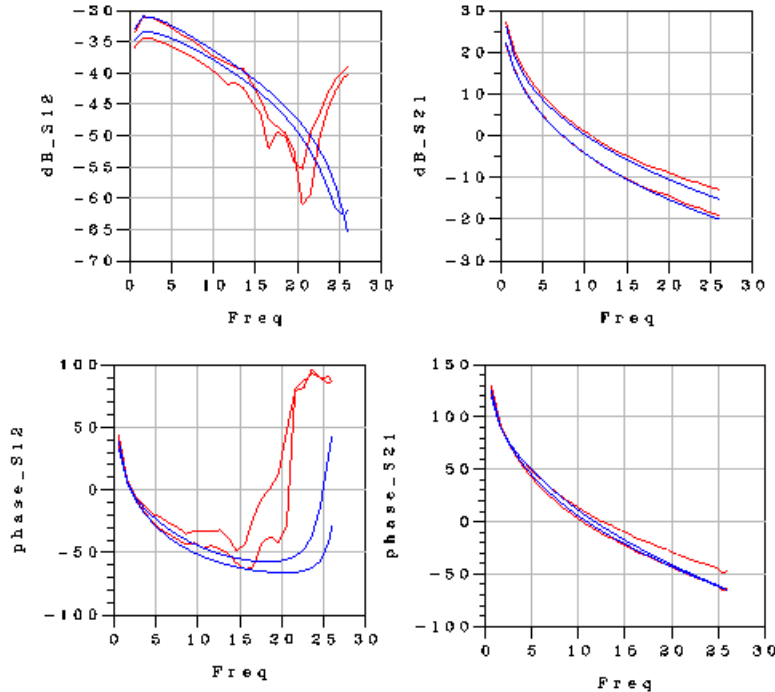


Figure 111 : 8x250µm transistor model validation. [S] parameters comparison. Measurement. vs Model 8x250µm @Vds0=42V and Ids0=50mA/mm

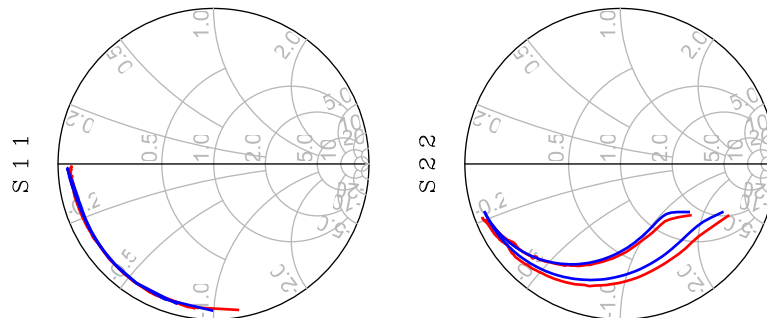


Figure 112 : 8x250µm transistor model validation. [S] parameters comparison. Measurement. vs Model 8x250µm @Vds0=42V and Ids0=50mA/mm

In Load-pull configuration, the comparison is performed at one frequency (1.5385GHz) and for several load impedances including the optimum ones. Next figures illustrate contour of max PAE & opt POUT @ 3dB respectively.

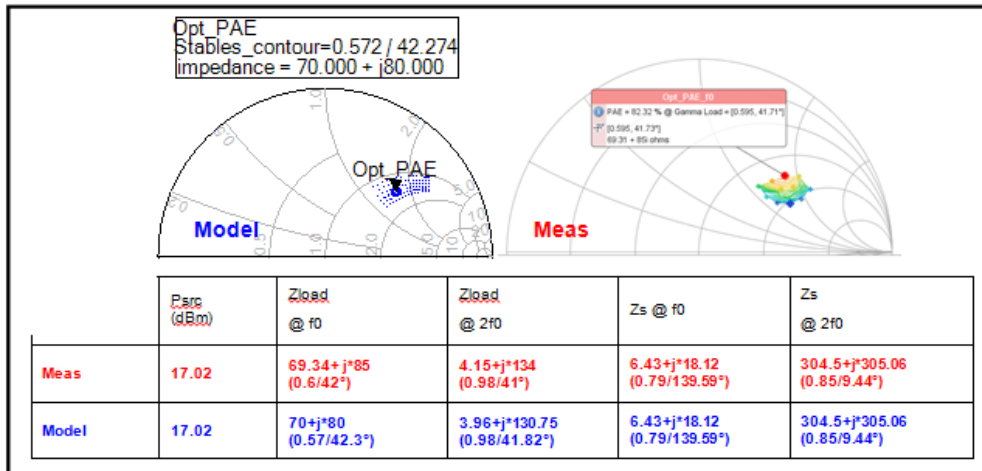


Figure 113 : Contour of Max PAE - Meas. vs Model 8x250µm

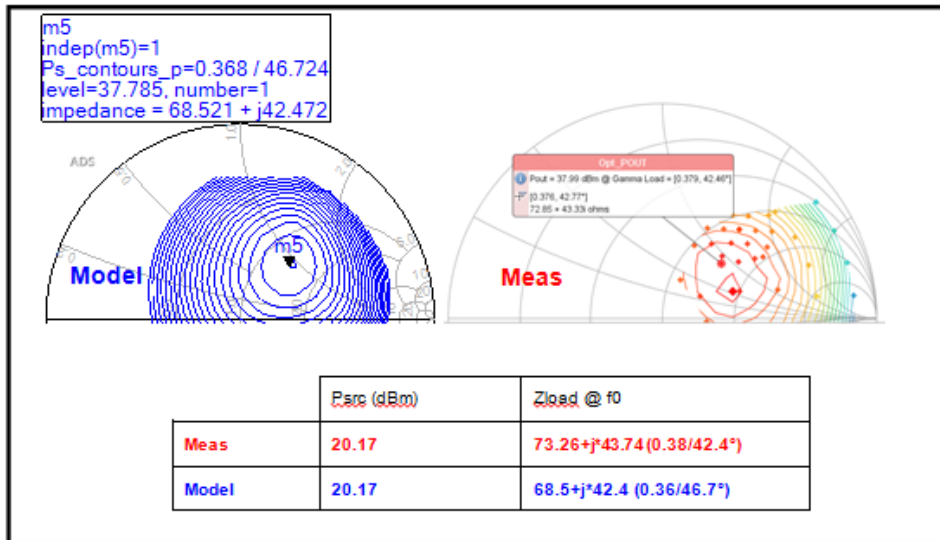


Figure 114 : Contour of opt POUT @ 3dB - Meas. vs Model 8x250µm

Opt PAE is reached at very near load impedance on measurements & simulations. On the following table, for comparison (simulation/measurement) exercise, opt PAE & Pout selected at f₀, including opt PAE @ 2f₀ are presented.

	Z _{load} @ f ₀	Z _{load} @ 2f ₀	Z _s @ f ₀	Z _s @ 2f ₀
Opt PAE	69.34+ j*85 (0.6/42°)	4.15+ j*134 (0.98/41°)	6.43+ j*18.12 (0.79/139.59°)	304.5+ j*305.06 (0.85/9.44°)
Opt POUT @ 3dB	73.26+ j*43.74 (0.38/42.4°)			

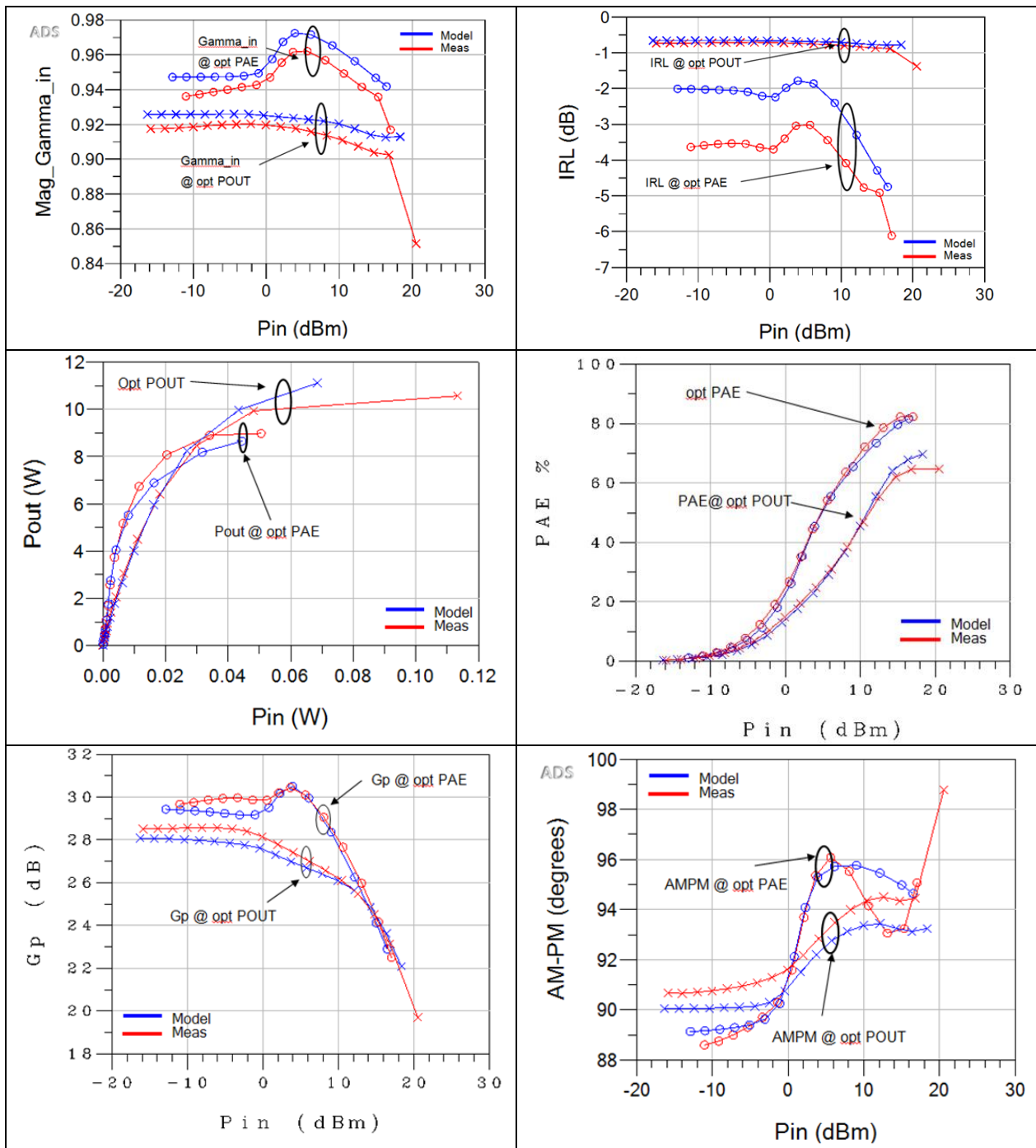


Figure 115 : 8x250µm transistor model validation. Loadpull simulations / measurements comparison. Vds0=42V and Ids0=50mA/mm

2.2.3.3 Power Bar measurements. Run-2

Load-pull measurements have been performed by TAS-F at Toulouse facilities. Conditions are:

- 3 power-bar mounted in jig test configuration and tested
- Measurements in CW mode with the following conditions:
- $V_{ds0}=42V$
- $I_{ds0}=800mA$ (50mA/mm)
- $F_c=1.5385GHz$
- The measurements have been performed in the SMA connectors plans (before de-embedding)
- De-embedding have been performed by AMCAD during the modeling activities.

The load-pull Optimization methodology used during this campaign is:

- Measurement on $Z_{out_H1}=Z_{out_H2}=50ohms$
- Measurement on $S22^*$
- Measurement with cloud of points in $S22^*$ area
- Measurement with cloud of points at Z_{out_H1} to obtain PAE_{opt}
- Measurement with cloud of points at Z_{out_H2} to obtain PAE_{opt}
- New optimization of Z_{load} @ F_0 with $Z_{load}@2F_0$ optimized
- Final optimization for max PAE: Z_{load} optimum @ F_0 and $2F_0$

Final performance after the different loadpull optimization steps are presented below:

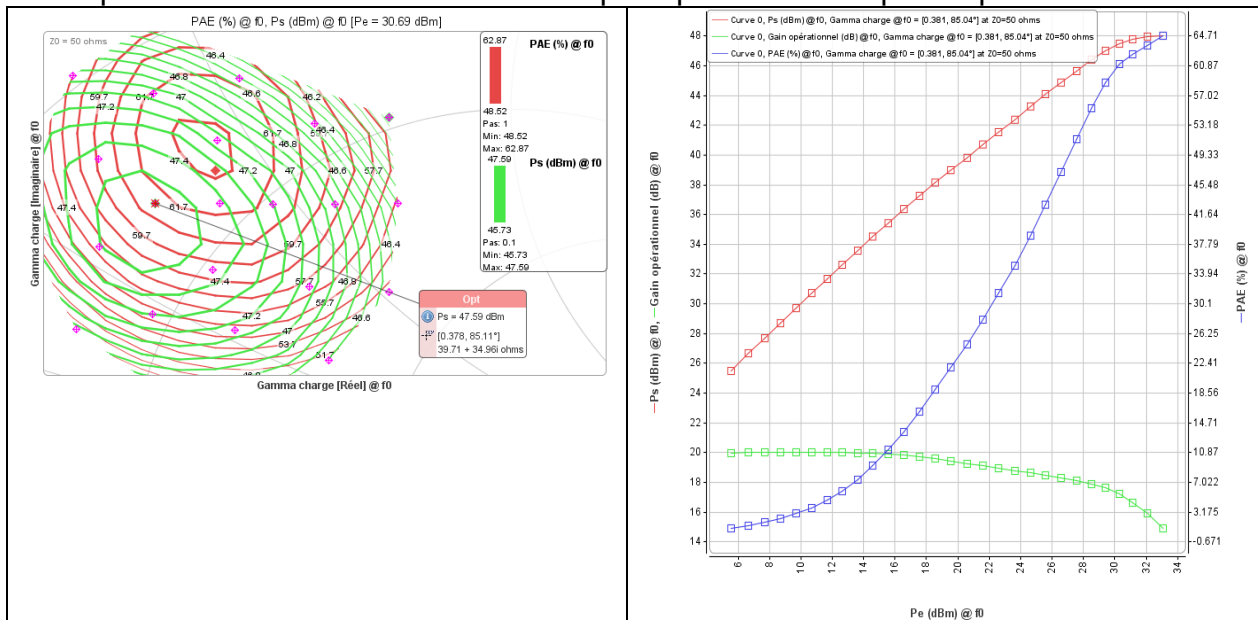


Figure 116 : SMA reference plane, Power bar N°2. Power Gain (dB)/ Pout(dBm) / PAE(%) of the power bar after final optimization of Z_{load} @ F_0 and $Z_{load}@2F_0$

Finally, the measured RF performance of the power bar after final optimization of $Z_{load} @ F_0$ and $Z_{load}@2F_0$ is With this second optimization at fundamental frequency ($2F_{0opt}$, $3F_0$ is set to 50 Ohms):

- $P_s = 63 \text{ W}$
- $PAE = 64,71 \%$
- $Gain = 20 \text{ dB}$
- $Z_{out_H1} : [0,378 ; 85,11^\circ]$
- $Z_{out_H2} : [0,507 ; 118,2^\circ]$

2.2.3.4 Power Bar modeling activity. Run-2

The power-bar model includes connections for 8 elementary transistors. These later are connected at the drain with a short circuit and through a resistor at the gate. Also, an input resistance "R" is added to describe parasitic effects due to the bonding connection at the input Power-bar. The power bar is connected through wire bondings to input and output circuit. Wires bounding are represented by their S parameters. Input circuit and output circuit are represented either by a simulated circuit or S parameters of these circuits.

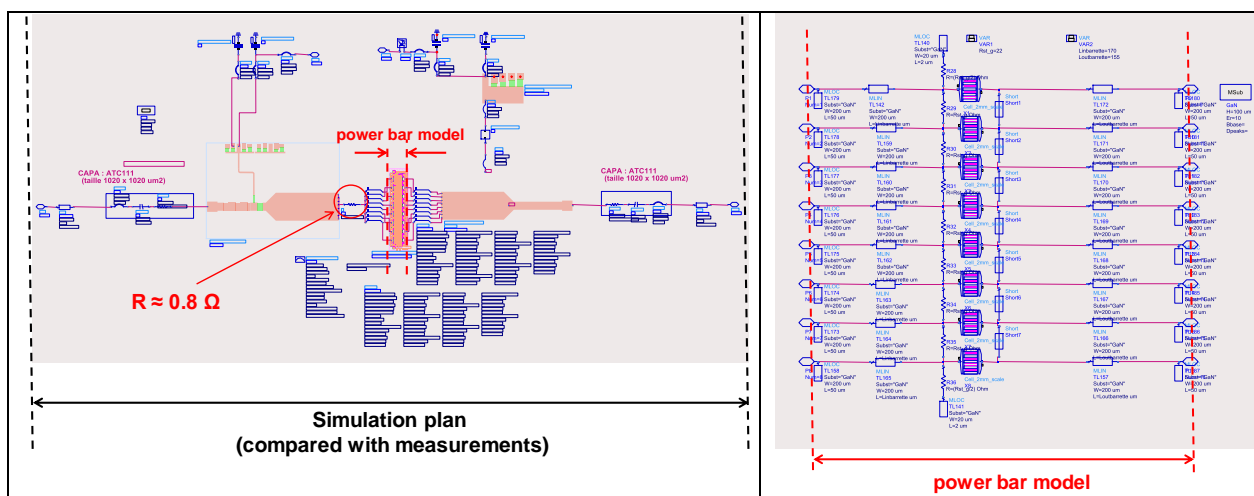
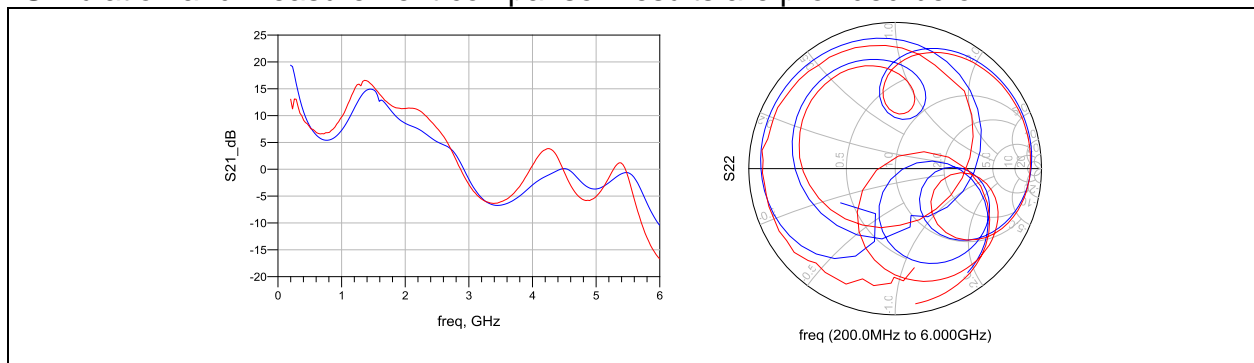


Figure 117 : Used power bar configuration for the simulation

Simulation and measurement comparison results are provided below:



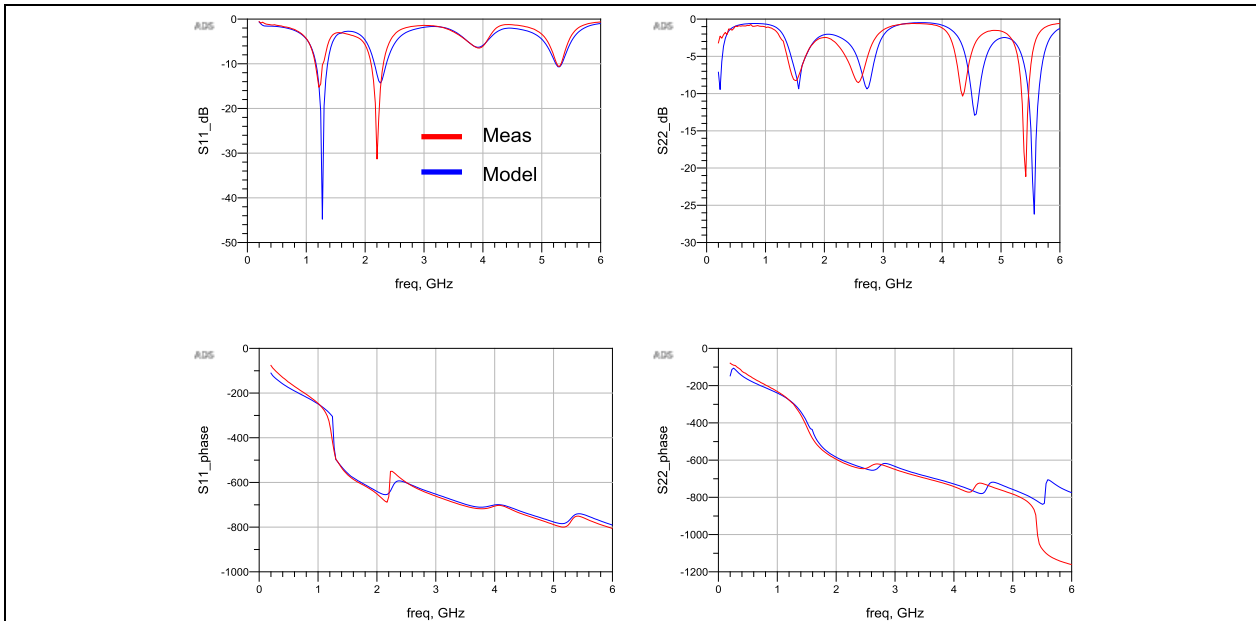


Figure 118 : Sparameter comparison between simulations and measurements for power bar Jig_Test_Barrette_N1

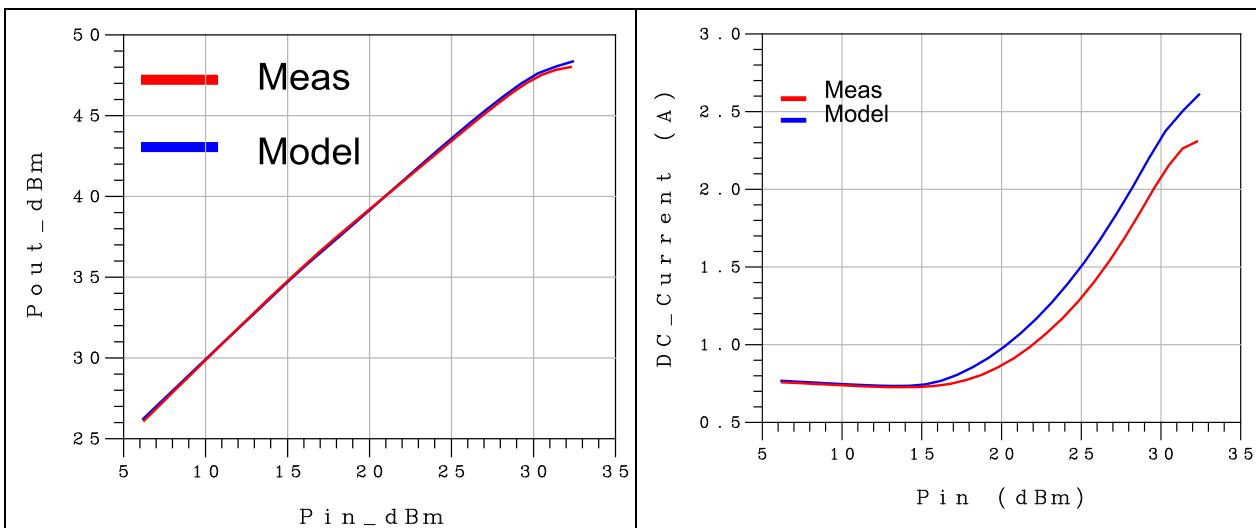


Figure 119 : Pout vs Pin and DC current vs Pin. Comparison between simulation and measurements for power bar N2

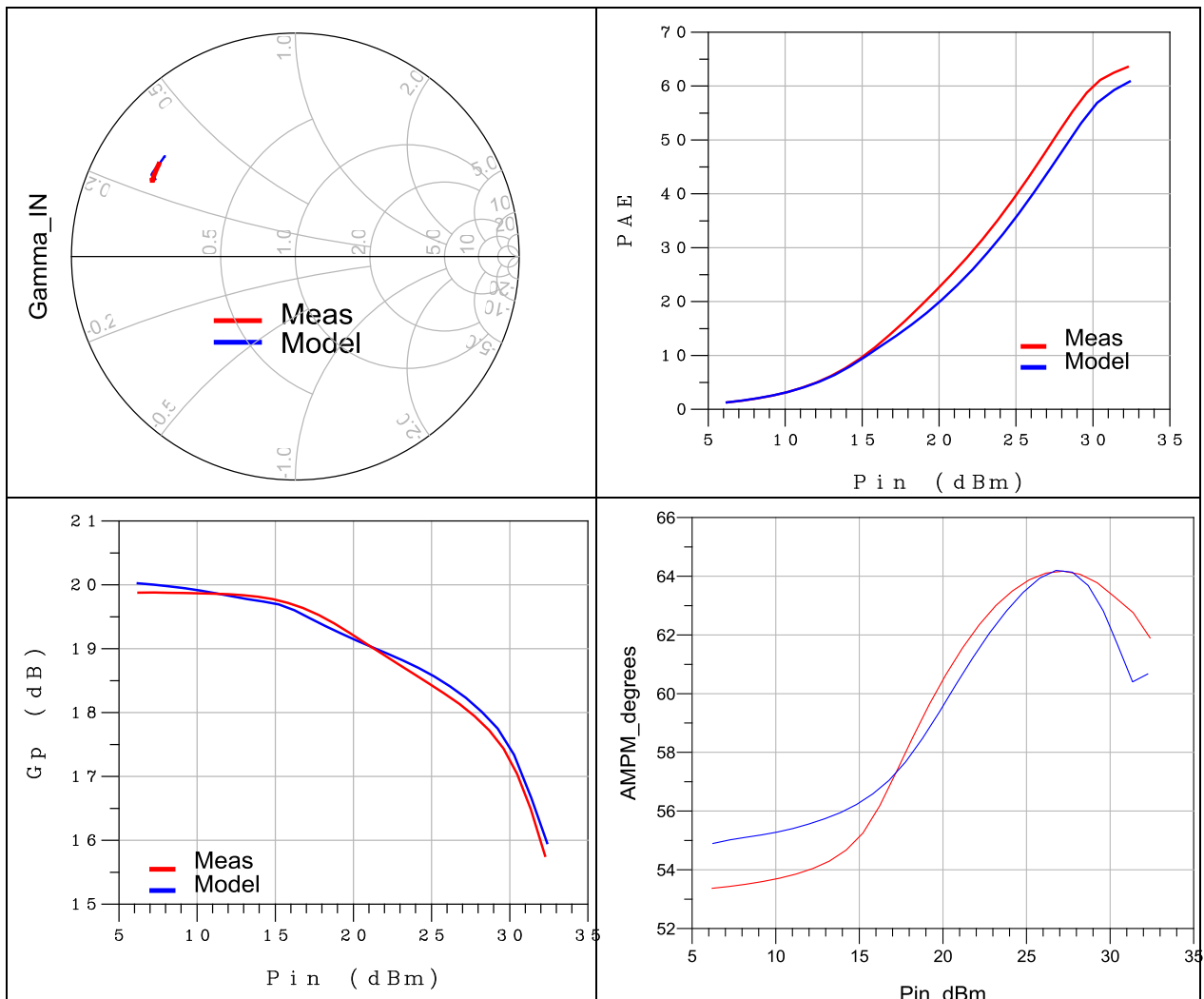


Figure 120 : Input reflexion coefficient / PAE / Gp / AMPM versus Pin. Comparison between simulation and measurements for powerbar N2

2.2.3.5 Synthesis of the performance Gate-Lag and Drain Lag monitored for Sabrina wafer (Run-1) and Stardust wafer (Run-2)

In the frame of this ESA ARTES 5.1 study two wafers have been manufactured:

- GH50 SABRINA wafer manufactured in 2011
- GH50 STARDUST wafer manufactured in 2014

Thus, monitoring of the UMS 0.5 μm GaN process evolution has been performed through the manufacturing of two wafers and associated to the characterizations of transistor cells and power-bars.

Regarding the evolution of the RF performance of the transistor cells between the two wafers, the following observations have been done:

- Gate Lag on SABRINA, no Gate Lag on STARDUST
- Same Drain Lag on SABRINA and STARDUST
- Kink's effect more important on SABRINA
- Current density high on STARDUST (+8%)

	Ids @ Vgs=+1,25V	% of Gate-lag	% of Drain-lag @ Vds=35V	Estimated Power Max @ Vds=35V on network (0,0)	Estimated Power Max @Vds=35V on network (-3,75, 35V)
Stardust AE50	857mA (714mA/mm)	1 %	16 %	6,3W (5.25W/mm)	5,1W (4,25W/mm)
Stardust AE62	842 (701)	0 %	17 %	6,1 (5,1)	5 (4,15)
Stardust AE74	829 (690)	0 %	22 %	6 (5)	4,7 (3,91)
Sabrina L65	793 (660)	8 %	22 %	5,8 (4,8)	4,1 (3,4)
Sabrina L54	766 (638)	11 %	13 %	5,5 (4,6)	4,2 (3,5)

Table 20 : Monitoring of the UMS 0.5 μ m GaN process evolution. Drain-Lag and Gate-Lag

2.2.4 Detailed Design. Run-2

Design of the HPA-1 Run-2 has been undertaken to reach the best possible performances with priority on PAE. first of all, optimal output load impedances at fundamental, second and third harmonic frequency have been searched and identified. Through CCN TAS has modified the center frequency from 1,5675GHz to 1,5385GHz. Indeed, this L-band HPA module is used as power stage of a new L-band GaN SSPA for MSS applications. The useful frequency range shall be [1,518-1,559 GHz] instead of [1,5425-1,5925GHz]. This new equipment will be dedicated to the entire renewal market of constellations of mobile communications satellites.

Performance within Environmental Requirements	L-Band HPA-1 module				
	Value	Test Conditions	C/NC	Proposed Value	Comments
Nominal Output power with Multicarrier Signal	>30W	@ 15dB NPR Worst case over temperature	C		
Power Added Efficiency with Multicarrier Signal	>55%	@ 15dB NPR Worst case over temperature	-	>50%	
Centre Frequency	1.5385 GHz	L-band	C		
Bandwidth	>50 MHz	@ Nominal output power	C		
Gain Flatness	+/- 0.25 dB	Over the whole BW for fixed input power	C		
Gain with Multicarrier Signal	> 16 dB	@ Nominal output power	C		
Gain Compression Level with Multicarrier Signal	Max 2dB	@ 15dB NPR Worst case over temperature	-	Max 5dB	@ 15dB NPR Worst case over temperature
Maximum Phase shift	<15 deg	From 30 dB back-off to 4dB compression	-	<30 deg	
Deviation from Linear Phase	2 deg pk-pk	versus frequency within BW	C		
Input Reflexion coefficient	<-10 dB	@ Nominal output power, over BW	C		
2nd harmonic rejection	>30 dBc		C		
Main DC voltage supply	>50V		-	45V	
Temperature	-10deg /+85deg		C		
Pressure	Ambient and 10e-6mbar		C		Multipactor free operation will be demonstrated by calculation with a sufficient margin

Table 21 : HPA-1 module. New required performances for Run-2

Optimum 8x250µm transistor output loads have been determined at both fundamental (H1) and second harmonic (H2) frequency using AMCAD 8x250µm transistor load-pull measurements data.

The results of the load-pull analysis after harmonics optimization is given below:

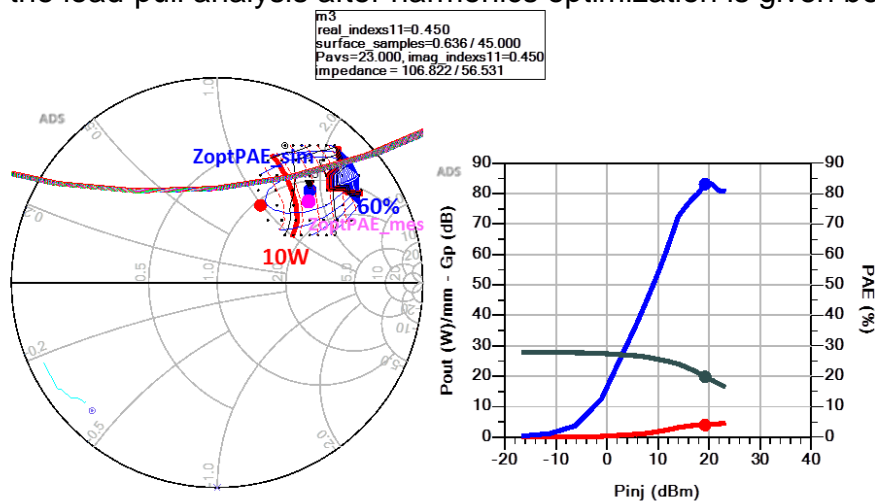


Figure 121 : 8x250µm transistor performance after harmonics loadpull optimization

Pin (dBm)	Zin (H1)	Zout (H1)	Zout (H2)	Gain lin (dB)	Gain comp (dB)	PAE (%)	Pout (dBm)	Pout (W)	Pout (W/mm)
20	4+j21	58.9+j89	5.5+j110	19.8	8	83	39	7.9	3.95

Table 22 : 8x250µm transistor performance after harmonics loadpull optimization

In order to optimize and predict accurately the HPA performances, package RF insert, capacitors and inductors have been carefully simulated and/or measured to secure the design result. In addition to that, the power-bar has been modeled as precisely as possible by stacking 8 elementary cells in parallel.

The UMS GH50 8x8x250µm power-bar have been made up of 8 elementary transistor stacked together in a way that respect, as much as possible, the power-bar layout provided by UMS. The UMS GH50 8x8x250µm power-bar has been modeled by AMCAD.

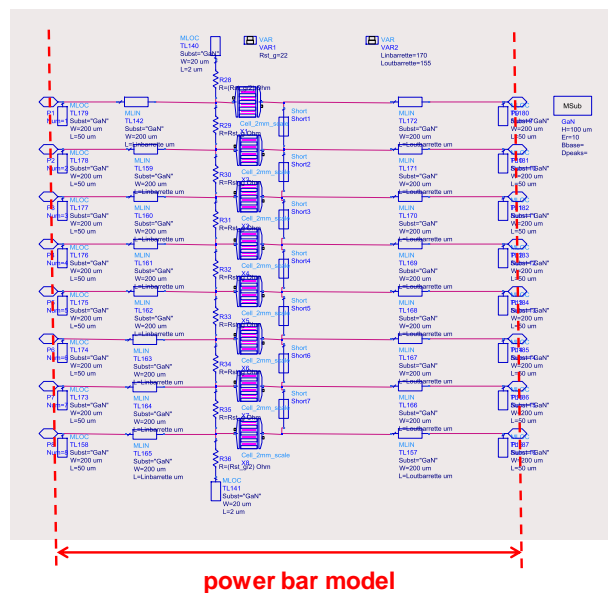


Figure 122 : ADS schematic of the GH50 8x8x250µm powerbar based on AMCAD transistor model

In order to optimize the simulation results, homemade discrete self-inductor model have been used whereas S-parameter files (coming from measurements data) have been used to simulate discrete self-inductors used for DC biasing. Hereafter, you can see the ADS schematic view of the HPA

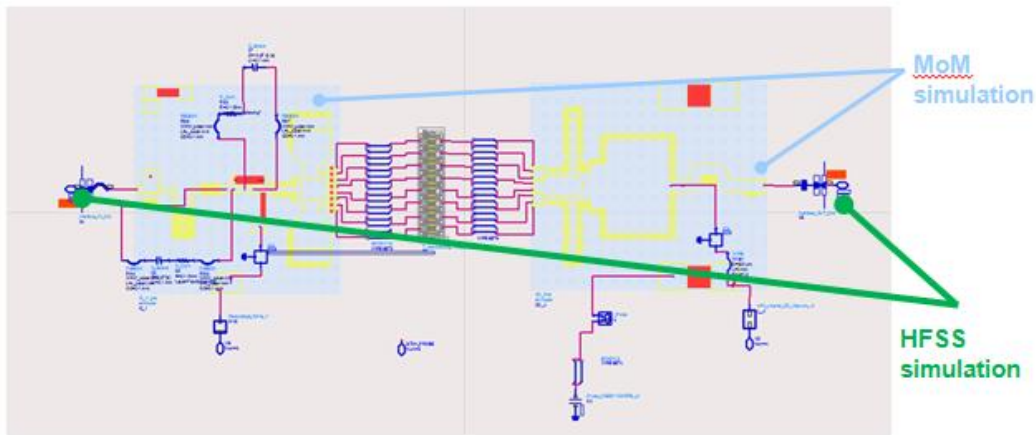


Figure 123 : ADS schematic view of the HPA-1 module Run-2

Due to both input and output matching networks size constraints and the need of high distributed capacitance effect to synthesize appropriate input and output load impedances, high dielectric constant material has been used : $\epsilon_r = 40$; $T = 381\mu\text{m}$; $\text{TanD} = 0.0003$. Input and output combiners have been fully optimized by means of EM simulation up to 10GHz. Engrave resistance sheet (red on Figure 31) has been chosen as low as possible ($6\Omega/\square$) to enable the design of resistors in series with the gate of each transistor. In this way, both even and odd mode stability issues have been managed at the same time.

In order to have a more realistic EM simulation result, the all passive components of hybrid HPA are simulated on HFSS, as shown in figure below.

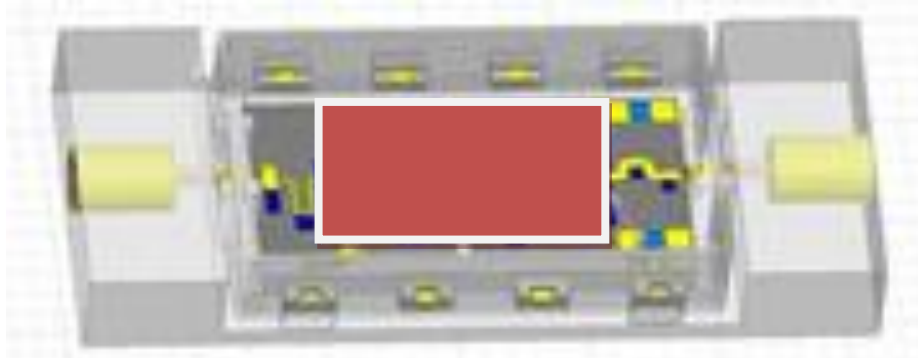


Figure 124 : HFSS schematic view of the HPA-1 module Run-2

The following figures shows the small signal behavior of the HPA in a wide frequency range

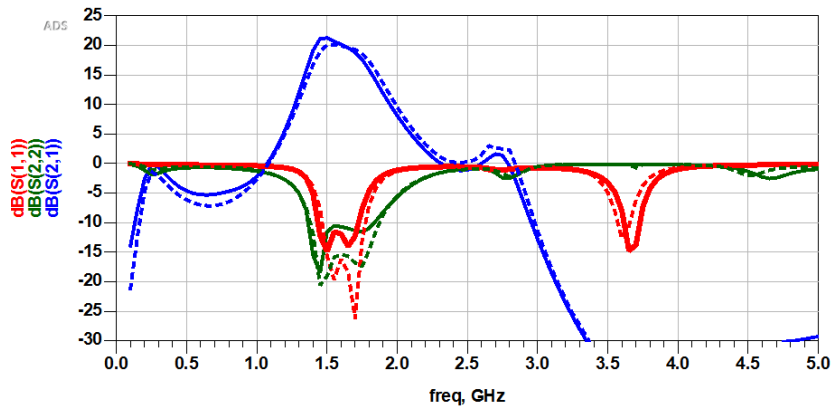


Figure 125 : HPA-1 module. Run-2. Simulated S-parameters wide frequency band analysis

This figure shows that S21 parameter drops below 0dB for frequency higher than 2.2GHz. HPA design have been managed to break the very high gain of the power bar at frequency below 1GHz. In that way, low frequency and Fo/2 oscillation issues will be prevented.

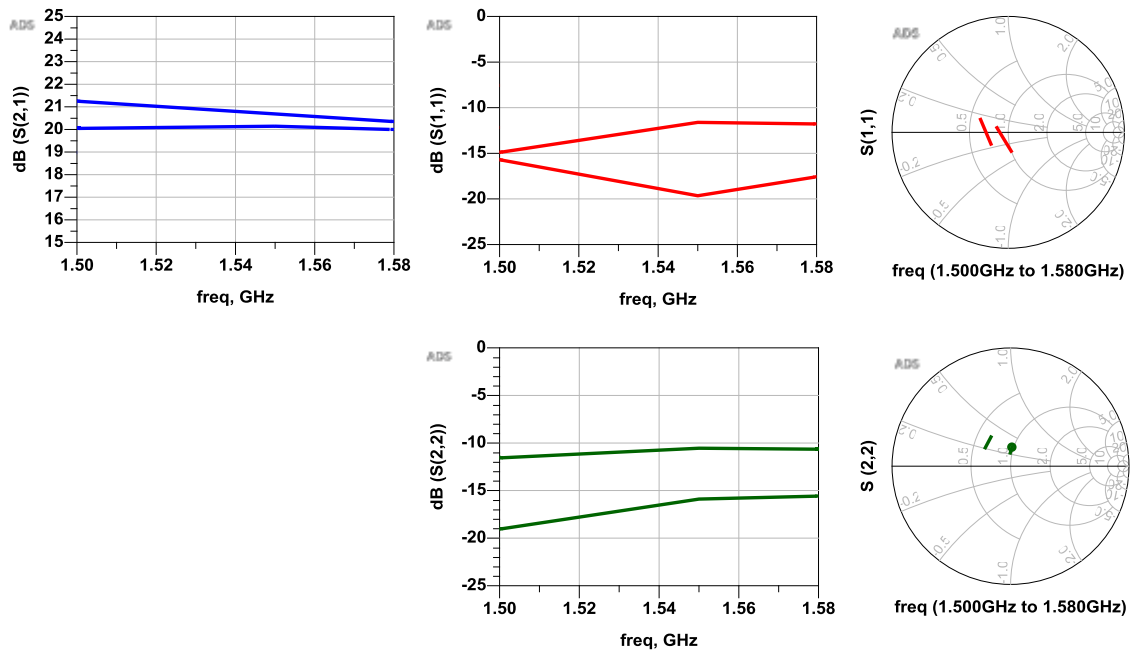


Figure 126 : HPA-1 module. Run-2. Simulated S-parameters in-band frequency analysis

The main RF performances obtained, output power, PAE and power gain are presented below versus input power and versus frequency

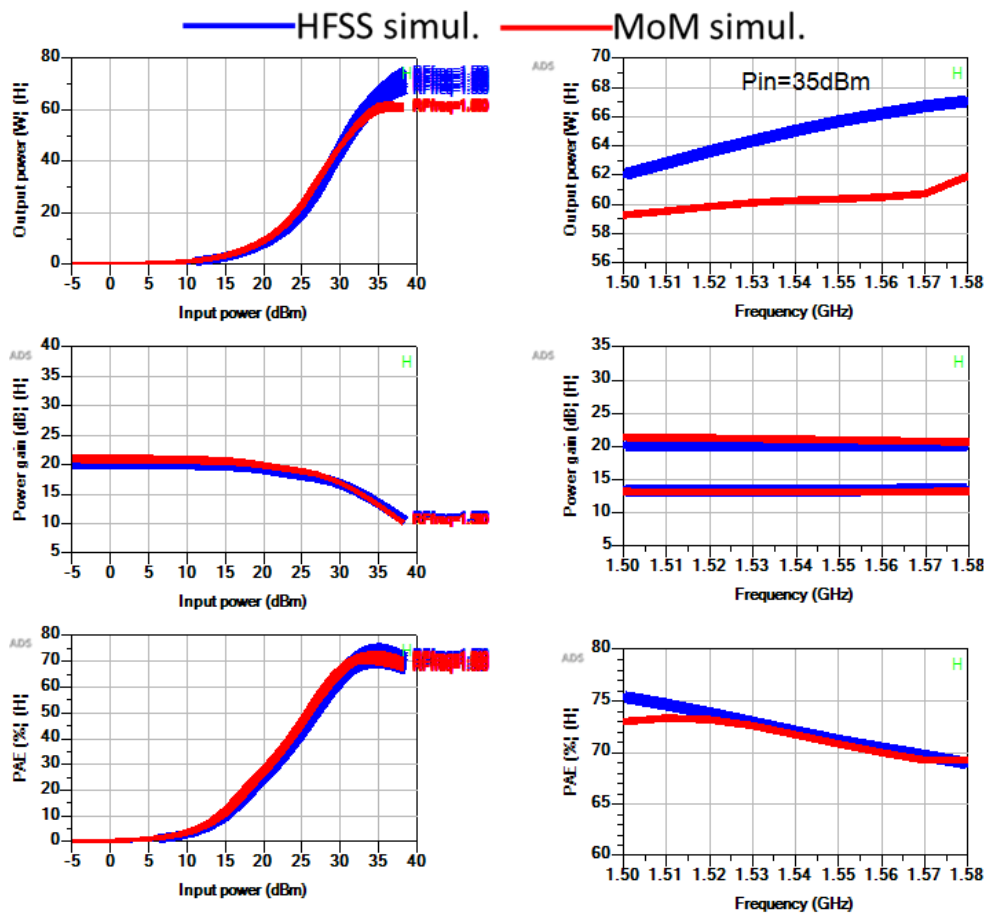


Figure 127 : HPA-1 module. Run-2. Simulated performances. Pout(W), PAE(%), Gain(dB) versus input power (dBm) and Frequency(GHz).

The frequency bandwidth reaches 50MHz for a center frequency of 1.5385 GHz. The maximum overall power added efficiency varies from 69 to 73-75% at Pin = 35dBm and is associated to an output power more than 58W. The maximum PAE value is reached with Pin = 35dBm, which corresponds to a 8 dB of compression. Therefore, the Safe Operating Area is defined as 10 dB of compression. At 35dBm of input power, the mean output power density is around 4 W/mm as shown in figure below.

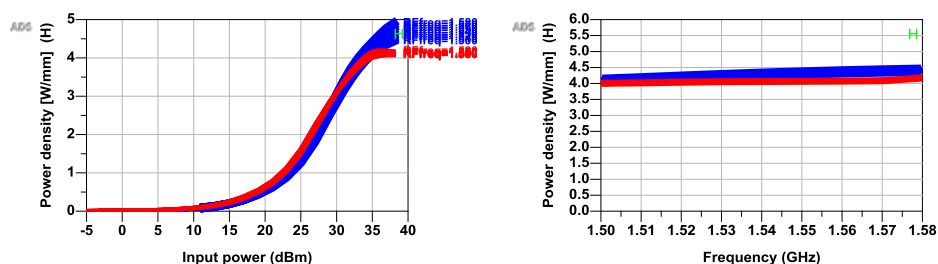


Figure 128 : HPA-1 module. Run-2. Simulated performances. Power density (W/mm) vs. input power(dBm) – from 1.50 to 1.58GHz

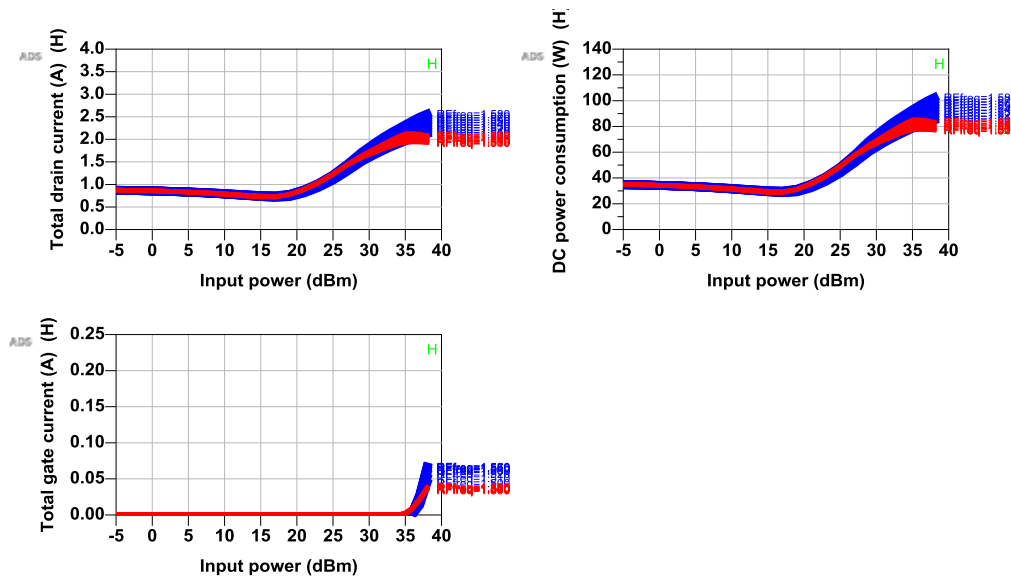


Figure 129 : HPA-1 module. Run-2. Simulated performances. Drain current and power consumption(W) vs. input power(dBm) – from 1.50 to 1.58GHz

Thanks to the electro-thermal capability of the transistor model, the main RF performances; output power, PAE and power gain; of HPA has been checked versus a temperature range from -10°C to 85°C. On figure below, main HPA performances with MoM simulation are shown for an input power (@35dBm) corresponding to the maximum of PAE (Pin = 35dBm)

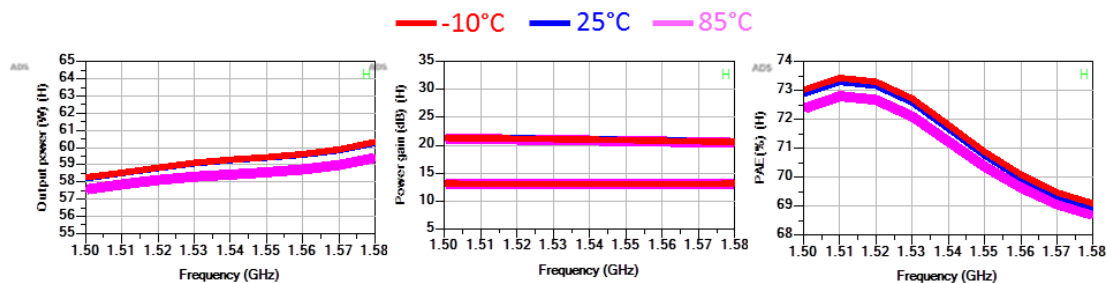


Figure 130 : HPA-1 module. Run-2. Simulated performances : Pout(W), PAE(%), Gain(dB) versus temperature [-10°C; 25°C, 85°C] @Pin(max PAE).

Stability analysis has to be consolidated by STAN software simulations during linear and non-linear operating modes at baseplate temperature equal to -10 °C. . Current probe was placed on transistor gate. For stability analysis is performed using the HPA with MoM simulation.

No critical behavior detected in linear simulation with the following biasing conditions:

- Fixed Ids=50 mA/mm and sweep of Vds from 0V to 45V (step 5V)
- Fixed Vds=40V and sweep of Vgs from -2.2V to -1.2 (step 0.1V)

No critical behavior detected in non-linear simulation at biasing condition (equal to 50mA/mm of drain current and Vds=45V) and with a sweep of input power from -10 dBm to 35 dBm.

Finally, a Volti analysis has been done at HPA level to check the feasibility of the PAE, output power, NPR trade-off.

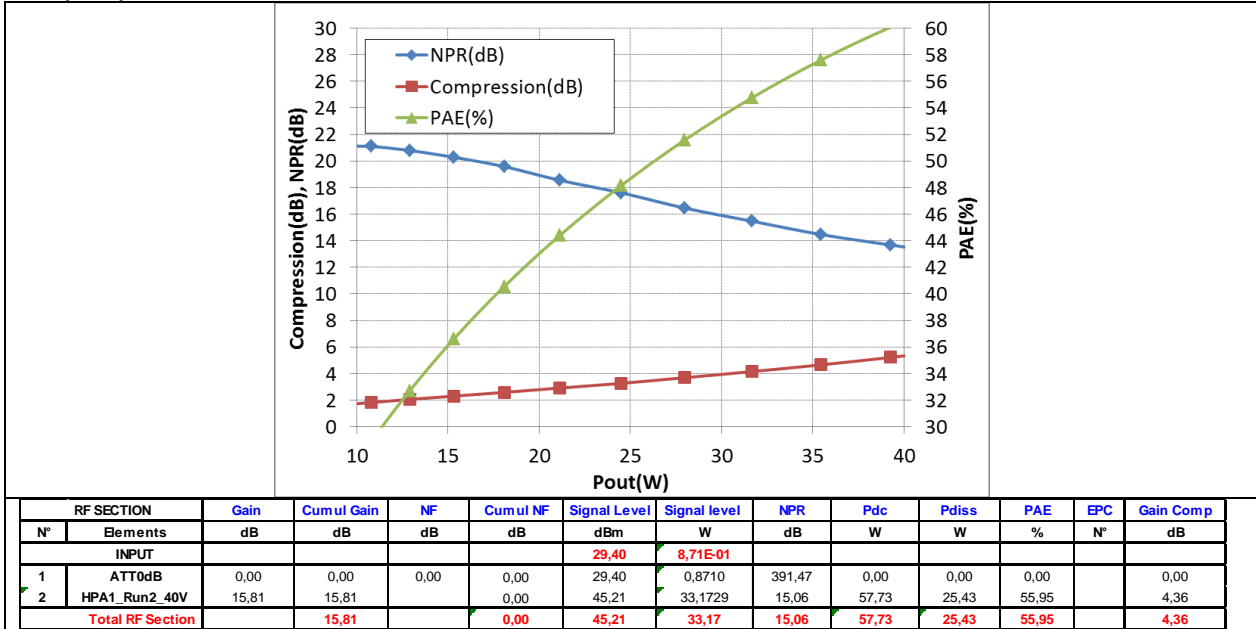


Figure 131 : HPA-1 module. Run-2. Simulated performances in multi-carrier mode : NPR(dB), compression(dB), PAE(%) versus Pin. Temp=25°C, Vds=40V and Ids=50mA/mm

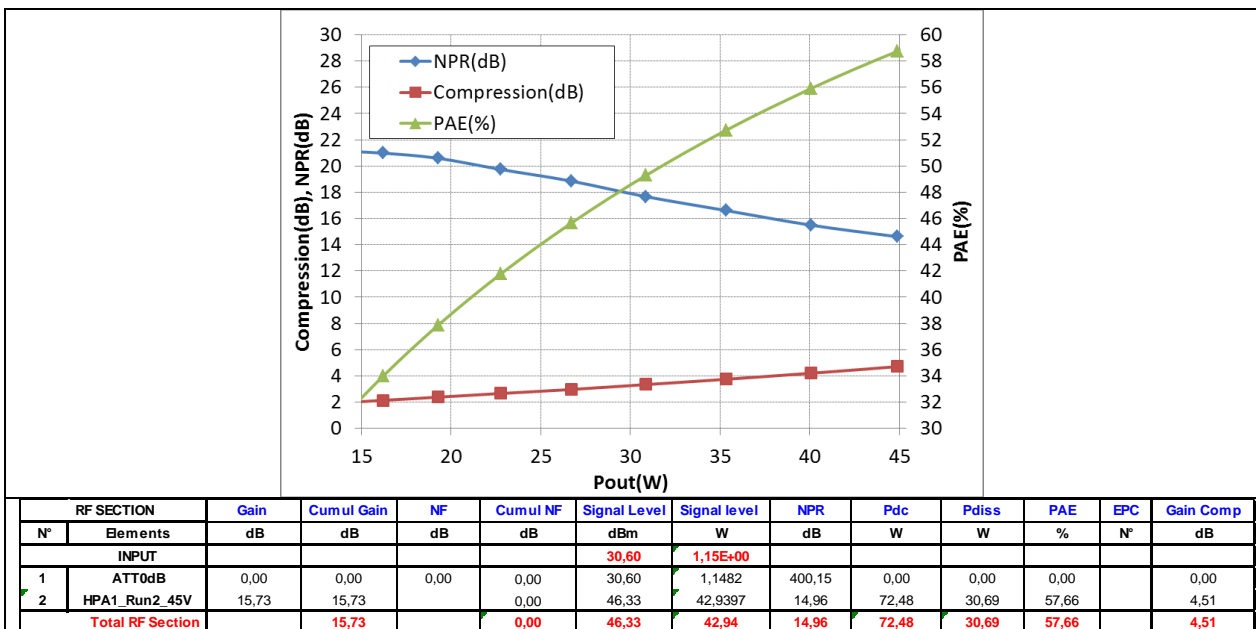


Figure 132 : HPA-1 module. Run-2. Simulated performances in multi-carrier mode : NPR(dB), compression(dB), PAE(%) versus Pin. Temp=25°C, Vds=45V and Ids=50mA/mm

The tables below summarize the HPA-1 module Run-2 simulated performances reached for the center frequency 1.5385GHz in multi-carriers mode.

Multi-carrier mode : VOLTI analysis Vds=40V and Ids=50mA/mm.		Multi-carrier mode : VOLTI analysis Vds=45V and Ids=50mA/mm.	
Parameters	Typ.	Parameters	Typ.
Output Power	33,5W	Output Power	43W
PAE	56%	PAE	57%
Gain compression	4,5dB	Gain compression	4,5dB
NPR	15,7dB	NPR	15dB

Table 23 : Summary of simulated multi-carriers performances at HPA-1 module. Run-2. Vd=450V and Vd=45V

2.2.5 HPA-1 Module Manufacturing and Tests. Run-2

3x L-band GaN HPA-1 modules (Sn#01, Sn#02, Sn#03) have been tested: In the frame of this study, tuning of the HPA modules has been performed at Temp=+25°C with CW signal in order to achieve maximum of PAE. Then [S] parameter measurements and power measurements with multi-carrier signal has been conducted.

The results are presented with the following outline

- [S] parameters measurements versus Temp=[-5°C, +25°C, +85°C]
- Power measurements (CW signal) versus Pin. Temp=[-5°C, +25°C, +85°C]. Vds=+40V and RF=[1,5135GHz / 1,5385GHz / 1,5635GHz]
- Power measurements (multi-carrier signal) versus Pin. Temp=[-5°C, +25°C, +85°C]. Vds=+40V, Ids=800mA]
- RF step stress measurements

2.2.5.1 [S] Parameter measurements. Run-2

Hereafter, the Sn#01 module S-parameters are given over a DC to 10GHz bandwidth with drain voltage of +40V and Ids=800mA (50mA/mm) fixed at Temp=+25°C. Measurements are performed versus Temp=[-5°C, +25°C, +85°C]

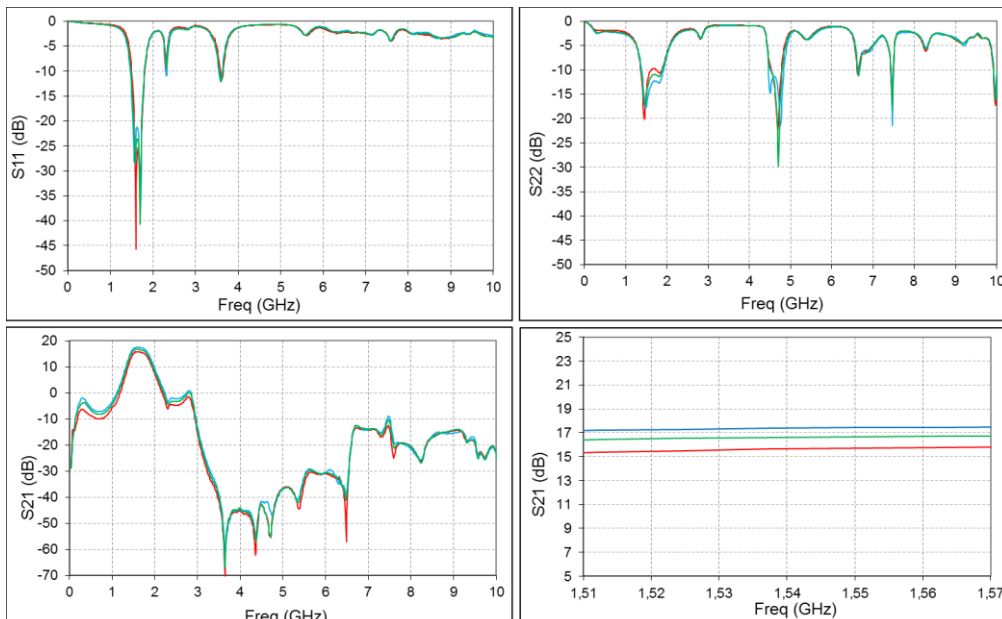


Figure 133 : Run-2. HPA-1 module(Sn#01). [S] parameters measurements. RF=[DC-10GHz], Vd=+40V, Fixed drain current I_{ds}=800mA @+25°C, Temp=[-5°C, +25°C, +85°C]

On the following figures, we focus on the Sn#01 module in-band frequency behavior. Figure shows that S11 and S22 parameters varies not in the same way:

- Input return loss is optimum at hot temperature
- Output return loss is optimum at room temperature.
- S21 variation is about 1,8dB between -5°C to +85°C at 1.5385GHz. At constant gate voltage current, the gain variation versus temperature is 0,2dB/°C

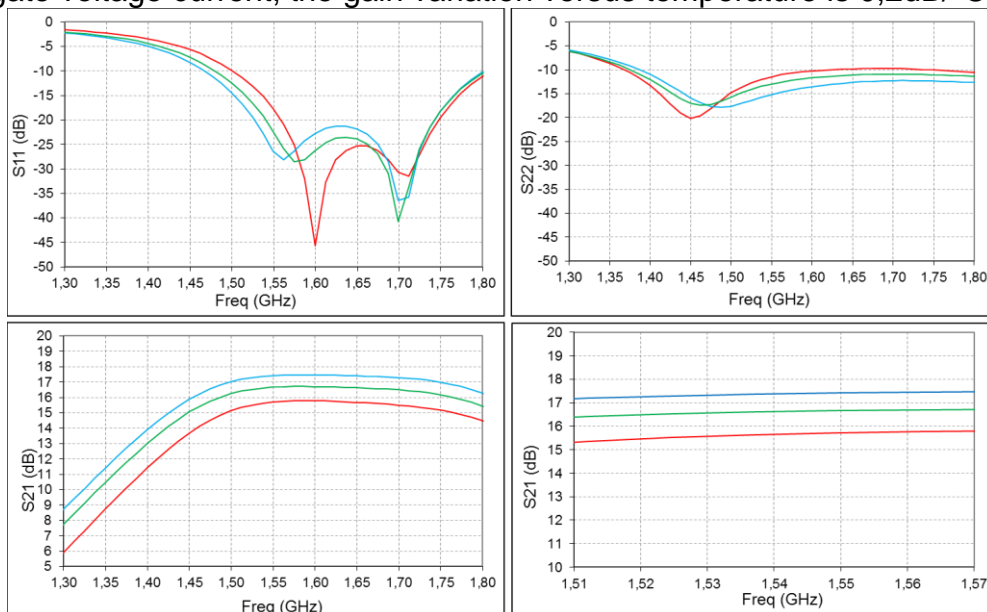


Figure 134 : Sn#01 module. [S] parameters measurements. RF=[1.3-1.8GHz], Vd=+40V, Fixed drain current I_{ds}=800mA @+25°C, Temp=[-5°C, +25°C, +85°C]

Hereafter, for three HPA modules, the S-parameters are given over a DC to 10GHz bandwidth with drain voltage of +40V and $I_{ds}=800\text{mA}$ (50mA/mm) fixed at $\text{Temp}=+25^\circ\text{C}$. Measurements are performed versus $\text{Temp}=[-5^\circ\text{C}, +25^\circ\text{C}, +85^\circ\text{C}]$

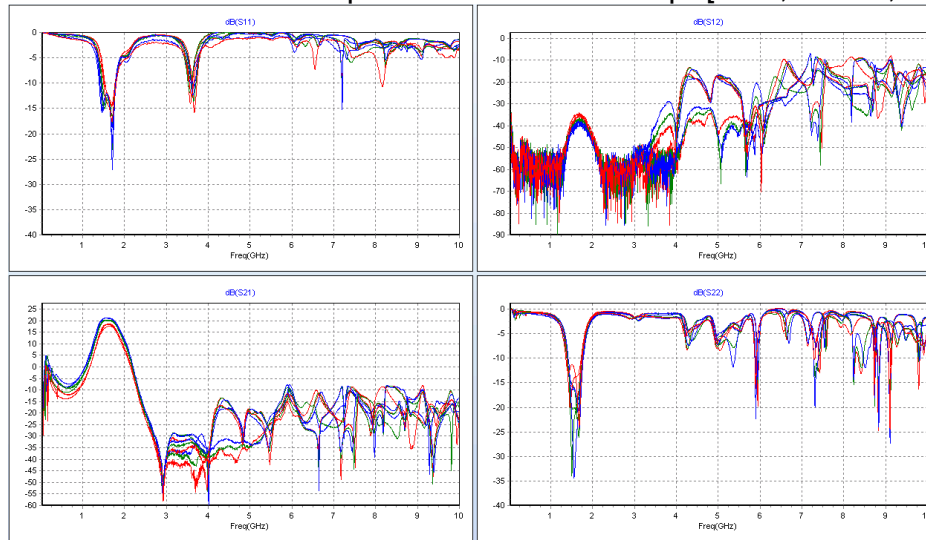


Figure 135 : Run-2. HPA-1 modules. Samples Sn#01 Sn#02 Sn#03 modules. [S] parameters measurements. RF=[DC-10GHz], $V_d=+40\text{V}$. Fixed drain current $I_{ds}=800\text{mA}$ @+25°C. $\text{Temp}=[-5^\circ\text{C}, +25^\circ\text{C}, +85^\circ\text{C}]$

On following figures, we focus on the HPA modules in-band frequency behavior. Figure shows the dispersion on S11, S22 and S21 parameters versus HPA modules. Measurements are performed versus $\text{Temp}=[-5^\circ\text{C}, +25^\circ\text{C}, +85^\circ\text{C}]$.

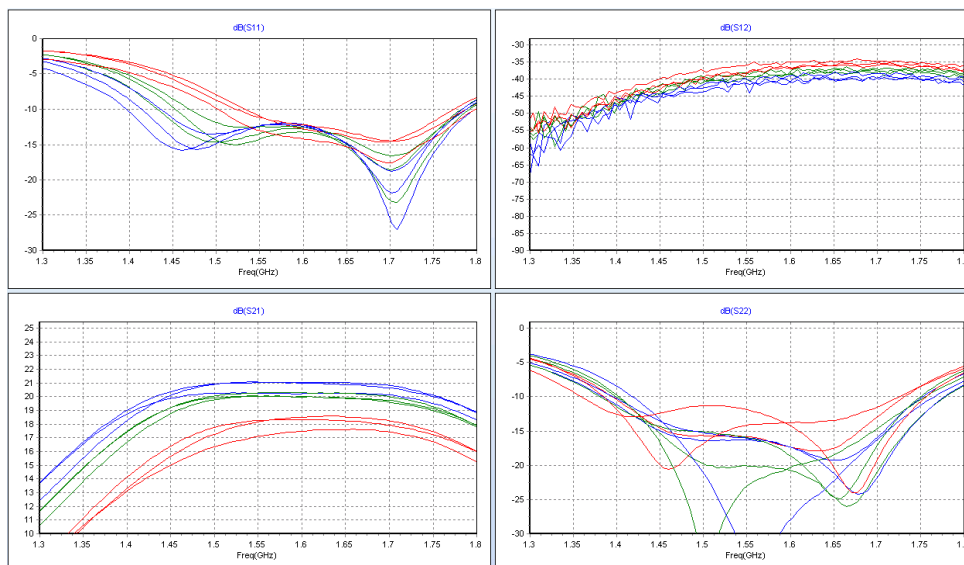


Figure 136 : Run-2. HPA-1 modules. Samples Sn#01 Sn#02 Sn#03 modules. [S] parameters measurements. RF=[1.3-1.8GHz], $V_d=+40\text{V}$. Fixed drain current $I_{ds}=800\text{mA}$ @+25°C. $\text{Temp}=[-5^\circ\text{C}, +25^\circ\text{C}, +85^\circ\text{C}]$

Regarding S21 parameter, at 1,5385GHz, a maximum dispersion of 1dB is observed between the three HPA modules. Regarding S11 parameter, at 1,5385GHz, a maximum dispersion of 2dB is observed between the three HPA modules. Regarding S22 parameter, dispersion is higher compared to the previous parameters. Indeed, depending of the HPA modules, the settings applied on the output combiner to obtain maximum of PAS have an impact of the output return loss behavior.

2.2.5.2 CW mode power measurements. Run-2

The RF performances obtained with a CW signal are presented in this paragraph chapter for Vds=+40V.

The main RF performances obtained, output power, PAE, power gain and phase are presented below versus input power and three frequency points [1,5135GHz, 1,5385GHz, 1,5635GHz]. Measurements have been performed versus Temp=[-5°C, +25°C, +85°C]. For each frequency and each temperature, drain current has been tuned in small signal: Ids=800mA with Vds=+40V.

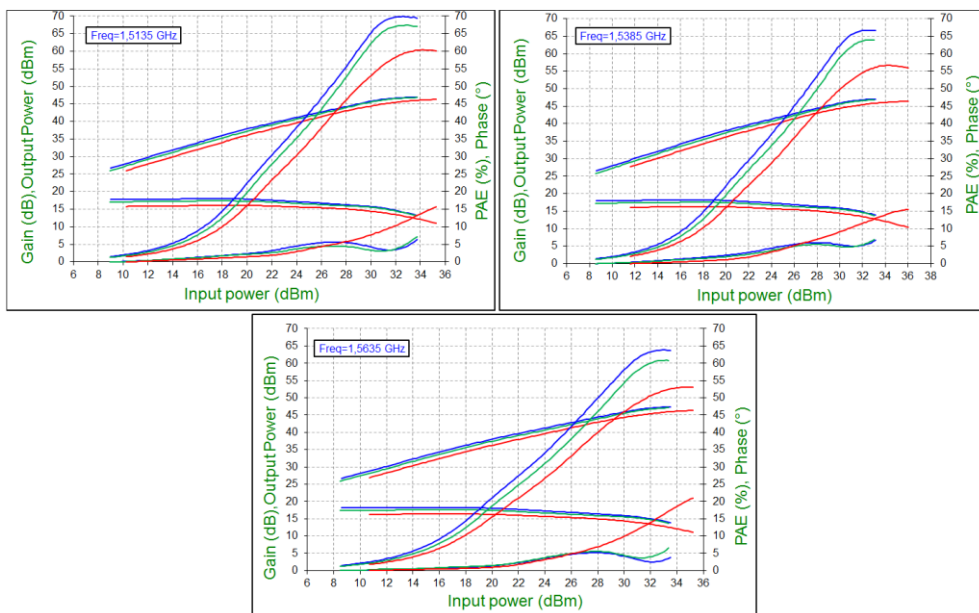


Figure 137 : Run-2. HPA-1 module. Sn#01 sample. Power measurements with CW signal. Temp=[-5°C, +25°C, +85°C], Vd=+40V, Id=800mA. RF=[1,5135GHz / 1,5385GHz / 1,5635GHz]. Gain(dB), PAE(%), Pout(dBm), Phase(deg) vs Pin(dBm)

The results (Pout, Gain, PAE) are presented versus frequency and temperature. Pin is fixed to obtain maximum of PAE

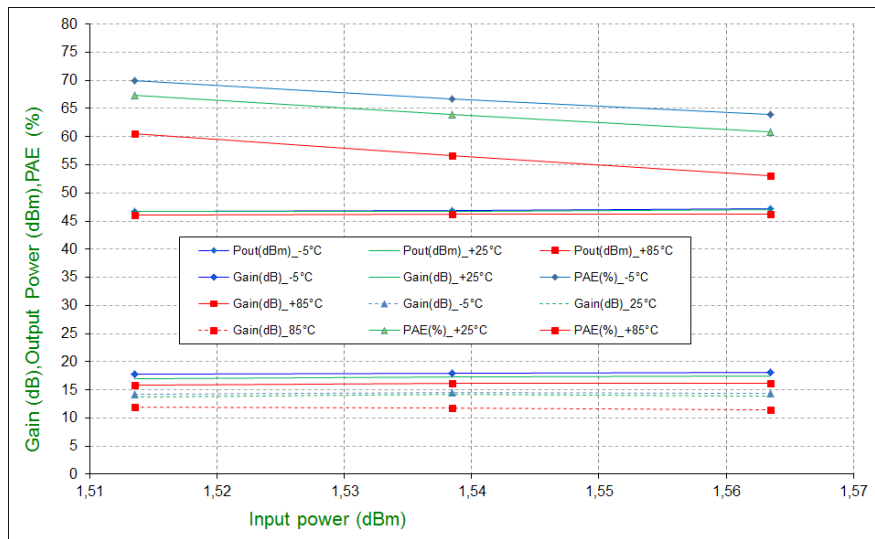


Figure 138 : Run-2. HPA-1 module. Sn#01 module. Power measurements with CW signal. Temp=[-5°C, +25°C, +85°C], Vd=+40V, Id=800mA. Gain(dB), PAE(%), Pout(dBm), Phase(deg) vs RFfreq(GHz) @PAE_max.

Synthesis of the RF performances measured with CW signal are provided in the following table

Temp (°C)	Biassing point	RFfreq (GHz)	Linear Gain (dB)	Pout (dBm)	Pout (W)	Power Density (W/mm)	PAE (%)	Phase (°)	Gain (dB)	Compression (dB)
85	Vd=40V, Id=800mA	1,5135	15,77	46,11	40,83	2,55	60,45	13,97	11,94	3,83
		1,5385	16,08	46,18	41,50	2,59	56,64	14,41	11,73	4,35
		1,5635	16,22	46,29	42,56	2,66	53,03	20,32	11,44	4,78
25	Vd=40V, Id=800mA	1,5135	17,04	46,72	46,99	2,94	67,42	5,45	13,69	3,35
		1,5385	17,26	46,74	47,21	2,95	63,92	5,98	14,26	3,00
		1,5635	17,39	47,08	51,05	3,19	60,87	5,98	13,89	3,50
-5	Vd=40V, Id=800mA	1,5135	17,72	46,78	47,64	2,98	69,90	4,03	14,20	3,52
		1,5385	17,94	46,89	48,87	3,05	66,64	5,46	14,56	3,38
		1,5635	18,11	47,26	53,21	3,33	63,89	2,86	14,37	3,74

Figure 139 : Run-2. HPA-1 module. Sn#01. Synthesis of power measurements with CW signal. Temp=[-5°C, +25°C, +85°C], Vd=+40V, Id=800mA. Gain(dB), PAE(%), Pout(dBm), Phase(deg) vs RFfreq(GHz) @PAE_max

Sn#02 and Sn#03 modules have been tested with the same approach. Synthesis of the RF performances measured with CW signal are provided in the following table

Temp (°C)	Biasing point	RFfreq (GHz)	Linear Gain (dB)	Pout (dBm)	Pout (W)	Power Density (W/mm)	PAE (%)	Phase (°)	Gain (dB)	Compression (dB)
85	Vd=40V, Id=800mA	1,5135	16,89	46,36	43,25	2,70	64,73	9,83	13,13	3,76
		1,5385	17,05	46,42	43,85	2,74	61,16	10,58	13,32	3,73
		1,5635	17,06	46,82	48,08	3,01	58,15	14,02	12,70	4,36
25	Vd=40V, Id=800mA	1,5135	18,06	46,63	46,03	2,88	69,33	2,16	14,46	3,60
		1,5385	18,21	46,73	47,10	2,94	65,92	3,56	14,66	3,55
		1,5635	18,26	47,07	50,93	3,18	62,93	2,15	14,42	3,84
-5	Vd=40V, Id=800mA	1,5135	18,57	46,68	46,56	2,91	71,62	1,48	14,80	3,77
		1,5385	18,77	46,84	48,31	3,02	68,49	2,34	14,90	3,87
		1,5635	18,87	47,25	53,09	3,32	65,68	0,35	14,62	4,25

Figure 140 : Run-2. HPA-1 module. Sn#02. Synthesis of power measurements with CW signal. Temp=[-5°C, +25°C, +85°C], Vd=+40V, Id=800mA. Gain(dB), PAE(%), Pout(dBm), Phase(deg) vs RFfreq(GHz) @PAE_max

Temp (°C)	Biasing point	RFfreq (GHz)	Linear Gain (dB)	Pout (dBm)	Pout (W)	Power Density (W/mm)	PAE (%)	Phase (°)	Gain (dB)	Compression (dB)
85	Vd=40V, Id=800mA	1,5135	15,87	46,59	45,60	2,85	63,89	10,90	12,66	3,21
		1,5385	15,67	46,77	47,53	2,97	60,65	15,76	12,32	3,35
		1,5635	15,24	47,06	50,82	3,18	57,61	16,90	12,03	3,21
25	Vd=40V, Id=800mA	1,5135	17,28	47,07	50,93	3,18	69,71	1,09	14,08	3,20
		1,5385	17,08	47,22	52,72	3,30	66,26	1,12	13,83	3,25
		1,5635	16,65	47,57	57,15	3,57	62,86	0,64	12,98	3,67
-5	Vd=40V, Id=800mA	1,5135	17,73	47,13	51,64	3,23	71,97	0,31	14,72	3,01
		1,5385	17,52	47,38	54,70	3,42	68,66	-1,44	13,96	3,56
		1,5635	17,09	47,69	58,75	3,67	65,28	-4,38	13,17	3,92

Figure 141 : Run-2. HPA-1 module. Sn#03. Synthesis of power measurements with CW signal. Temp=[-5°C, +25°C, +85°C], Vd=+40V, Id=800mA. Gain(dB), PAE(%), Pout(dBm), Phase(deg) vs RFfreq(GHz) @PAE_max

2.2.5.3 Multi-carrier mode power measurements. Run-2

In the following part, multicarrier measurements are presented for two HPA modules: SN#02 and Sn#04. HPA modules have been tested with Vds=40V and biasing point fixed in small signal Ids=800mA. Multi-carrier measurements have been performed at Temp=[-20°C, 25°C, 85°C].

Characteristics of the multicarrier signal applied:

- Centre Frequency: Fc=1.5385GHz
- Bandwidth: Span=50MHz
- Number of carriers: 3000
- Notch: 1%
- Position of the notch: centered at 1.5385GHz

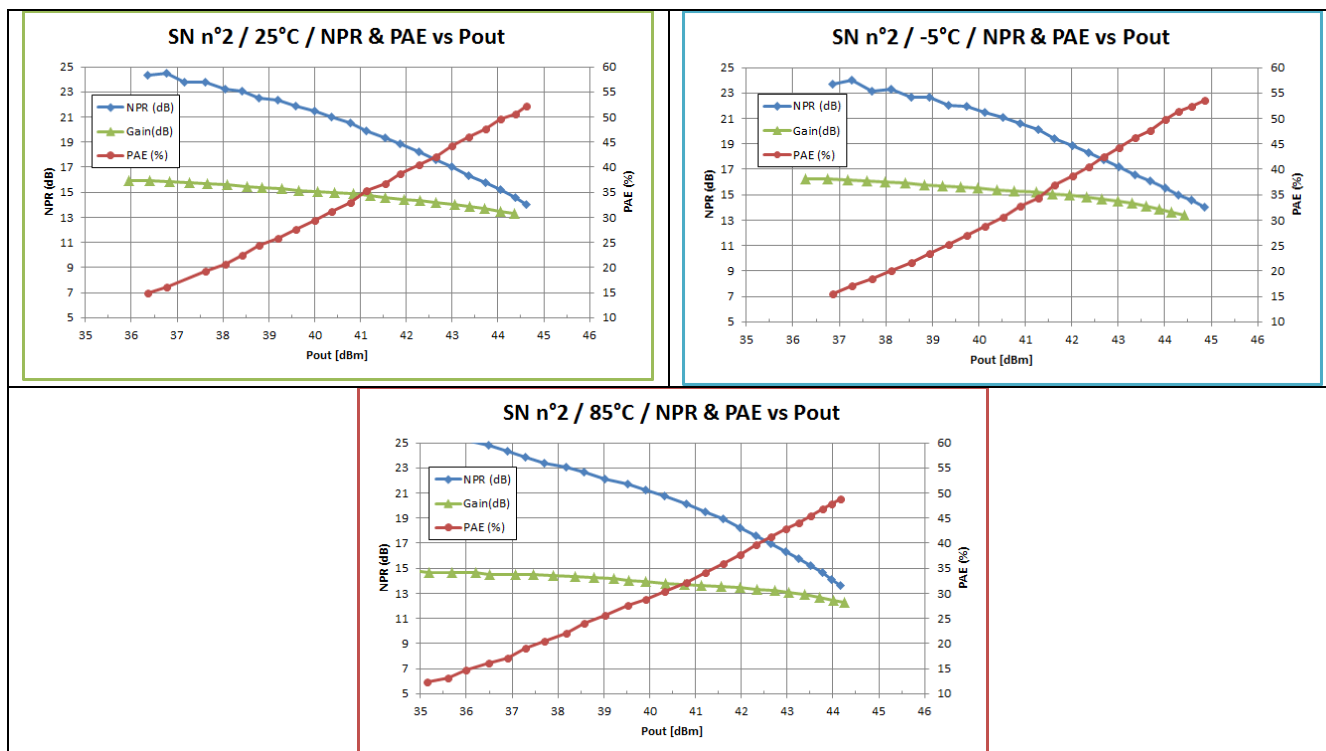


Figure 142 : Run-2. HPA-1 module. Sn#02 Power measurements with multi-carrier signal. Temp=[-5°C, +25°C, +85°C]. Vds=40V, RF=1,5385GHz, Gain(dB), PAE(%), NPR(dB) vs Pout(dBm)

	Linear Gain(dB)	Pin(dBm)	Pout (dBm)	Pout(W)	Power Density (W/mm)	PAE (%)	NPR (dB)	Gain (dB)	Compression (dB)
Vd=40V, Id=800mA, Temp=25°C	15,9	30,3	43,9	24,5	1,5	50,1	14,9	13,6	2,3
		31,1	44,4	27,2	1,7	52,1	14,1	13,3	2,6
Vd=45V, Id=800mA, Temp=-10°C	16,3	30,0	43,9	24,5	1,5	51,4	15,0	13,9	2,4
		31,1	44,4	27,7	1,7	53,6	14,0	13,4	2,9
Vd=45V, Id=900mA, Temp=85°C	14,8	30,0	44,0	25,0	1,6	46,2	14,9	12,8	2,0
		31,8	44,1	25,9	1,6	48,4	13,9	12,4	2,5

Figure 143 : Run-2. HPA-1 module. Sn#02 module. Synthesis of power measurements with multi-carrier signal. Temp=[-20°C, +25°C, +90°C]. Vds=40V,

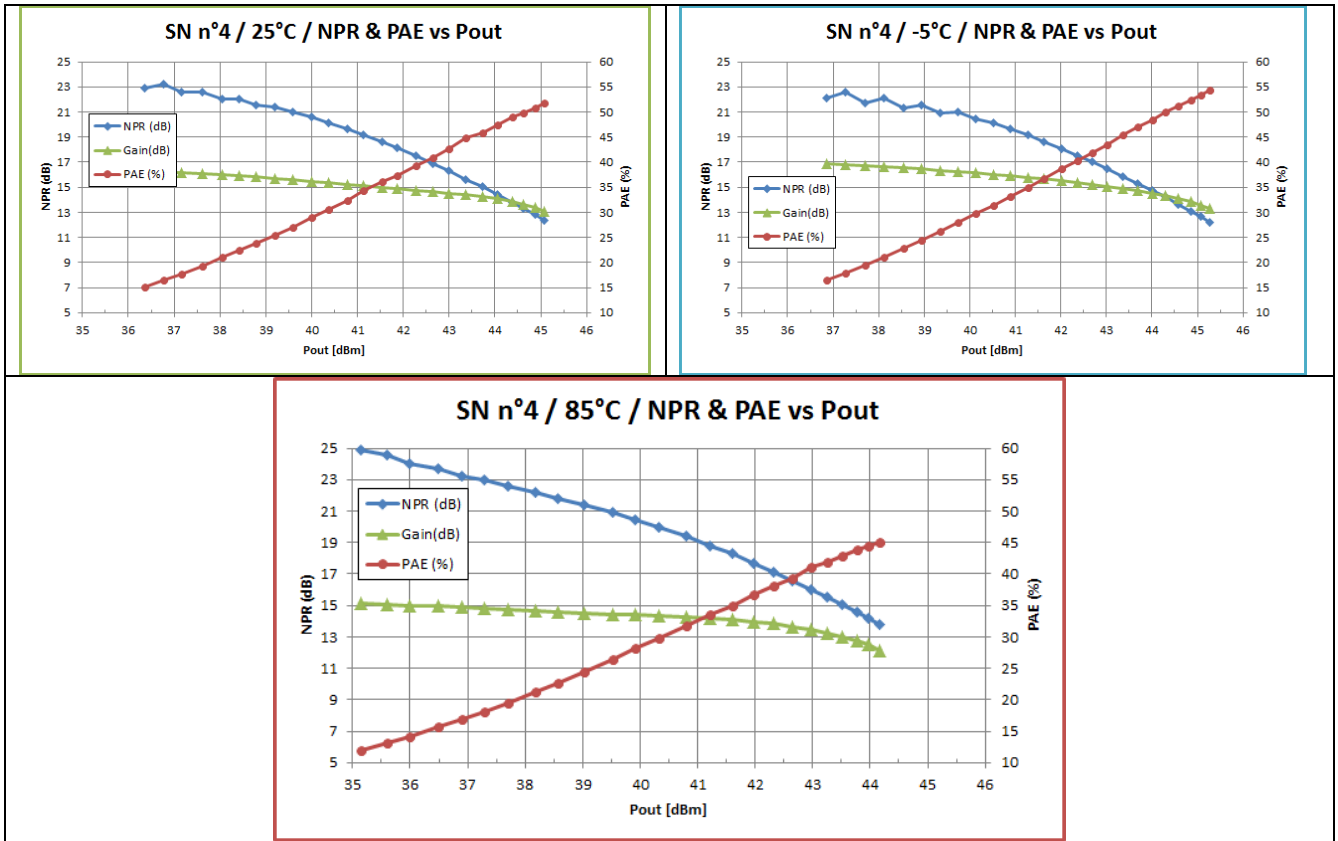


Figure 144 : Run-2. HPA-1 module. Sn#04 Power measurements with multi-carrier signal. Temp=[-5°C, +25°C, +85°C]. Vds=40V, RF=1,5385GHz, Gain(dB), PAE(%), NPR(dB) vs Pout(dBm)

	Linear Gain(dB)	Pin(dBm)	Pout (dBm)	Pout(W)	Power Density (W/mm)	PAE (%)	NPR (dB)	Gain (dB)	Compression (dB)
Vd=40V, Id=800mA, Temp=25°C	16,3	29,5	43,7	23,6	1,5	45,8	15,0	14,2	2,1
		30,3	44,2	26,4	1,7	48,2	14,1	14,0	2,3
Vd=45V, Id=800mA, Temp=-10°C	16,8	29,2	43,9	24,3	1,5	47,7	15,0	14,6	2,2
		30,2	44,4	27,8	1,7	52,9	13,9	14,2	2,6
Vd=45V, Id=900mA, Temp=85°C	15,1	30,5	43,5	22,5	1,4	42,9	15,0	13,0	2,1
		31,7	44,1	25,5	1,6	44,7	14,0	12,3	2,8

Figure 145 : : Run-2. HPA-1 module. Sn#04 module. Synthesis of power measurements with multi-carrier signal. Temp=[-20°C, +25°C, +90°C]. Vds=40V,

2.2.5.4 RF step measurements with multi-carrier signal: reliability of GH50-10 technology. Run-2

This paragraph summarizes the reliability test performed on GaN HPA L Band in the frame of the ARTES 5.1 "SSPAs with European GaN Devices" study. The goal of this reliability study is to define a Safe Operating Area through RF Multicarrier step stress

(1 dB compression, 3 dB compression, 5 dB compression). For that, a dedicated multicarrier test bench have been developed. Intermediate RF measurements and in situ monitoring are performed during this qualification.

Test plan is provided in the following table:

DC Life test	Function	HPA 50 WATTS 16 mm
	Process	UMS GH50.10
	Frequency	1.56 GHz
	DC Bias	V _d =45V, I _d = 100 mA (6,25 mA / mm) ² samples + 1 sample I _d =400 mA (25 mA / mm)
	Number of Sample	NA
	T° JUNCTION (Objective)	NA
	Electrical constraint	NA
Duration	NA	
RF Life test	Number of Sample	3 + 1
	T°	25°C
	DC Biases	Nominal DC biases
	Electrical Constraint	Multicarrier
		1 - Step stress :
		2 weeks / step from 4 dBc to 8 dBc
		2 - RF Life test :
		2000 hours @ X _{dBc} - 2 dB or max PAE
Monitoring	Gate, drain current, Input, output power	
Initial, Final & Intermediate Measurement	RF Characteristic : P _{out} , Gain, I _d , I _g vs P _{in} , Phase vs input power	

Table 24 : Test plan for RF step stress measurements of L-band GH50 HPA-1 module

4 samples have been tested during RF step stress with multicarrier signal:

- Sample n°2 = SN2
- Sample n°3 = SN3(control sample reference)
- Sample n°4 = SN4
- Sample n°5 = SN5

Multi carrier signal is generated using white noise source. The « white noise » bandwidth is = 28 MHz. All the spike > 40 dBc outside the signal band width are eliminated. Synoptic and photographs of the multi-carrier test bench are provided in the following figures.

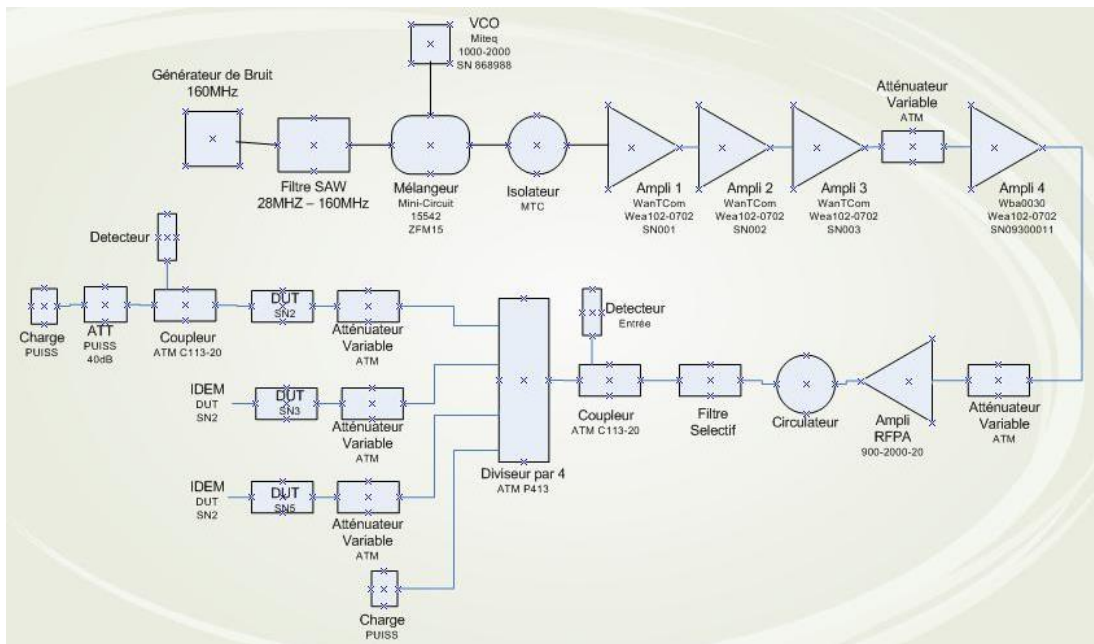


Figure 146 : Multi-carrier test bench

A dedicated test bench for initial, intermediate and final measurement bench is used for [S], AM/AM and AM/PM measurements after each step of compression (2 weeks / step from 1dBc to 5dBc). Synoptic and photographs of this test bench are provided in the following figures.

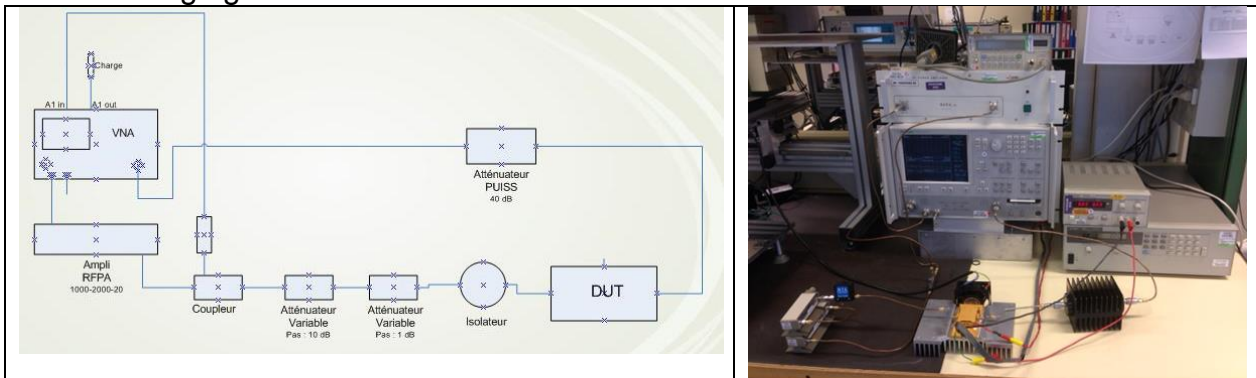


Figure 147 : Photography of the CW test bench for CW initial/intermediate and final measurements

In order to determine the power value during the in situ monitoring we use a detector. The power value versus the detected voltage is represented in the following graph.

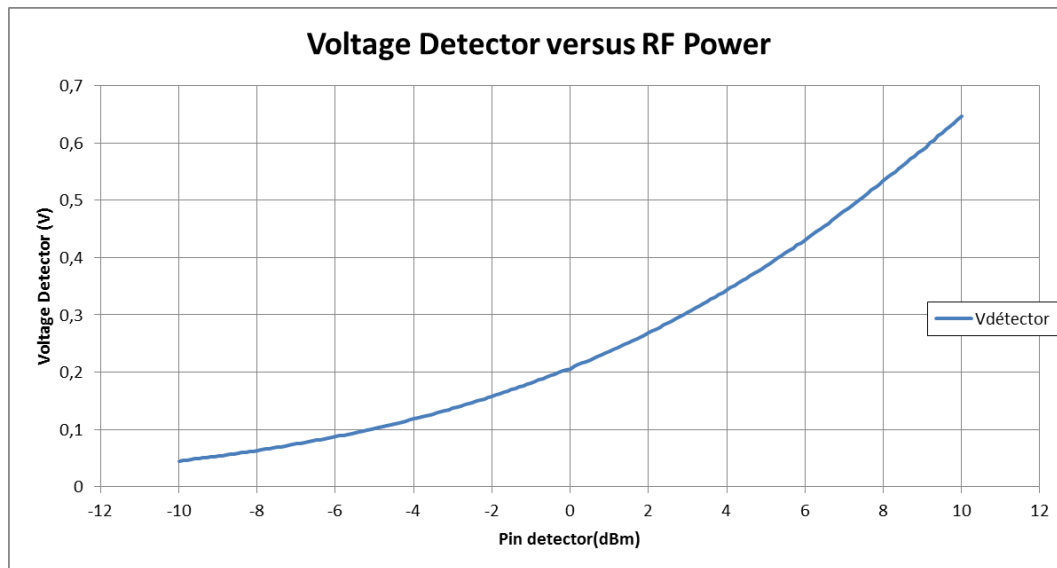
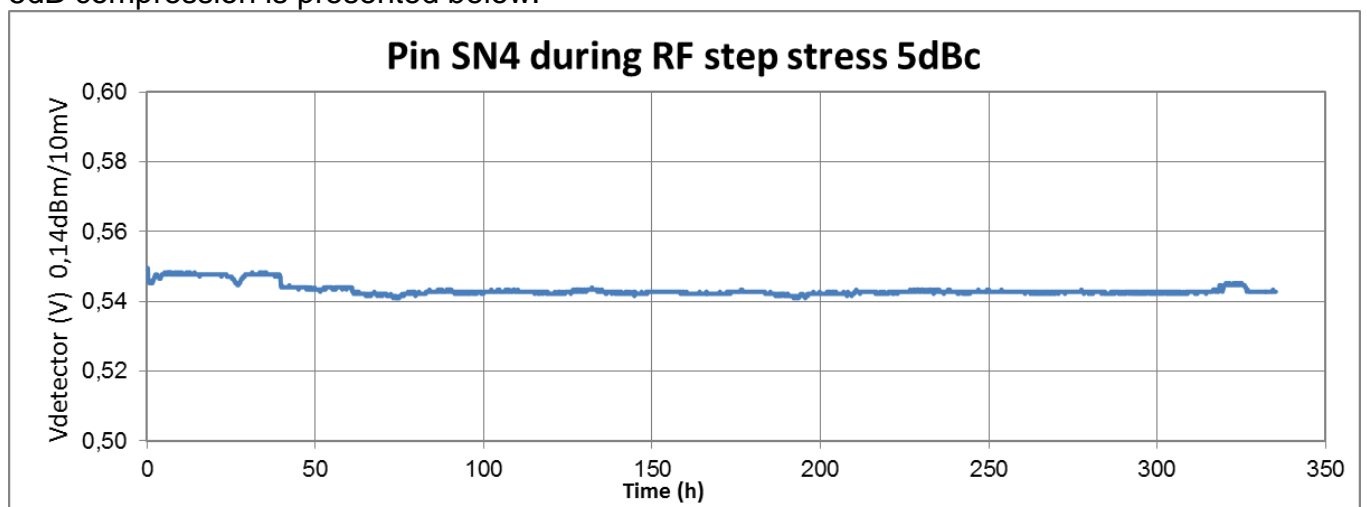


Figure 148 : Detector characterization : Detected voltage value (mV) versus power range(dBm)

On three HPA-1 (Run-2) modules (#2, #4, #5), in Situ measurements have been continuously performed during steps @1dB, @3dB, @5dB. The different parameters monitored are:

- Input power (dBm) and output power (dBm)
- Temperature (°C)
- Drain voltage (V) and Drain current (mA)
- Gate voltage (V) and gate current (mA)

An example of the in situ monitoring performed on HPA-1 (Run-2) module (#4) at Step 5dB compression is presented below:



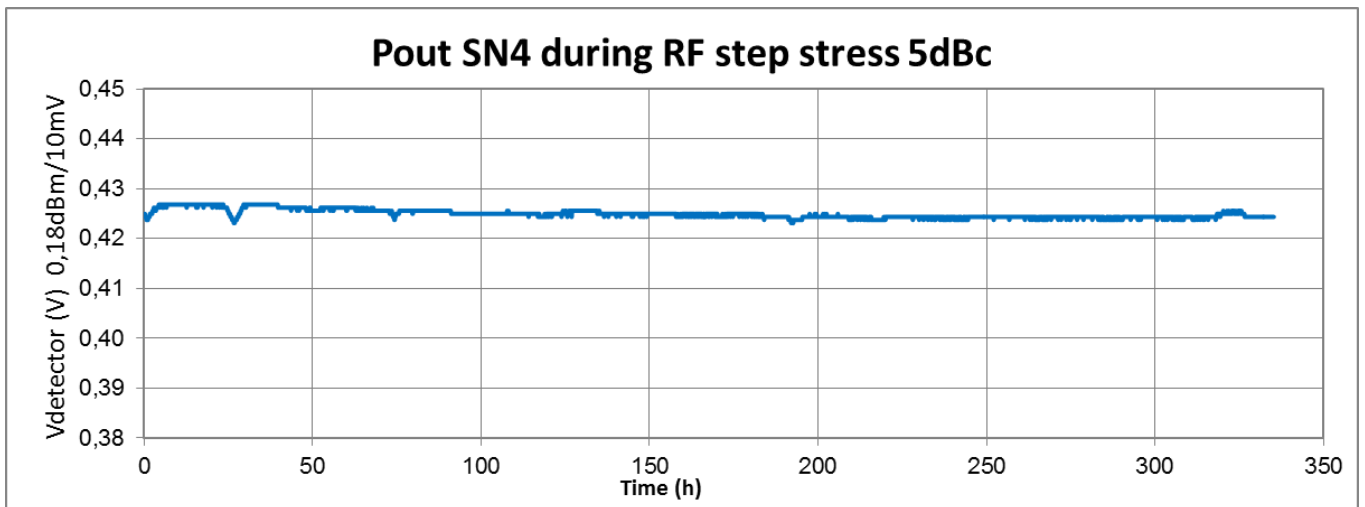


Figure 149 : HPA-1 module Run-2 (#4). RF step stress measurement. Input power and output power monitoring during 5dBc compression step

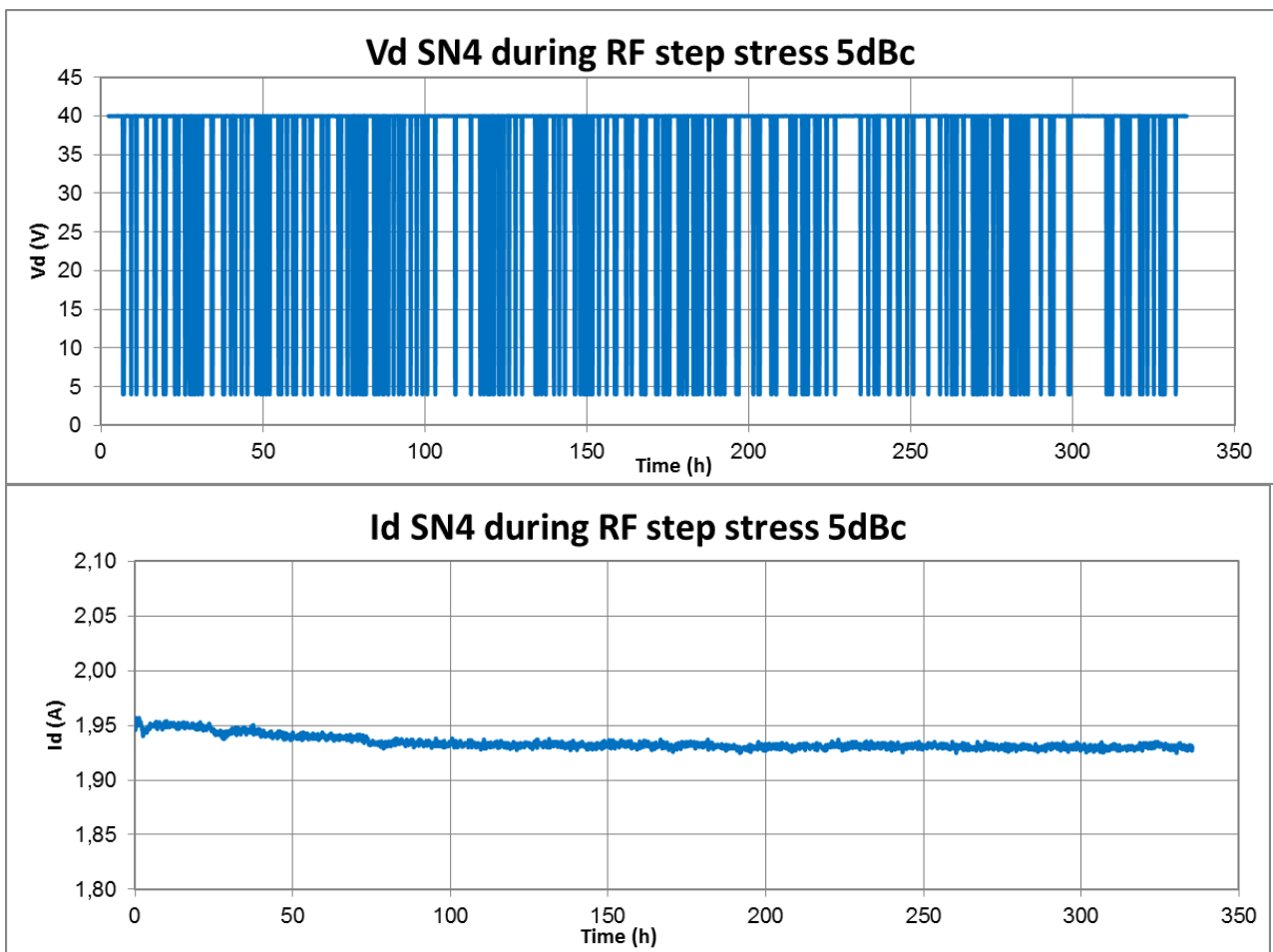


Figure 150 : HPA-1 Run-2 module (#4). RF step stress measurement (5dBc step). Drain voltage drift(V). Drain current drift (mA).

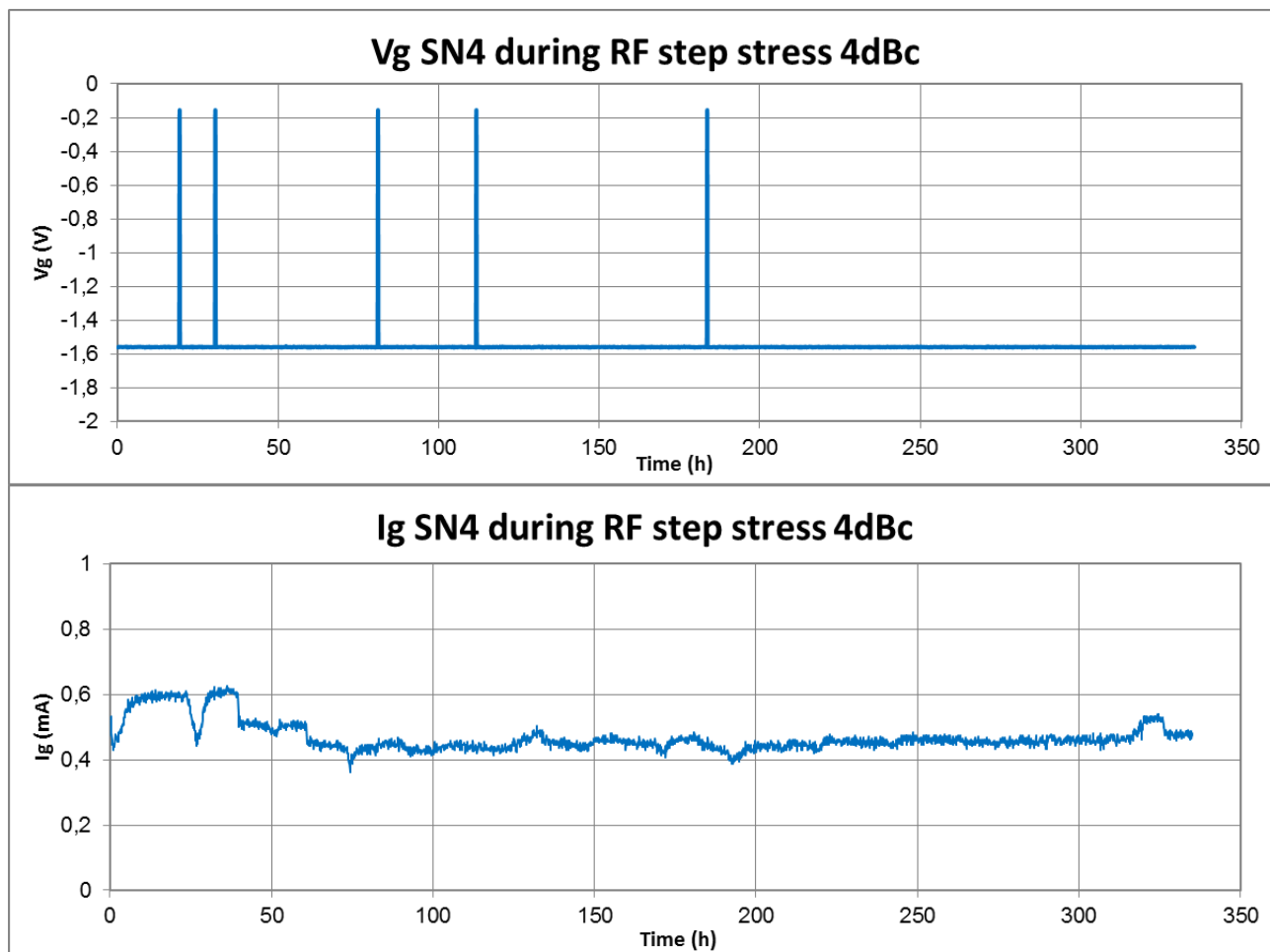


Figure 151 : HPA-1 Run-2 module (#4). RF step stress measurement (5dBc step). Gate voltage drift (V) & Gate current drift (mA).

For each HPA-1 module (#2, #4, #5), initial, intermediate and final have been performed. These measurements have consisted of:

- [S] parameters measurements
- CW characterizations (AMAM and AMPM)
- Static measurements

Measurement data are presented for HPA-1 Run-2 module #4 in the following graphs.

For the following graphs, the legend is:

- Et0 -> Initial measurements
- Et1 -> Measurements after step @ 1 dBc
- Et2 -> Measurements after step @ 3 dBc
- Et3 -> Measurements after step @ 5 dBc

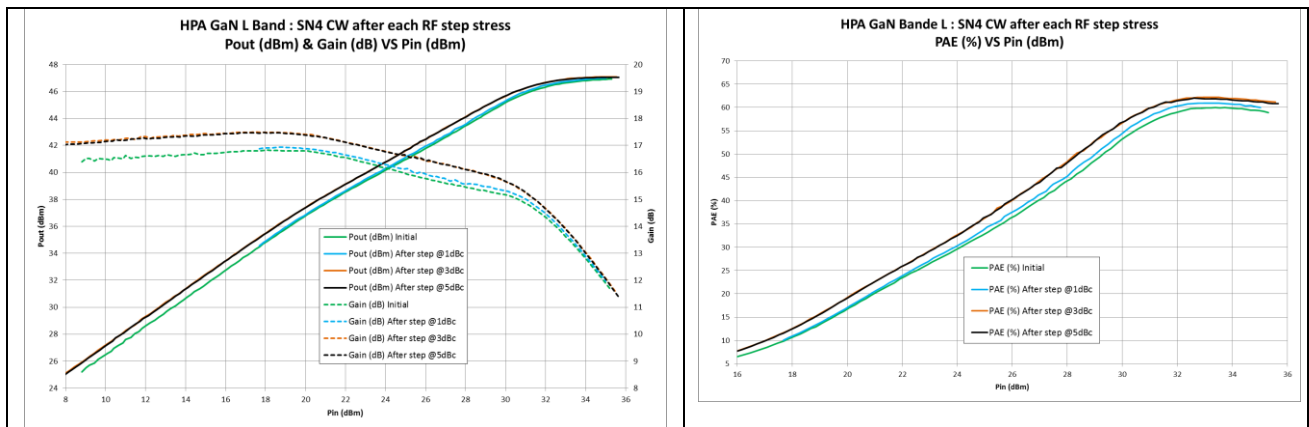
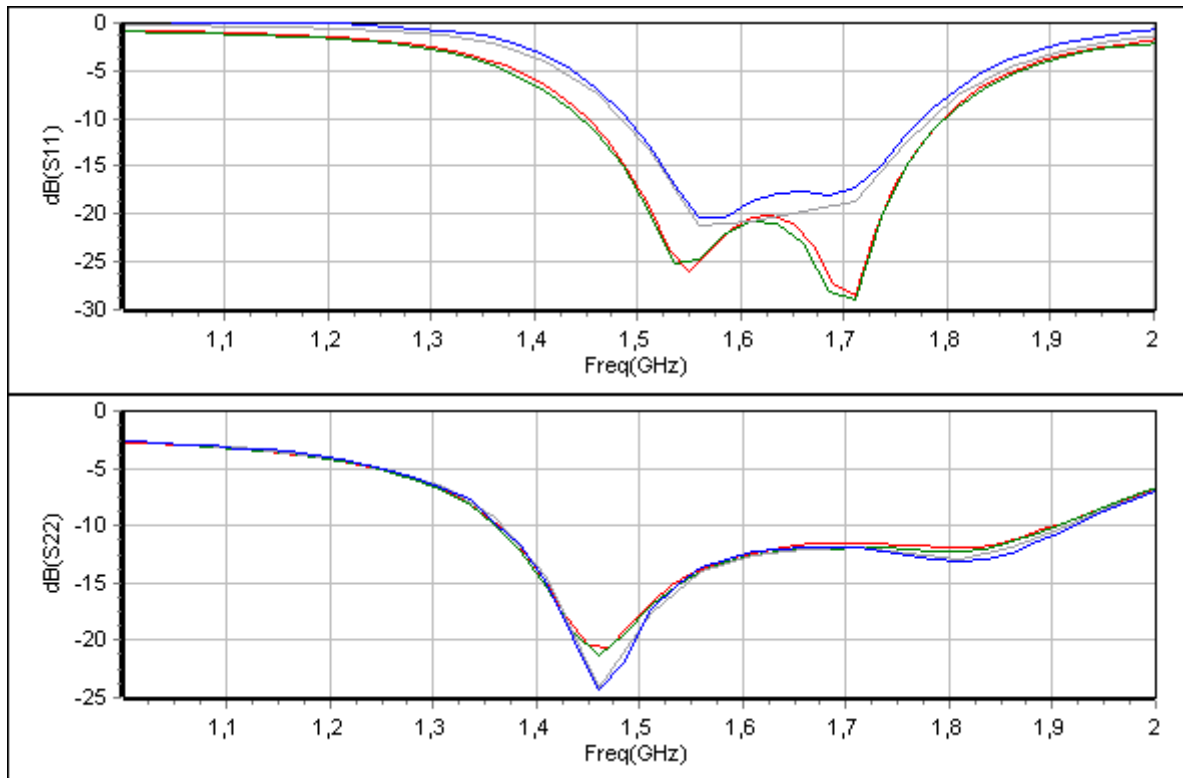


Figure 152 : HPA-1 Run-2 module #4. AMAM and AMPM characterization in CW mode after each compression step of the RF step stress measurements



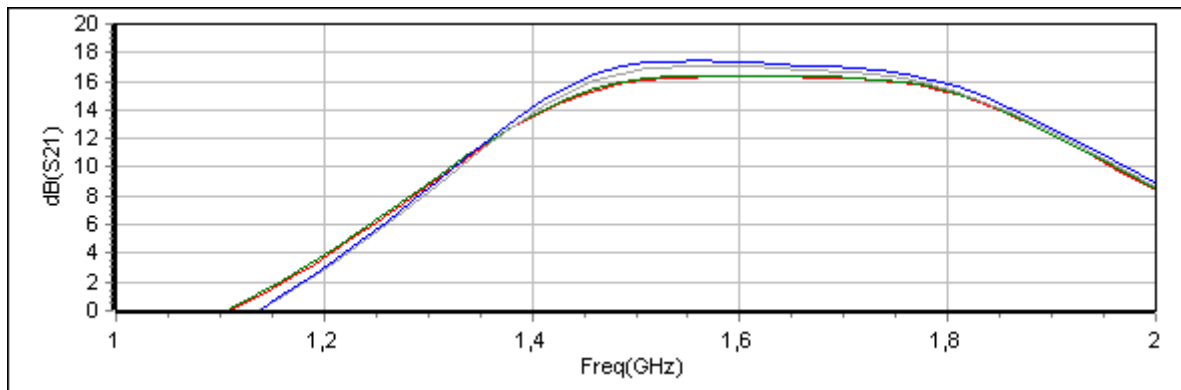


Figure 153 : HPA-1 Run-2 module #4. [S] parameters measurements after each compression step of the RF step stress measurements

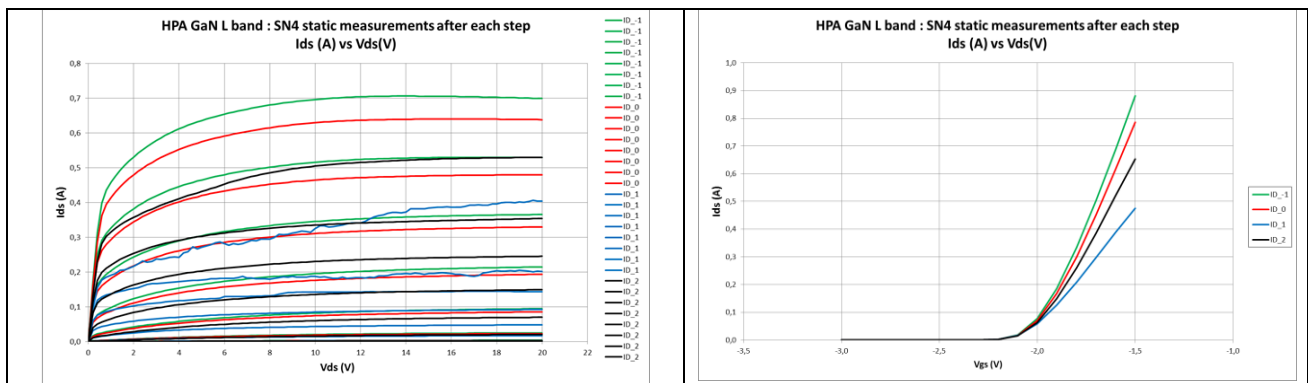


Figure 154 : HPA-1 Run-2 module #4. Static measurements after each compression step of the RF step stress measurements

Regarding the compression parameter of 3dBc obtained at NPR=15dB: the RF step stress measurements have been performed up to 5dBc gain compression for two HPA modules (One HPA module destroyed during RF step measurement due to parametric oscillations). No degradation has been observed on dynamic performances, showing that high level of compression could be used.

3. DEVELOPMENT OF KU-BAND MMIC GH25 HPA MODULES (HPA-2 MODULE)

3.1 Market trends survey

TAS-F has conducted a survey in order to give a more accurate picture (future) of the market trends for telecom application in Ku-band and to better justify the targeted SSPA equipment applications. A detailed justification in collaboration with the TAS SSPA product line, the TAS Telecom and Equipment Business Segment has been prepared. Two markets are identified: TX for TTC and SSPA for Telecom.

- Regarding TX for TTC applications in Ku-band, the main characteristics of the

market which is targeted:

- Required quantity: 8x equipment to be delivered per year
- Pout>20W in CW mode
- Regarding GaN LC-SSPA for Telecom in Ku-band:
 - Objective would be to replace current LCTWTA solutions
 - Expected quantity: 200x SSPA to be delivered per year
- Regarding satellites constellation for Ku-band internet data application:
 - Pout>20W in CW mode
 - Pout=10W in multi-carrier mode at 15dB
 - Expected quantity: 900x satellites

Frequencies bandwidth for TX and Telecom SSPA are the same: 10.7 to 12.95GHz to be cover in two sub-bands. One Ku-band GaN HPA module would be used as output stage of the TX equipment . The same Ku-band GaN HPA module would be used as elementary building block of the output power section of the LC-SSPA. Based on this market trends activity, new electrical specifications are proposed for the Ku-band HPA module.

3.2 HPA specifications

This activity is dedicated to the definition of the HPA-2 baseline design and the transistor level requirements to achieve the following technical performances :

In First table are provided the initial specifications from the ESA SoW. In this document, the electrical analysis and thermal simulations are based on the preliminary HPA design based on these initial specifications

In second Table 2 are provided the new specifications from TAS requirements. Through a new CCN, TAS has proposed new specification for the Ku-band HPA. The market trends survey has been performed for Ku-band Telecom applications justifying the needs to adapt the specification of the HPA modules to the new requirements. Market trends survey results have presented in the previous chapter. In WP5300, the detailed design of the HPA module will be based on these specifications.

Ku-Band HPA-2					
Performance within Environmental Requirements	Value	Test Conditions	C/NC	Proposed Value	Comments
Nominal Output power with Multicarrier Signal	>6W	@ 15dB NPR Worst case over temperature	C		
Power Added Efficiency with Multicarrier Signal	>25%	@ 15dB NPR Worst case over temperature	C		
Centre Frequency	11.9 GHz	Ku-band	C		
Bandwidth	>1GHz	@ Nominal output power	C		
Gain Flatness	+/- 0.3 dB	Over the whole BW for fixed input power	C		
Gain with Multicarrier Signal	> 15 dB	@ Nominal output power	C		
Gain Compression Level with Multicarrier Signal	Max 2dB	@ 15dB NPR Worst case over temperature	-	Max 7dB	@ 15dB NPR Worst case over temperature
Maximum Phase shift	<15 deg	From 30 dB back-off to 4dB compression	-	<30deg	
Deviation from Linear Phase	6 deg pk-pk	versus frequency within BW	C		
Input Reflexion coefficient	<-10 dB	@ Nominal output power, over BW	C		
2nd harmonic rejection	>30 dBc		C		
Main DC voltage supply	>40V		-	22.5V	Value confirmed with UMS
Temperature		-10deg /+85deg	C		
Pressure		Ambient and 10e-6mbar	C		Multipactor free operation will be demonstrated by calculation with a sufficient margin

Table 25 : HPA-2 Specifications (initial version from ESA proposal)

Performance within Environmental Requirements	Unity	Specification		Test Conditions	Comments
		Min	Max		
Nominal Output power with CW signal	dBm	43	44	Max PAE	
Operating frequency	GHz	11.5	13	Ku-band	
Gain Flatness	dB		+/- 0.3	Over the whole BW for fixed input power	
Gain with CW Signal	dB	16		@ Nominal output power, over operating frequency bandwidth	
Gain Compression Level with CW Signal	dB		5	Max PAE	
Power Added Efficiency	%	42	45		Ideal target 50% of PAE
Maximum Phase shift	deg		15	From 30 dB back-off to 5dB compression	
Deviation from Linear Phase	deg pk-pk		6	versus frequency within operating frequency bandwidth	
Output Reflexion coefficient	dB		-10		
Input Reflexion coefficient	dB		-15		
2nd harmonic rejection	dBc	30		@ Nominal output power, over operating frequency bandwidth	
Main DC voltage supply				30V	Value confirmed with UMS
Temperature	deg	-10	85		
Pressure	mbar	Ambient and 10e-6mbar			Multipactor free operation will be demonstrated by calculation with a sufficient margin

Table 26 : New HPA-2 Specifications after CCN

3.3 Baseline Design

3.3.1 Loadpull simulations

The optimum operating class depends on the application area, this high power amplifier discussed in this work is designed for space application. The requirements are both output power and high power added efficiency at same time. So the class-AB is the best to fulfill this requirements. In our design, both of the transistors (stage 1&2)

have been biased at 80mA/mm (deep AB class) to ensure PAE performances. This biasing point also guaranties an accurate non-linear simulation: the transistor model will be developed at this biasing condition (WP5200 performed by AMCAD).

Load-pull simulations have been undertaken to evaluate 8x100 μ m and 8x125 μ m GH25 transistor performances. To reach the maximum possible PAE performances, the following simulation procedure has been applied for each transistor at a given biasing point:

- Input impedance determination to maximize injected input power (close to perfect matching)
- Load pull at fundamental frequency to highlight maximum output power and PAE, harmonics 2 and 3 are set to 50 ohms
- Harmonic 2 load-pull optimization to maximize PAE performances, H1 set to optimal impedance previously fund and H3 set to 50ohms
- Re-optimization of H1, with H2 fixed to impedance exhibiting the maximum PAE performance, H3 on 50ohms.
- Harmonic 3 is not optimized, no significant influence on PAE due to its very high frequency

GH25 technology enables designs up to 30 (AMR) of drain voltage. In the following study, spatial de-rating ratio of 75% has been applied regarding AMR drain voltage, leading to a maximum biasing drain voltage $V_{DS0} = 22.5V$. This value has been consolidated by UMS.

Starting from the following biasing conditions:

- $I_{DS0} = 50mA/mm$
- $V_{DS0} = 22.5V$ (Maximum drain voltage derated at 75%). During the study and based on updated information from UMS, V_{ds0} will be increased to 30V. Thus, detailed design, manufacturing and test will be based on 30V.

Load-pull analysis have been undertaken at 12.5GHz (higher frequency) following the specific methodology previously detailed and have highlighted the following performances. According to the GH25_10 v1.2 DK, load-pull simulations have been done at transistor level. The results of the 8x125 μ m load-pull analysis with harmonic 1 and harmonic 2 optimization is given below :

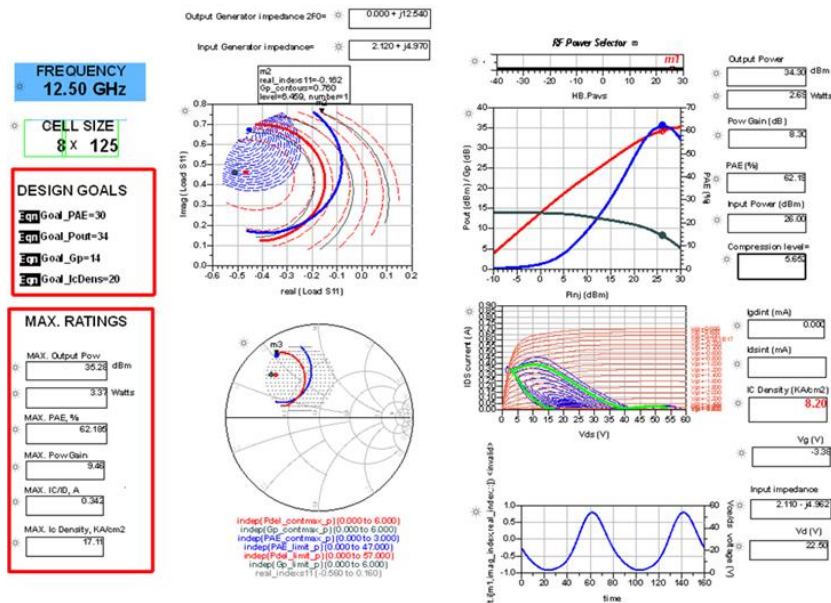


Figure 155 : Loadpull simulation of GH25 8x125µm transistors

For 8x125µm transistor, PAE peak of 62% was simulated with optimum output load at fundamental and second harmonic frequencies (H3 set to 50ohms).

3.3.2 MMIC architecture

PAE performances were considered of primary importance in the frame of this demonstrator. As a consequence this high power amplifier (HPA-2) has been designed to maximize the power added efficiency (PAE) performances. Single-ended configuration was chosen since the required narrow bandwidth (nearly 10% around the center frequency) allows to meet the requirements avoiding balanced solutions (which would require larger chip size). Transistor size of 8x125µm exhibits the best PAE / output power trade-off with a maximum peak PAE of 62% associated to an output power of 34,3dBm. The active device periphery best configuration has been found out to be:

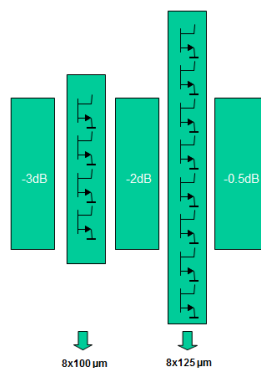


Figure 156 : Preliminary topology of the GH25 HPA-2

The HPA topology is based on two stages of amplification with an arborescent structure. Two stages were required to reach the power gain of 15dB at nominal operating point with multi-carrier signal.

The active device periphery best configuration (for both designs) has been found out to be:

- Stage 1 : 4 x 8x100µm
- Stage 2 : 8 x 8x125µm

3.3.3 RF performance simulation

Non-linear simulations have been performed using Volti software with the following setup :

- Use of AMAM / AMPM / AMPdc curves from loadpull simulations of 8x100µm and 8x125µm transistors
- Input power : -10 to 34dBm
- Center Frequency : 12.5GHz

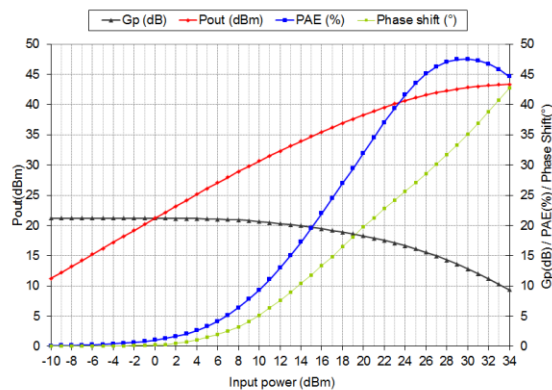


**Figure 157 : Performance versus Pin in CW mode of the GH25 HPA-2.
Vds=22,5V, RFfreq=12.5GHz**

With multi-carrier signal, contribution of each parts of the GH25 HPA-2 module is presented in the next table. Simulation results are presented at NPR=15,2dB.

RF SECTION		Gain	Cumul Gain	Signal Level	Signal level	Linearity	Pdc	Pdiss	PAE	Gain Comp
N°	Elements	dB	dB	dBm	W	dB	W	W	%	dB
INPUT				22,00	1,58E-01					
1	INPUT	-3,00	-3,00	19,00	0,0794	285,19	0,00	0,08	0,00	0,00
2	4x8x100	11,74	8,74	30,74	1,1847	22,12	4,34	3,23	25,48	1,57
3	INTERSTAGE	-2,00	6,74	28,74	0,7475	22,12	0,00	0,44	0,00	0,00
4	8x8x125	10,53	17,27	39,27	8,4454	15,25	17,28	9,58	44,55	2,87
5	OUTPUT	-0,50	16,77	38,77	7,5270	15,25	0,00	0,92	0,00	0,00
Total RF Section			16,77	38,77	7,53	15,25	21,61	14,25	34,09	4,45

**Table 27 : Performance in multi-carrier mode of the GH25 HPA-2. Vds=22,5V,
RFfreq=12,5GHz**

With a multi-carrier signal, at NPR=15,2dB, the PAE performance match the required performance with a PAE of 34%. At NPR=15,2dB, output power is 48,77dBm (7,53W).

3.3.4 Packaging solution

An existing Ku-band dissipative hermetic package based on CuW material will be used for the assembly of the HPA-2 module. Layout of the package including preliminary HPA-2 is given hereafter. This package is space compliant and have been developed by TAS. Baseplate material is CuW. This Ku-band package have also been designed taking into account both electrical and mechanical design constraints, multipactor and DC current constraints on RF feedthrough. CuW baseplate and relevant interface optimization have demonstrates up to 200 W/mK thermal resistance. In future, TAS expects to develop a new Ku-band high dissipative package based on CuD material

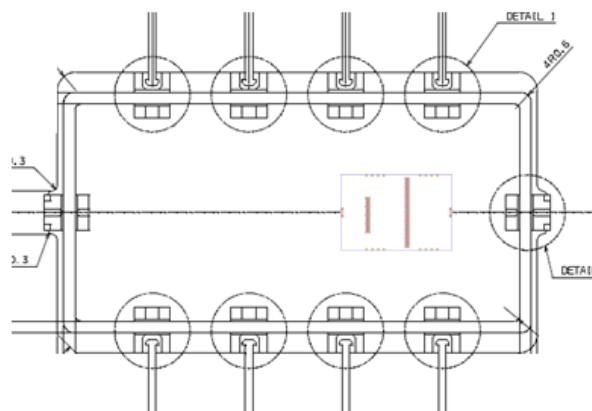


Figure 158 : Layout of the Ku-band hermetic package including preliminary MMIC HPA-2

3.3.5 Thermal simulations

Thermal analysis on the GH25 HPA-2 module including the transistor physical description and packaging environment will be launched in order to evaluate junction temperature. The thermal behavior of the 0.25 μ m device represented by a multi-port inputs and outputs SPICE thermal circuit will be generated and used for non-linear modeling activities. Several cases will be studied to provide to the designer an overview in terms of thermal performances.

Two different baseplate materials will be considered for thermal simulation.

- CuW with $K=210\text{W/m}^{\circ}\text{C}$
- CuD with $K=400\text{W/m}^{\circ}\text{C}$

Description of the thermal stack used in thermal simulation is provided below

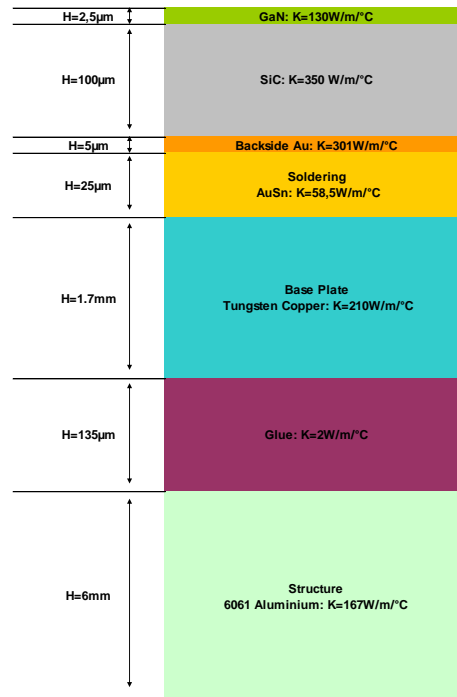


Figure 159 : Description of the thermal stack used for thermal simulation: baseplate material of the package: CuW

In this paragraph, thermal simulations results are provided for second transistor stage.

3.3.5.1 Thermal study of GH25 8x125µm transistor

The mesh of the device is presented in Figure 160 after simplification for symmetry consideration. Simulation has been performed for several baseplate temperatures (25°C, 50°C, 75°C, 100°C). The dissipated power in the ¼ of the device is 0.25W. Materials are supposed to be linear excepted GaN material which is nonlinear.

Figure 160 show the temperature map for different baseplate temperatures. Figure 160 presents also the temperature along a line in the channel layer. The following table reports the values for temperature and thermal resistances in the devices. The thermal resistance is around 11.8°C/W with a small variation of 5% due to material non-linearity.

Baseplate temperature (°C)	25	50	75	100
Dissipated power(W)	1	1	1	1
Thermal resistance (°C/W)	11.6	11.81	12.02	12.21
Temperature (°C)	36.6	61.81	87.02	112.21

Table 28 : GH25 8x125µm transistor. Thermal resistance(°C/W) for various base plate temperatures and dissipated power.

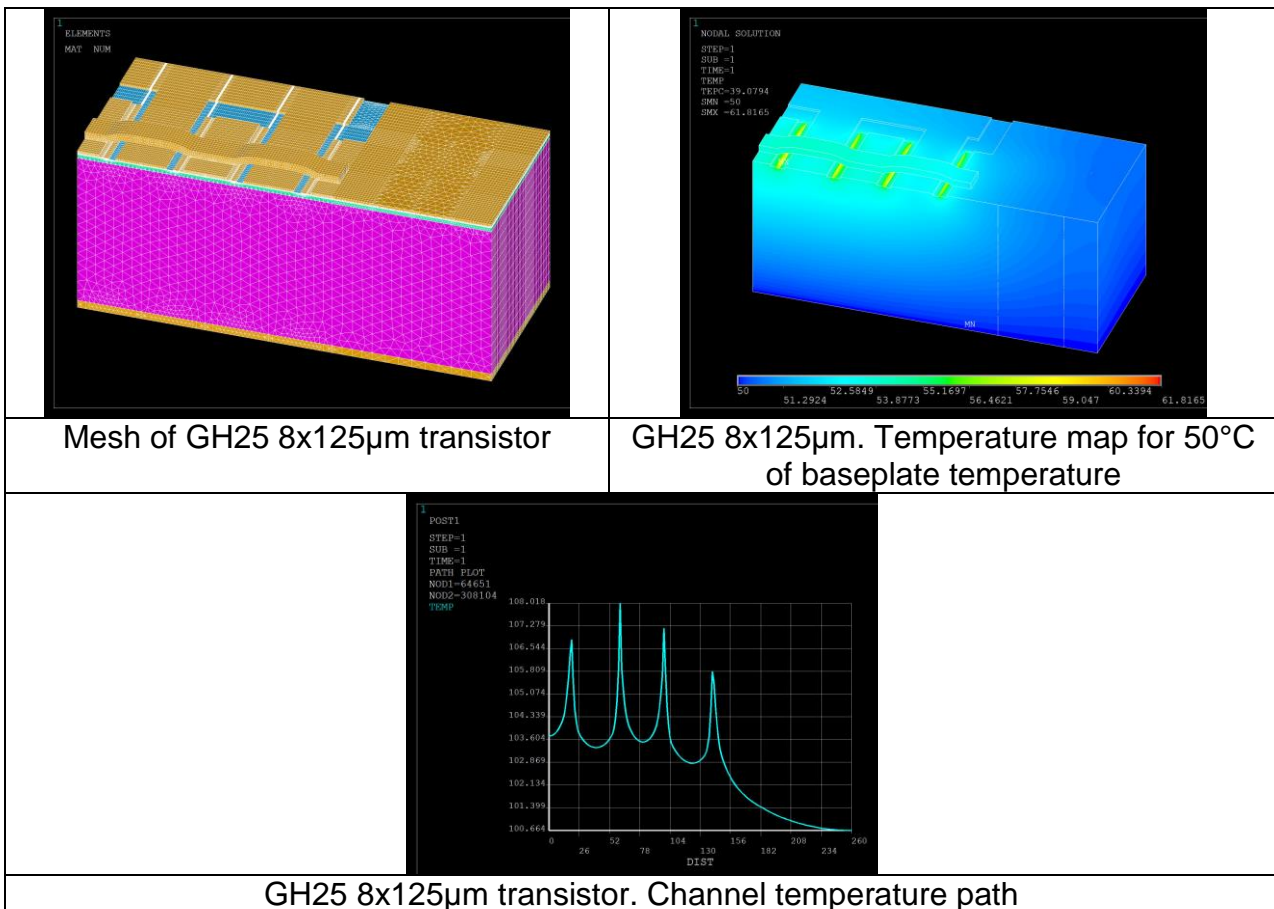


Figure 160 : 8x125µm transistor thermal simulations

3.3.5.2 Thermal study of the GH25 8x8x125µm power-bar

The mesh of the device is presented in figure below after simplification for symmetry consideration. Simulation has been performed for several baseplate temperatures (25°C, 50°C, 75°C, 100°C). The dissipated power in the ¼ of the device is 2.5W corresponding to 10W in the whole device. Figure below shows also the temperature map for different baseplate temperatures. The following table reports the values for temperature and thermal resistances in the devices.

The thermal resistance is around 1.48°C/W with a small variation of 5% due to material non-linearity.

Baseplate temperature (°C)	25	50	75	100
Dissipated power(W)	10	10	10	10
Thermal resistance (°C/W)	1.46	1.48	1.50	1.53
Temperature (°C)	39.59	64.84	90.10	115.34

Table 29 : GH25 8x8x125µm power-bar. Thermal resistance(°C/W) for various base plate temperatures and dissipated power.

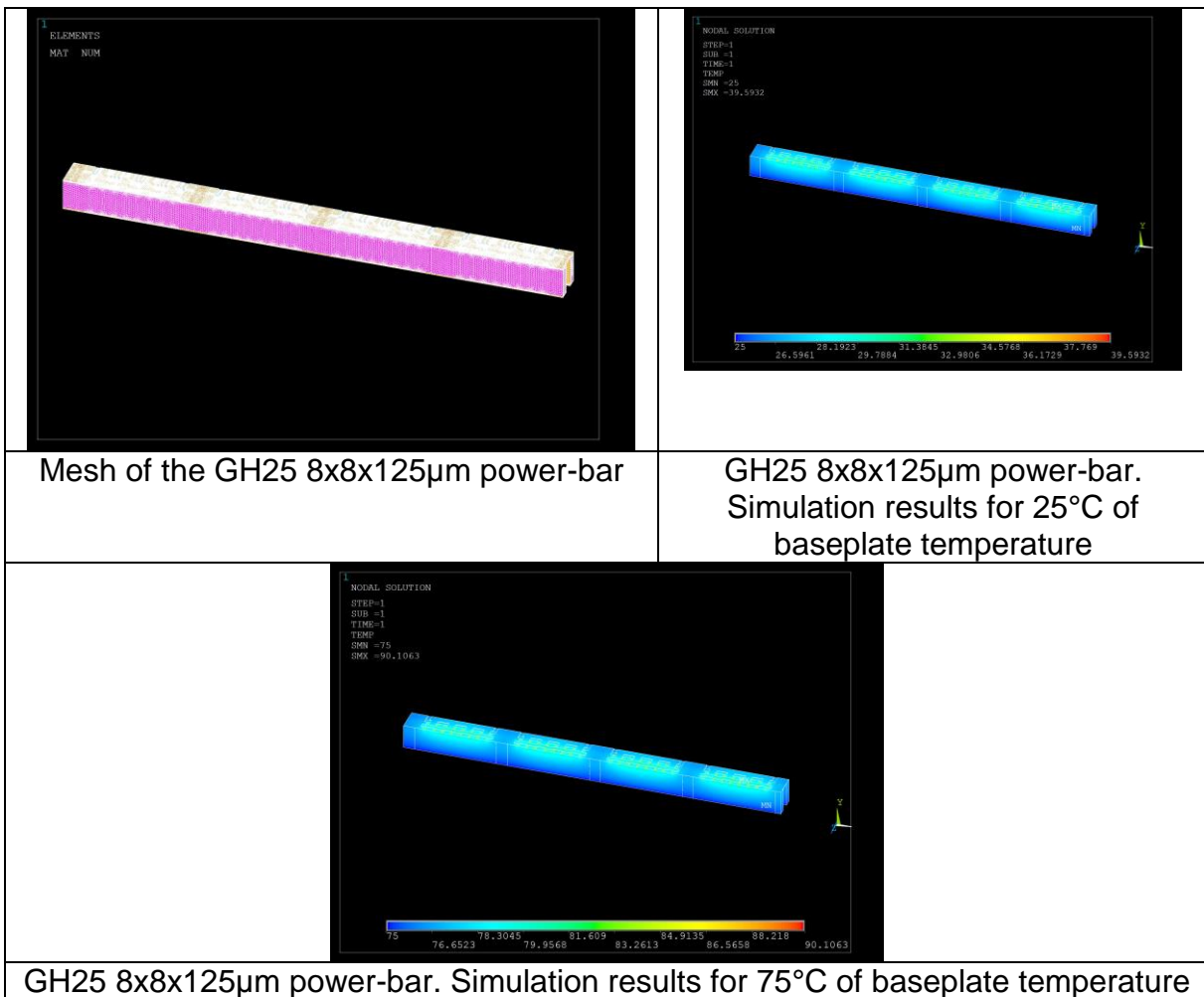


Figure 161 : 8x8x125µm transistor thermal simulations

3.3.5.3 Thermal study of the packaging of the power amplifier

In this part, we consider the part of the thermal stack presented in Figure 159 corresponding to the packaging. Each power-bar is replaced by a rectangle. The dimensions of the rectangle correspond to the footprint of the power-bar. The mesh of the structure is presented in figure below. The thermal network is extracted by injecting power in first and second stage alternatively. Results are presented in figures below. Validation is proposed by injecting power simultaneously in both stages as shown in Figure 162

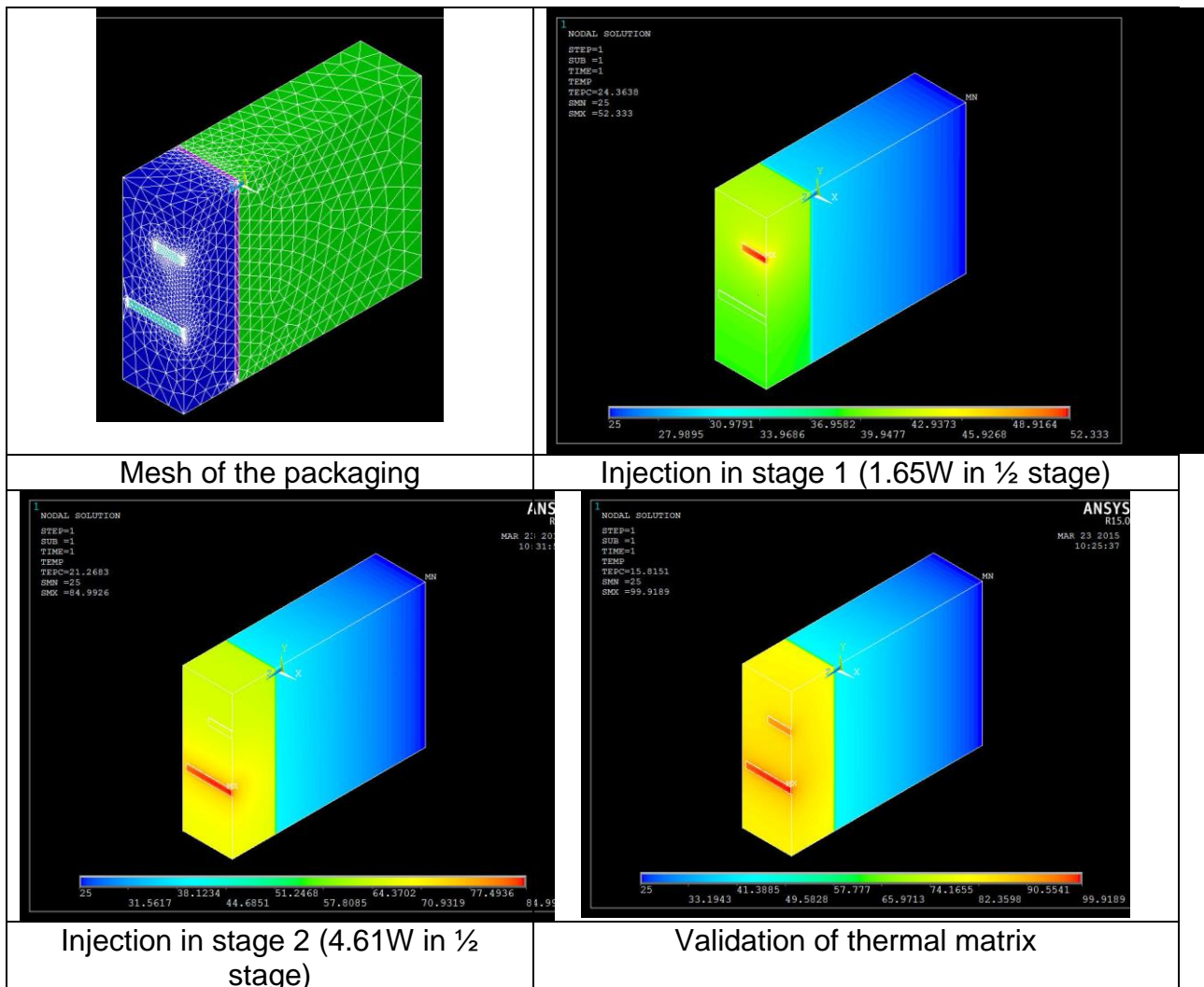


Figure 162 : Thermal study of the packaging

3.3.5.4 Temperature evaluation

Hypothesis for thermal calculation is presented below :

Tr = transistor of stage 1 or 2

Rth packaging = matrix of thermal resistances

Tj1, Tj2 = temperature of transistor in stage 1, stage 2

Tbase = T baseplate

Tp1, Tp2 = Tpackaging under powerbar1 or 2

Rj1=14.5 (thermal resistance transistor of stage 1)

Rj2=11.8 (thermal resistance transistor of stage 2)

P1, P2= power in stage 1 or 2

Pj1, Pj2 = P1/4, P2/8

For CuW baseplate material:

For CuD baseplate material:

<ul style="list-style-type: none"> • Z11=4.42°C/W • Z12=0.89°C/W • Z21=Z12 • Z22=2.93°C/W 	<ul style="list-style-type: none"> • Z11=2.92°C/W • Z12=0.694°C/W • Z21=Z12 • Z22=1.97°C/W
---	--

For example, if you want to compute Tj1 or Tj2 (junction temperature of transistor in stage 1 or transistor in stage 2), calculation is:

Case 1 : Pout RF=7,53W NPR=15,25dB, Tbase=50°C, CuW material:

- Dissipated power in stage 1 : **3.2W**
- Dissipated power in stage 2 : **9.6W**

$$Tj1 = 14.5 \cdot Pj1 + Tp1 = 14.5 \cdot 0.8 + 4.42 \cdot 3.2 + 0.89 \cdot 9.6 + 50 = 84.3^\circ\text{C}$$

$$Tj2 = 11.8 \cdot Pj2 + Tp2 = 11.8 \cdot 1.2 + 0.89 \cdot 3.2 + 2.93 \cdot 9.6 + 50 = 95.14^\circ\text{C}$$

Case 2 : Pout RF=7,53W NPR=15,25dB, Tbase=85°C, CuW material:

- Dissipated power in stage 1 : **3.2W**
- Dissipated power in stage 2 : **9.6W**

$$Tj1 = 14.5 \cdot Pj1 + Tp1 = 14.5 \cdot 0.8 + 4.42 \cdot 3.2 + 0.89 \cdot 9.6 + 85 = 119.3^\circ\text{C}$$

$$Tj2 = 11.8 \cdot Pj2 + Tp2 = 11.8 \cdot 1.2 + 0.89 \cdot 3.2 + 2.93 \cdot 9.6 + 85 = 130.1^\circ\text{C}$$

Case 3 : Pout RF=7,53W NPR=15,25dB, Tbase=85°C, CuD material:

- Dissipated power in stage 1 : **3.2W**
- Dissipated power in stage 2 : **9.6W**

$$Tj1 = 14.5 \cdot Pj1 + Tp1 = 14.5 \cdot 0.8 + 2.92 \cdot 3.2 + 0.694 \cdot 9.6 + 85 = 112.6^\circ\text{C}$$

$$Tj2 = 11.8 \cdot Pj2 + Tp2 = 11.8 \cdot 1.2 + 0.694 \cdot 3.2 + 1.97 \cdot 9.6 + 85 = 120.3^\circ\text{C}$$

3.4 0.25µm Technology Modelling and Performance

In this chapter, first part synthesizes AMCAD Engineering I(V) / S-Parameters and Load Pull measurements achieved on the GH25 transistors 8x125µm. For this study, UMS provided four samples of GH25 transistors. Second part synthesizes AMCAD Engineering modelling activity achieved on the GH25 transistors 8x125µm

3.4.1 Unitary cell measurements

The system set up for the transistor (8x100µm, 8x125µm GH25 UMS) characterization is described below. The bias voltages and S-parameters are performed in CW mode.

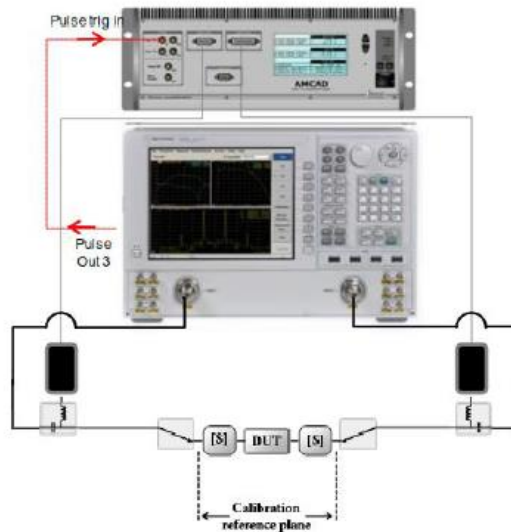


Figure 163 : AMCAD I(V) and [S] test bench for transistors characterizations

The principle of measurement pulse is to describe the I(V) network by quasi-isothermal measurements using short pulses around a quiescent bias point selected. The quiescent bias point of rest is provided by the voltage levels and V_{gs0} v_{ds0} . This results in a current I_{ds0} polarization. Pulses, whose levels are represented by V_{gs1} , I_{gs1} , V_{ds1} I_{ds1} and describe all the characteristics of input and output of the transistors.

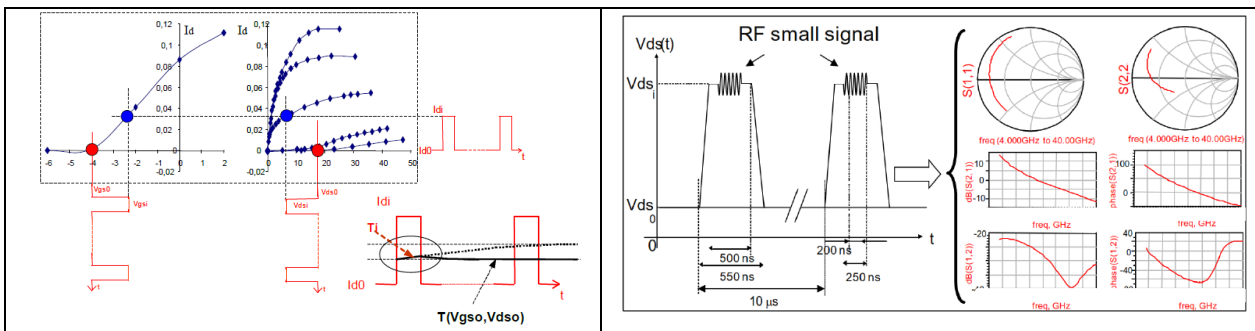


Figure 164 : Typical timings (DC bias / RF) used for pulsed measurements

4 samples for each development are supplied by UMS:

- 8x100 -> Ref: N17, T12, T7, N12
- 8x125 -> Ref: N17, T12, T7, N12

Preliminary continuous I(V)/RF measurements have been performed on each development in order to estimate the process dispersion and to select the most representative samples for the complete characterizations. These dispersive measurements have been performed at ambient temperature (25°C). The results for the different transistor have shown that the representative sample is referred T7. In this final report, results are presented only for 8x125µm transistor size.

In figure below are presented the results for Quiescent bias : $V_{ds0}=0V$, $V_{gs0}=0V$. I_{dss} is reduced by 8% to a rise of 75 °C the chuck temperature

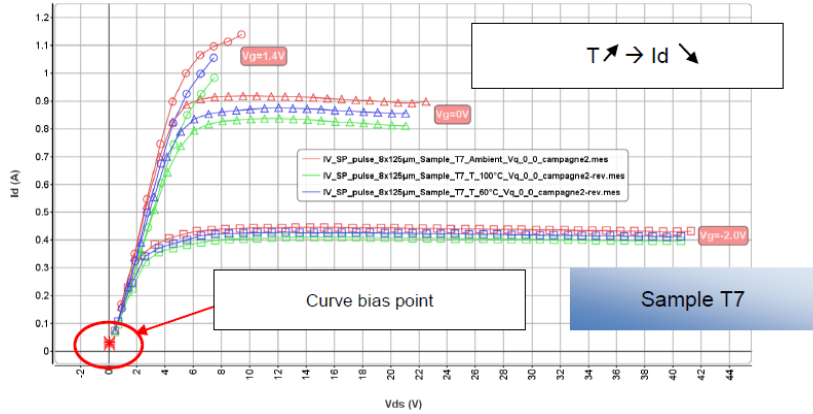


Figure 165 : Output current with different chuck temperature (25°C, 60°C, 100°C), transistor 8x125 GH25 measurements (bias points $V_{ds0}=0V$, $V_{gs0}=0V$)

In figure below are presented the results for Quiescent bias : $V_{ds0}=27V$, $I_{ds0} = 50mA/mm$. I_{dss} is reduced by 8% to a rise of 75 °C the chuck temperature.

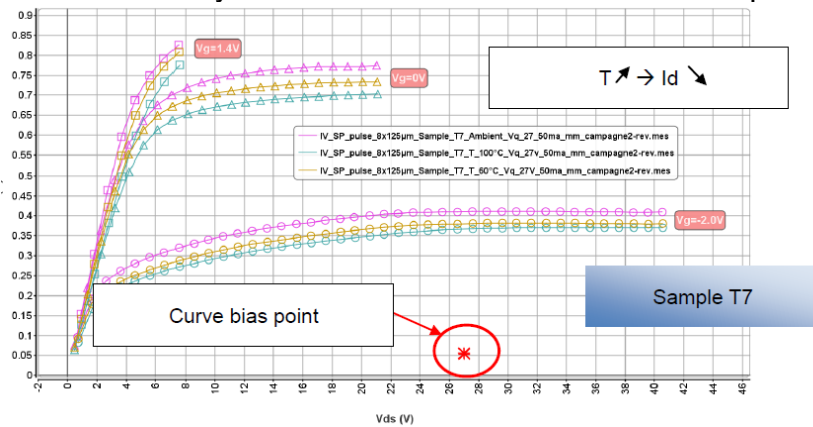


Figure 166 : Output current with different chuck temperature (25°C, 60°C, 100°C), transistor 8x125 GH25 measurements (bias points $V_{ds0}=27V$, $I_{ds0}=50mA$)

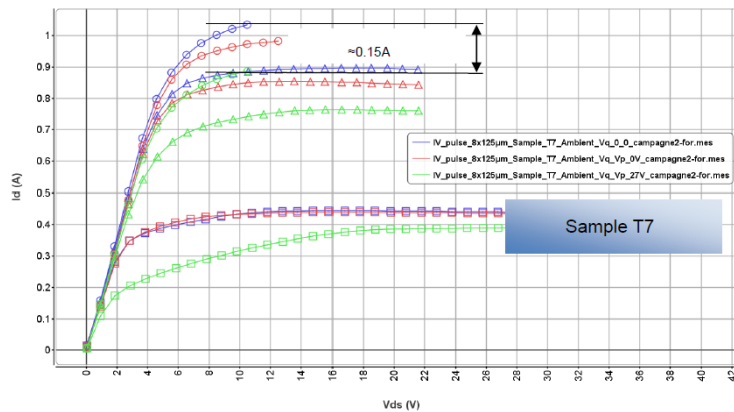


Figure 167 : Highlighted phenomena traps

Regarding the phenomena traps, the effect on the output characteristic is a reduction of the drain current of 14%

Measurement for classical AB class ($V_{ds0}=27V$, $I_{ds}=50mA/mm$) is presented below.

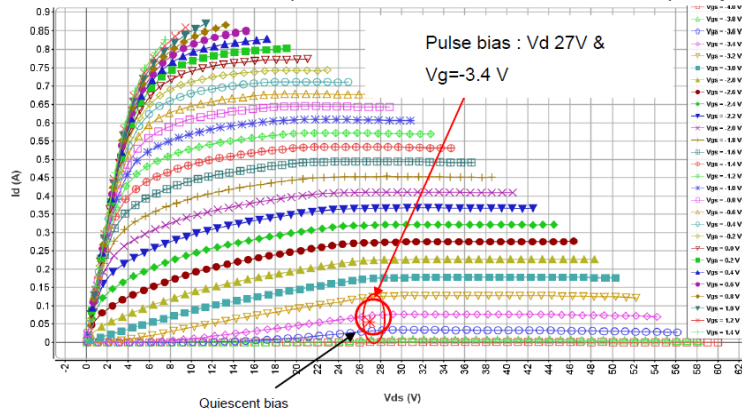


Figure 168 : Output current, quiescent bias: (27V, 50mA), (chuck temperature = 25°C), transistor 8x125 GH25

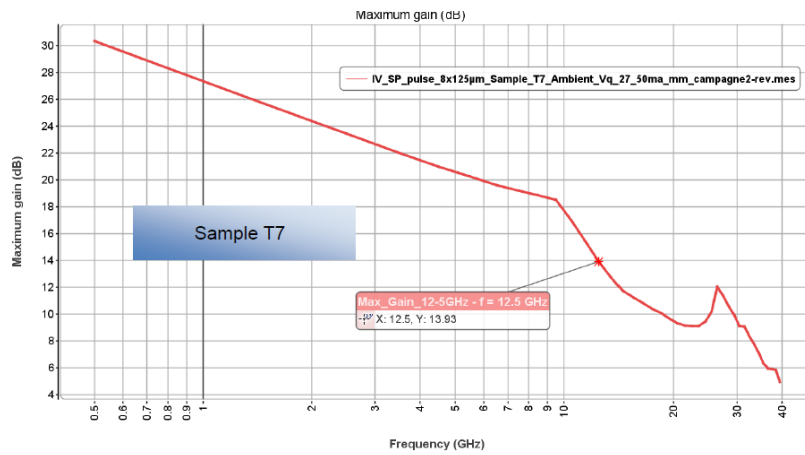


Figure 169 : Maximum Gain @ $V_{ds0}=27V$, $I_{ds0}=50mA$

The loadpull system set up for the devices characterization is described below

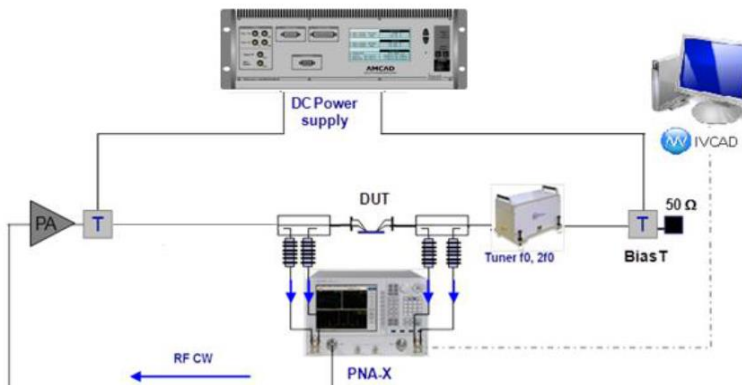


Figure 170 : AMCAD VNA-based load-pull system

The objective is to find the optimal load impedance power added efficiency (PAE) for $f_0 = 12.5\text{GHz}$ CW mode for $P_{out} > 3\text{W/mm}$.

The loadpull methodology used for performance optimization is :

- Measurement and optimization of f_0 load impedance
- Measurement and optimization of $2f_0$
- Re-optimization of f_0 load impedance

Final performance obtained after loadpull optimization are presented below:

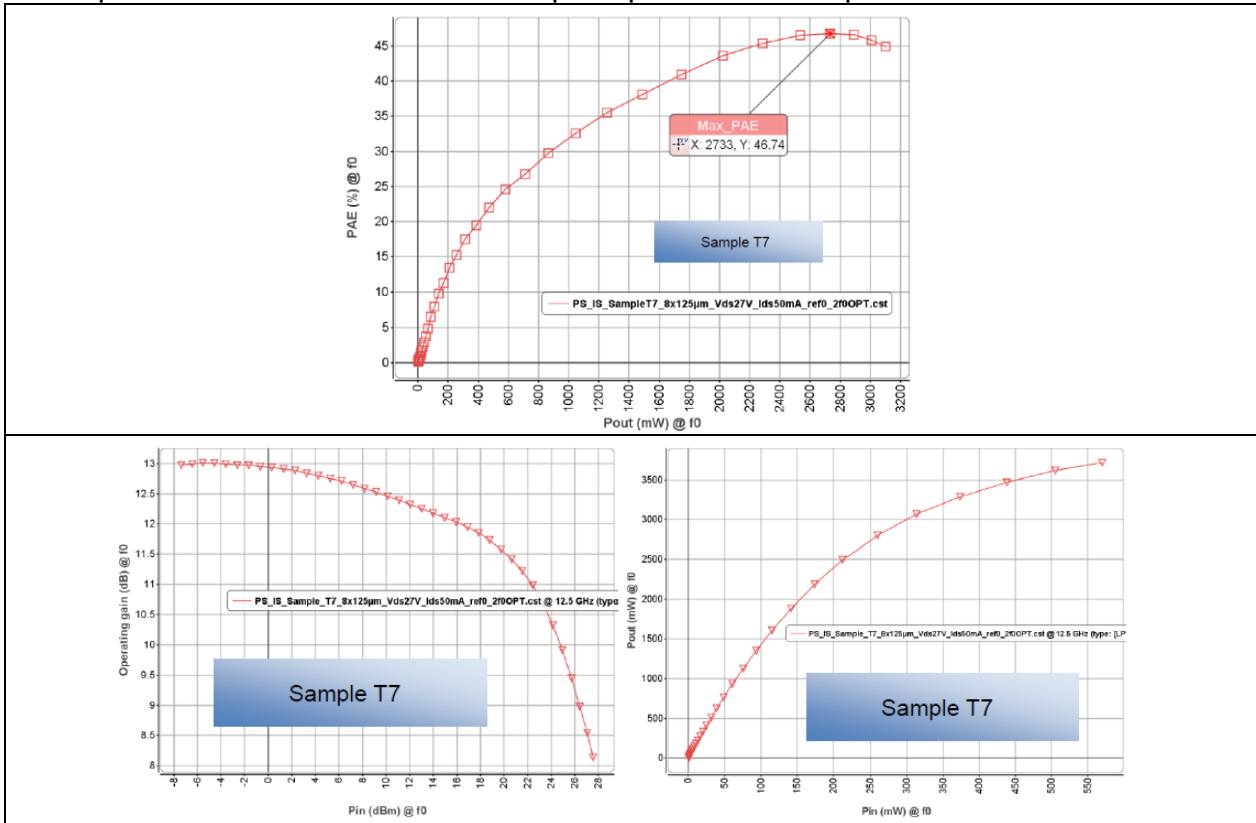


Figure 171 : 8x125µm performance at 12.5GHz after loadpull optimization

Development	Linear Gain (dB)	Output Power (W)	PAE foOPT (%)	PAE AllOPT (%)	Zload f0 opt PAE (Ω)	Zload 2f0 opt PAE (Ω)	Zsource (Ω)
8x125µm	12.97	3.180	46.45	47.31	$10.19 + j23.39$	$4.85 + j25.69$	50

Table 30 : 8x125µm performance at 12.5GHz after loadpull optimization

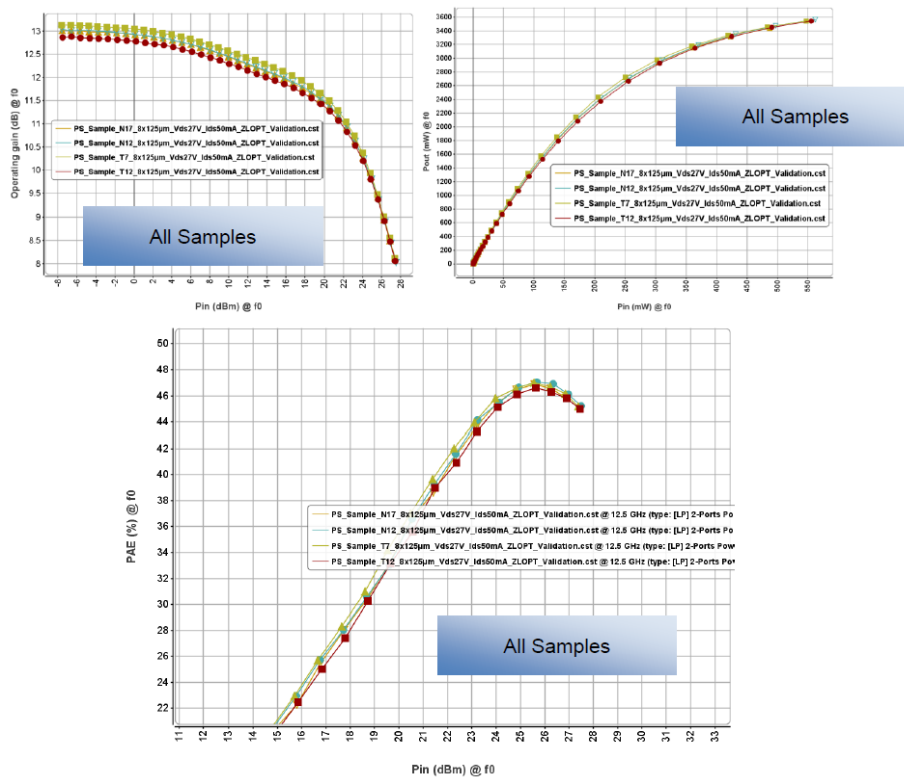


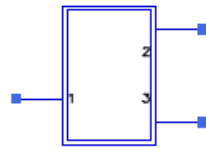
Figure 172 : Sample dispersion for optimal PAE load impedances @ 12.5GHz (Vds=27V, 50mA)

Sample	Linear Gain (dB)	Output Power (W)	PAE max (%)	Zload f0 opt PAE (Ω)	Zload 2f0 opt PAE (Ω)	Zsource (Ω)
T7	13.13	3.46	47	9.26+J23.33	8.87+j26.11	50
N12	13.04	3.47	47.1	9.26+J23.33	8.87+j26.11	50
N17	13.01	3.44	46.9	9.26+J23.33	8.87+j26.11	50
T12	12.87	3.45	46.6	9.26+J23.33	8.87+j26.11	50

Figure 173 : Synthesis of sample dispersion for optimal PAE load impedances @ 12.5GHz (Vds=27V, 40mA)

3.4.2 Unitary cell modeling activity.

The provided model is a 3 ports transistor. All the parameters are available as well as the chuck temperature and selfheating effects



Demo_Model
X4
temp_chuck=25 °C
ratio_self_heating=100 %

Figure 174 : 3 ports transistor model

The model is adjusted through several measurements (I(V), [S], load-pull...) in different operating conditions (bias, temperature, frequency...) in order to have a coherent model. Comparisons between the pulsed I(V) measurements and the model @ T_chuck=25°C are illustrated below, for the quiescent bias conditions : Vds0=27V, Ids0=50mA.

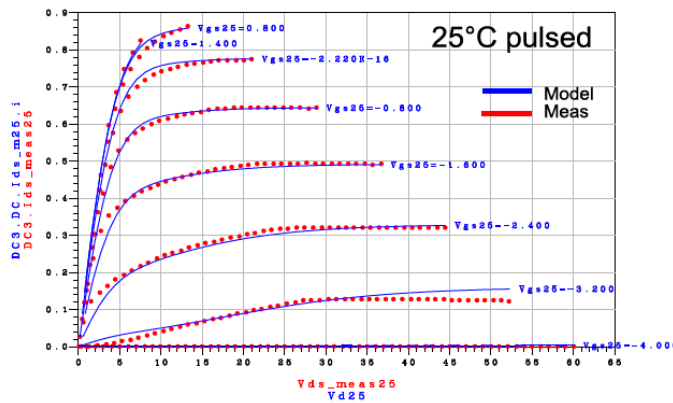


Figure 175 : Meas. vs Model 8x125µm @ 25°C

Thermal resistance Rth is extracted from DC and pulsed measurements at ambient temperature and 100°C respectively. For the same Vgs, the intercept of the two curves describe the same thermal state.

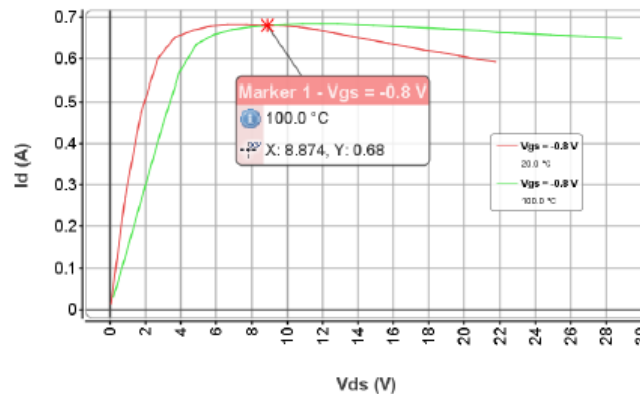


Figure 176 : Thermal resistance extraction for 8X125µm

Finally, thermal parameters of the model are extracted from measurements at ambient and 100°C in pulsed mode. Thermal dependence is then implemented to the relevant elements such as the drain current which is directly impacted.

Comparisons between the pulsed I(V) measurements and the model @ T_{chuck} = 60°C & 100°C are illustrated below, for the quiescent bias conditions : V_{ds0}=27V, I_{ds0}=50mA.

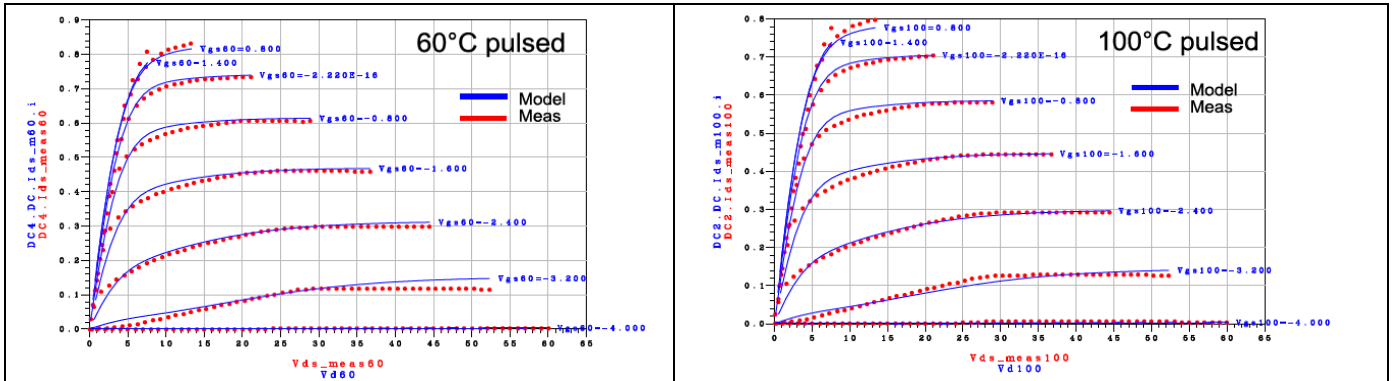


Figure 177 : Meas. vs Model 8x125µm @ 60°C

For S parameters [0.5 to 39.5 GHz] validation, the model is compared to the measurement on several bias points.

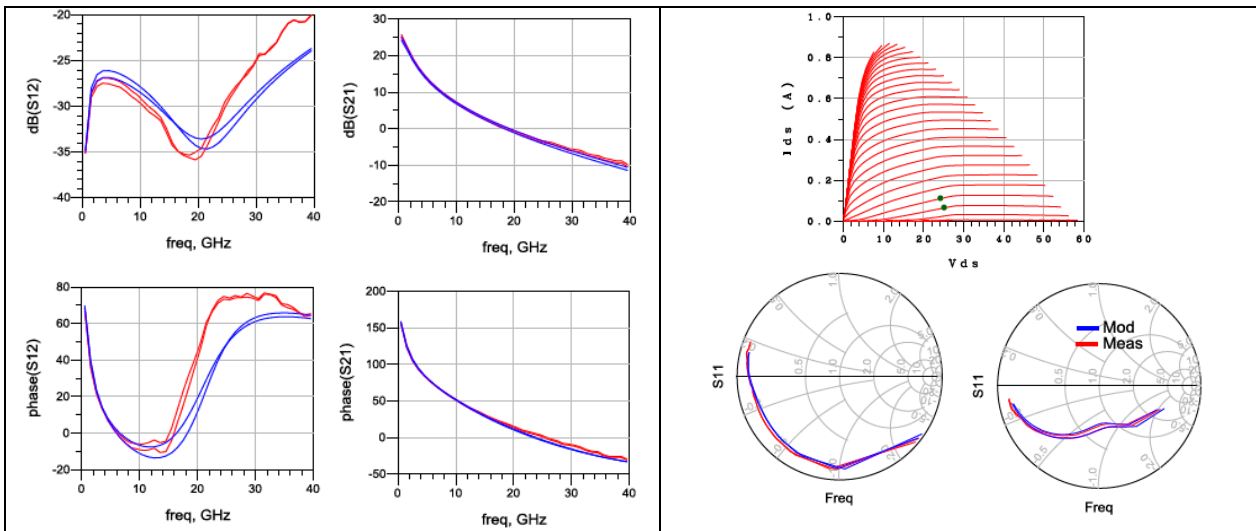


Figure 178 : [S] parameter Meas. vs Model 8x125µm @ 25°C

In Load-pull configuration, the comparison is performed at one frequency (12.5GHz) and for several load impedances including the optimum ones. Next figure illustrates contour of max PAE @ 3dB respectively.

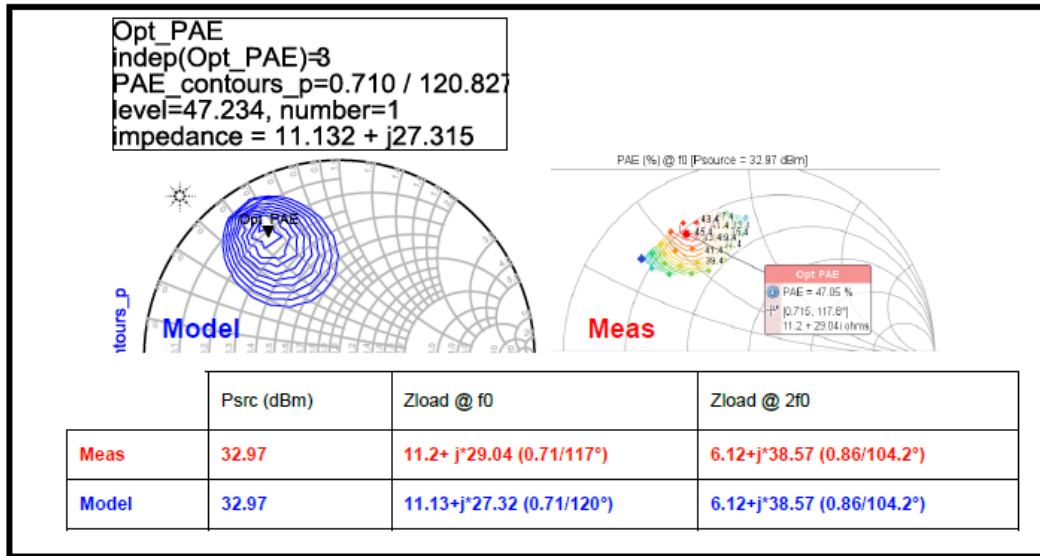


Figure 179 : Contour of Max PAE - Meas. vs Model 8x125µm

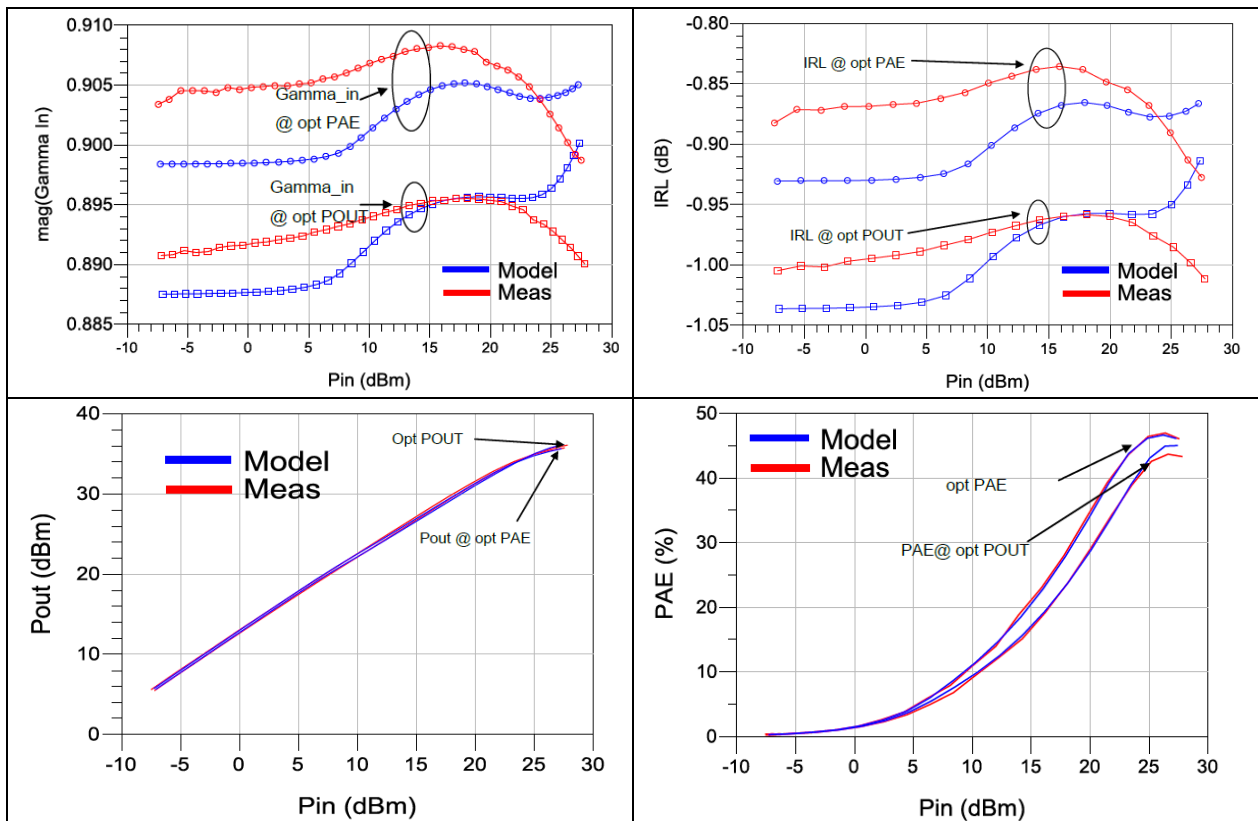


Figure 180 : Gamma_in / IRL / Pout / PAE - Meas. vs Model 8x125µm

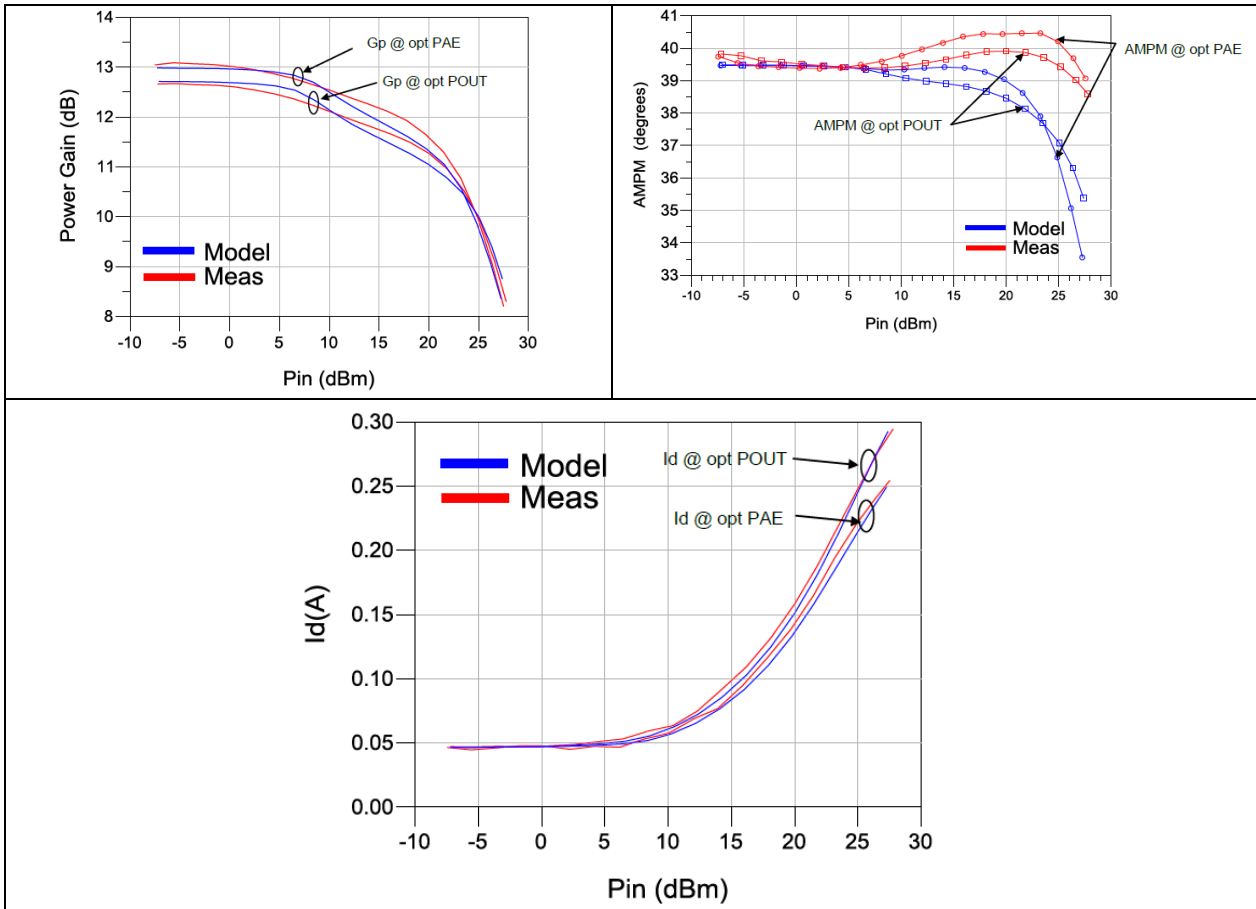


Figure 181 : Power Gain / AM-PM / Id - Meas. vs Model 8x125µm

3.5 Detailed Design

Three versions have been designed and are presented in this chapter

- Version 1: HPA-2 module which is a Class AB Ku-band GH25 MMIC HPA module has been finalized with NL electrothermal model of the transistor cell provided by AMCAD.
- Version 2: Doherty Ku-band GH25 MMIC HPA module has been designed using NL electro-thermal model of the transistor cell from the UMS DK
- Version 3: Doherty Ku-band GH25 MMIC-Hybrid HPA module has been designed using NL electro-thermal model of the transistor cell from the UMS DK

Regarding these three HPA versions, a common electrical specifications matrix has been used and is recalled below:

Performance within Environmental Requirements	Unity	Specification			Ku-Band HPA	
		Min		Max	Test Conditions	Comments
Nominal Output power with CW signal	dBm	43	44		Max PAE	
Operating frequency	GHz	11.5		13	Ku-band	
Gain Flatness	dB			+/- 0.3	Over the whole BW for fixed input power	
Gain with CW Signal	dB	16			@ Nominal output power, over operating frequency bandwidth	
Gain Compression Level with CW Signal	dB			5	Max PAE	
Power Added Efficiency	%	42	45			
Maximum Phase shift	deg			15	From 30 dB back-off to 5dB compression	
Deviation from Linear Phase	deg pk-pk			6	versus frequency within operating frequency bandwidth	
Output Reflexion coefficient	dB			-10		
Input Reflexion coefficient	dB			-15		
2nd harmonic rejection	dBc	30			@ Nominal output power, over operating frequency bandwidth	
Main DC voltage supply				30V		Value confirmed with UMS
Temperature	deg	-10		85		
Pressure	mbar	Ambient and 10e-6mbar				Multipactor free operation will be demonstrated by calculation with a sufficient margin

Table 31 : Specifications of the HPA-2 Module and Doherty HPA modules

3.5.1 Detailed Design of version 1 : HPA-2 module

PAE performances were considered of primary importance in the frame of this demonstrator. As a consequence this high power amplifier (HPA) has been designed to maximize the power added efficiency (PAE) performances. Single-ended configuration was chosen since the required narrow bandwidth (nearly 10% around the

center frequency) allows to meet the requirements avoiding balanced solutions (which would require larger chip size).

According to the transistor mode provided by AMCD, load-pull simulations have been done at transistor level. Transistor size of $8 \times 125 \mu\text{m}$ exhibits the best PAE / output power trade-off with a maximum peak PAE of 48% associated to an output power of 36.3dBm. The active device periphery best configuration has been found out to be:

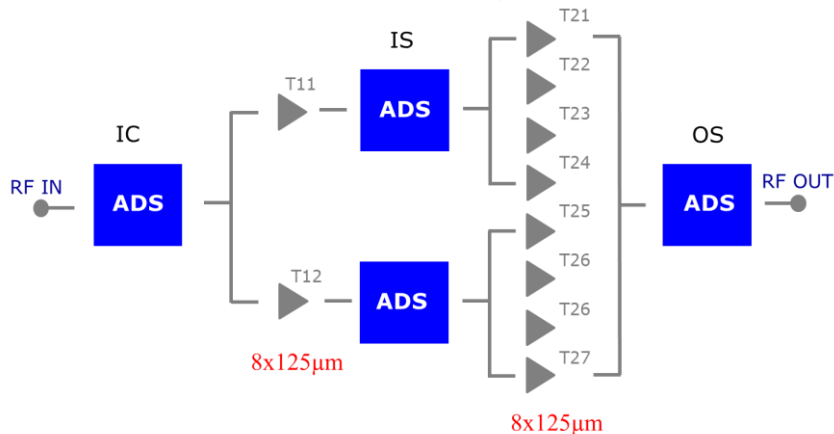


Figure 182 : HPA-2 module. Amplifier topology

The HPA topology is based on two stages of amplification with an arborescent structure. Two stages were required to reach the power gain of 17dB at compression level for 7dB of gain compression.

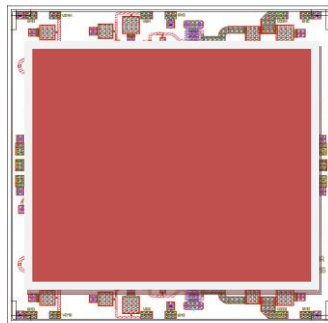


Figure 183 : HPA-2 module. MMIC circuit layout

Spiral inductors are used in matching-networks and for DC bias de-coupling. It is advised for high power amplifier to avoid inductors on output matching combiner and Drain bias voltage due to high current that will flow under small microstrip line width.

- The capacitors are crucial for the realisation of the matching networks and DC-decoupling networks. The capacitors used for this discussed high power amplifier is the MIM capacitor. This capacitor is formed by two metal plates on top of each other with a dielectric in between. The main features regarding passive elements of the GH25-10 technology are as follows:
- 30 W/ TaN thin film resistors
- 1000 W/ TiWSi thin film resistors

- 250 pF/mm² MIM capacitors
- 1.8 μ m evaporated and 7 μ m electroplated gold layers for interconnects and lines
- Air bridges to overcome device topography and realization of integrated inductors
- SiN-protection of the wafer front side
- 100 μ m substrate thickness and via interconnects for source contacting / connection to ground
- Pads

CW Harmonic Balance simulation have been performed with the non-linear transistor model realized by AMCAD for this specific 8x125 μ m GH25 HEMT

At both input and output RF ports of the MMIC, two half-wires bonding have been considered to take into account a gap length of 650 μ m from the MMIC RF PAD to the external 50 Ω line. A variation of $\pm 33\%$ of this equivalent inductance has been included in the statistical analysis. Simulation of the performances of the HPA have been also verified with a dedicated ADS DELF model representative of the RF connexion of the MMIC (input and output) to the hermetic package. At each DC PAD the simplified circuit shown below has been considered to model the connection of the MMIC with the external circuit.

The optimum operating class depends on the application area, this high power amplifier discussed in this work is designed for space application. The requirements are both output power and high power added efficiency at same time. So the class-AB is the best to fulfil this requirements. In our design, both of the transistors (stage 1&2) have been biased at 50mA/mm (deep AB class) to ensure PAE performances. This biasing point also guarantees an accurate non-linear simulation: the transistor model has been developed at this biasing condition.

Regarding loadpull simulations, the following approach has been used:

- Load-pull simulations have been undertaken to evaluate 8x125 μ m GH25 transistor performances. To reach the maximum possible PAE performances, the following simulation procedure has been applied for each transistor at a given biasing point: Input impedance determination to maximize injected input power (close to perfect matching)
- load pull at fundamental frequency to highlight maximum output power and PAE, harmonics 2 and 3 are set to 50 ohms
- Harmonic 2 load-pull optimization to maximize PAE performances, H1 set to optimal impedance previously found and H3 set to 50ohms
- Re-optimization of H1, with H2 fixed to impedance exhibiting the maximum PAE performance, H3 on 50ohms.
- Harmonic 3 is not optimized, no significant influence on PAE due to its very high frequency

Starting from the following biasing conditions:

- $I_{DS0} = 50\text{mA/mm}$
- $V_{DS0} = 28\text{V}$ (leading to 30V (ROR) of drain voltage)

Load-pull analysis have been undertaken at 12.25GHz (centre frequency) following the specific methodology previously detailed and have highlighted the following performances. The results of the load-pull analysis after optimization is given below :

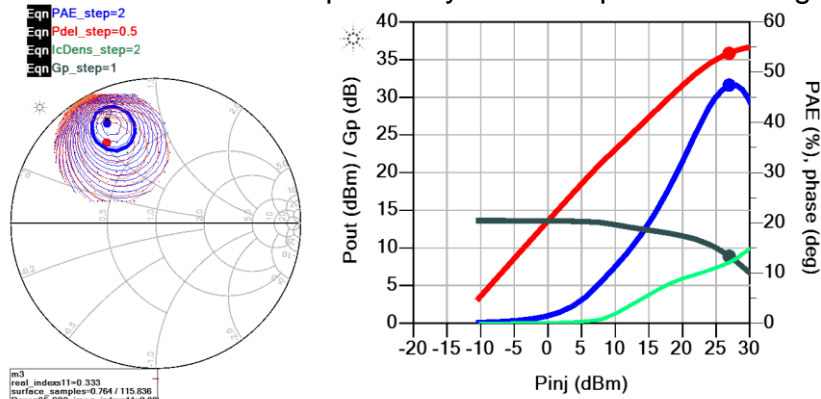


Figure 184 : Final load-pull optimization results

The S-parameter HPA simulation results, at biasing point condition equal to $IDS_0=50\text{mA/mm}$ and $VDS=28\text{V}$, are shown below:

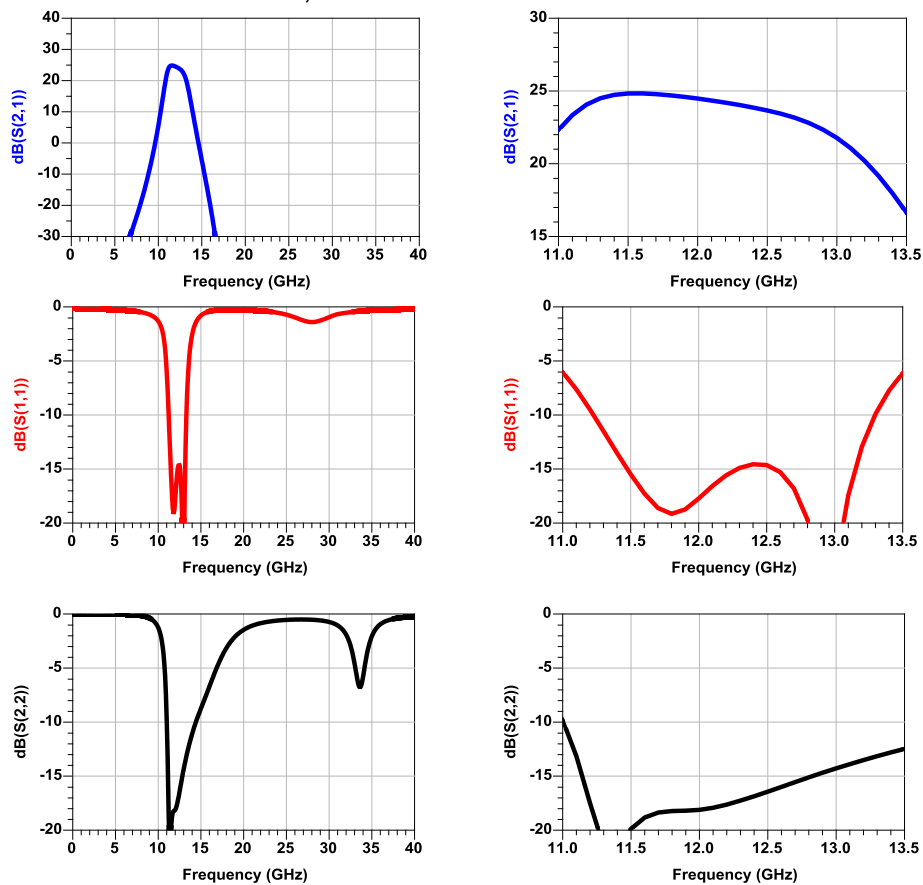


Figure 185 : S-parameters simulation (S21, S11, S22) at room temperature

Non-linear simulations have been performed with the following setup :

- Input power : -10 to 28dBm (with narrow 0.5dB input power step from 23 to 28dBm)
- Frequency bandwidth : 11 GHz to 13.5 GHz step 0.25GHz

Main RF power performances are:

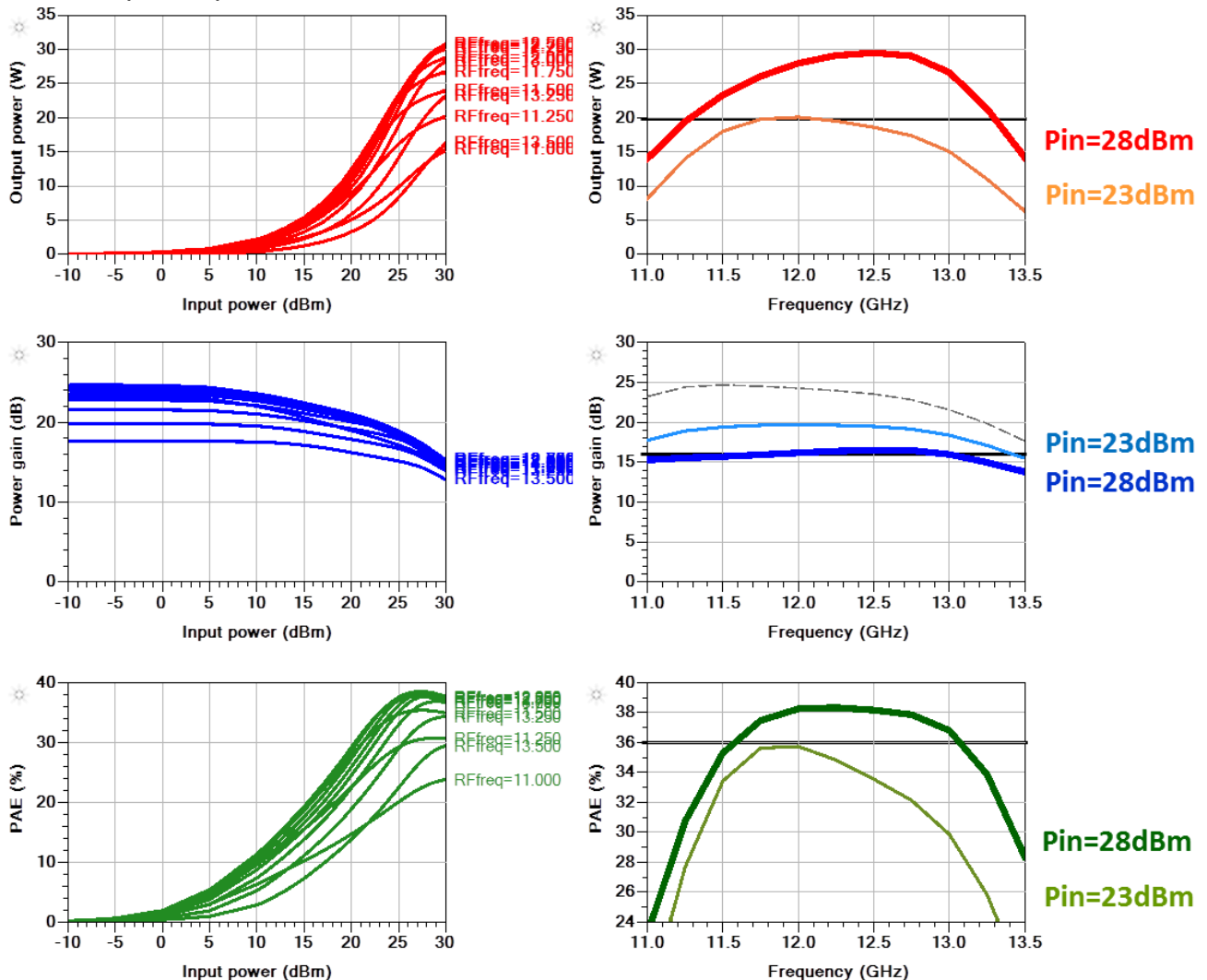


Figure 186 : HPA-2 module. Simulation results. Output power, power gain and PAE performances

The PAE performances don't match the required performances with a peak PAE of 38% at 12.25GHz. Within the frequency bandwidth the minimum power added efficiency is 37%. The output power performances match the required specifications. Maximum output power is 44.62dBm (29W). Regarding the gain performance at compression level, 15dB is reached for the peak PAE which is under the 16dB required in the specifications table.

PAE by transistor for each stage versus input power is given below:

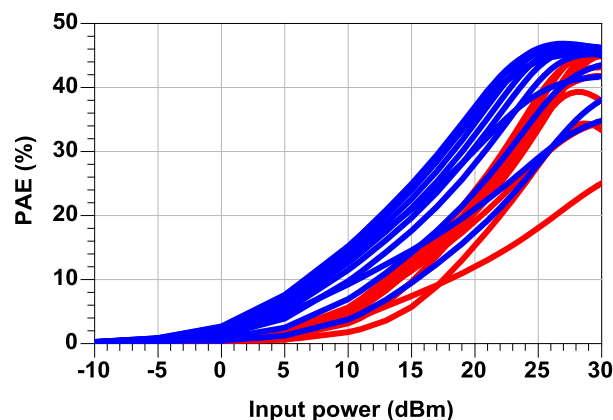


Figure 187 : PAE of stage 1 & 2 versus input power

As expected, the HPA peak PAE corresponds to a maximum peak PAE of stage 2 (46%) close to the maximum PAE found in load pull simulation at 12.25GHz (58%) in the overall frequency bandwidth. The PAE overall HPA power added efficiency remains constant close to 46% in the frame of 11.5 GHz to 13GHz .

The load cycles of the transistors of each stage at biasing point condition equal to $IDS0=50\text{mA/mm}$ and $VDS=28\text{V}$, at $PIN=28\text{ dBm}$ and several frequencies are shown in Figure 18.

The load cycle for all frequencies, all input power are drawn in red . The remarkable load cycle in blue corresponds to the 12.25GHz (center frequency) for the peak PAE at 28dBm. Load-cycles are correlated to the theoretical optimum PAE shape.

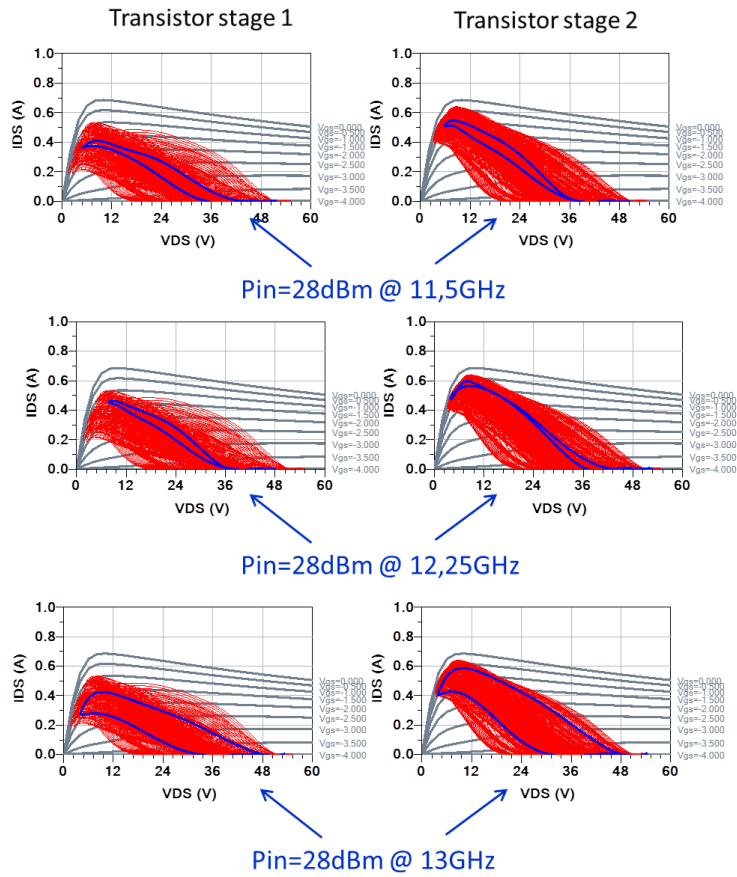


Figure 188 : Transistor load-cycle at 11.5GHz, 12.25GHz and 13GHz (Pin = 28dBm), stage 1 & 2

DC Power Consumption of HPA-2 module is presented below:

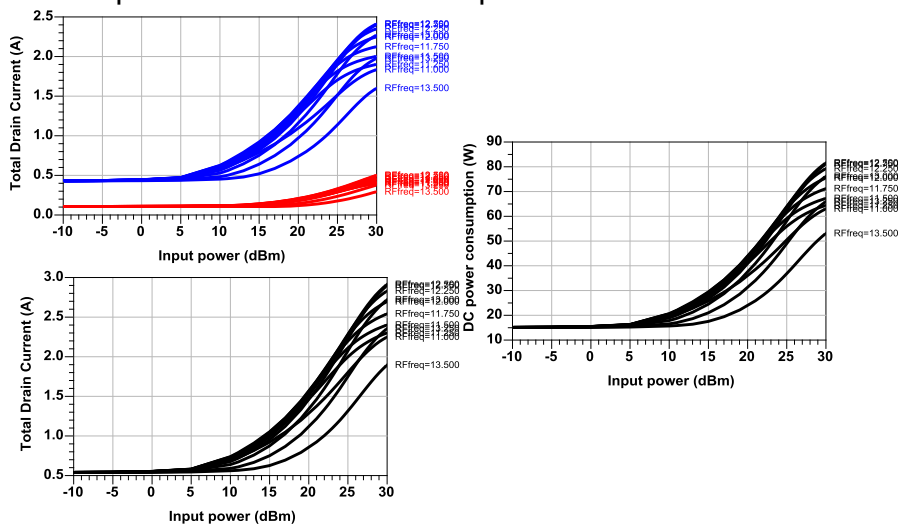


Figure 189 : DC current and power consumption

Stability analysis has been consolidated by STAN software simulations during linear and non-linear operating modes at baseplate temperature equal to -10 °C.

No critical behavior detected in linear simulation with the following biasing conditions:

- Fixed $I_{ds}=50$ mA/mm and sweep of V_{ds} from 0V to 30V (step 5V)
- Fixed $V_{ds}=28$ V and sweep of V_{gs} from -4V to -3V (step 0.1V)

No critical behavior detected in non-linear simulation at biasing condition (equal to 50mA/mm of drain current and $V_{ds}=28$ V) and with a sweep of input power from -10 dBm to 30 dBm. This analysis has been performed in the broadband frequency between 11.5 GHz and 13 GHz.

3.5.2 Detailed Design of version 2: MMIC Doherty HPA module

For this design, elementary building blocks from previous HPA-2 module have been used. Thus, two half HPA-2 modules have been used:

- One half HPA-2 module is used for carrier path
- One half HPA-2 module is used for peaking path

The 2 amplifiers (peaking and carrier) have the same gate length of $4 * 8 * 125\mu\text{m}$ ie 4 mm for last stage. For the input coupler, a Lange coupler which has 90 ° of phase shift over a wide frequency band has been used. For output coupler, solution used is based on the outputs of the following publication « Designing an Octave-Bandwidth doherty amplifier using a novel power combination method N. Sahan and S. Demir Progress In Electromagnetics Research B, Vol. 56, 327-346, 2013 »

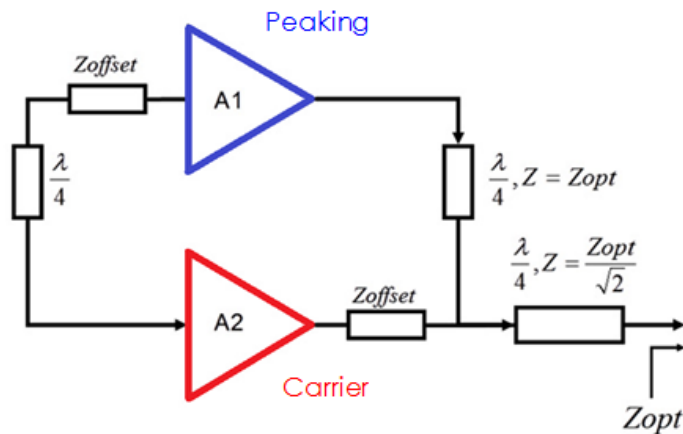


Figure 190 : Doherty MMIC HPA module. Topology

The design methodology has followed the sequence presented below:

1. Use of 2x 10W amplifier cells from HPA-2 module as basic building blocks: the HPA-2 module is divided in two identical and separated parts. Then
 - a. One part has been optimized as “peaking” amplifier
 - b. Second part has been optimized as “carrier” amplifier

2. Use of an ideal 90° coupler input/output and tuning of the VGs _peaking value in order to optimize the operating are of the peaking amplifier vs carrier amplifier)
3. Optimization of the output coupler in order to obtain the bandwidth, the minimum of losses and the required phase shift
4. Optimization in harmonic balance of the input coupler and the inter-stages (of peaking amplifier and carrier amplifier) at Pin=19 dBm (5dB OBO) and Pin=29 dBm (0dB OBO)



Figure 191 : Doherty MMIC HPA module. MMIC circuit layout

Carrier and peaking transistor loadpull simulations are presented in the two following figures:

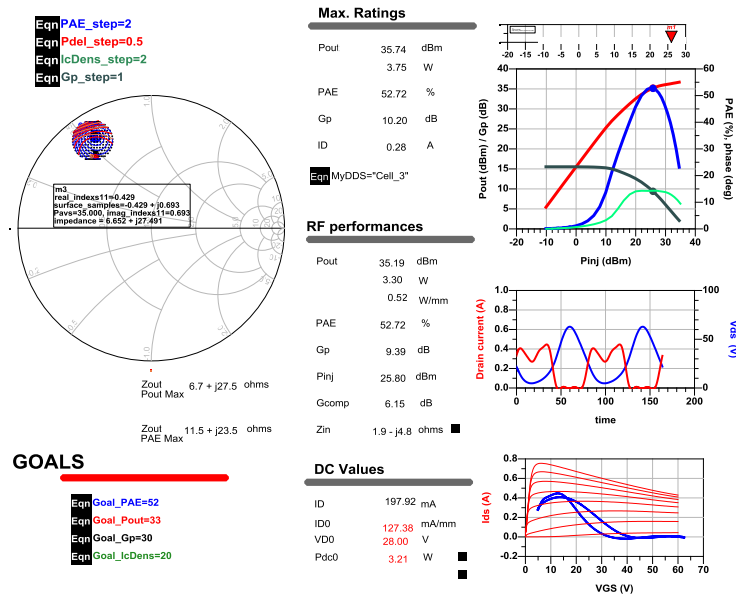


Figure 192 : Load pull 8x125um @12.2GHz @130mA/mm as Carrier transistor

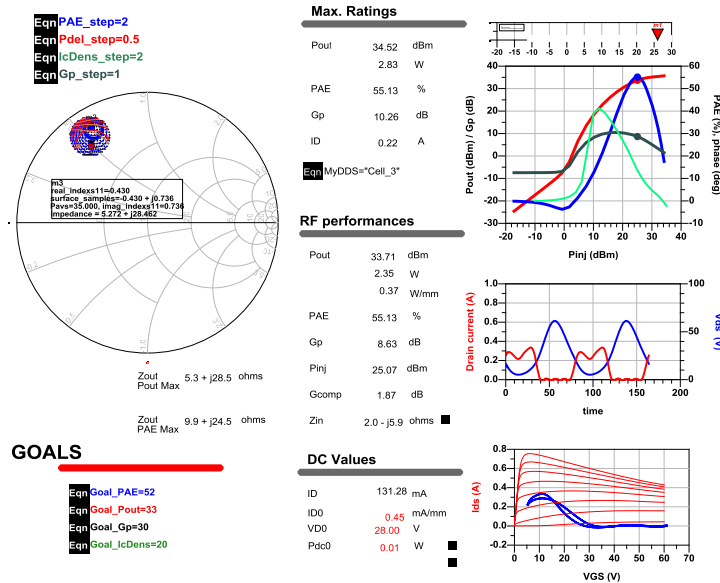


Figure 193 : Load pull @12.2GHz @0mA/mm as peaking transistor

Vg1 of peaking amplifier is optimised to have $K > 1$, it has very low impact on PAE at low signal. The behaviour of the gain is improved as the RF power rise a sufficient value to polarized the peaking amplifier. Due to the large bandwidth of the output coupler and for some cases with low power and $RFfreq = [11.5GHz-13GHz]$, it is observed that some energy produced by the carrier amplifier is absorbed by the peaking amplifier. This behaviour disappears during the increasing of gain of the peaking amplifier.

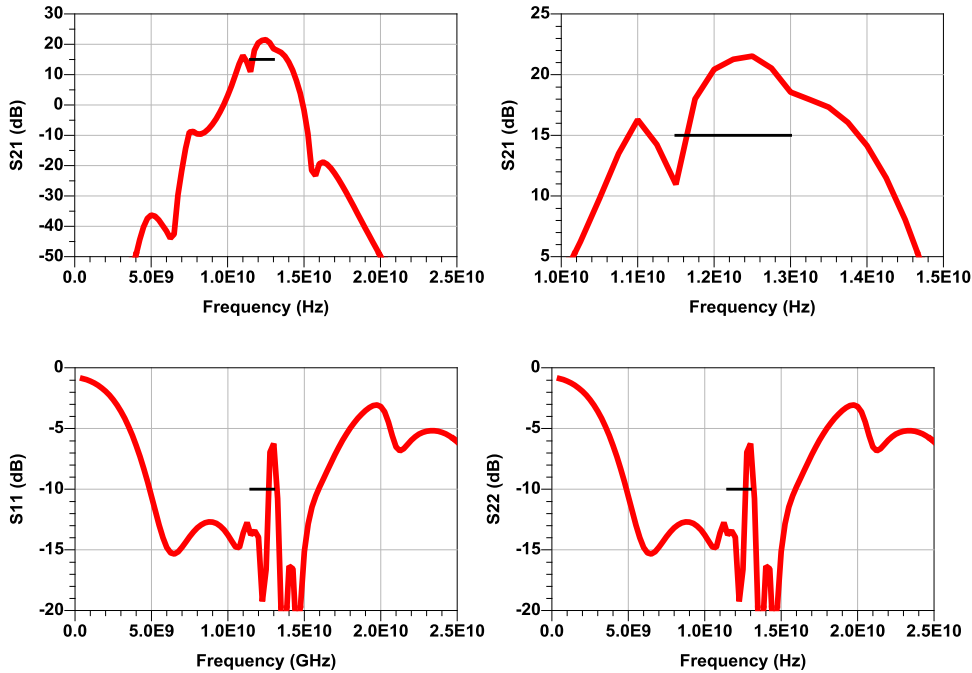


Figure 194 : S Parameters simulation of MMIC Doherty HPA module

Comparison between Doherty and a classical 20W HPA regarding PAE parameter is provide below:

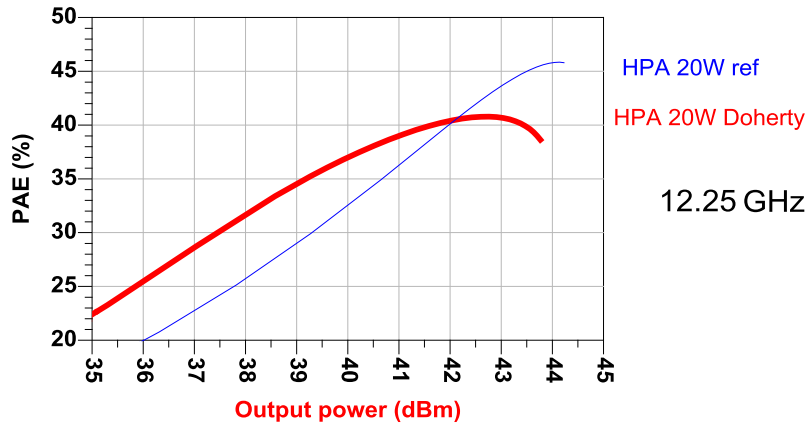


Figure 195 : Comparison between Doherty and a classical 20W HPA regarding PAE parameter

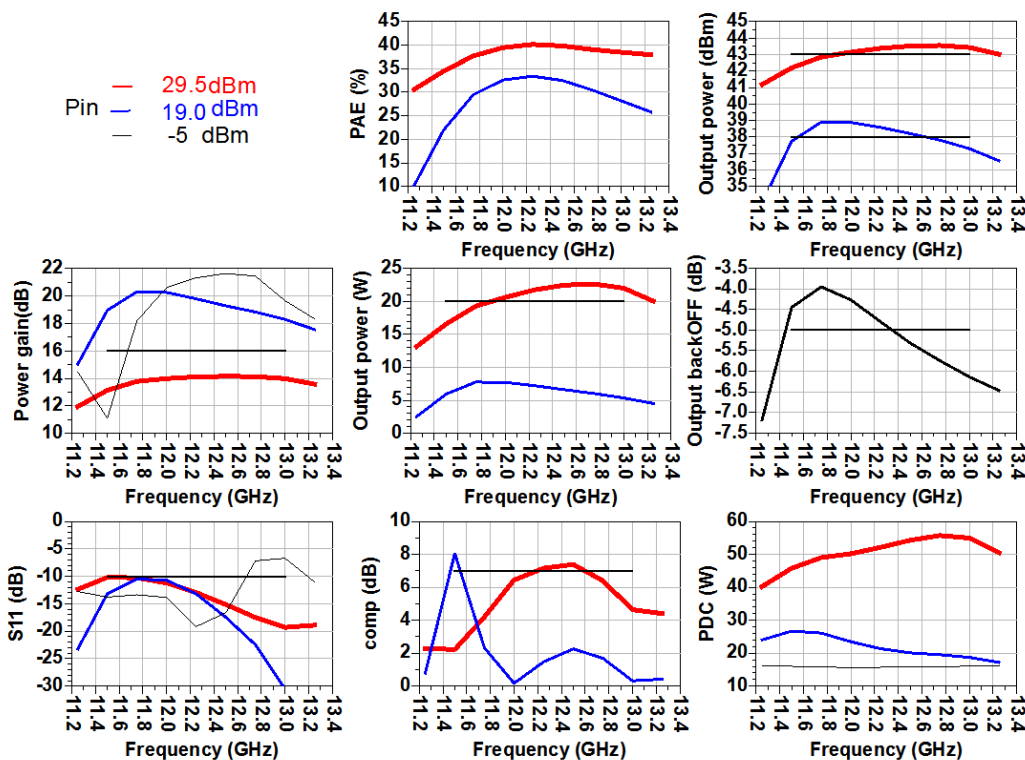


Figure 196 : MMIC Doherty HPA module. Performance over frequency for two different input power

Hereafter are presented the impedances presented at the transistor of both amplifier (carrier and peaking) in function of input power and for each frequency. In low signal, the impedance is outside the smith chart for the peaking amplifier (it means it is off, there no amplification). Moreover, the impedance on the carrier amplifier is also a function of the input power

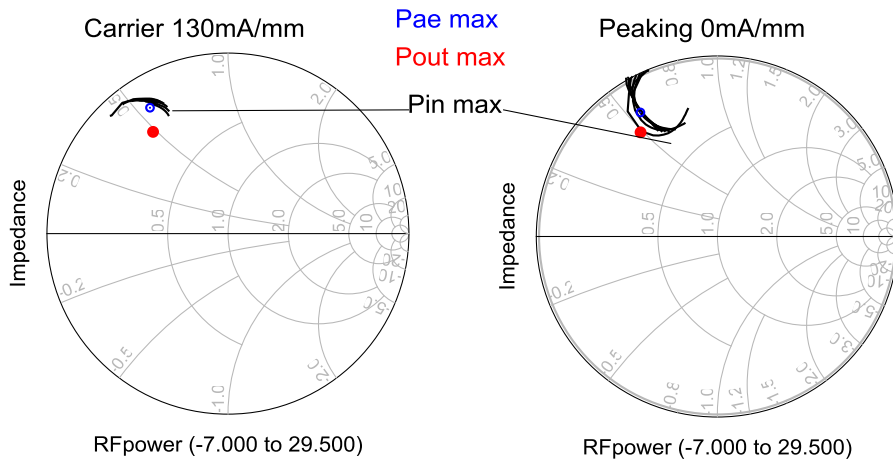


Figure 197 : 2nd stage Transistor Load Pin -7 to 29.5dBm Freq 11.5 to 13 GHz

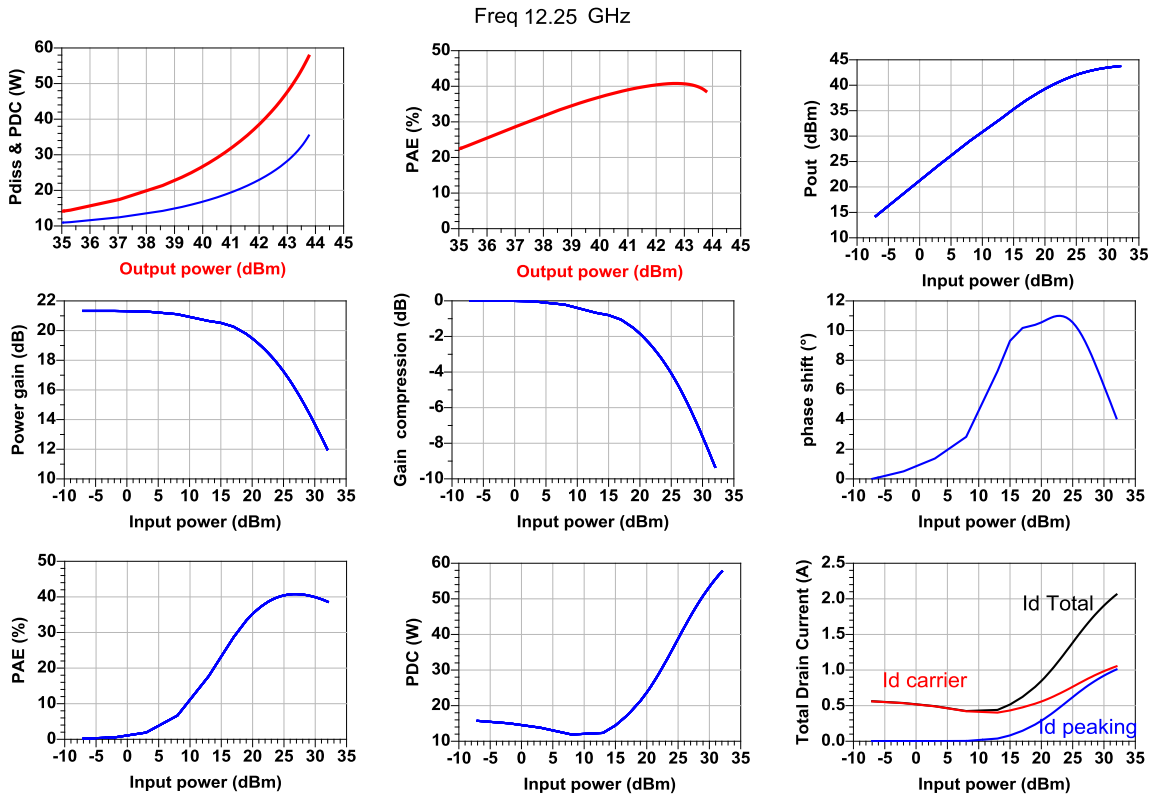


Figure 198 : MMIC Doherty HPA module. NL simulation versus Pin at 12.25 GHz

By tuning the vg peaking value a trade-off between maximum output power and PAE in back-off can be obtained:

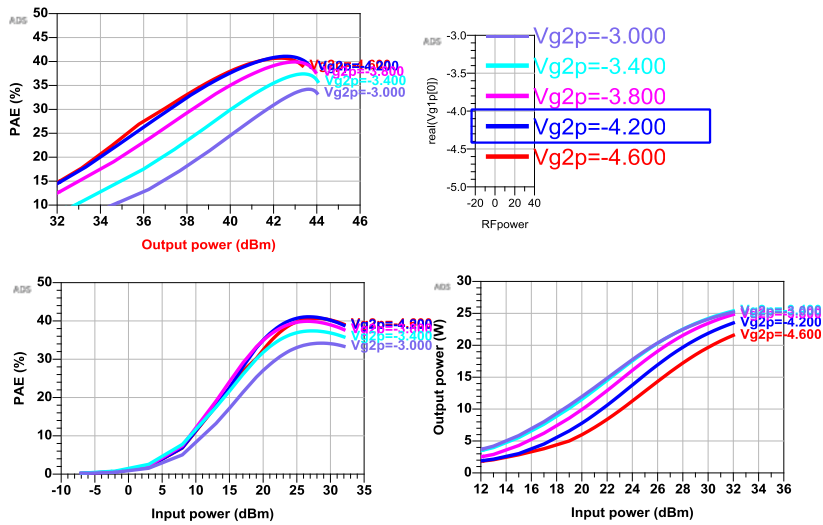


Figure 199 : MMIC Doherty HPA module. Performance versus VG peaking

Stability analysis is consolidated by STAN software simulations during linear and non-linear operating modes at baseplate temperature equal to -20 °C.

No critical behaviour detected in linear simulation with the following biasing conditions:
Probe on Drain and Gate of peaking and carrier amplifier

- Fixed Vgs = -2.95V on Carrier and -4.2V on peaking
- Sweep of Vds from 0V to 30V (1 to 10V step 1V 10 to 30V step 5V)
- Sweep frequency 0.1 to 20GHz

3.5.3 Detailed Design of version 3: MMIC-Hybrid Doherty HPA module

For this third version, a dedicated MMIC test pattern is used. Starting from MMIC Doherty HPA version (version 2), the input and output combiners have been suppressed from MMIC. Thus, this dedicated MMIC test cell is including to separated amplifiers (1x carrier amplifier and 1x peaking amplifier)

To build the MMC-Hybrid Doherty HPA module:

- 1x MMIC test cells is used
- The input combiner (Lange coupler) is processed and alumina circuit
- The output combiner is processed and alumina circuit

Tuning possibilities will be performed on alumina circuit.

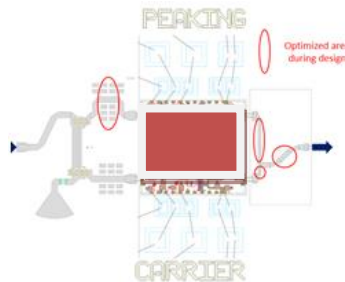


Figure 200 : MMIC-Hybrid Doherty HPA module. Configuration using two MMIC test cells.

The design methodology has followed the methodology presented below:

1. Load pull simulation on carrier and peaking amplifier. Simulations have been performed for different frequencies in the targeted bandwidth.
2. Design (through EM Simulation) of a an input 90° divider: a Lange coupler topology has been selected and designed.
3. Optimization in harmonic balance of the input offset and of the output coupler offset at Pin=19 dBm (5dB OBO) and Pin=29 dBm (0dB OBO)
4. Global NL simulation of the hybrid Doherty Ku-band amplifier and cross-check that the hybrid output combiner presents the optimum loads to the carrier amplifier and to the peaking amplifier (vs OBO)

The carrier amplifier loadpull simulation is presented in the following figure. We can observe that optimum load to present to the carrier amplifier at nominal operating point (Pae_max) is close to 50ohms: 57-13.1*j ohms.

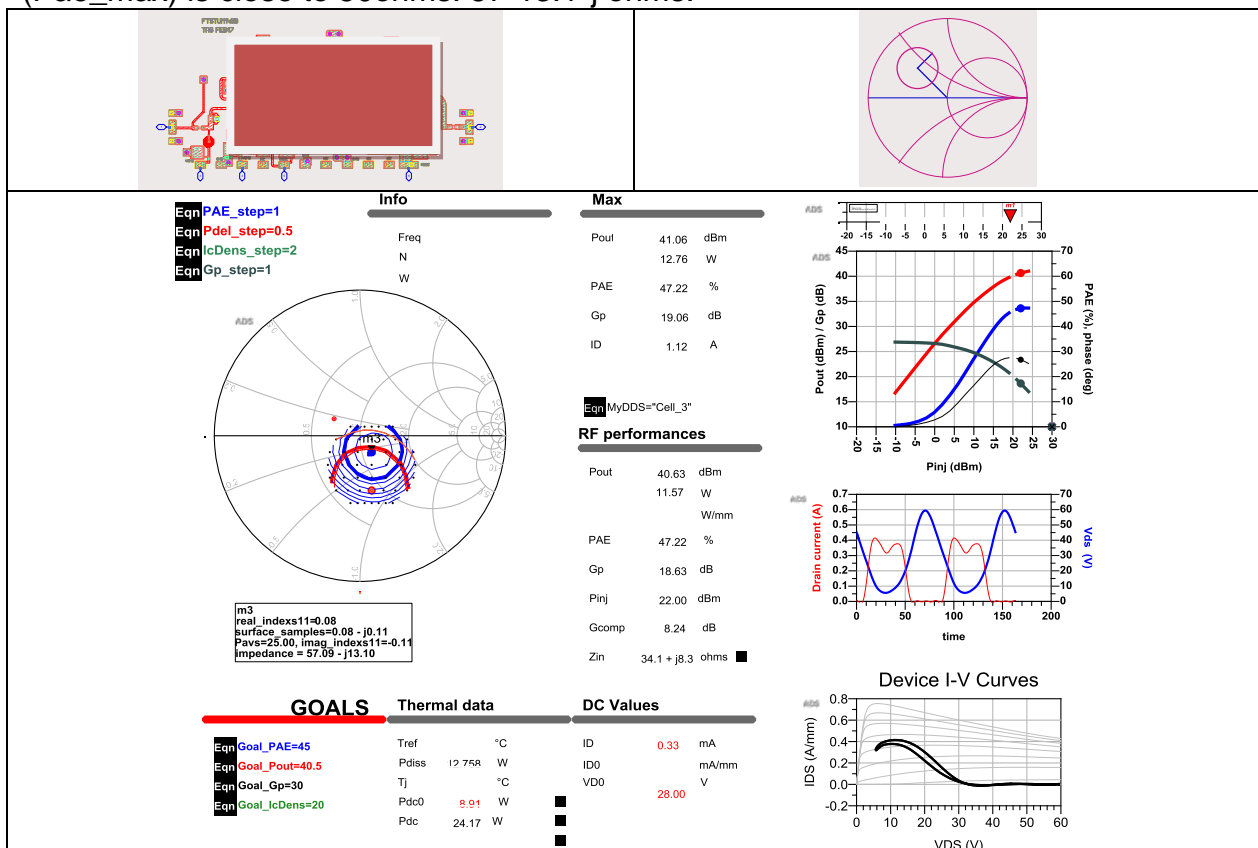


Figure 201 : Load pull simulation and carrier amplifier

The peaking amplifier loadpull simulation is presented in the following figure. We can observe that optimum load to present to the peaking amplifier at Pae_max is equal to 16.6+7.9*j ohms.

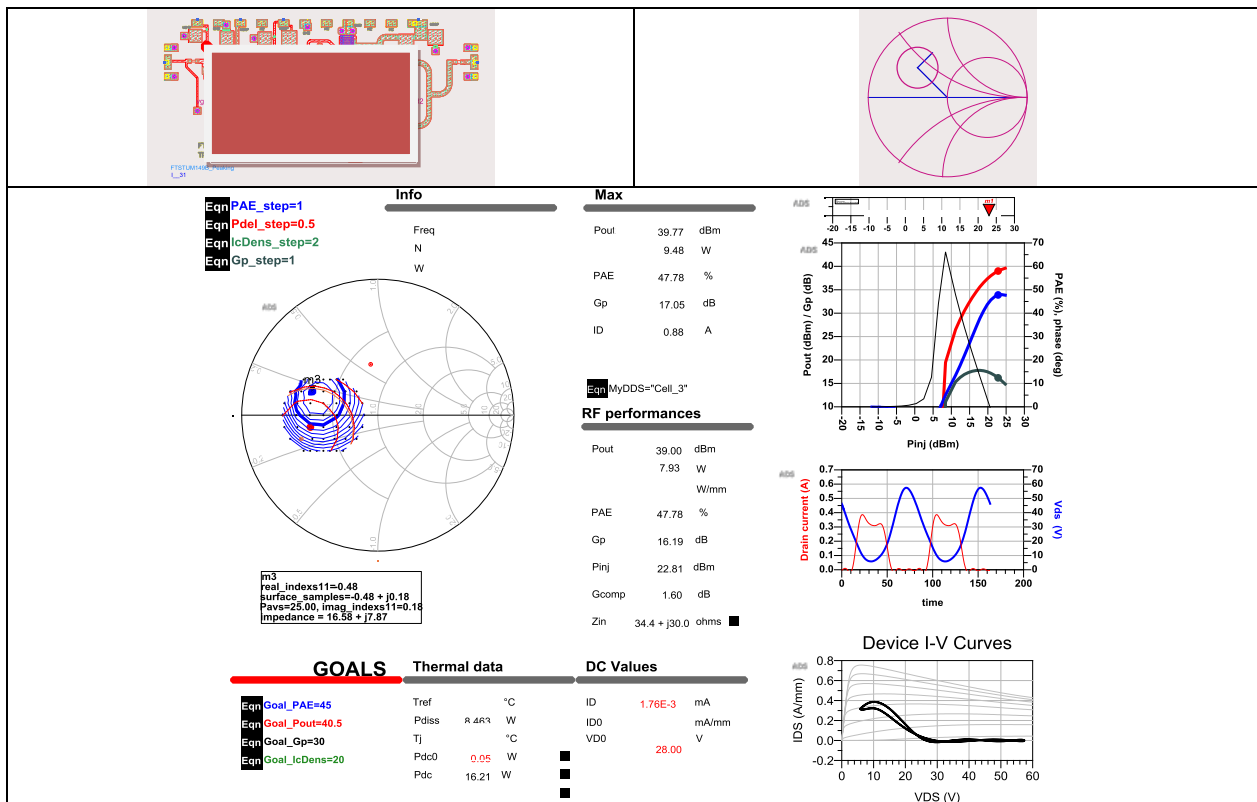


Figure 202 : Load pull simulation and peaking amplifier

Vg1 of peaking amplifier has been optimized in order to have $K > 1$: it has very low impact on PAE at low signal. The behavior of the gain is improved as the RF power rise a sufficient value to polarized the peaking amplifier. Due to the large bandwidth of the output coupler and for some cases (low power and some frequency points into [11.5GHz-13GHz]), it is observed that some level of RF energy produced by the carrier amplifier is absorbed by the peaking amplifier. This behavior disappears during the increasing of gain of the peaking amplifier.

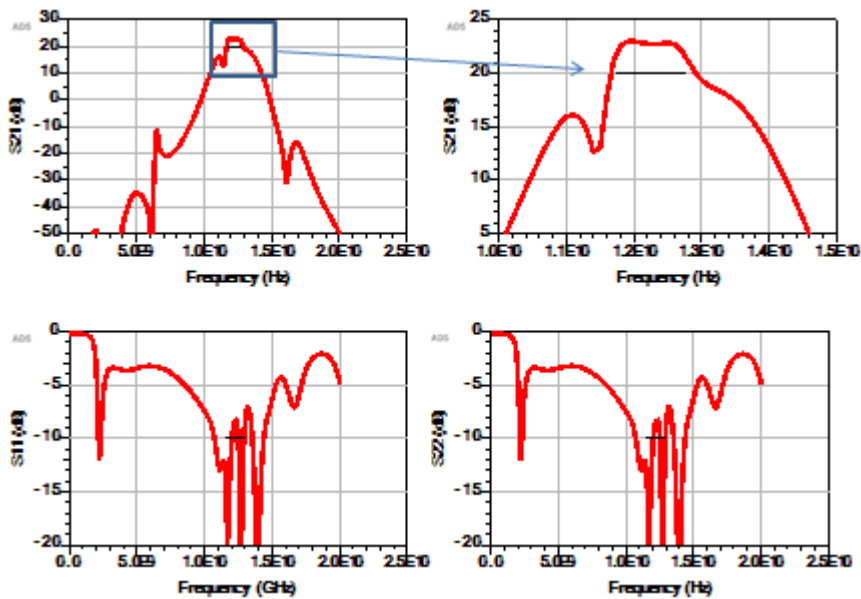


Figure 203 : S Parameters simulation of MMIC-Hybrid Doherty HPA

Comparison between MMIC Doherty / MMIC-Hybrid Doherty and a classical 20W HPA regarding PAE parameter is provide below:

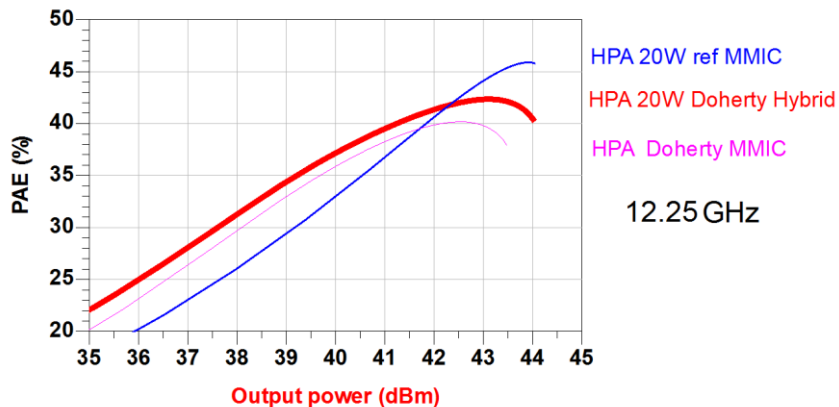


Figure 204 : Comparison between Doherty and a classical 20W HPA regarding PAE parameter

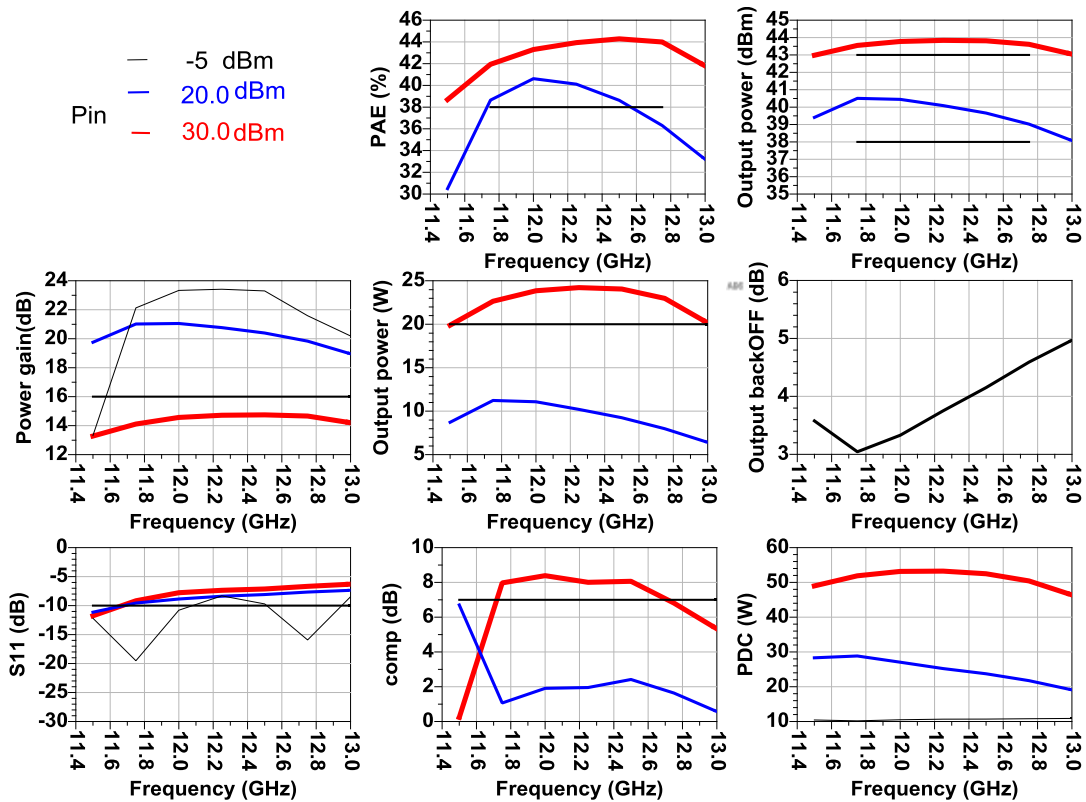


Figure 205 : MMIC-Hybrid Doherty HPA module. Performance over frequency for different input power

Hereafter are presented the impedances presented at the 2nd stage transistors of both amplifier in function of input power and for each frequency. In low signal, the impedance is outside the smith chart for the peaking amplifier (it means it is off, there no gain amplification). Moreover, the impedance on the carrier amplifier is also a function of the input power

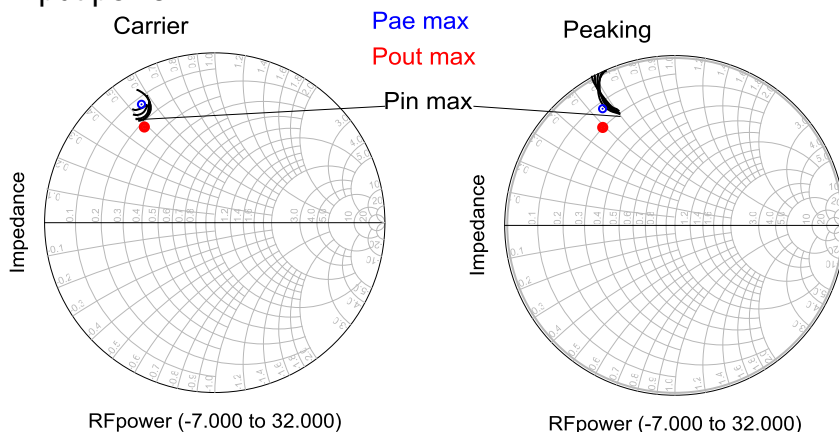


Figure 206 : MMIC-Hybrid Doherty HPA module. 2nd stage Transistor output load for Pin=[-7 to 30dBm]. Freq=[11.5 to 13 GHz]

Hereafter are presented the impedances presented at the both amplifier in function of input power and for one frequency. In low signal, the impedance is outside the smith chart for the peaking amplifier (it means it is off, there no amplification).

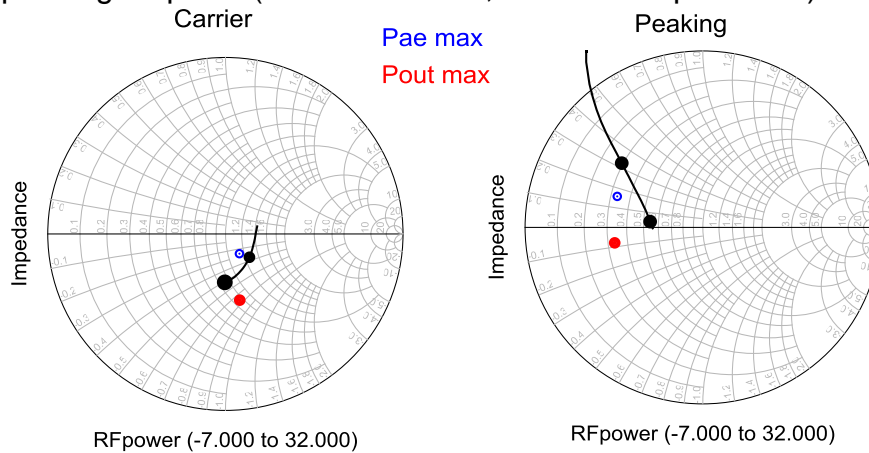


Figure 207 : MMIC-Hybrid Doherty HPA module. Amplifier (Carrier & Peaking) loads for Pin=[-7 to 30dBm]. Freq 12.25 GHz

Three types of Ku-Band HPA module using UMS GH25 technology have been designed. Objective of the manufacturing and tests is to identify solution to achieve best trade-off for Pout/PAE/NPR/bandwidth performance.

3.6 0,25 μ m MMIC and transistors Manufacturing and on-wafer Test

A complete GH25 wafer (Run "Wind") including the different MMICs designed and presented in the previous chapter has been manufactured by UMS at Ulm facilities. On-wafer tests have been conducted by UMS at Villebon facilities:

- Process monitoring
- On-wafer DC&RF tests of the transistor cells and the different MMIC

3.6.1 PCM Results

PCMs results are presented in the table below. These PCM results demonstrate very low spread on the WIND wafer on both active and passive devices.

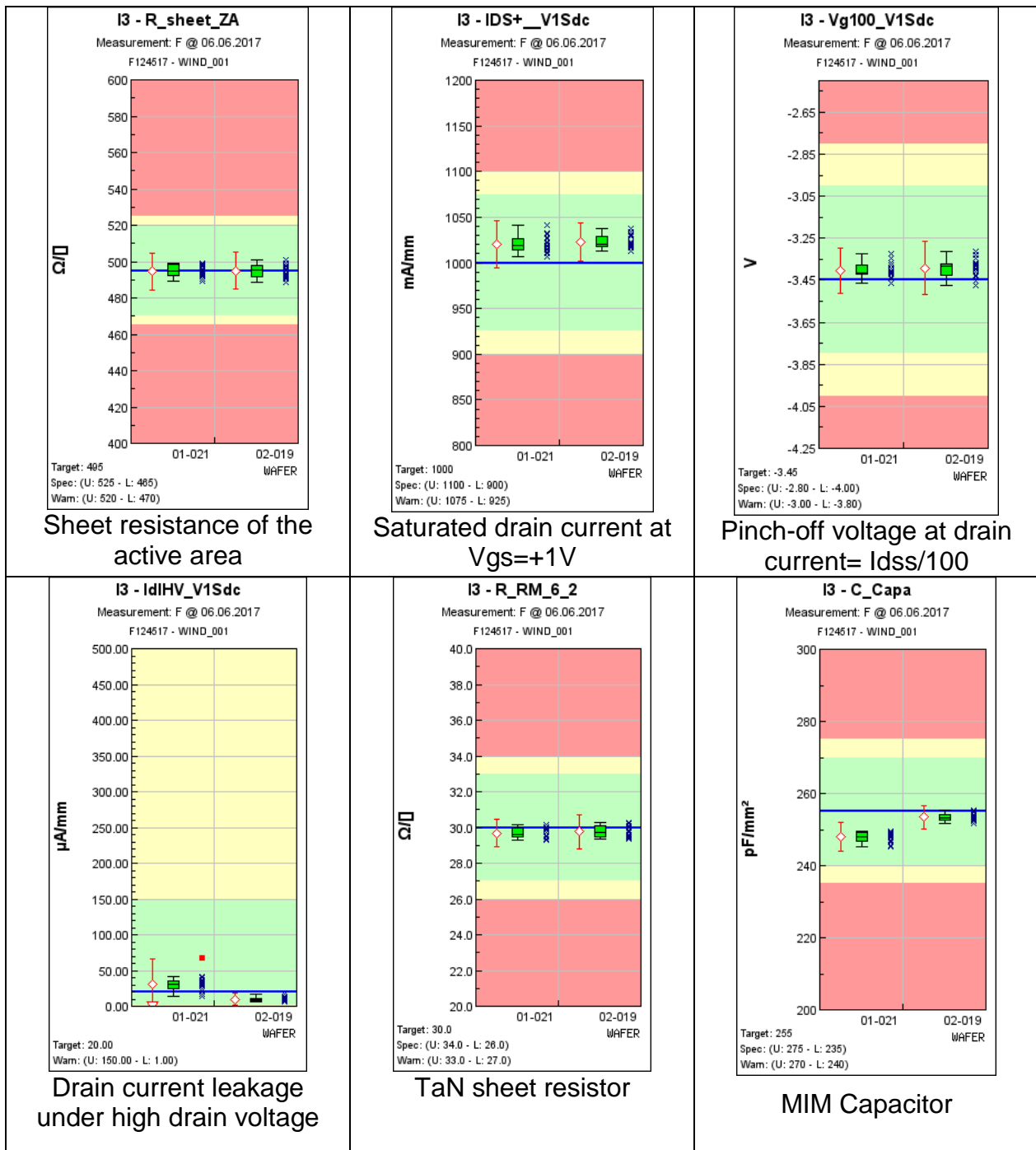


Figure 208 : PCM results of GH25 wafer

3.6.2 HPA-2 MMIC On wafer-measurements

The test conditions are reminder below:

<p>Pulsed S-Parameters measurement:</p> <ul style="list-style-type: none"> • Vd 28V Pulsed Vg 25µs / 10%, Idq=50mA/mm • From 0.5 to 20 GHz (step 0.1 GHz) 	<p>Power pulsed measurement:</p> <ul style="list-style-type: none"> • Vd 28V Pulsed Vg 25µs / 10%, Idq=50mA/mm • Freq=[11.5-13GHz] step 0.25 GHz. • Pin 0 to 30 dBm (0 , 10 ,20 to 30 step 1dB) • Record : Pin, Pout, Ig, Id
--	---

Table 32 : HPA-2 MMIC On wafer-measurements. Test conditions

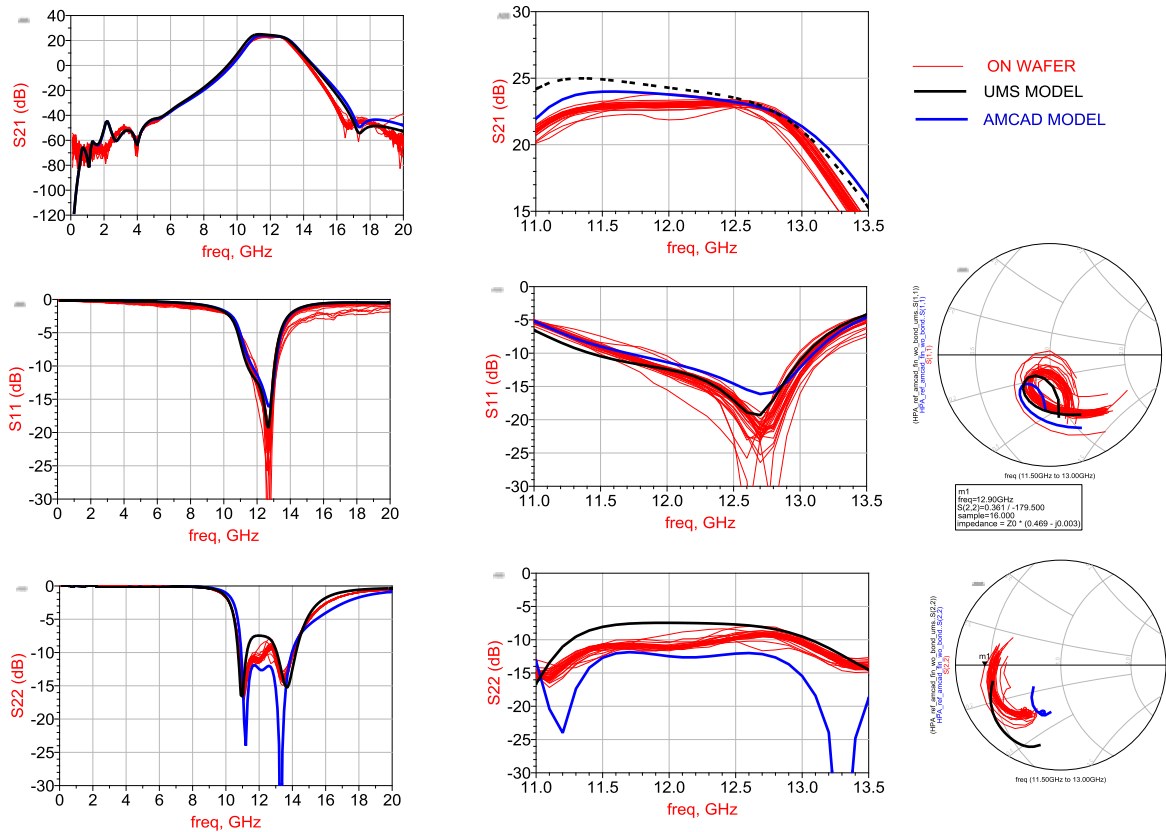


Figure 209 : HPA-2 MMIC On wafer-measurement. [S] Parameter measurements and simulation

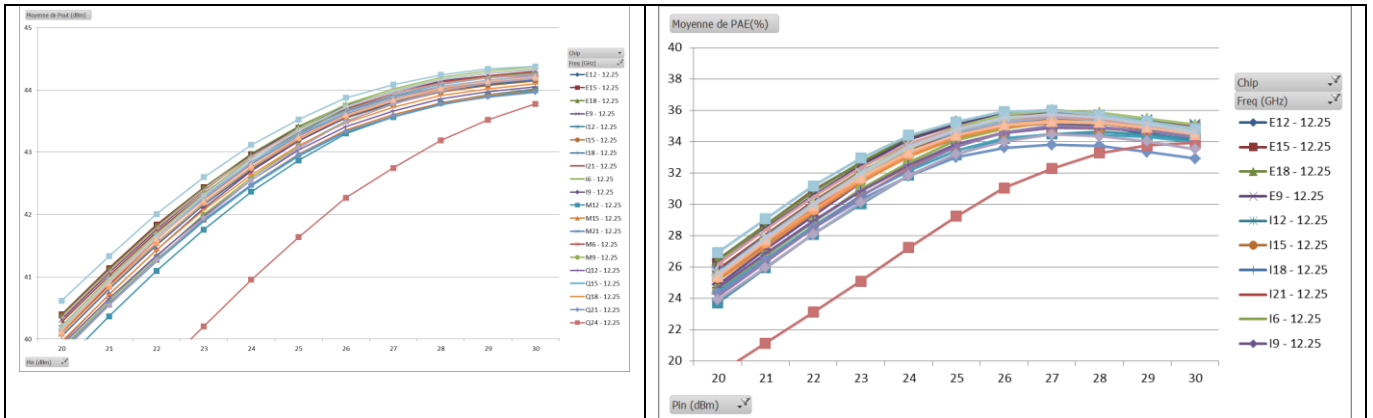


Figure 210 : HPA-2 MMIC On wafer-measurement. Power measurements. Pout and PAE vs Pin at 12,25 GHz

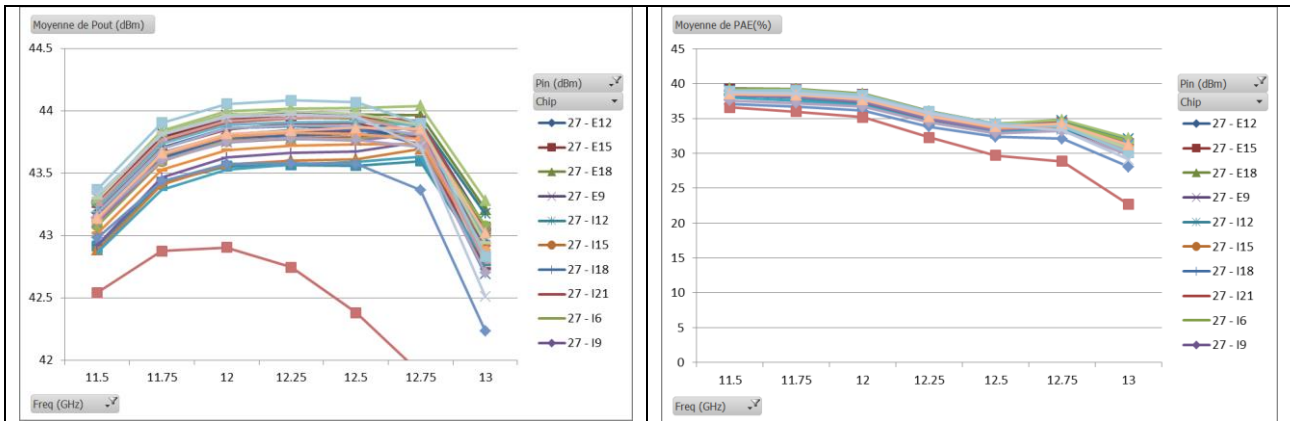


Figure 211: HPA-2 MMIC On wafer-measurement. Power measurements. Pout and PAE vs freq at Pin=27 dBm

3.6.3 Doherty HPA MMIC On wafer-measurements

The test conditions are reminder below:

Pulsed S-Parameters measurement:

- Vd 28V Pulsed Vg 25µs / 10%, Idq=50mA/mm
- From 0.5 to 20 GHz (step 0.1 GHz)

Power pulsed measurement:

- Vd 28V Pulsed Vg 25µs / 10%, Idq=50mA/mm
- Freq=[11.5-13GHz] step 0.25 GHz.
- Pin 0 to 30 dBm (0 , 10 ,20 to 30 step 1dB)
- Record : Pin, Pout, Ig, Id

Table 33 : Doherty HPA MMIC On wafer-measurements. Test conditions

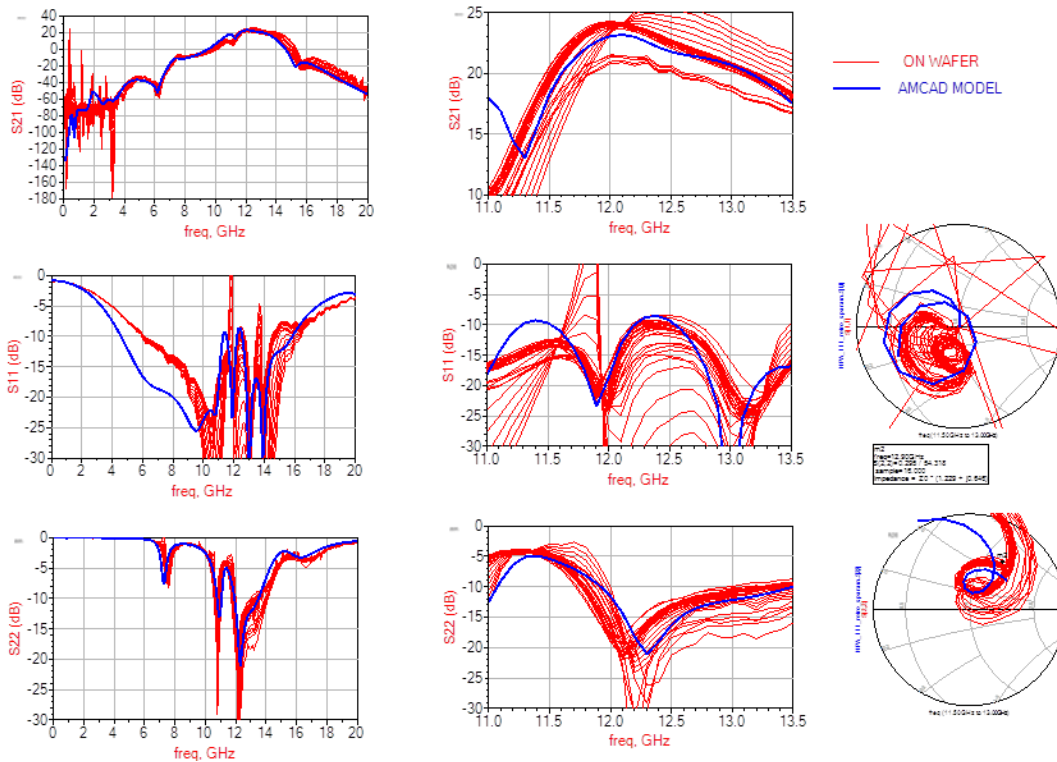


Figure 212 : Doherty HPA MMIC On wafer-measurement. [S] Parameter measurements and simulation

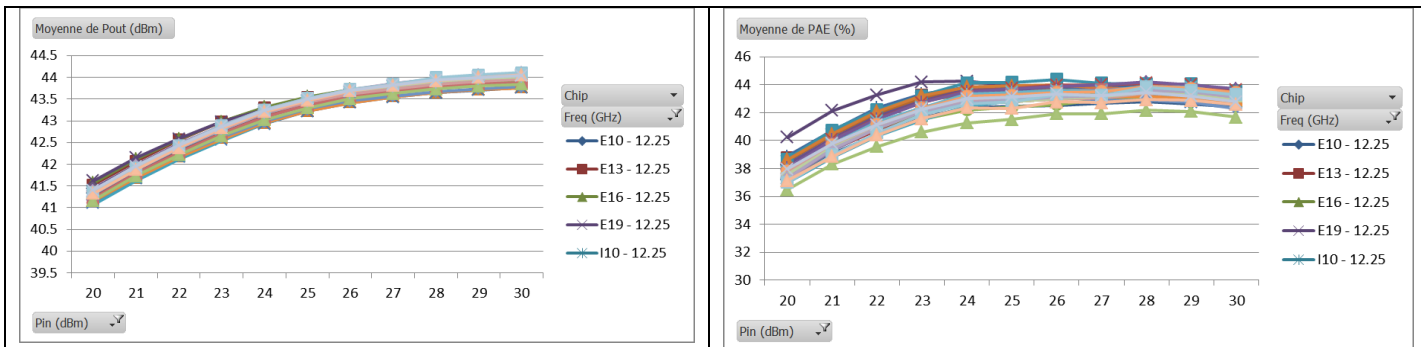
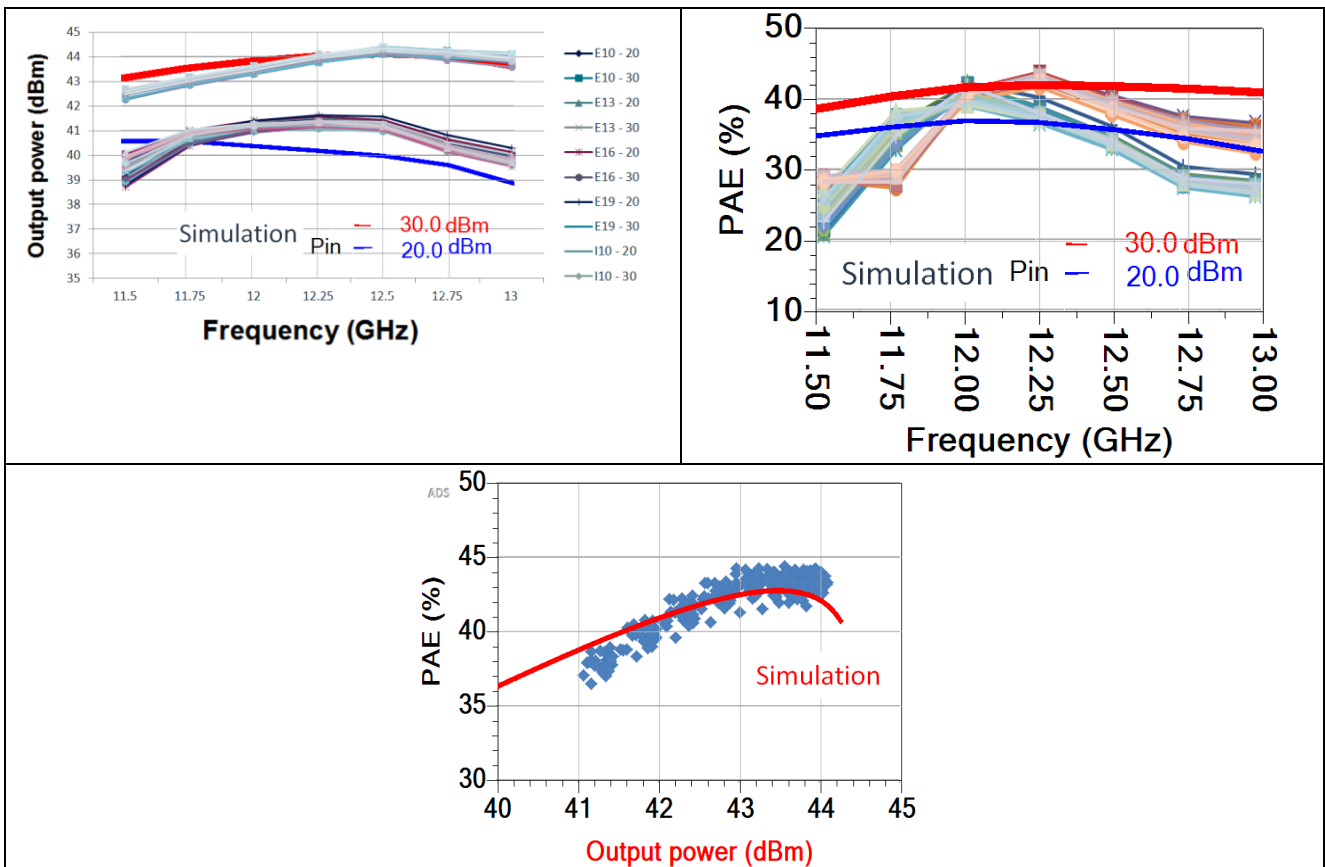


Figure 213 : Doherty HPA MMIC On wafer-measurement. Power measurements. Pout and PAE vs Pin at 12,25 GHz

Some comparison simulations vs measurements are provided in the following figures:



**Figure 214 : Doherty HPA MMIC On wafer-measurement. Pout & PAE vs freq
Measurements and simulation at Pin=20&30 dBm**

3.7 HPA-2 Module and Doherty HPA Module Test

The manufacturing and testing activities conducted are:

- HPA-2 modules:
 - 4x samples have been mounted in jig test fixture
 - [S] parameter measurements vs temperature
 - CW-mode multi-carrier mode measurements vs temperature
 - RF step measurements at room temperature
- MMIC Doherty HPA modules:
 - 3x samples have been mounted in jig test fixture
 - [S] parameter measurements vs temperature
 - CW-mode multi-carrier mode measurements vs temperature
- MMIC-Hybrid Doherty HPA modules:
 - 2x samples have been mounted in jig test fixture
 - [S] parameter measurements vs temperature
 - CW-mode mode measurements at room temperature

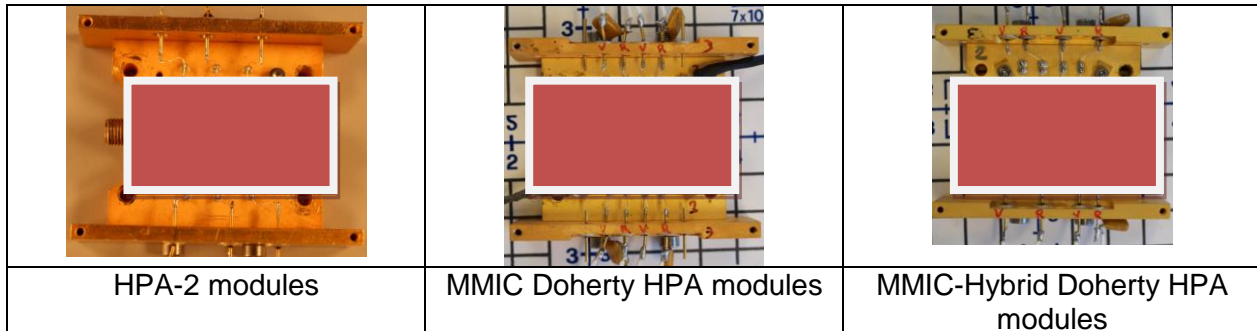


Figure 215 : Photography of HPA-2 modules and Doherty HPA modules

3.7.1 HPA-2 Modules test results

3x GH25 HPA-2 modules have been tested: in the frame of this study, tuning of the HPA modules has been performed at **Temp=25°C** with CW signal in order to achieve maximum of PAE. Then [S] parameter measurements and power measurements with multi-carrier signal has been conducted.

The results are presented with the following outline

- [S] parameters measurements versus Temp=[-10°C, 25°C, 85°C]
- Power measurements (CW signal) versus Pin. Temp=[-10°C, 25°C, 85°C]. Vds=40V RF=[11.5 to 13GHz] with RF step=500MHz
- Power measurements (multi-carrier signal) versus Pin. Temp=[-10°C, 25°C, 85°C]. Vds=30V, Ids=450mA at centre frequency = 12 GHz
- RF step stress measurements

3.7.1.1 [S] Parameter measurements.

Hereafter, the HPA-2 #1 module S-parameters are given over a DC to 20GHz bandwidth with drain voltage of 30V and Ids=450mA (45mA/mm) fixed at Temp=25°C. Measurements are performed versus Temp=[-10°C, 25°C, 85°C]

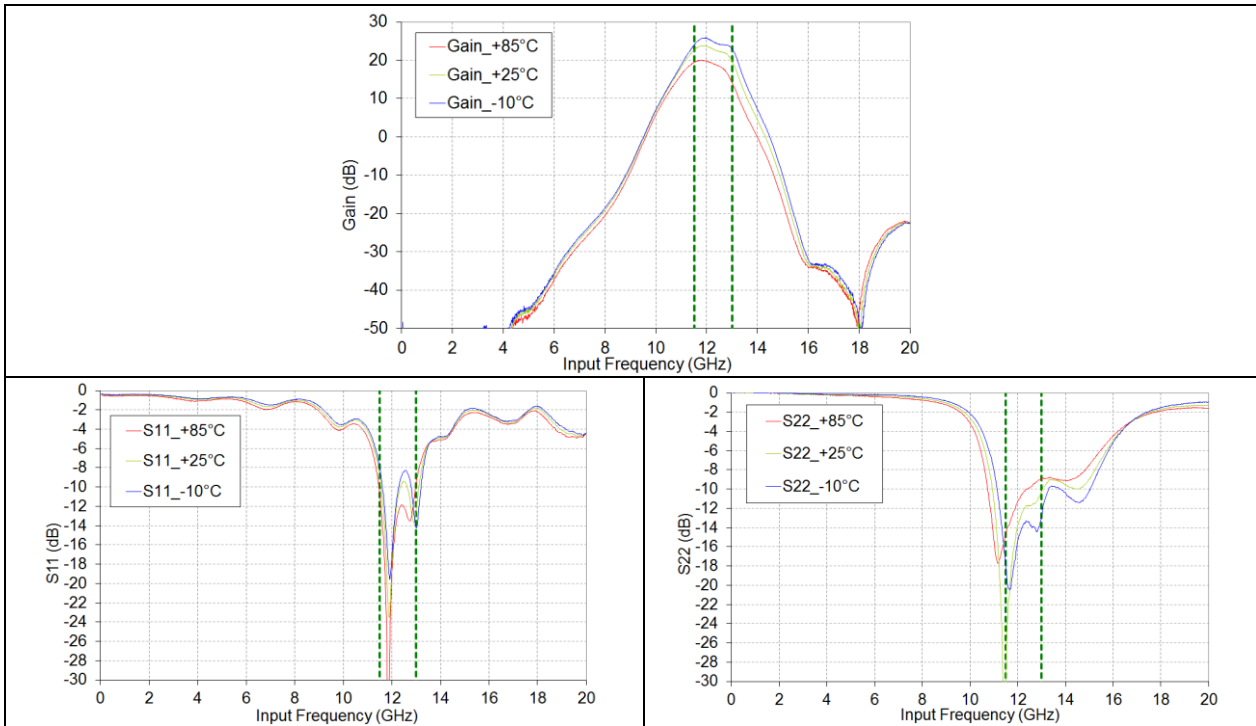
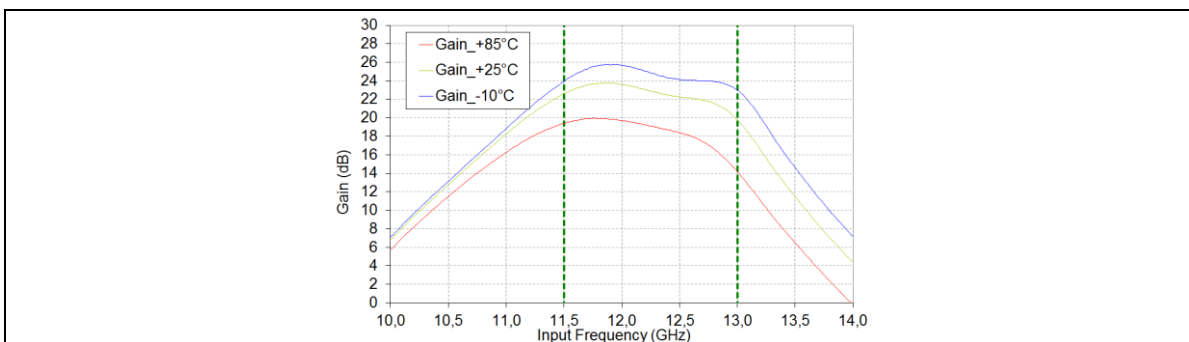


Figure 216 : HPA-2 #1 module. [S] parameters measurements. RF=[DC-20GHz], Vd=30V, Fixed drain current Ids=450mA @25°C, Temp=[-10°C, 25°C, 85°C]

On the following figures, we focus on the HPA-2 #1 module in-band frequency behavior. **Erreur ! Source du renvoi introuvable.** shows that S11 and S22 parameters varies not in the same way:

- Input return loss is optimum at hot temperature
- Output return loss is optimum at room temperature.

S21 variation is about 6dB between -10°C to 85°C at 12 GHz. At constant gate voltage current, the gain variation versus temperature is 0,31dB/°C



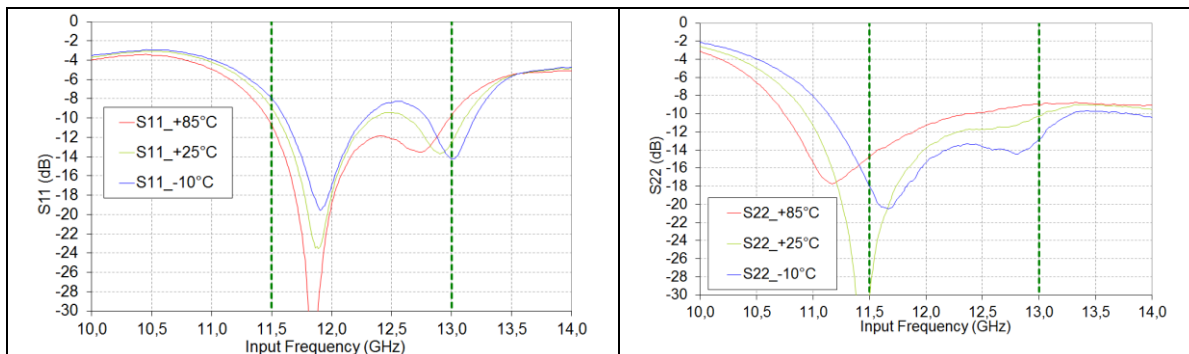


Figure 217 : HPA-2 #1 module. [S] parameters measurements. RF=[10-14GHz], Vd=30V, Fixed drain current Ids=450mA @25°C, Temp=[-10°C, 25°C, 85°C]

Hereafter, for three HPA modules, the S-parameters are given over a DC to 20 GHz bandwidth with drain voltage of 30V and Ids=450mA (25mA/mm) fixed at Temp=25°C. Measurements are performed versus Temp=[-10°C, 25°C, 85°C]

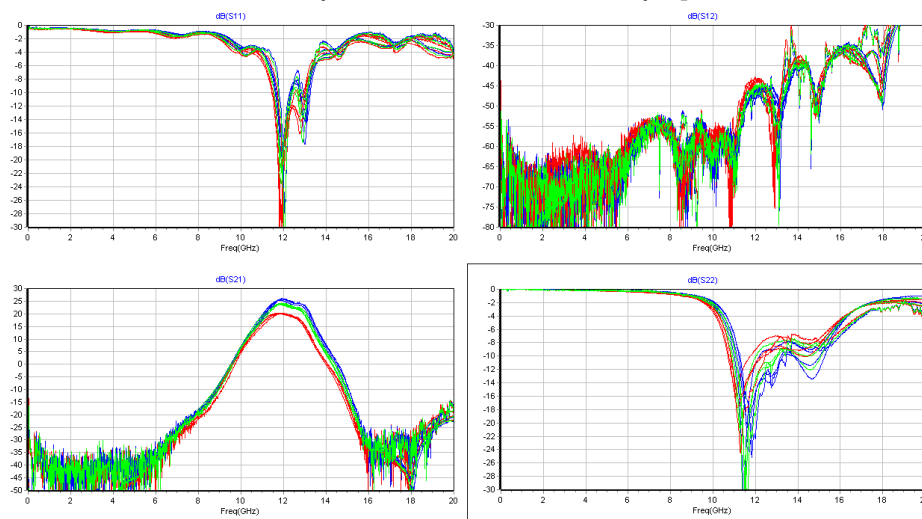


Figure 218 : HPA-2 #1 HPA-2 #2 HPA-2 #3 HPA-2 #4 modules. [S] parameters measurements. RF=[DC-20 GHz], Vd=30 V. Fixed drain current Ids=450mA @25°C. Temp=[-10°C, 25°C, 85°C]

On following figures, we focus on the HPA modules in-band frequency behavior. **Erreur ! Source du renvoi introuvable.** shows the dispersion on S11, S22 and S21 parameters versus HPA modules. Measurements are performed versus Temp=[-10°C, 25°C, 85°C]

- Regarding S21 parameter, at 12 GHz, a maximum dispersion of 1dB is observed between the three HPA modules
- Regarding S11 parameter, at 12 GHz, a maximum dispersion of 2dB is observed between the three HPA modules
- Regarding S22 parameter, at 12 GHz, a maximum dispersion of 2dB is observed between the three HPA modules

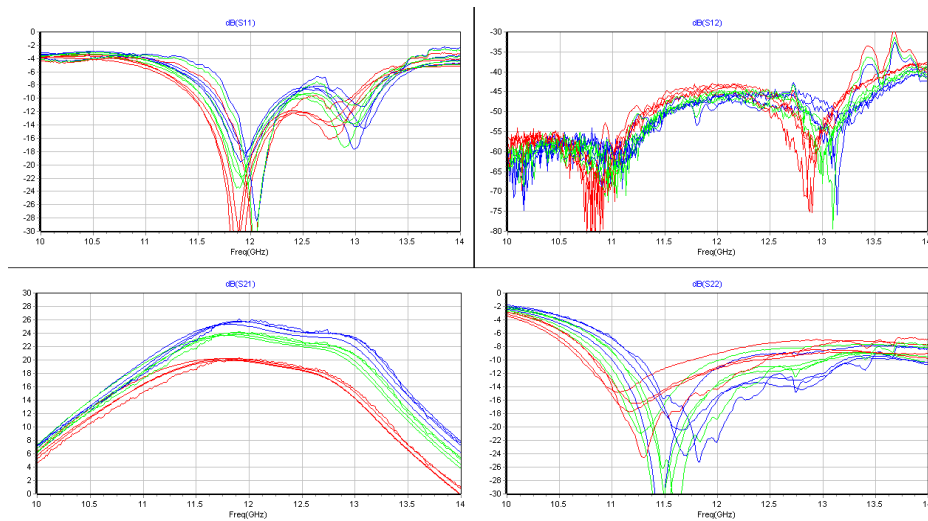
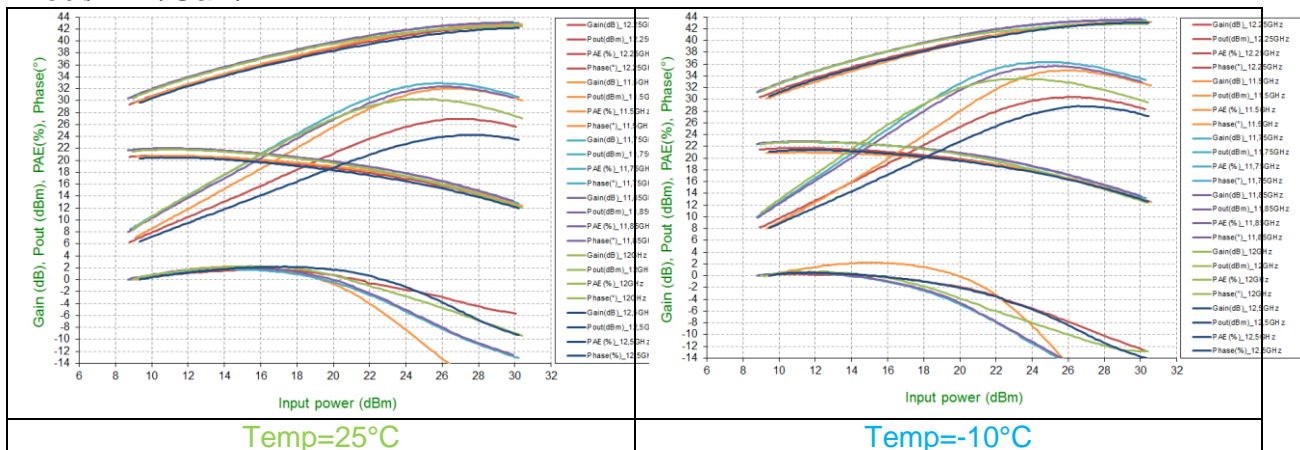


Figure 219 : HPA-2 #1 HPA-2 #2 HPA-2 #3 HPA-2 #4 modules. [S] parameters measurements. RF=[10-14GHz], Vd=30 V, Fixed drain current Ids=450mA @25°C. Temp=[-10°C, 25°C, 85°C].

3.7.1.2 CW mode power measurements.

The main RF performances obtained, output power, PAE, power gain and phase are presented below versus input power and different frequency points from [11.5GHz to 13GHz]. Measurements have been performed for Temp=[-10°C, 25°C, 85°C]. For each frequency, drain current has been tuned in small signal: Ids=450mA (fixed at 25°C) with Vds=30V which represents the best trade-off in term of Pout/PAE/Gain/AMPM.



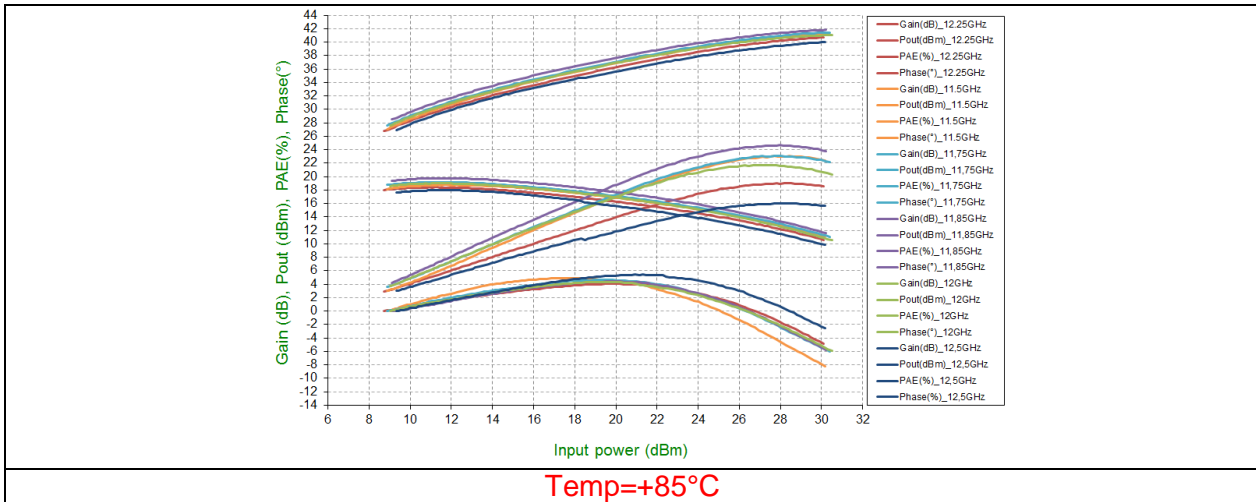


Figure 220: HPA-2 #1 module. Power measurements with CW signal. Temp=[-10°C, 25°C, 85°C], Vd=30 V, Id=450mA. RF=[11,5 GHz to 13 GHz]. Gain(dB), PAE(%), Pout(dBm), Phase(deg) vs Pin(dBm)

In figure below, the results (Pout, Gain, PAE, Compression) are presented versus frequency and temperature. For each temperature, Pin has been fixed to obtain maximum of PAE.

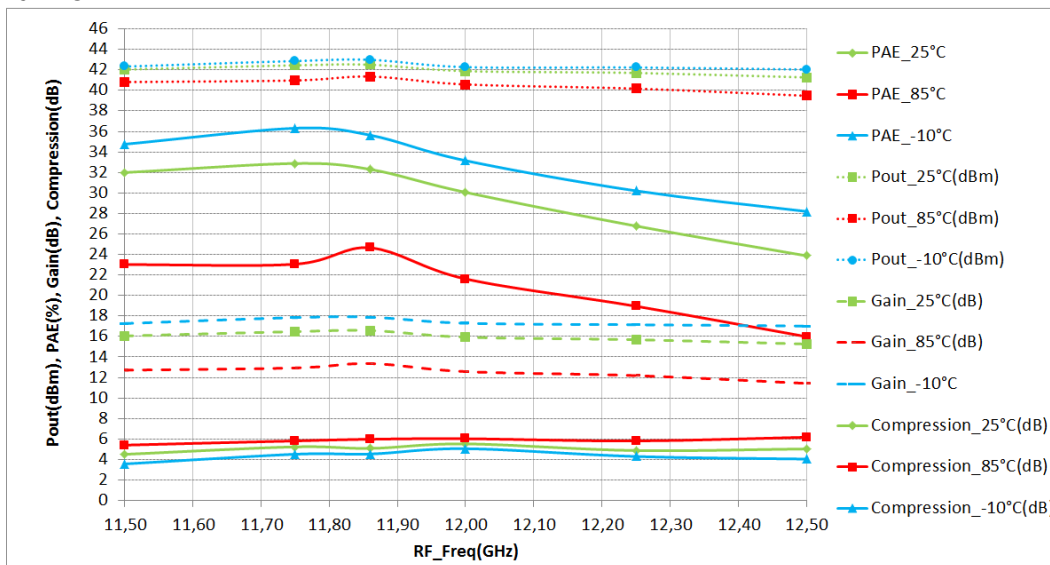


Figure 221 : HPA-2 #1 module. Power measurements with CW signal. Temp=[-10°C, 25°C, 85°C], Vd=30 V, Id=450mA. Gain(dB), PAE(%), Pout(dBm), Phase(deg) vs RFFreq(GHz) @PAE_max.

At Vds=30 V and room temperature, the maximum overall power added efficiency varies from 25 to 32% and is associated to an output power of 14W to 16W. Synthesis of the RF performances measured with CW signal are provided in the following table. Data are provided at PAE_max.

Freq (GHz)	Pin (dBm)	Pout (dBm)	Pout (W)	Gain (dB)	Compression (dB)	Phase (°)	PAE (%)	Freq (GHz)	Pin (dBm)	Pout (dBm)	Pout (W)	Gain (dB)	Compression (dB)	Phase (°)	PAE (%)
11,50	25,98	42,04	16,00	16,06	4,51	-13,15	32,00	11,50	28,10	40,82	12,08	12,72	5,41	-4,74	23,02
11,75	25,97	42,45	17,58	16,48	5,24	-8,20	32,88	11,75	28,04	40,98	12,53	12,94	5,82	-2,50	23,06
11,86	25,92	42,51	17,82	16,59	5,09	-7,84	32,31	11,86	27,99	41,36	13,68	13,37	5,98	-2,23	24,66
12,00	25,95	41,89	15,45	15,94	5,53	-4,67	30,07	12,00	28,01	40,59	11,46	12,58	6,03	-2,16	21,62
12,25	26,02	41,71	14,83	15,69	4,88	-2,94	26,78	12,25	27,99	40,18	10,42	12,19	5,82	-1,62	18,95
12,50	26,00	41,27	13,40	15,27	5,04	-3,77	23,88	12,50	28,05	39,48	8,87	11,43	6,18	0,55	15,99

Freq (GHz)	Pin (dBm)	Pout (dBm)	Pout (W)	Gain (dB)	Compression (dB)	Phase (°)	PAE (%)
11,50	25,06	42,33	17,10	17,27	3,58	-11,86	34,76
11,75	25,02	42,87	19,36	17,85	4,52	-13,27	36,32
11,86	25,10	42,99	19,91	17,89	4,54	-13,09	35,64
12,00	24,98	42,28	16,90	17,30	5,06	-9,00	33,16
12,25	25,09	42,24	16,75	17,15	4,30	-6,77	30,21
12,50	25,01	42,04	16,00	17,03	4,05	-7,01	28,20

Table 34 : HPA-2 #1 module. Synthesis of power measurements with CW signal. Temp=[-10°C, 25°C, 85°C], Vd=30V, Id=450mA. Gain(dB), PAE(%), Pout(dBm), Phase(deg) vs Rffreq(GHz) @PAE_max

HPA-2 #2, HPA-2 #3 and HPA-2 #4 modules have been tested with the same approach. Synthesis of the RF performances measured with CW signal are provided in the following tables.

Freq (GHz)	Pin (dBm)	Pout (dBm)	Pout (W)	Gain (dB)	Compression (dB)	Phase (°)	PAE (%)	Freq (GHz)	Pin (dBm)	Pout (dBm)	Pout (W)	Gain (dB)	Compression (dB)	Phase (°)	PAE (%)
11,50	26,06	42,35	17,18	16,29	4,89	-12,08	33,97	11,50	28,00	41,62	14,52	13,62	5,30	-7,00	27,45
11,75	26,12	42,88	19,41	16,76	5,67	-5,50	35,45	11,75	26,10	41,35	13,65	15,25	4,41	0,93	27,54
11,86	26,01	42,95	19,72	16,94	5,47	-5,98	34,71	11,86	25,98	41,34	13,61	15,36	4,21	-1,52	26,94
12,00	26,01	42,14	16,37	16,13	5,82	-1,78	31,34	12,00	26,07	40,74	11,86	14,67	4,40	1,79	24,62
12,25	25,97	42,31	17,02	16,34	4,80	-0,73	29,40	12,25	25,98	40,34	10,81	14,36	4,09	1,69	21,47
12,50	26,07	42,07	16,11	16,00	4,68	-2,12	27,00	12,50	25,94	39,76	9,46	13,82	4,10	3,35	18,40

Freq (GHz)	Pin (dBm)	Pout (dBm)	Pout (W)	Gain (dB)	Compression (dB)	Phase (°)	PAE (%)
11,50	25,01	42,38	17,30	17,37	4,02	-8,24	35,83
11,75	24,98	43,16	20,70	18,18	5,08	-9,88	38,83
11,86	25,07	43,32	21,48	18,25	4,93	-7,51	38,09
12,00	25,11	42,52	17,86	17,41	5,64	-1,17	34,84
12,25	25,09	42,81	19,10	17,72	4,88	-4,96	32,48
12,50	25,10	42,70	18,62	17,60	4,08	-2,31	30,66

Table 35 : HPA-2 #2 module. Synthesis of power measurements with CW signal. Temp=[-10°C, 25°C, 85°C], Vd=30V, Id=450mA. Gain(dB), PAE(%), Pout(dBm), Phase(deg) vs Rffreq(GHz) @PAE_max

Freq (GHz)	Pin (dBm)	Pout (dBm)	Pout (W)	Gain (dB)	Compression (dB)	Phase (°)	PAE (%)	Freq (GHz)	Pin (dBm)	Pout (dBm)	Pout (W)	Gain (dB)	Compression (dB)	Phase (°)	PAE (%)
11,50	27,01	41,91	15,52	14,90	5,44	-13,93	27,54	11,50	28,04	41,16	13,06	13,12	5,64	-8,67	23,22
11,75	27,02	42,14	16,37	15,12	5,97	-9,21	26,83	11,75	27,97	41,07	12,79	13,10	5,92	-5,99	21,41
11,86	27,02	42,26	16,83	15,24	5,78	-6,86	27,09	11,86	27,96	41,22	13,24	13,26	5,66	-3,98	21,99
12,00	26,98	40,98	12,53	14,00	6,38	-7,89	20,66	12,00	28,07	39,84	9,64	11,77	6,30	-4,95	15,98
12,25	27,09	41,34	13,61	14,25	5,61	-6,56	21,14	12,25	27,94	40,07	10,16	12,13	5,60	-3,13	16,70
12,50	27,13	40,93	12,39	13,80	5,60	-6,16	18,62	12,50	28,04	39,60	9,12	11,56	5,68	-0,63	14,63

Freq (GHz)	Pin (dBm)	Pout (dBm)	Pout (W)	Gain (dB)	Compression (dB)	Phase (°)	PAE (%)
11,50	25,06	42,08	16,14	17,02	4,06	-7,55	31,48
11,75	24,99	42,64	18,37	17,65	4,74	-7,63	32,56
11,86	25,12	42,74	18,79	17,62	4,73	-7,57	32,37
12,00	24,96	41,65	14,62	16,69	5,29	-1,36	26,76
12,25	25,12	42,03	15,96	16,91	4,26	-2,40	26,75
12,50	25,09	41,74	14,93	16,65	3,98	-3,89	23,85

Table 36 : HPA-2 #3 module. Synthesis of power measurements with CW signal. Temp=[-10°C, 25°C, 85°C], Vd=30V, Id=450mA. Gain(dB), PAE(%), Pout(dBm), Phase(deg) vs RFfreq(GHz) @PAE_max

Freq (GHz)	Pin (dBm)	Pout (dBm)	Pout (W)	Gain (dB)	Compression (dB)	Phase (°)	PAE (%)	Freq (GHz)	Pin (dBm)	Pout (dBm)	Pout (W)	Gain (dB)	Compression (dB)	Phase (°)	PAE (%)
11,50	26,95	42,26	16,83	15,31	5,02	-12,55	33,07	11,50	28,11	41,52	14,19	13,41	5,39	###	27,61
11,75	27,00	42,80	19,05	15,80	5,90	-11,23	34,27	11,75	28,02	41,93	15,60	13,91	5,71	-5,30	28,49
11,86	26,92	42,83	19,19	15,91	5,98	-10,33	33,54	11,86	28,03	41,97	15,74	13,94	5,78	-4,90	28,03
12,00	27,01	42,11	16,26	15,10	6,53	-6,04	30,02	12,00	28,13	41,25	13,34	13,12	6,25	-4,16	24,60
12,25	27,08	42,28	16,90	15,20	5,76	-5,91	28,69	12,25	28,13	41,17	13,09	13,04	5,60	-3,91	23,13
12,50	27,18	42,42	17,46	15,24	5,36	-5,95	28,35	12,50	28,02	40,84	12,13	12,82	5,40	-2,20	21,26

Freq (GHz)	Pin (dBm)	Pout (dBm)	Pout (W)	Gain (dB)	Compression (dB)	Phase (°)	PAE (%)
11,50	25,98	42,28	16,90	16,30	3,60	-19,63	35,26
11,75	25,98	43,08	20,32	17,10	4,72	-19,64	38,13
11,86	26,08	43,14	20,61	17,06	5,17	-19,52	37,00
12,00	26,12	42,46	17,62	16,34	5,90	-10,67	33,86
12,25	26,05	42,66	18,45	16,61	5,03	-11,32	31,93
12,50	25,97	42,91	19,54	16,94	4,24	-10,68	32,18

Table 37 : HPA-2 #4 module. Synthesis of power measurements with CW signal. Temp=[-10°C, 25°C, 85°C], Vd=30V, Id=450mA. Gain(dB), PAE(%), Pout(dBm), Phase(deg) vs RFfreq(GHz) @PAE_max

3.7.1.3 Multi-carrier mode power measurements.

In the following part, multicarrier measurements are presented. 4x HPA modules have been tested with Vds=30V and Ids=450mA for biasing point fixed in small signal. Multi-carrier measurements have been performed at Temp=[-10°C, 25°C, 85°C]. Characteristics of the multicarrier signal applied are:

- Centre frequency=12GHz
- Span=1GHz
- Nb of carriers=3000
- Notch=1% centered at 12GHz

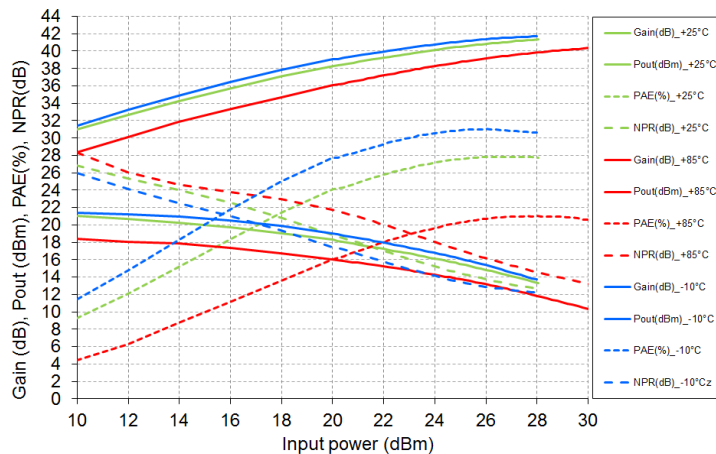


Figure 222 : HPA-2 #1 module. Power measurements with multi-carrier signal. Temp=[-10°C, 25°C, 85°C]. Vds=30V, RF=12GHz, Span=1GHz, 3000 carriers, 1% notch. Gain(dB), PAE(%), NPR(dB), Pout(dBm) vs Pin(dBm)

In the following table are summarized the main parameters measured during multi-carrier measurements : Pout / NPR / PAE

	NPR(dB)	Pin(dBm)	Pout(dBm)	Pout(W)	Gain(dB)	PAE(%)
Temp=25°C	15,05	24,22	40,20	10,48	15,99	27,25
	13,98	25,63	40,71	11,78	15,08	27,76
Temp=85°C	15,01	27,41	39,65	9,23	12,24	20,98
	14,03	28,79	40,06	10,13	11,27	20,95
Temp=-10°C	15,1	22,79	40,30	10,71	17,51	29,89
	13,99	23,01	40,84	12,12	16,65	30,66

Table 38 : HPA-2 #1 module. Synthesis of power measurements with multi-carrier signal. Temp=[-10°C, +25°C, +85°C]. Vds=30V, RF=12GHz, Span=1GHz, 3000 carriers, 1% notch

HPA-2 #2, HPA-2 #3 and HPA-2 #4 modules have been tested with the same approach. Synthesis of the RF performances measured with multi-carrier signal are provided in the following tables.

	NPR(dB)	Pin(dBm)	Pout(dBm)	Pout(W)	Gain(dB)	PAE(%)
Temp=25°C	14,95	23,58	40,27	10,65	16,69	28,55
	13,99	24,81	40,74	11,86	15,93	29,11
Temp=85°C	14,99	26,59	39,70	9,34	13,11	21,91
	14,05	27,84	40,12	10,27	12,27	22,14
Temp=-10°C	15,05	21,63	40,06	10,13	18,43	30,57
	14,04	23,00	40,61	11,51	17,61	31,74

Table 39 : HPA-2 #2 module. Synthesis of power measurements with multi-carrier signal. Temp=[-10°C, +25°C, +85°C]. Vds=30V, RF=12GHz, Span=1GHz, 3000 carriers, 1% notch.

	NPR(dB)	Pin(dBm)	Pout(dBm)	Pout(W)	Gain(dB)	PAE(%)
Temp=25°C	14,99	23,99	39,83	9,62	15,84	22,89
	13,98	25,39	40,33	10,79	14,94	23,37
Temp=85°C	14,96	26,79	39,24	8,40	12,46	17,90
	13,94	28,20	39,68	9,29	11,48	18,00
Temp=-10°C	15,08	22,01	39,78	9,51	17,77	24,96
	14,03	23,60	40,39	10,93	16,79	25,71

Table 40 : HPA-2 #3 module. Synthesis of power measurements with multi-carrier signal. Temp=[-10°C, +25°C, +85°C]. Vds=30V, RF=12GHz, Span=1GHz, 3000 carriers, 1% notch.

	NPR(dB)	Pin(dBm)	Pout(dBm)	Pout(W)	Gain(dB)	PAE(%)
Temp=25°C	15	23,60	40,19	10,44	16,59	27,91
	13,99	25,01	40,70	11,74	15,69	28,50
Temp=85°C	15,04	26,21	39,78	9,51	13,57	22,83
	13,92	27,81	40,27	10,64	12,46	23,01
Temp=-10°C	15,03	21,97	40,07	10,15	18,09	30,33
	14,02	23,38	40,58	11,42	17,20	31,37

Table 41 : HPA-2 #4 module. Synthesis of power measurements with multi-carrier signal. Temp=[-10°C, +25°C, +85°C]. Vds=30V, RF=12GHz, Span=1GHz, 3000 carriers, 1% notch

3.7.1.4 RF step measurements with multi-carrier signal : reliability of GH25 technology

The goal of this reliability study is to define a Safe Operating Area through RF Multicarrier step stress (2 dB compression, 4 dB compression, 6 dB compression, 8 dB compression). For that, a dedicated multicarrier test bench have been developed. Initial Measurements, intermediate RF measurements, final measurements and in situ monitoring are performed during this evaluation. Test plan is provided in the following table:

	Function	HPA
	FONDERIE	UMS GH25
	Frequency	12 GHz
	DC Bias	Vd = 28 Id = 460mA (Id1 = 60 mA; Id2 = 400 mA)
DC Life test	Number of Sample	NA
	T° JUNCTION (Objective)	NA
	Electrical constraint	NA
	Duration	NA
RF Life test	Number of Sample	3 + 1
	T°	25°C
	DC Biases	Nominal DC biases
	Electrical Constraint	Multicarrier
		Step stress : 2 weeks at 2dBc, 4 dBc, 6dBc and 8 dBc
	Monitoring	Gate, drain current, Input, output power
	Initial, Final & Intermediate Measurement	DC characteristics : Ids (Vds, Vgs) -> Ids=500 mA, Schottky Characteristic RF Characteristic : Pout, Gain, Id vs Pin Phase vs input power

Table 42 : Test plan for RF step stress measurements of Ku-Band GH25 HPA-2 module

3 samples have been tested during RF step stress with multicarrier signal:

- Sample n°2 = SN2
- Sample n°3 = SN3
- Sample n°1 = SN1 (control sample reference)

Multi carrier signal is generated using white noise source. The « white noise » bandwidth is = 1GHz . Synoptic and photographs of the multi-carrier test bench are provided in the following figures.

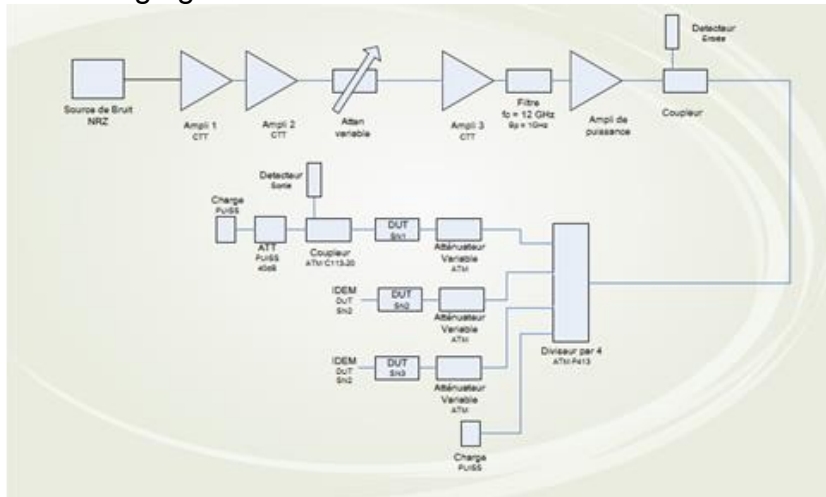


Figure 223 : Ku-Band Multi-carrier test bench

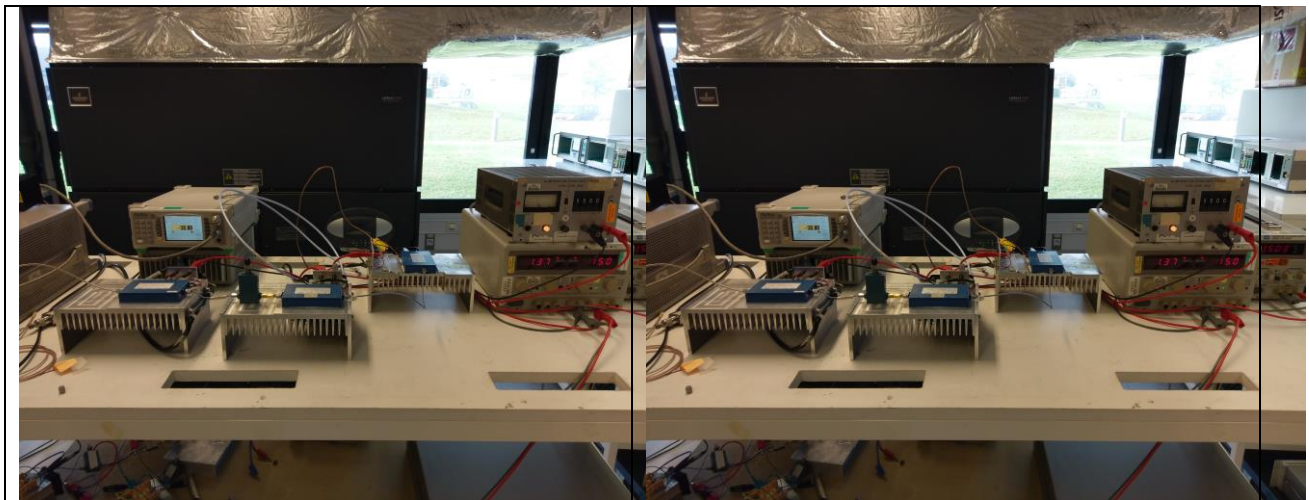


Figure 224 : Photographs of the Ku-Band multi-carrier test bench

The figure here above describes the signal level generated by the RF step stress test bench.

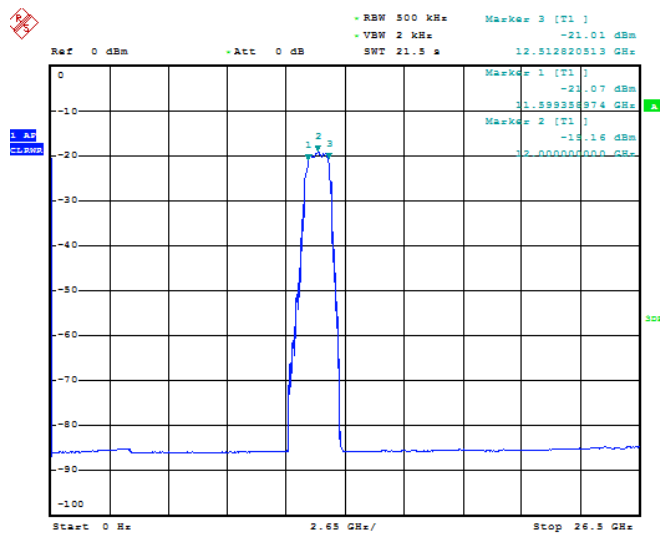


Figure 225 : Noise signal level at different point of the test bench

A dedicated test bench for initial, intermediate and final measurement bench is used for [S], AM/AM and AM/PM measurements after each step of compression (2 weeks / step from 4dBc to 8dBc). Synoptic and photographs of this test bench are provided in the following figures.

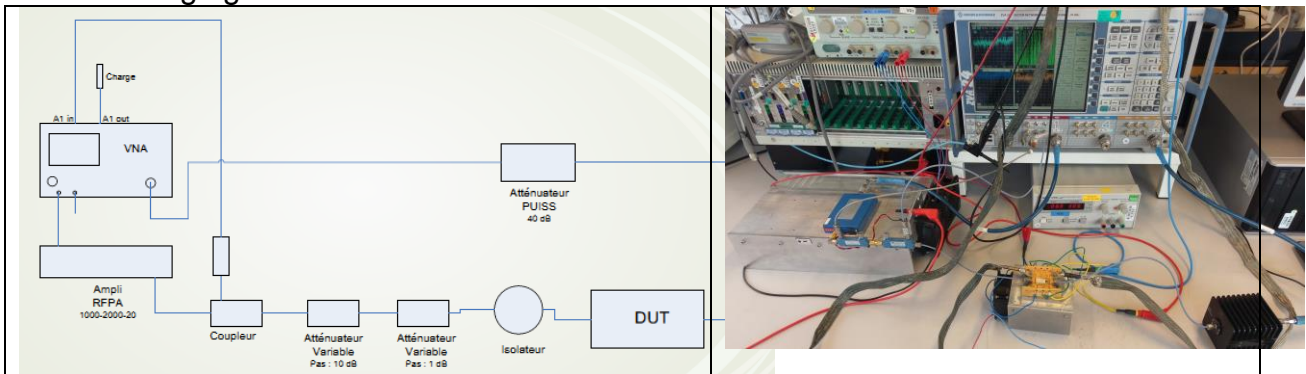


Figure 226 : Photography of the CW test bench for CW initial/intermediate and final measurements

Before starting the RF step stress campaign, initial characterization with the multicarrier signal have been performed in order to determine the non-linear characteristic of each samples.

In order to determine the power value during the in situ monitoring we use a detector. The power value versus the detected voltage is represented in the following graph.

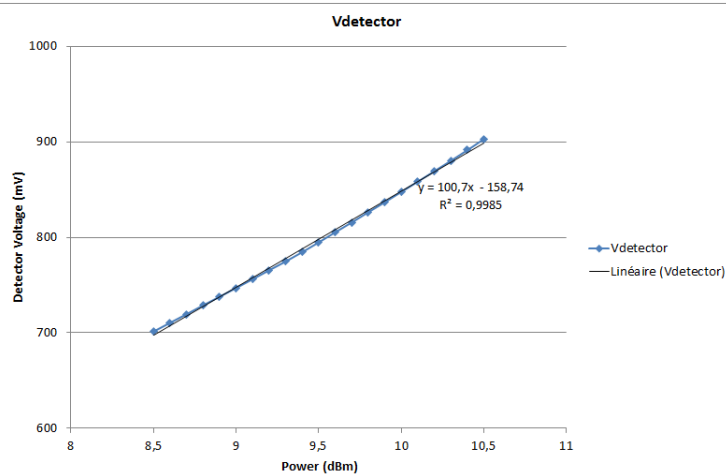


Figure 227 : Detector characterization : Detected voltage value (mV) versus power range(dBm)

On two HPA-2 modules (#2, #3), in Situ measurements have been continuously performed during steps @2dB, @4dB, 6dB, 8dB compression. The different parameters monitored are:

- Input power (dBm) and output power (dBm)
- Temperature (°C)
- Drain voltage (V) and Drain current (mA)
- Gate voltage (V) and gate current (mA)

An example of the in situ monitoring performed on HPA-2 module (#2) at Step 8dB compression is presented below:

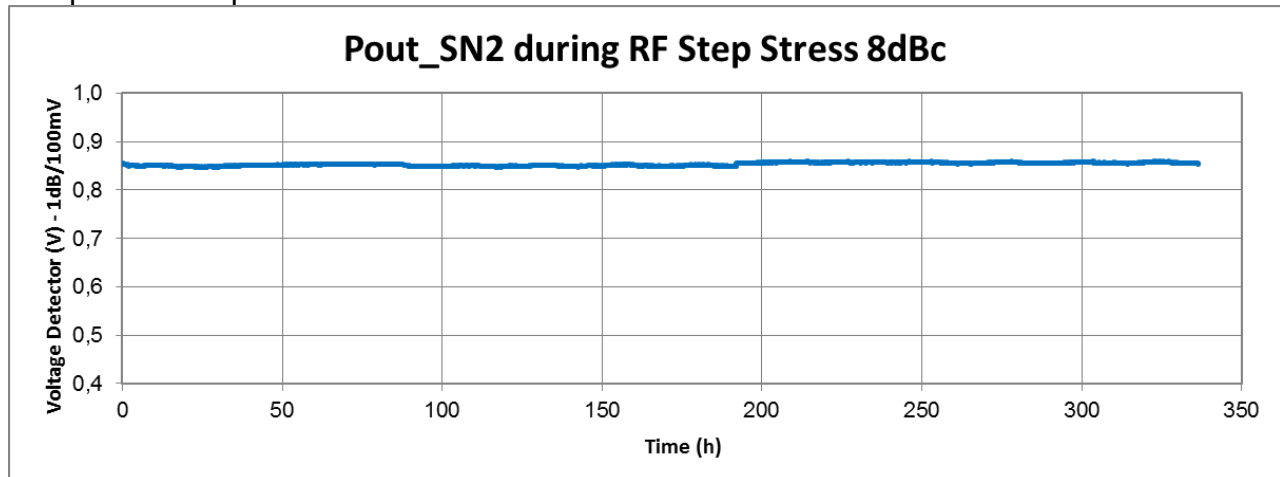


Figure 228 : HPA-2 module (#2). RF step stress measurement. Monitoring of Pout drift (detected voltage in V) during 8dBc compression step

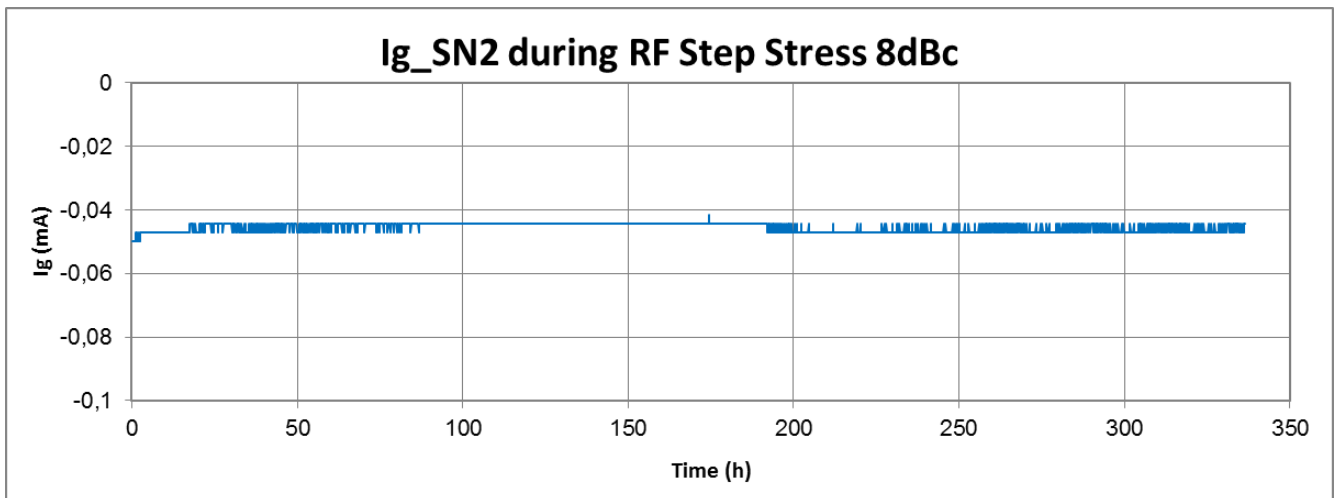


Figure 229 : HPA-2 module (#2). RF step stress measurement. Monitoring of Gate current drift during 8dBc compression step

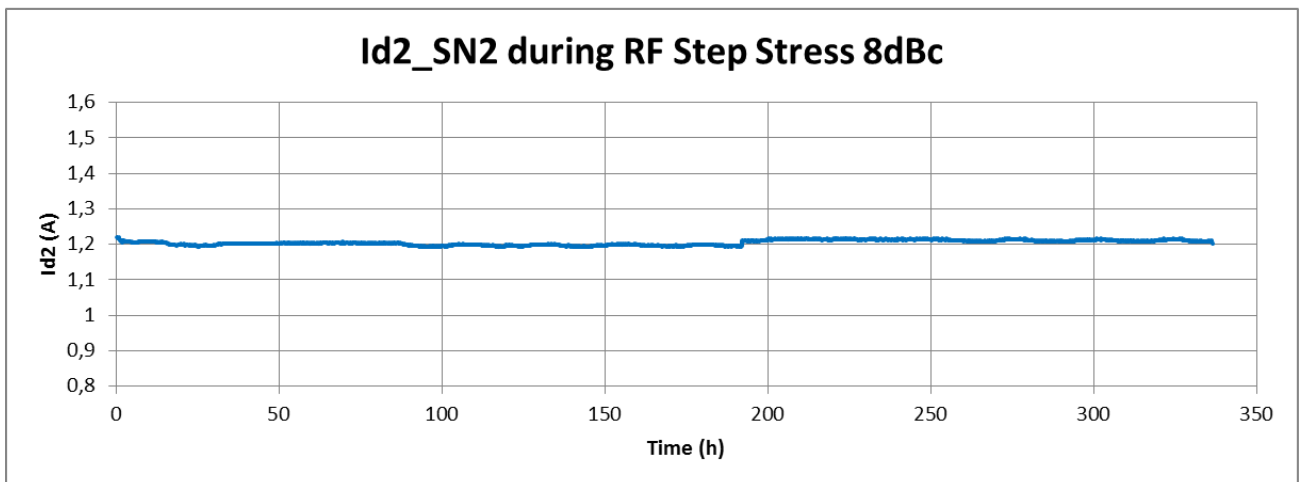
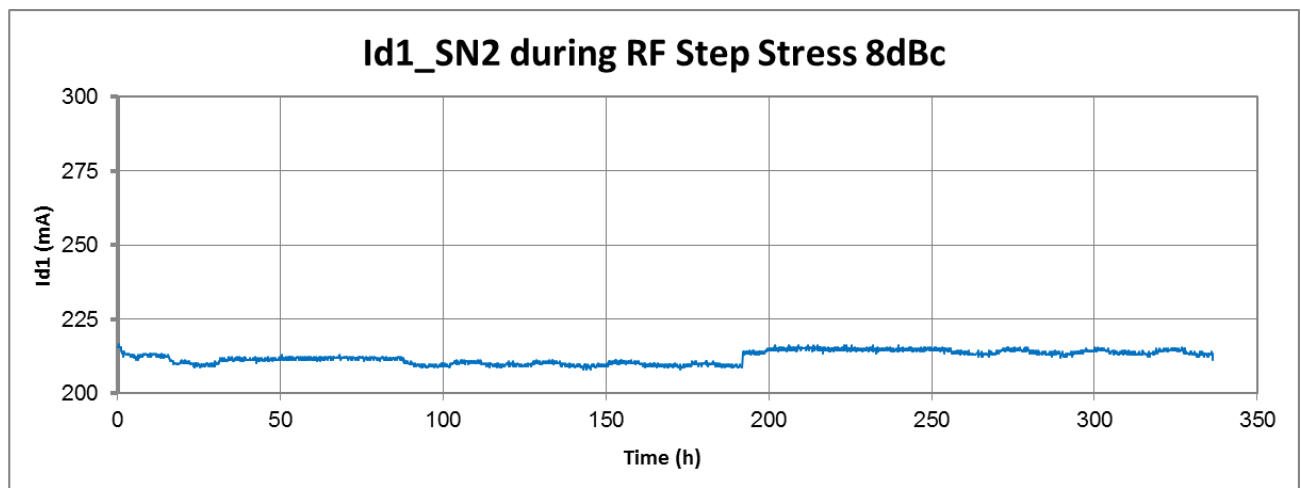


Figure 230 : HPA-2 module (#2). RF step stress measurement. Monitoring of Drain current drift during 8dBc compression step

For each HPA-2 module (#2, #3) initial, intermediate and final have been performed. These measurements have consisted of:

- [S] parameters measurements
- CW characterizations (AMAM and AMPM)
- Static measurements

Measurement data are presented for HPA-2 module #2 in the following graphs.

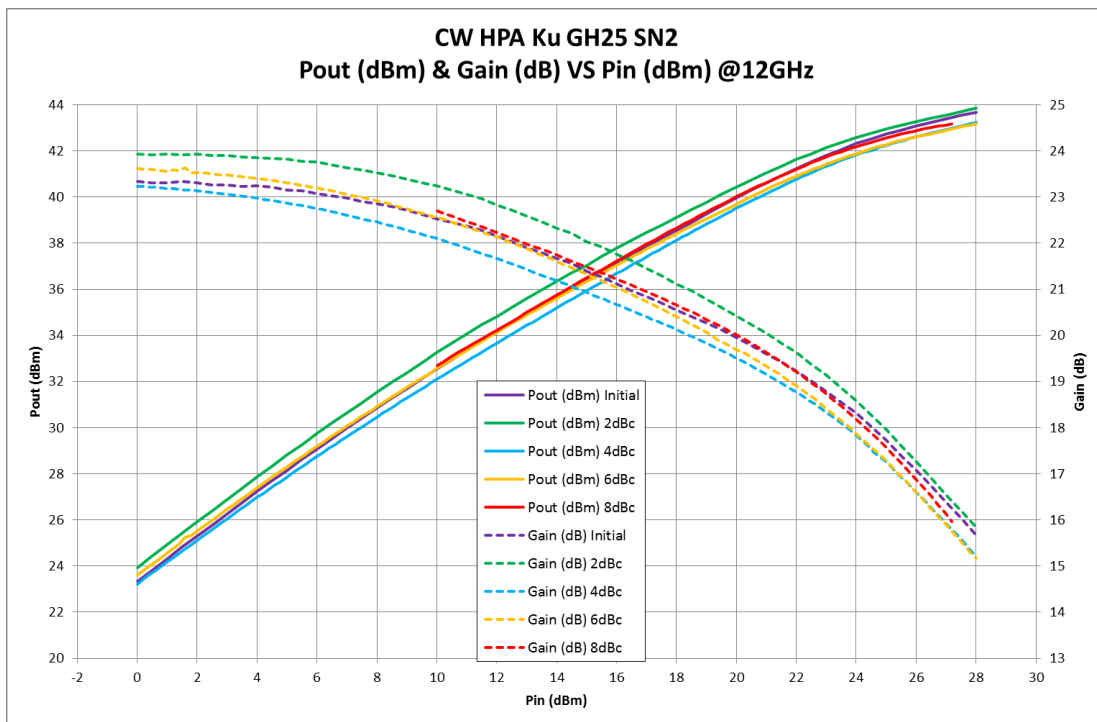


Figure 231 : HPA-2 module #2. AMAM characterization in CW mode after each compression step of the RF step stress measurements

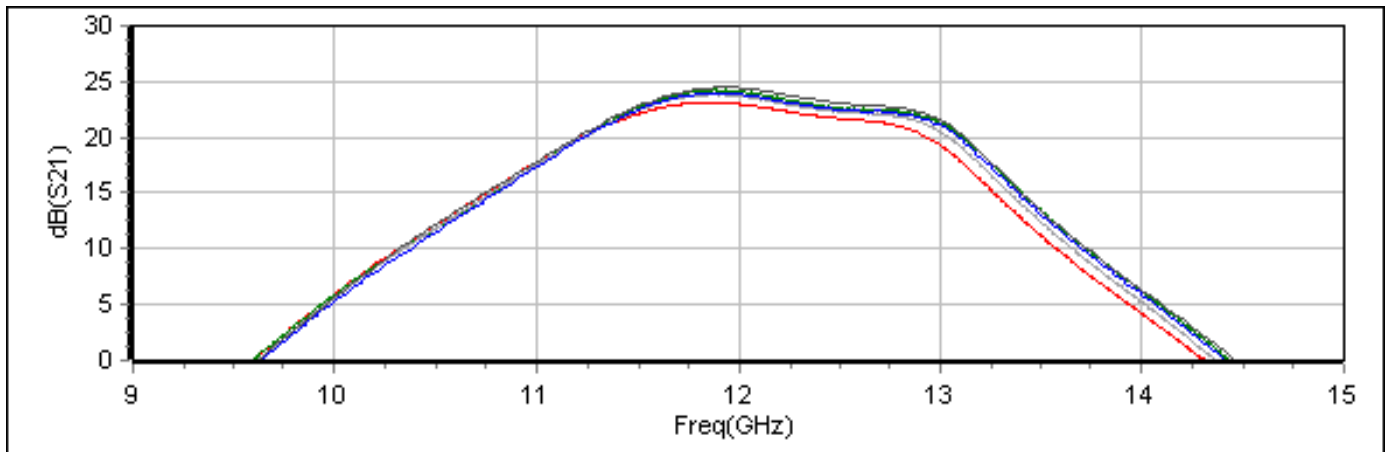


Figure 232 : HPA-2 module #2. [S] parameters measurements after each compression step of the RF step stress measurements

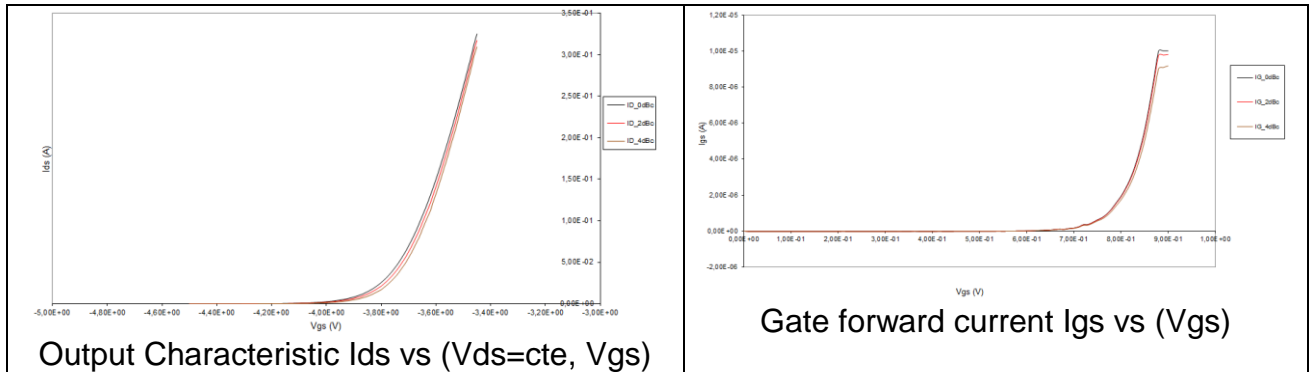


Figure 233 : HPA-2 module #2 Static measurements after each compression step of the RF step stress measurements

No significant drift have been pointed out during these stress steps. The drift observed on the 2 samples are also observed on the control sample.

In conclusion, TAS has performed during this evaluation, 2 kinds of measurements :

- In situ measurements (Pout, drain & gate current)
- Initial, intermediate (after each step) and final measurements :
 - CW (Pout vs Pin)
 - [S] measurements

During the monitoring no significant drifts have been observed.

3.7.2 MMIC Doherty HPA Modules test results

3.7.2.1 [S] Parameter measurements

On figure below the Doherty HPA module #1 (Full MMIC) S-parameters are given over a DC to 20GHz bandwidth with drain voltage of 30V and $I_{ds_carrier}=400mA$ (80mA/mm) and $I_{ds_peaking}=100mA$ (20mA/mm) fixed at **Temp=25°C**. This biasing point has been obtained during the multicarrier measurements and represent the best trade-off Pout/PAE/NPR. Measurements are performed versus Temp=[-10°C, 25°C, 85°C]

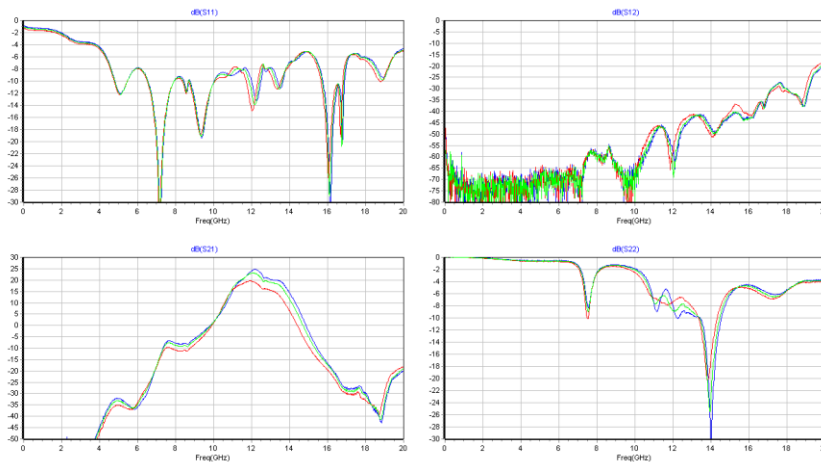


Figure 234 : MMIC Doherty HPA module #1 (Full MMIC). [S] parameters measurements. RF=[DC-20GHz], Vd=30V. Fixed I_{ds_carrier}=400mA (80mA/mm) and Fixed I_{ds_peaking}=100mA (20mA/mm) @25°C, Temp=[-10°C, 25°C, 85°C]

On the following figures, we focus on the Doherty HPA module #1 (Full MMIC) in-band frequency behavior. S₂₁ variation is about 4dB between -10°C to 85°C at 12 GHz. At constant gate voltage current, the gain variation versus temperature is 0,21dB/°C

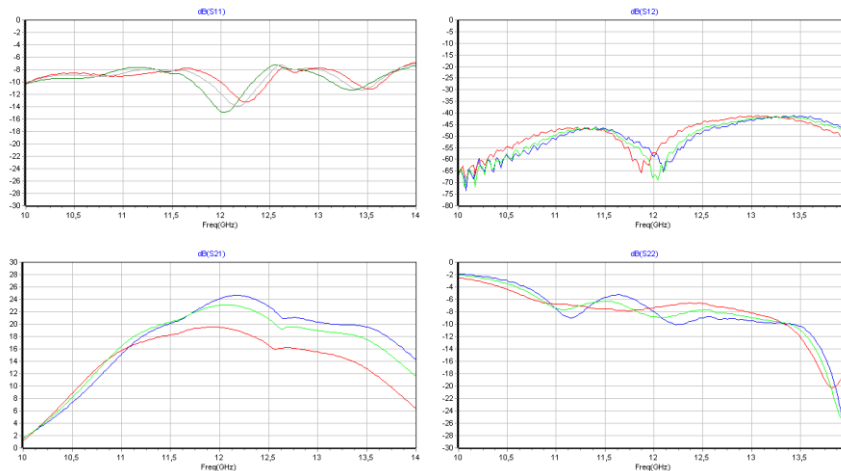


Figure 235 : MMIC Doherty HPA module #1 (Full MMIC). [S] parameters measurements. RF=[10-14GHz], Vds=30V. Fixed I_{ds_carrier}=400mA (80mA/mm) and Fixed I_{ds_peaking}=100mA (20mA/mm) @25°C, Temp=[-10°C, 25°C, 85°C]

Hereafter, for three Doherty HPA modules (Full MMIC), the S-parameters are given over a DC to 20 GHz bandwidth with drain voltage of 30V and I_{ds_carrier}=400mA (80mA/mm) and I_{ds_peaking}=100mA (20mA/mm) fixed at Temp=25. Measurements are performed versus Temp=[-10°C, 25°C, 85°C]

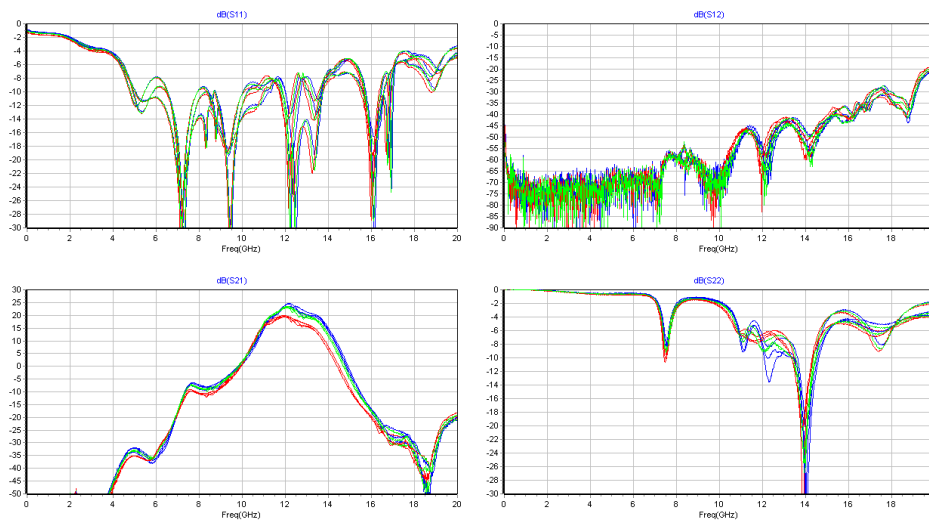


Figure 236 : 3x MMIC Doherty HPA module (Full MMIC). [S] parameters measurements. RF=[DC-20 GHz]. Vds=30V. Fixed Ids_carrier=400mA (80mA/mm) and Fixed Ids_peaking=100mA (20mA/mm) @25°C, Temp=[-10°C, 25°C, 85°C]

On following figures, we focus on the Doherty HPA modules in-band frequency behavior. **Erreur ! Source du renvoi introuvable.** shows the dispersion on S11, S22 and S21 parameters versus HPA modules. Measurements are performed versus Temp=[-10°C, 25°C, 85°C]. Regarding S21 parameter, at 12 GHz, a maximum dispersion of 1dB is observed between the three HPA modules.

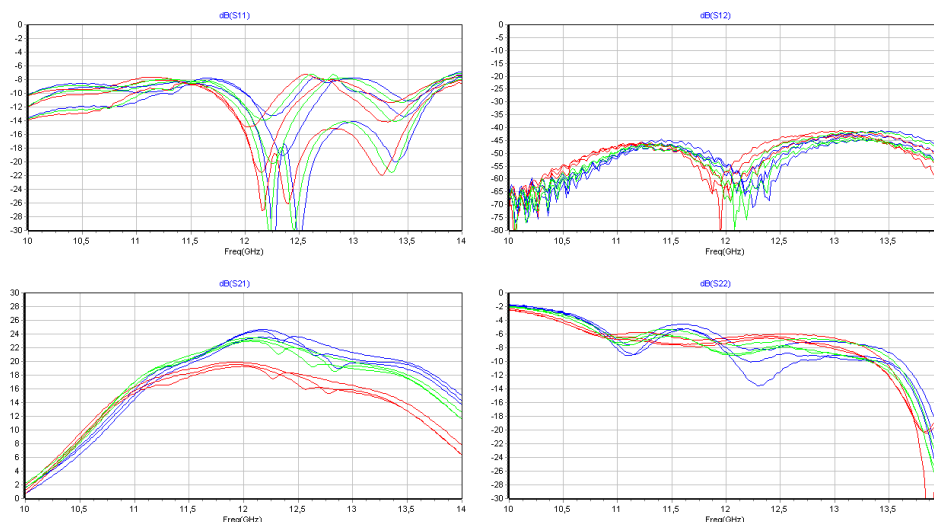


Figure 237 : 3x MMIC Doherty HPA module (Full MMIC). [S] parameters measurements. RF=[10-14 GHz]. Vds=30V. Fixed Ids_carrier=400mA (80mA/mm) and Fixed Ids_peaking=100mA (20mA/mm) @25°C, Temp=[-10°C, 25°C, 85°C]

3.7.2.2 CW mode power measurements.

The RF performances measured with a CW signal are presented in this chapter. The selected biasing point is: $V_{ds}=30V$ with $I_{ds_carrier}=400mA$ (80mA/mm) and $I_{ds_peaking}=100mA$ (20mA/mm). This biasing point is fixed at $Temp=25^{\circ}C$. This biasing point has been obtained during the multicarrier measurements and represents the best trade-off Pout/PAE/NPR. The presented measurements are performed versus $Temp=[-10^{\circ}C, 25^{\circ}C, 85^{\circ}C]$.

The main RF performances obtained, output power, PAE, power gain and phase are presented below versus input power and different frequency points from [11.5GHz to 13GHz]. Measurements have been performed for $Temp=[-10^{\circ}C, 25^{\circ}C, 85^{\circ}C]$.

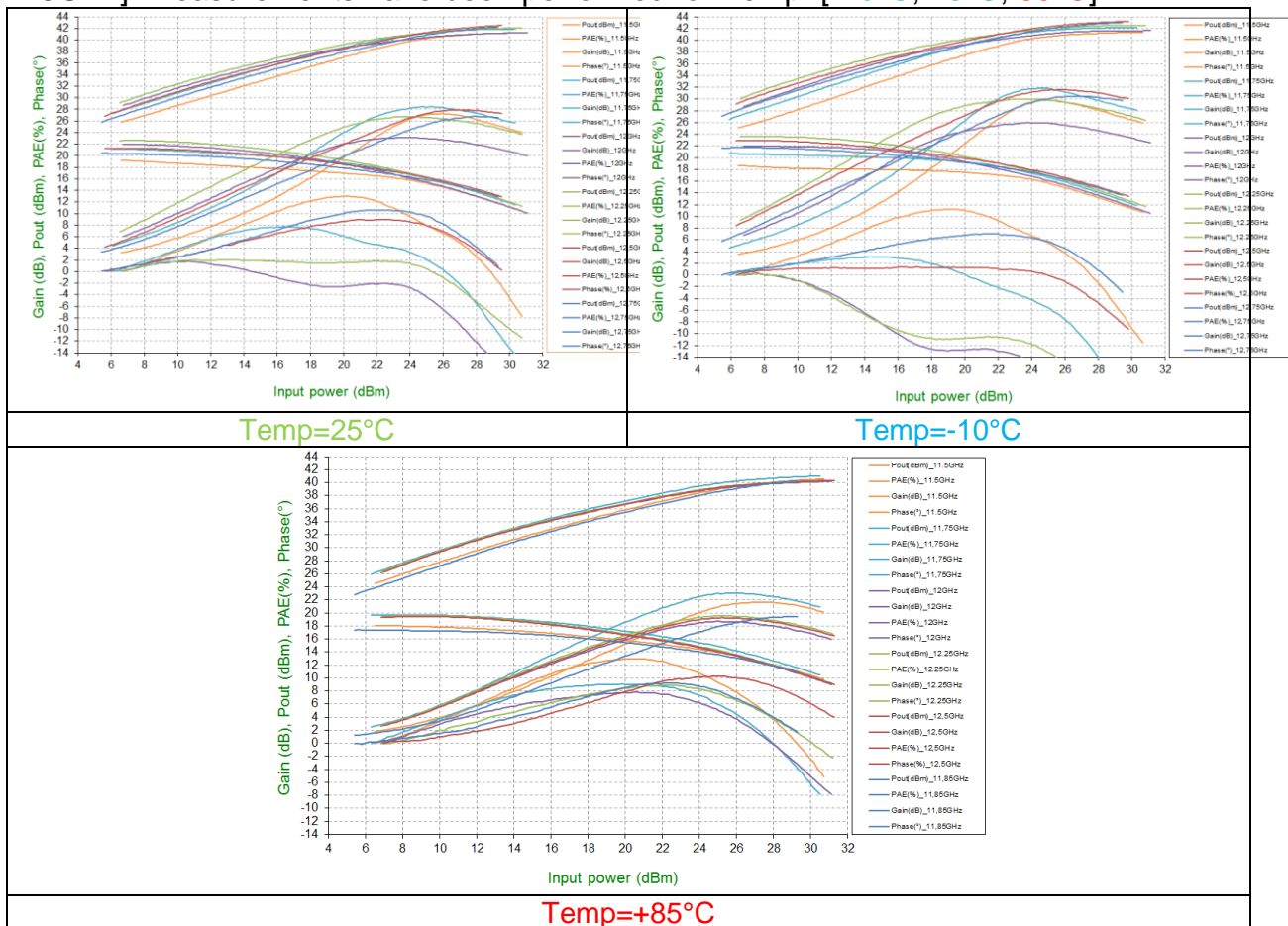


Figure 238 : MMIC Doherty HPA module#1 (Full MMIC). Power measurements with CW signal. $V_{ds}=30V$. Fixed $I_{ds_carrier}=400mA$ (80mA/mm) and Fixed $I_{ds_peaking}=100mA$ (20mA/mm) @ $25^{\circ}C$. $Temp=[-10^{\circ}C, 25^{\circ}C, 85^{\circ}C]$. RF=[11,5 GHz to 13 GHz]. Gain(dB), PAE(%), Pout(dBm), Phase(deg) vs Pin(dBm)

The results (Pout, Gain, PAE, Compression) are presented versus frequency and temperature. For each temperature, Pin has been fixed to obtain maximum of PAE.

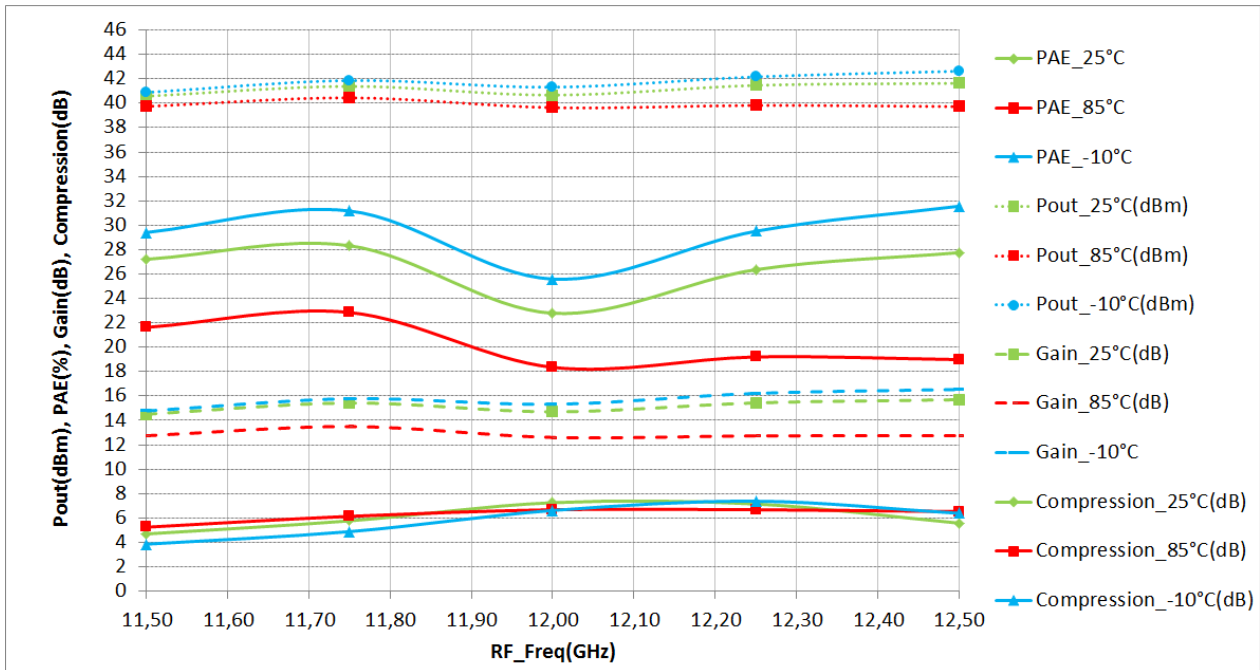


Figure 239 : MMIC Doherty HPA module#1 (Full MMIC). Power measurements with CW signal. Temp=[-10°C, 25°C, 85°C]. Vds=30V. Fixed Ids_carrier=400mA (80mA/mm) and Fixed Ids_peaking=100mA (20mA/mm) @25°C. Gain(dB), PAE(%), Pout(dBm), Phase(deg) vs Rffreq(GHz) @PAE_max.

Synthesis of the RF performances measured with CW signal are provided in the following table. Data are provided at PAE_max

Freq (GHz)	Pin (dBm)	Pout (dBm)	Pout (W)	Gain (dB)	Compression (dB)	Phase (°)	PAE (%)	Freq (GHz)	Pin (dBm)	Pout (dBm)	Pout (W)	Gain (dB)	Compression (dB)	Phase (°)	PAE (%)
11,50	26,07	40,58	11,43	14,51	4,70	6,51	27,21	11,50	26,99	39,74	9,42	12,75	5,25	5,94	21,63
11,75	25,96	41,39	13,77	15,43	5,77	0,33	28,33	11,75	26,95	40,45	11,09	13,50	6,14	2,54	22,85
12,00	25,96	40,67	11,67	14,71	7,26	-6,45	22,79	12,00	27,03	39,64	9,20	12,61	6,68	1,82	18,36
12,25	26,03	41,47	14,03	15,44	7,15	-1,08	26,36	12,25	27,09	39,83	9,62	12,74	6,68	5,17	19,21
12,50	25,94	41,64	14,59	15,70	5,58	7,01	27,76	12,50	26,98	39,73	9,40	12,75	6,53	9,55	18,99

Freq (GHz)	Pin (dBm)	Pout (dBm)	Pout (W)	Gain (dB)	Compression (dB)	Phase (°)	PAE (%)
11,50	26,11	40,89	12,27	14,78	3,86	3,55	29,41
11,75	26,09	41,87	15,38	15,78	4,89	-7,77	31,18
12,00	25,99	41,32	13,55	15,33	6,62	-19,28	25,59
12,25	25,95	42,17	16,48	16,22	7,38	-14,91	29,51
12,50	26,09	42,63	18,32	16,54	6,39	-1,29	31,56

Figure 240 : MMIC Doherty HPA module#1 (Full MMIC). Synthesis of power measurements with CW signal. Temp=[-10°C, 25°C, 85°C], Vds=30V. Fixed Ids_carrier=400mA (80mA/mm) and Fixed Ids_peaking=100mA (20mA/mm) @25°C. Gain(dB), PAE(%), Pout(dBm), Phase(deg) vs Rffreq(GHz) @PAE_max

Two other MMIC Doherty HPA modules have been tested with the same approach. Synthesis of the RF performances measured with CW signal are provided in the following tables.

Freq (GHz)	Pin (dBm)	Pout (dBm)	Pout (W)	Gain (dB)	Compression (dB)	Phase (°)	PAE (%)	Freq (GHz)	Pin (dBm)	Pout (dBm)	Pout (W)	Gain (dB)	Compression (dB)	Phase (°)	PAE (%)
11,50	25,08	40,51	11,25	15,43	4,51	1,03	27,27	11,50	26,08	39,66	9,25	13,58	5,01	1,38	21,87
11,75	25,08	41,29	13,46	16,21	5,62	-1,99	28,56	11,75	26,08	40,30	10,72	14,22	5,70	1,60	23,05
12,00	24,97	40,63	11,56	15,66	6,94	-3,85	23,24	12,00	26,09	39,58	9,08	13,49	6,18	3,25	18,75
12,25	24,98	41,42	13,87	16,44	6,57	2,25	26,75	12,25	26,14	40,16	10,38	14,02	5,52	5,53	21,40
12,50	25,02	41,84	15,28	16,82	5,16	7,68	28,57	12,50	26,01	40,19	10,45	14,18	4,49	7,84	21,77

Freq (GHz)	Pin (dBm)	Pout (dBm)	Pout (W)	Gain (dB)	Compression (dB)	Phase (°)	PAE (%)
11,50	23,97	40,60	11,48	16,63	3,47	3,64	29,68
11,75	23,95	41,47	14,03	17,52	4,61	-2,39	31,33
12,00	24,01	40,95	12,45	16,94	6,49	-8,04	25,88
12,25	24,10	41,85	15,31	17,75	6,86	-2,64	29,78
12,50	24,00	42,36	17,22	18,36	5,42	6,80	32,10

Figure 241 : MMIC Doherty HPA module#2 (Full MMIC). Synthesis of power measurements with CW signal. Temp=[-10°C, 25°C, 85°C], Vds=30V. Fixed Ids_carrier=400mA (80mA/mm) and Fixed Ids_peaking=100mA (20mA/mm) @25°C. Gain(dB), PAE(%), Pout(dBm), Phase(deg) vs Rffreq(GHz) @PAE_max

Freq (GHz)	Pin (dBm)	Pout (dBm)	Pout (W)	Gain (dB)	Compression (dB)	Phase (°)	PAE (%)
11,50	26,00	40,13	10,30	14,13	5,16	6,69	24,96
11,75	25,97	40,99	12,56	15,02	6,01	-2,51	25,99
12,00	26,08	40,24	10,57	14,16	7,55	-6,57	20,23
12,25	25,96	41,05	12,74	15,09	6,81	-0,03	24,65
12,50	26,02	41,56	14,32	15,54	5,50	5,52	24,86

Figure 242 : MMIC Doherty HPA module#3 (Full MMIC). Synthesis of power measurements with CW signal. Vds=30V. Fixed Ids_carrier=400mA (80mA/mm) and Fixed Ids_peaking=100mA (20mA/mm) @25°C. Gain(dB), PAE(%), Pout(dBm), Phase(deg) vs Rffreq(GHz) @PAE_max

3.7.2.3 Multi-carrier mode power measurements.

The multicarrier signal characteristics is presented below:

- Centre frequency: 12GHz
- Bandwidth : 1GHz
- Number of carriers: 3000
- Notch: 1%
- Position of notch: centred at 12GHz

Performance of the Ku-Band Doherty HPA module (Full MMIC) has been optimized directly during the multicarrier measurements by tuning the biasing point of the peaking path and the carrier path.

In the table below, the performance (Pout/PAE) for NPR=15dB and NPR=14dB are presented versus different biasing points:

- Drain current of the carrier path from 300mA (60mA/mm) to 700mA(140mA)
- Drain current of the peaking path from 0mA(0mA/mm) to 100mA(20mA/mm)

At NPR15	Gain	Pin	Pout	PAE	NPR
Data (500mA_100mA)	17.41	21.61	38.93	24.69	14.96
Data (400mA_100mA)	17.00	21.81	38.81	24.59	15.02
Data (500mA_150mA)	17.52	21.42	38.95	24.49	15.07
Data (500mA_5mA)	16.60	21.78	38.38	24.21	15.02
Data (600mA_100mA)	16.95	22.00	38.96	24.18	15.02
Data (300mA_5mA)	16.25	21.86	38.11	24.01	14.97
Data (500mA_0mA)	15.32	22.61	37.93	23.50	15.05
Data (700mA_5mA)	16.00	22.59	38.59	23.14	15.05

At NPR15	Gain	Pin	Pout	PAE	NPR
Data (500mA_100mA)	17.41	21.61	38.93	24.69	14.96
Data (400mA_100mA)	17.00	21.81	38.81	24.59	15.02
Data (500mA_150mA)	17.52	21.42	38.95	24.49	15.07
Data (500mA_5mA)	16.60	21.78	38.38	24.21	15.02
Data (600mA_100mA)	16.95	22.00	38.96	24.18	15.02
Data (300mA_5mA)	16.25	21.86	38.11	24.01	14.97
Data (500mA_0mA)	15.32	22.61	37.93	23.50	15.05
Data (700mA_5mA)	16.00	22.59	38.59	23.14	15.05

Figure 243 : MMIC Doherty HPA module#1 (Full MMIC). Optimization of the biasing point. Multi-carrier measurements. Temp=25°C

Best compromise is obtained for $I_{ds_carrier}=400mA$ and $I_{ds_peaking}=100mA$ corresponding to a minimum of AMPM variation vs Pin with CW signal. On figure below, multi-carrier measurements are given versus input power.

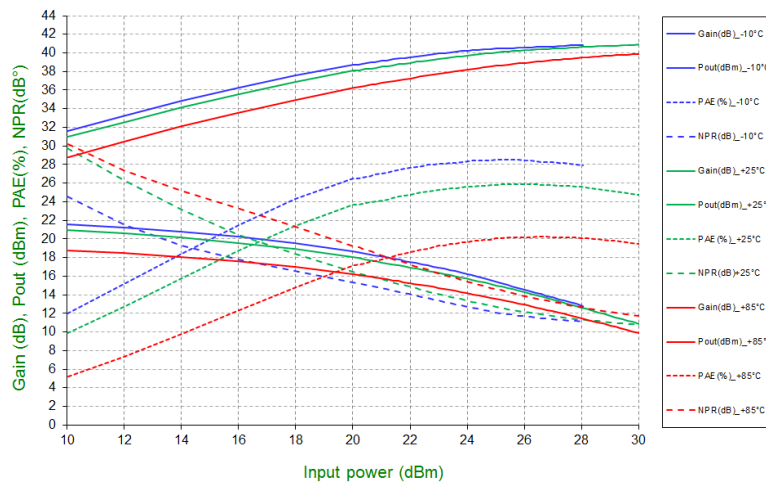


Figure 244 : Doherty HPA module#1 (Full MMIC). Power measurements with multi-carrier signal. Temp=[-10°C, 25°C, 85°C]. Vds=30V, RF=12GHz, Span=1GHz, 3000 carriers, 1% notch. Gain(dB), PAE(%), NPR(dB), Pout(dBm) vs Pin(dBm)

In the following table are summarized the main parameters measured during multi-carrier measurements : Pout / NPR / PAE

	NPR(dB)	Pin(dBm)	Pout(dBm)	Pout(W)	Gain(dB)	PAE(%)
Temp=25°C	15,05	21,77	38,84	7,66	17,07	24,63
	14,12	22,97	39,35	8,60	16,38	25,24
Temp=85°C	14,97	24,57	38,42	6,95	13,85	19,89
	14,02	25,80	38,87	7,70	13,06	20,18
Temp=-10°C	15	20,63	38,96	7,87	18,26	26,76
	14,08	21,98	39,54	8,99	17,56	27,62

Figure 245 : Doherty HPA module#1 (Full MMIC). Synthesis of power measurements with multi-carrier signal. Temp=[-10°C, +25°C, +85°C]. Vds=30V, RF=12GHz, Span=1GHz, 3000 carriers, 1% notch.

Two other MMIC Doherty HPA modules have been tested with the same approach. Synthesis of the RF performances measured with multicarrier signal are provided in the following tables.

	NPR(dB)	Pin(dBm)	Pout(dBm)	Pout(W)	Gain(dB)	PAE(%)
Temp=25°C	15,06	20,99	38,83	7,64	17,84	24,74
	14,06	22,39	39,40	8,71	17,01	25,39
Temp=85°C	14,98	23,63	38,40	6,92	14,78	20,12
	13,97	25,05	38,92	7,80	13,88	20,45
Temp=-10°C	14,88	20,00	39,21	8,34	19,22	27,31
	14,02	21,41	39,73	9,40	18,33	27,79

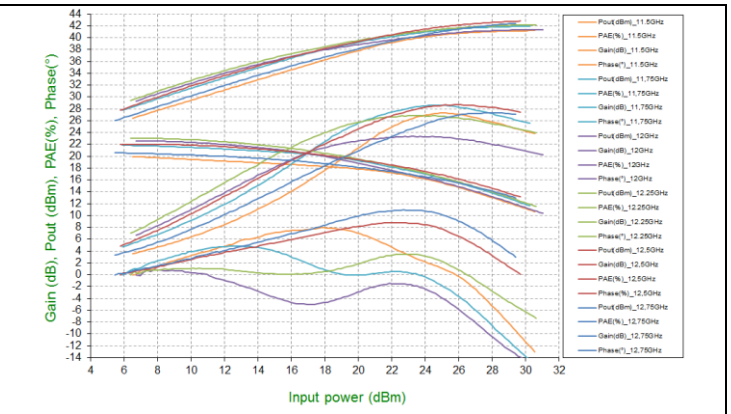
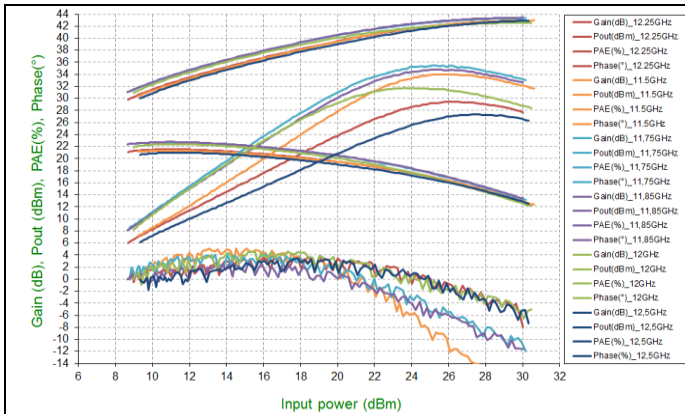
Figure 246 : Doherty HPA module#2 (Full MMIC). Synthesis of power measurements with multi-carrier signal. Temp=[-10°C, +25°C, +85°C]. Vds=30V, RF=12GHz, Span=1GHz, 3000 carriers, 1% notch.

	NPR(dB)	Pin(dBm)	Pout(dBm)	Pout(W)	Gain(dB)	PAE(%)
Temp=25°C	15,01	21,61	38,29	6,75	16,68	21,82
	14,06	22,98	38,84	7,65	15,86	22,34
Temp=85°C	15,07	24,40	38,02	6,33	13,62	17,89
	14,05	25,78	38,52	7,12	12,74	18,18
Temp=-10°C	14,98	21,19	38,89	7,75	17,71	24,83
	14,08	22,39	39,35	8,62	16,96	25,34

Figure 247 : Doherty HPA module#3 (Full MMIC). Synthesis of power measurements with multi-carrier signal. Temp=[-10°C, +25°C, +85°C]. Vds=30V, RF=12GHz, Span=1GHz, 3000 carriers, 1% notch.

3.7.2.4 Comparison results between HPA-2 module and MMIC Doherty HPA module

The table below, presents the comparison results between HPA-2 module and MMIC Doherty HPA module



HPA-2 module. Power measurements with CW signal. Temp=25°C. RF=[11,5 GHz to 12.5 GHz]. Gain(dB), PAE(%), Pout(dBm), Phase(deg) vs Pin(dBm)

MMIC Doherty HPA module (Full MMIC). Power measurements with CW signal. Temp=25°C. RF=[11,5 GHz to 12.5 GHz]. Gain(dB), PAE(%), Pout(dBm), Phase(deg) vs Pin(dBm)

Freq (GHz)	Pin (dBm)	Pout (dBm)	Pout (W)	Gain (dB)	Compression (dB)	Phase (°)	PAE (%)
11,50	26,06	42,35	17,18	16,29	4,89	-12,08	33,97
11,75	26,12	42,88	19,41	16,76	5,67	-5,50	35,45
11,86	26,01	42,95	19,72	16,94	5,47	-5,98	34,71
12,00	26,01	42,14	16,37	16,13	5,82	-1,78	31,34
12,25	25,97	42,31	17,02	16,34	4,80	-0,73	29,40
12,50	26,07	42,07	16,11	16,00	4,68	-2,12	27,00

Freq (GHz)	Pin (dBm)	Pout (dBm)	Pout (W)	Gain (dB)	Compression (dB)	Phase (°)	PAE (%)
11,50	25,08	40,51	11,25	15,43	4,51	1,03	27,27
11,75	25,08	41,29	13,46	16,21	5,62	-1,99	28,56
12,00	24,97	40,63	11,56	15,66	6,94	-3,85	23,24
12,25	24,98	41,42	13,87	16,44	6,57	2,25	26,75
12,50	25,02	41,84	15,28	16,82	5,16	7,68	28,57

HPA-2 module. Power measurements with CW signal. Temp=25°C. RF=[11,5 GHz to 13 GHz]. Gain(dB), PAE(%), Pout(dBm), Phase(deg) vs Rffreq(GHz) for PAE_max

MMIC Doherty HPA module (Full MMIC). Power measurements with CW signal. Temp=25°C. RF=[11,5 GHz to 13 GHz]. Gain(dB), PAE(%), Pout(dBm), Phase(deg) vs Rffreq(GHz) for PAE_max

	NPR(dB)	Pin(dBm)	Pout(dBm)	Pout(W)	Gain(dB)	PAE(%)
Temp=25°C	14,95	23,58	40,27	10,65	16,69	28,55
	13,99	24,81	40,74	11,86	15,93	29,11
Temp=85°C	14,99	26,59	39,70	9,34	13,11	21,91
	14,05	27,84	40,12	10,27	12,27	22,14
Temp=-10°C	15,05	21,63	40,06	10,13	18,43	30,57
	14,04	23,00	40,61	11,51	17,61	31,74

	NPR(dB)	Pin(dBm)	Pout(dBm)	Pout(W)	Gain(dB)	PAE(%)
Temp=25°C	15,06	20,99	38,83	7,64	17,84	24,74
	14,06	22,39	39,40	8,71	17,01	25,39
Temp=85°C	14,98	23,63	38,40	6,92	14,78	20,12
	13,97	25,05	38,92	7,80	13,88	20,45
Temp=-10°C	14,88	20,00	39,21	8,34	19,22	27,31
	14,02	21,41	39,73	9,40	18,33	27,79

HPA-2 module. Power measurements with multicarrier signal.

MMIC Doherty HPA module. Power measurements with multicarrier signal.

Table 43 : Comparison results between HPA-2 module and MMIC Doherty HPA module

Based on the comparisons provided in the previous table, the preliminary conclusions on the development of a Large-band (1GHz bandwidth) and high power Ku-Band GH25 MMIC Doherty HPA module are:

- In CW mode:
 - Maximum of PAE for Doherty architecture is lower than the PAE obtained with a classical Class AB architecture
 - The Pout associated to the PAE_max is lower for Doherty architecture
 - AMPM vs Pin and frequency bandwidth is much more important for Doherty architecture

- In Multicarrier-mode (NPR=14dB and NPR=15dB), PAE and Pout for PAE are lower for Doherty architecture

4. CRITICAL ASSESMENT OF HPA MODULE

4.1 L-band applications: comparison of SSPA using GaN HPA-1 module with a conventional GaAs flat mounted SSPA and TWTA

A Trade-Off between solutions with LTWTA and SSPA has been conducted. Results are presented in the following table. For the new generation of payload, a L-band GaN SSPA solution using HPA-1 module developed in this study and improved thermal management solutions brings many benefits, compared to a LTWTA solution and to a conventional GaAs SSPA, in term of:

- Improved electrical performances with multi-carrier signal
- Mass reduction
- Footprint reduction
- Higher operating temperature
- Simplified implementation during payload integration

	Solution with L-band TWT	Solution with L-band SSPA	
	TWTA	GaAs SSPA with standard housing and 2x GaAs HPA modules in RF chain	GaN SSPA with vertical housing and single GaN HPA-1 module in RF chain
RF performances with CW signal	Pout=43W PAE=57% (at 65°C)	Pout=43W PAE=45% (at 65°C)	Pout=50W PAE=58% (at 85°C)
RF performances with multi-carrier signal	Pout=25W PAE=45% @NPR=14dB (at 85°C)	Pout=25W PAE=36% @NPR=14dB (65°C)	Pout=32W PAE=45,5% @NPR=14dB (Temp=85°C)
Mass	4340g	1300g	1439g
Temperature	2 zones: 65°C (CAMP) 85°C (TWT)	Single zone: 65°C	Single zone: 85°C
Footprint	5 box: CAMP + TWT + EPC + Circulator + Load + (DC cable + RF cable)	Single box: 250x123mm ²	Single box: 240x105mm ²
	7,1dm ²	3,1dm ²	2,5dm ²
Payload Integration complexity	Reference	++	+++

Table 44 : Trade-Off GaAs SSPA vs GaN SSPA (using HPA-1 module) vs TWTA

The target market is composed of the historical MSS market, the FSS and data relay satellite market, the high power SSPA market.

- Mobile Satellite Service (MSS) Market: even if the MSS market cannot be considered as a steady market, there are regular opportunities for replacement satellites in existing constellations such as Inmarsat, Thuraya. It is forecast that one such replacement satellite will be ordered each year. Each satellite includes a large number of SSPA's (typically 100). We have conservatively figured a commercial success rate in this market of 50%, hence the number of 50/year on average.

- Fixed Service Satellite (FSS) & Data Relay Satellite Market: there is also a number of opportunities in L- and S-band in this market,. The number of SSPA's per payload is smaller (in the order of 4 to 10 per satellite) and the number of opportunities estimated at 1 per year.
- High power SSPA market: beyond the proposed 50W SSPA, further developments in higher power (by e.g. paralleling output HPA's) will be able to address the higher-power L-band SSPA market for navigation repeaters (WAAS, EGNOS) which is also relatively steady at 1 payload per year with 4 SSPA's each.

4.2 Ku-band applications: comparison of SSPA using GaN HPA-2 module with a LC-TWTA equipment.

Based on HPA-2 module developed in the frame of this study, a trade-off has been performed achieved by TAS-F on a LC-SSPA.

This trade-off, presented in the following table, shows that a Ku-Band LC-SSPA using a current commercial European 0.25 μ m GaN technology (GH25 from UMS) and a low loss space combiner technique for output power section was not able to compete with a Ku-Band LC-TWTA solution regarding the electrical performance: LC-TWTA PAE was 30 points higher than the LC-SSPA one at saturation. If this gap was reduced down to 24 points in multi-carrier mode, the comparison remained clearly at LC-SSPA disadvantage.

It is then clear that a GH25 based LC-SSPA would present insufficient electric performances (low PAE and reduced frequency bandwidth) and that a technological breakthrough is required to increase this performance (Pout/PAE/NPR/Instantaneous frequency bandwidth).

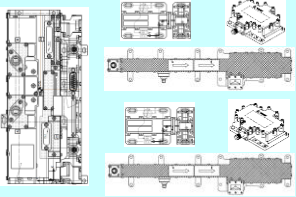
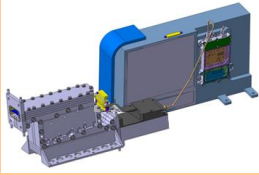
		Ku-band Linearized Equipment	
		Solution with TWT	Solution with SSPA
Mechanical characteristics	Equipment's display		
	Technology for RF chain	GaAs for low level RF chain(LDLA) TWT for power section	GaAs for low level RF chain(LDLA) UMS GH25 for RF power section
	Architecture's description for 1x RF chain:	<u>Assembly of 4 box</u> 1x TWTs + Dual LC-EPC + 1x Circulator + 1x Load <u>DC and RF cables:</u> + 1x High Power DC cables (LC-EPC to TWT) + 1x RF cables (LC-EPC to TWT) + 2x High Power RF cables (TWT to circulator and circulator to load)	<u>Stand-alone (1x box) including:</u> + 1x RF power GaN section (8x HPA) + EPC / TMTC board + Low level RF chain (LDLA) + HPI
	Temperature	2 areas: 65°C (LC-EPC) 85°C (TWT)	1 area: 75°C and 85°C
	Mass for single RF chain	2800g	2300g
	Footprint for single RF chain	4,5dm ²	3,4dm ²
	Functions	LDLA functions	Yes
	Power Flexibility	No	Yes
Performance	Frequency Bandwidth	1GHz	0,5 GHz (up to 1GHz to be confirmed by measurements)
Performance with Multi-carrier Signal	NPR	15dB	15dB
	Pout	95W	95W
Performance with CW Signal	PAE	46,0%	22%
	Pout	175W	175W
	PAE	61%	30%

Table 45 : Current comparison between Ku-Band a LC-TWTA and a LC-SSPA based on the GH25 GaN technology associated to the space combiner technique